Population Pharmacokinetic and Pharmacodynamic Modelling and Simulation of Linagliptin, a Novel Dipeptidyl-Peptidase 4 Inhibitor for the Treatment of Type 2 Diabetes

Dissertation

zur Erlangung des Doktorgrades (Dr. rer. nat.)
der Mathematisch-Naturwissenschaftlichen Fakultät
der Rheinischen Friedrich-Wilhelms-Universität Bonn

vorgelegt von

Silke Retlich
geboren in Schorndorf, Deutschland

Bonn 2010

Angefertigt mit Genehmigung der Mathematisch-Naturwissenschaftlichen Fakultät
der Rheinischen Friedrich-Wilhelms-Universität Bonn.

Erstgutachter:	Prof. Dr. Ulrich Jaehde
Zweitgutachter:	Prof. Dr. Charlotte Kloft
Tag der mündlichen Prüfung:	15. Juli 2010
Erscheinungsjahr:	2010

Für Mama.

Table of Contents

List of abbreviations

°C	degree Celsius
ACE	angiotensin-converting enzyme
AIC	Akaike information criterion
ALAG	lag time
ALT	alanine transaminase
$A_{max,P}$	amount of binding partner in the peripheral compartment
AP	alkaline phosphatase
AST	aspartate transaminase
AUC	area under the plasma concentration-time curve
AUC_{0-24h}	area under the plasma concentration-time curve from time point 0 to 24 hours
$AUC_{24h,SS}$	area under the plasma concentration-time curve of one day at steady-state
AUC_{0-inf}	area under the plasma concentration-time curve from time point 0 to infinity
AUC_{τ}	area under the plasma concentration-time curve of one dosing interval
$AUC_{\tau,ss}$	area under the plasma concentration-time curve at steady-state of one dosing interval
BCS	biopharmaceutics classification system
bid	*bis in die* (twice daily)
BIL	total bilirubin
$B_{max,C}$	concentration of binding partner in the central compartment
BMI	body mass index
BSA	body surface area
BSL	pre-dose DPP-4 activity (parameter estimate)
CB_{plasma}	plasma concentration of linagliptin bound to DPP-4

CHOL	cholesterol
CK	creatine kinase
CL	clearance
C_{max}	maximum linagliptin plasma concentration
CRCL	creatinine clearance
CRF	case report form
CRP	C-reactive protein
C_{trough}	trough plasma concentration, i.e. concentration at the end of the dosing interval, taken directly before next administration
CU_{plasma}	unbound plasma linagliptin concentration
CV%	coefficient of variation
CYP	cytochrome P450
df	degree of freedom
DPP	pre-dose DPP-4 activity in RFU
DPP-4	dipeptidyl-peptidase 4
DPP-8	dipeptidyl-peptidase 8
DPP-9	dipeptidyl-peptidase 9
EC_{50}	concentration resulting in half-maximum effect
$EC_{80\%}$	concentration resulting in 80% DPP-4 inhibition
ECG	electrocardiogram
EDTA	ethylendiaminetetraacetic acid
E_{max}	maximum effect
EMEA	European Medicines Agency
F	bioavailability
FDA	U.S. Food and Drug Administration
fe	fraction excreted

FO	first-order estimation method
FOCE	first-order conditional estimation method
FOCE-I	first-order conditional estimation method with interaction
FPG	fasting plasma glucose
fu	fraction unbound
gMean	geometric mean
GAM	generalised additive modelling
gCV	geometric coefficient of variation
GGT	gamma glutamyl transferase
GIP	glucose-dependent insulinotropic peptide
GLP-1	glucagon-like peptide 1
HGT	height
HPLC-MS/MS	high performance liquid chromatography coupled to tandem mass spectrometry
HV	healthy volunteers
IC_{50}	concentration leading to half-maximal inhibition
i.v.	intravenous
K_a	absorption rate constant
K_d	dissociation constant
K_{OFF}	dissociation rate constant
K_{ON}	association rate constant
L	litre
M	mol/L
min	minute
NA	not applicable
nc	nonclinical
OCT2	organic cation transporter 2

OBJF	objective function
OGTT	oral glucose tolerance test
p	probability
PD	pharmacodynamic
PK	pharmacokinetic
p.o.	peroral
qd	*quaque die* (every day, once daily)
Q_P	intercompartmental clearance between central and peripheral compartment
Q_{P1}	intercompartmental clearance between central and first peripheral compartment
Q_{P2}	intercompartmental clearance between central and second peripheral compartment
$R_{A,\ AUC}$	accumulation ratio based on area under the plasma concentration-time curve
RFU	relative fluorescence units
RSE	relative standard error
SCR	serum creatinine
SD	single dose
SD	standard deviation
SS	steady-state
$t_{1/2}$	terminal half-life
T2D	type 2 diabetic patients
t_{max}	time of maximum plasma concentration
TRIG	triglycerides
V_C	central volume of distribution
V_P	volume of distribution of the peripheral compartment

V_{P1}	volume of distribution of the first peripheral compartment
V_{P2}	volume of distribution of the second peripheral compartment
V_{SS}	volume of distribution at steady-state
V_z	volume of distribution of the terminal phase
WHO	World Health Organization
WT	weight
ε	residual variability
η	interindividual variability
θ	typical model parameter
κ	intraindividual variability
π^2	estimate of the variance of intraindividual variability
σ^2	estimate of the variance of residual variability
σ_{add}	estimate of the additive residual variability
σ_{prop}	estimate of the proportional residual variability
τ	dosing interval
χ^2	chi square distribution
ω^2	estimate of the variance of interindividual variability
Ω-matrix	variance-covariance matrix of interindividual random effects

Acknowledgements

I am most grateful to my supervisor, Professor Ulrich Jaehde, for his valued support and expert advice throughout my work on which I could always rely.

I am deeply indebted to Dr. Alexander Staab for his ceaseless support and encouragement throughout my work. His experience and structured, critical thinking were of invaluable help. I learned so much from you Alexander, thanks!

Boehringer Ingelheim Pharma GmbH & Co KG, Biberach provided me with financial support, the permission to use the data and the working facilities. This is gratefully acknowledged. I would like to thank Dr. Hans Günter Schaefer, Dr. Paul Tanswell, Dr. Willy Roth, and Dr. Ulrich Roth for their confidence in entrusting me with this project as my PhD thesis. Paul's native speaker help is also gratefully acknowledged.

I would like to express my gratitude to my colleagues in the Pharmacometrics Team, Dr. Thorsten Lehr for the helpful comments on my work and the aid with SAS scripts, Dirk Zeumer for the help with the PROPHET system, Reinhilde Krug-Schmid for the QC checks, Dr. Matthias Freiwald, Christiane Göde, Charlie Liesenfeld, Dr. Chantaratsamon Dansirikul, and especially to Dr. Vincent Duval for teaching me the use of NONMEM and Splus and the fruitful discussions of my work.

I am grateful to my colleagues in the PCPK team, especially Dr. Ulrike Graefe-Mody, Dr. Christian Friedrich, and Dr. Katja Boland. Thank you Ulrike and Christian for our most enjoyable collaboration, valuable discussions, and for keeping me informed on the linagliptin project beyond pharmacometrics.

The non-clinical pharmacokinetic group allowed me to extend my research to animal models. I would especially like to thank Dr. Holger Fuchs for the pleasant collaboration.

Modesta Wiersema from the data management group helped me with the large datasets. Thank you very much, Mo!

For their good collaboration, I would also like to thank the bioanalytics group, especially Dr. Barbara Withopf, Dr. André Liesener, Dr. Frank Runge, and Dr. Christine Rentzsch.

Thanks also to Prof. Iñaki F. Trocóniz for my pleasant stay in Pamplona and the helpful discussions about estimating the absolute bioavailability.

I am very thankful to all my colleagues at the Department of Clinical Pharmacy at the University of Bonn, in particular those of the pharmacokinetics group, Anne Drescher,

Andreas Lindauer, and especially Dr. Frederike Lentz for the enjoyable collaboration and the valuable discussions.

Finally, I would like to thank my family and friends for their loving support and incredible patience. It is wonderful to have you! I am most grateful to Michael, my ‘Fels in der Brandung’. Thanks for everything, I love you!

1 Introduction

In this work pharmacometric analyses were performed to investigate the pharmacokinetics and the pharmacokinetic/pharmacodynamic relationship of the novel dipeptidyl-peptidase 4 (DPP-4) inhibitor linagliptin, which is undergoing clinical development for the treatment of type 2 diabetes.

1.1 Type 2 diabetes mellitus

1.1.1 Epidemiology and pathology

Recent estimates revealed that in the year 2007, 246 million people suffered from diabetes worldwide (1). This number is projected to rise to 366 million people affected in the year 2030 (2). Diabetes mellitus is defined by the current World Health Organization (WHO) (3,4) and American Diabetes Association (5) diagnostic criteria based on plasma glucose levels. If a venous fasting plasma glucose (FPG) ≥7.00 mmol/L or a venous plasma glucose ≥11.1 mmol/L, 2 h after ingestion of a 75 g oral glucose load is diagnosed, a patient is considered to be diabetic. The WHO classifies diabetes mellitus based on aetiology in four types: type 1, type 2, other specific types and gestational diabetes (4). Type 2 diabetes is the common major type, affecting 85–95% of diabetic patients in developed countries and an even higher percentage in developing countries (1). It is caused by impaired pancreatic insulin secretion, almost always with a major contribution of insulin resistance (4,6,7), the reduced susceptibility of muscle, liver, and adipose tissue to insulin.

Insulin resistance plays a central role in the pathogenesis of type 2 diabetes mellitus. It is influenced by genetic (e.g. mutations in the PPARγ gene) (8,9) and environmental (e.g. obesity) factors (10,11). Initially, insulin resistance in muscle leads to reduced insulin-dependent glucose uptake compensated by increases in pancreatic insulin secretion to maintain normal blood glucose levels (12). However, as the disease progresses, insulin secretion decreases (11). Lower levels of insulin diminish the insulin-dependent uptake of glucose in muscle and thus lead to higher post-prandial glucose levels. In addition, hepatic glucose production, which is normally inhibited by insulin, is augmented. This in turn

leads to an increase of fasting plasma glucose levels. Increasing hyperglycemia on the other hand deteriorates both insulin sensitivity and insulin secretion – a phenomenon known as 'glucose toxicity'(13). Insulin resistance also affects adipose tissue, leading to an increase in free fatty acids from enhanced lipolysis, which further diminishes the insulin response in skeletal muscle and liver and may in addition further impair pancreatic insulin secretion ('lipotoxicity') (14). An overview of factors contributing to hyperglycemia is provided in Figure 1-1.

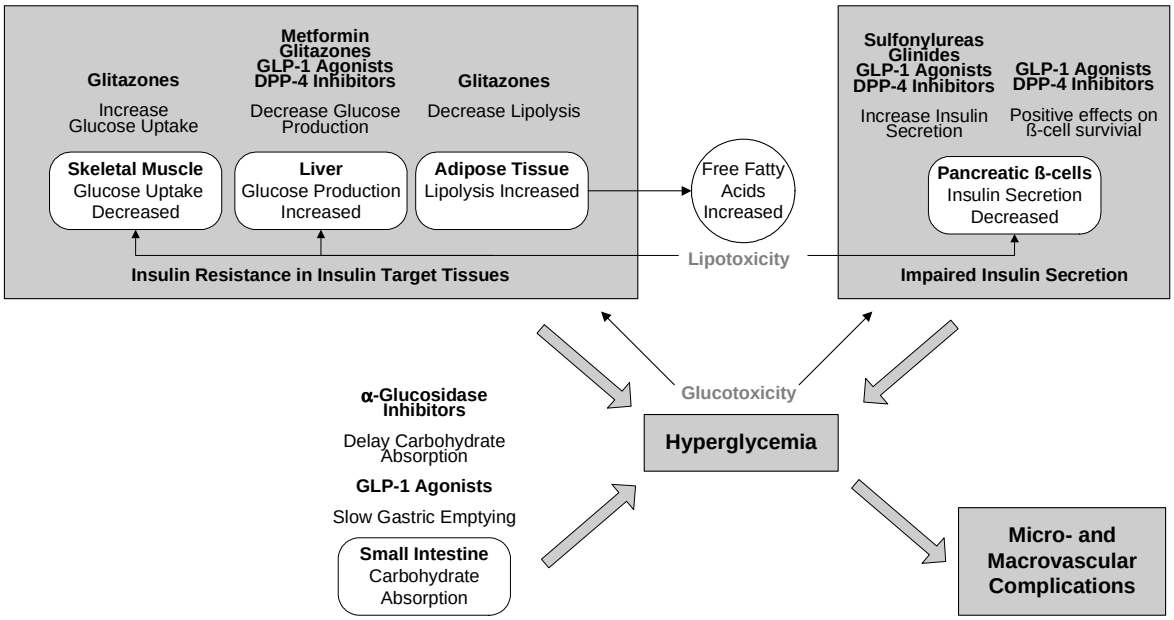

Figure 1-1 Major metabolic defects and treatment options of type 2 diabetes, adapted from (12).

Hyperglycaemia resulting from type 2 diabetes leads to a diminished life expectancy and quality of life (3). It is associated with risk of microvascular complications, e.g. retinopathy, nephropathy, and neuropathy, as well as macrovasular complications, e.g. ischaemic heart disease, stroke, and peripheral vascular disease. Cardiovascular disease accounts for approximately 70% of the mortality in diabetic patients (15). Controlled clinical studies demonstrated that intensive glycaemic control slows down the progression of microvascular complications in patients with type 2 diabetes (16-18). A positive effect of intensive diabetes therapy on macrovasular complications like cardiovascular disease however could so far only clearly be shown in type 1 diabetes (19,20) and is controversial for type 2 diabetes (21-23).

1.1.2 Treatment

For type 2 diabetic patients, several treatment options are available (12,24). While the major focus of diabetes treatment is glycaemic control, other strategies target coincident features of the disease such as insulin resistance or obesity. The current consensus treatment of type 2 diabetes follows a stepwise manner, starting with lifestyle interventions (e.g. diet and exercise) and pharmacotherapy with metformin. Eventually, combination therapy with lifestyle interventions, oral agents, and/or insulin is generally indicated for many type 2 diabetic patients (24). The success of the antidiabetic therapy is controlled by measuring blood glucose, as an index of acute glycaemia and HbA1c, i.e. glycosylated haemoglobin, as an index of chronic glycaemia (24).

Lifestyle interventions to promote weight loss and increase exercise should, if possible, always be included in the treatment of diabetes (24). While weight loss can effectively ameliorate hyperglycaemia (25), the long-term success of incorporating such intervention programs into the usual lifestyle and maintaining them is limited. For pharmacotherapy, several classes of antidiabetic medications are currently available, targeting different angles of the disease (Figure 1-1). Hepatic glucose production is decreased by metformin, resulting in decreased fasting glycaemia. Sulfonylureas and glinides act by enhancing insulin secretion. α-Glucosidase inhibitors reduce the rate of digestion of polysaccharides, thereby lowering postprandial glucose levels (26). Glitazones increase the sensitivity of muscle, fat, and liver to insulin (27). Finally, insulin is the oldest and most effective treatment for lowering glycaemia, and over time, as β-cell function decreases, many diabetics require intensive insulin therapy. Metformin, sulfonylureas and glinides lower HbA1c by ~1.5% (12,24), more than the other oral antidiabetics, but not as much as insulin. Metformin is indicated at every stage of the disease (24). In the United Kingdom Prospective Diabetes Study it was shown not to affect body weight (28) and to decrease mortality compared to other antidiabetic treatments (17).

These currently available therapies for type 2 diabetes have several disadvantages including increased risk of hypoglycaemia (sulphonylureas, insulin), gastrointestinal side effects (metformin, α-glucosidase inhibitors, amylin agonists), weight gain (sulphonylureas, glitazones, glinides, insulin), fluid retention and congestive heart failure (glitazones) (29), as well as myocardial infarction (rosiglitazone) (30,31). One new approach yielding

promising results is the use of agents that mimic or enhance the effect of incretin hormones. This new approach is discussed in detail in section 1.2.3.

1.2 New treatment options based on incretins

1.2.1 Incretins

An oral glucose load leads to a greater insulin secretion compared to an intravenous (i.v.) glucose load matched to produce a similar glycaemic profile (32,33). This phenomenon is called 'incretin effect'. The incretin hormones mainly responsible for this effect are glucagon-like peptide 1 (GLP-1) and glucose-dependent insulinotropic peptide (GIP) (34,35). Incretin hormones are secreted from intestinal endocrine cells in response to oral but not intravenous glucose administration. GLP-1 is secreted from L-cells, GIP from K-cells (34). Secretion occurs in response to oral intake of carbohydrates, lipids and, in the case of GLP-1, also proteins (36). GLP-1 and GIP both enhance the insulin secretion in pancreatic ß-cells (35,37-39). In addition, GLP-1 acts on glucose homeostasis by inhibiting the glucagon secretion of pancreatic α-cells, thereby further decreasing the hepatic glucose production (40-42). Both mechanisms directly lower the plasma glucose levels in a glucose-dependent manner. For rodents, GLP-1 and GIP have been shown to have protective effects on pancreatic ß-cells by enhancing their proliferation and increasing their resistance to apoptosis (43-47). Moreover, the survival of isolated human islets of Langerhans was prolonged in the presence of GLP-1 (48). Other beneficial aspects of GLP-1 are the prolongation of gastric emptying (49,50) and the induction of satiety, both supporting dietary goals in diabetes treatment.

In type 2 diabetic patients, incretin levels (mainly GLP-1) are reduced (51) and the incretin effect is markedly decreased compared to healthy volunteers (52). In line with these studies, patients with impaired glucose tolerance show a reduced suppression of glucagon following an oral glucose load compared to healthy volunteers (53). In type 2 diabetic patients, the insulinotropic activity of GLP-1, in contrast to GIP, remains relatively intact (54). Pharmacotherapy therefore mainly focuses on GLP-1. Continuous subcutaneous infusion of GLP-1 over six weeks normalised blood glucose levels, decreased HbA1c and body weight and greatly improved the first-phase insulin response in type 2 diabetic patients (55).

1.2.2 Dipeptidyl-peptidase 4

DPP-4 rapidly inactivates the incretins, making the long-term diabetes treatment with GLP-1 itself difficult. The hydrolytic activity of DPP-4 results in half-lives of 1–2 min for GLP-1 and 7 min for GIP (36). In fact, more than 50% of secreted GLP-1 is degraded by DPP-4 immediately following release into intestinal capillaries, i.e. before reaching the general circulation (56).

DPP-4 (EC 3.4.14.5) is an ubiquitous serine-type peptidase that cleaves dipeptide fragments from the N-terminus of polypeptides with either proline or alanine as their second residue most effectively (57). Furthermore, DPP-4 acts as regulatory peptidase on a large number of bioactive peptides. Substrates that have been identified for DPP-4 (58) include, besides gastrointestinal hormones like GLP-1 and GIP (59), the neuropeptides (58) endomorphin, neuropeptide Y (60), substance P (61) and bradykinin, as well as growth hormone-releasing hormone (59,62) and several chemokines (63). Apart from its catalytic activity, it interacts with a number of other proteins, e.g. collagen (64), the chemokine receptor CXCR4 (65), adenosine deaminase (66), and the human immunodeficiency virus gp120 surface protein (65,67). In the immune system, DPP-4, also known as CD26, acts as a co-stimulatory molecule in T cell activation (57). It also plays a role in malignant transformation, cancer progression (68-70), and possibly human immunodeficiency virus entry (71).

DPP-4 is expressed in a variety of tissues, primarily on the apical membrane of epithelial and endothelial cells (57,72-75). The distribution of DPP-4 when determined with a polyclonal antibody corresponds to the distribution of DPP-4 activity determined histochemically (74). In blood vessels, lung, myocardium and striated muscles, almost the total DPP-4 activity is located endothelially (75). In kidney, intestine, and liver however, where DPP-4 is abundantly expressed (58,72,76), endothelial DPP-4 activity accounts for only a small part of the total DPP-4 activity (75). The membrane-bound form of DPP-4 is also found on fibroblasts (76), T-cells (77) and other cell types (57). In addition to the membrane-bound form, DPP-4 exists as a soluble form lacking the intracellular part and the transmembrane region (78). Soluble DPP-4 is present in low nanomolar concentrations in plasma (79,80) and other body fluids (57). The origin of soluble DPP-4 in human plasma is not completely understood, but several lines of evidence suggest that soluble DPP-4 may originate from endothelial or epithelial cells or from circulating leukocytes.

A substrain of Fischer rats (F344/DuCrlCrlJ) bred by Charles River, Japan exhibits a mutation resulting in the complete loss of DPP-4 activity (81). In these animals, most of the immature protein is retained and degraded in the endoplasmic reticulum (82). A DPP-4 knockout mouse model has also been developed (83). Despite its ubiquitous localisation and its multiple functions, DPP-4-deficient rats and DPP-4 knockout mice are viable and show no evident pathology. In both animal models, the lack of DPP-4 interferes with blood glucose regulation. After a glucose challenge, intact GLP-1 levels rise higher than in the respective wildtype animals leading to elevated insulin levels accompanied by lower blood glucose levels (83,84). For DPP-4-deficient rats it was also demonstrated that the development of diabetes under a high fat diet is less frequent compared to wildtype rats (85,86).

1.2.3 GLP-1 agonists and DPP-4 inhibitors

With the aim of obtaining clinical benefit from the positive effects of incretins despite their short half-life, GLP-1 analogues resistant to DPP-4 degradation and compounds inhibiting DPP-4 have been developed. GLP-1 agonists such as exenatide or liraglutide bind to the GLP-1 receptor on pancreatic ß-cells and augment glucose-mediated insulin secretion. They also suppress glucagon secretion, resulting in a decreased hepatic glucose production, and they slow down gastric emptying (87). GLP-1 agonists mainly reduce post-prandial glucose levels and do not cause hypoglycaemia (24). Clinical studies have indicated that the administration of GLP-1 agonists lowers body weight by ~2–3 kg over 30 weeks (88-91), and by ~4 kg after 80 weeks (92). The main adverse effects are nausea, vomiting, and diarrhoea, but these apparently abate over time (87-91). Some patients were shown to develop antibodies against GLP-1 agonists, albeit with weak binding affinity and low titres (88-91). Being peptide molecules, GLP-1 agonists require subcutaneous injection. In April 2005, the U.S. Food and Drug Administration (FDA) approved the first GLP-1 agonist, synthetic exendin-4, exenatide. Exenatide needs to be administered twice daily due to its short half-life. Liraglutide is a new GLP-1 agonist with a longer half-life, submitted to the FDA in 2008, that can be given once daily.

While GLP-1 agonists mimic the biologic function of GLP-1, DPP-4 inhibitors prevent the degradation of incretins by DPP-4, prolonging the beneficial effects of these regulatory peptides for type 2 diabetic patients. They stimulate insulin secretion and inhibit glucagon secretion, but unlike GLP-1 agonists they are not associated with the prolongation of gastric emptying (87) and clinical studies demonstrated that DPP-4 inhibitors do not affect body weight (87,93,94). In general, they are well tolerated and, like GLP-1 agonists, do not

cause hypoglycaemia (24,94). As DPP-4 is involved in the immune system, DPP-4 inhibitors carry the potential risk of interfering with immune function. In fact, an increase in infections, e.g. of the upper respiratory tract was reported for sitagliptin, but not for vildagliptin (94). In October 2006, the FDA approved the first DPP-4 inhibitor sitagliptin. The second DPP-4 inhibitor vildagliptin is so far only approved in Europe, since February 2008. Alogliptin and saxagliptin were submitted to the FDA in 2007 and 2008, respectively.

In general, GLP-1 agonists and DPP-4 inhibitors are well tolerated and lower HbA1c by 0.5–1%, comparable to α-glucosidase inhibitors (24). Both classes have the potential advantage of preserving the ß-cell mass through stimulation of cell proliferation and inhibition of apoptosis, as demonstrated in animal models (95-98). However, these effects need yet to be confirmed in human. In addition, apart from surrogate endpoints like reduction in fasting plasma glucose and HbA1c, clinically important endpoints like reduction of the incidence of cardiovascular events have to be examined in order to prove the long-term efficacy of these new compounds.

1.3 Linagliptin

Linagliptin is a novel competitive DPP-4 inhibitor under clinical development for the treatment of type II diabetes. Its chemical structure is depicted in Figure 1-2 (99). It binds to the active site of the DPP-4 enzyme, as shown by the crystal structure of human DPP-4 in complex with linagliptin (100).

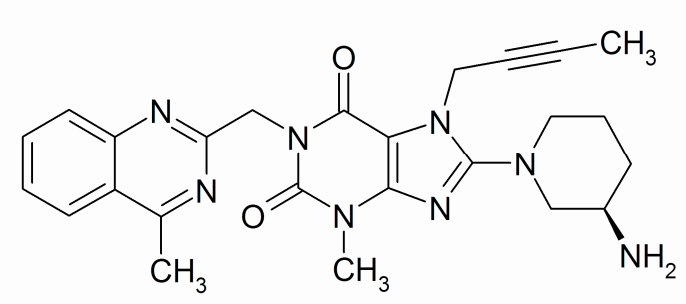

Figure 1-2 Chemical structure of linagliptin

Linagliptin is highly soluble in water at the physiological pH of 7.4 (>5 g/L) (100), at acidic pH linagliptin solubility is increased (107). It displays a log D value of 0.4 at pH 7.4 indicating that its solubility in the lipophilic octanol phase is greater compared to the

aqueous phase (100). The linagliptin pK_a values of 1.9 and 8.6 correspond to the protonation of the nitrogen of the quinazoline group and the primary amino group, respectively (100).

1.3.1 Pharmacodynamic properties

1.3.1.1 *In Vitro* investigations and preclinical pharmacodynamics

In vitro studies revealed linagliptin to be a highly potent, competitive DPP-4 inhibitor. The concentration leading to half-maximal inhibition (IC_{50}) of DPP-4 *in vitro* was approximately 1 nM, and thus linagliptin was more potent compared to sitagliptin (IC_{50}: 19 nM), alogliptin (IC_{50}: 24 nM), saxagliptin (IC_{50}: 50 nM), and vildagliptin (IC_{50}: 62 nM). Linagliptin binding to DPP-4 exhibits a slow off-rate ($3.0 \cdot 10^{-5}$ s^{-1}) (101).

The potent DPP-4 inhibition of linagliptin was confirmed *in vivo* in various species including male Wistar rats, Beagle dogs, and Rhesus monkeys. In all three species, linagliptin was highly efficacious and resulted in long-lasting and potent DPP-4 inhibition of >70% for >7 h after oral administration of 1 mg/kg (100). After a single oral dose of 3 mg/kg, linagliptin increased active GLP-1 and insulin levels, and reduced the glucose levels compared to the control group after an oral glucose tolerance test (OGTT) in Zucker fatty rats (101). The effect on glucose tolerance was long-lasting. Glucose excursion was significantly reduced 16 h after a single administration in C57/BL6 mice, or 24 h in Zucker fatty (fa/fa) rats (101). Glucose excursion was measured by an OGTT, as the increment of the area under the plasma concentration-time curve (AUC) of glucose. In addition, basal active GLP-1, but not basal insulin levels, were elevated in Zucker fatty rats and in the postprandial phase, plasma glucagon values tended to be lower (101). The effects of linagliptin after a single dose were confirmed for multiple dosing in two animal models for diabetes, high-fat diet/streptozotocin-induced diabetic mice and Zucker diabetic fatty rats (102). In addition, HbA1c was decreased after 4–5 weeks of treatment. In both animal models, body weight was unaffected compared to placebo treatment.

1.3.1.2 Clinical pharmacodynamics

Linagliptin treatment resulted in a rapid, potent and long-lasting inhibition of plasma DPP-4 in clinical studies. Already after a single dose of linagliptin, DPP-4 was effectively inhibited as shown by maximum DPP-4 inhibitions of 72.7 and 86.1% for 2.5 and 5 mg, and >95% for doses ≥25 mg (103). At steady-state, plasma DPP-4 activity was inhibited

over 24 h by >80% in most patients receiving 5 or 10 mg linagliptin once daily (104). Generally, DPP-4 inhibition ≥80% over 24 h is aimed for, as this was shown to be related to maximum effects in incretin response and glucose reduction (105,106).

The effects of linagliptin on the incretins and the glucose levels in type 2 diabetic patients were investigated during an OGTT after twelve days of treatment. Treatment with 2.5, 5, and 10 mg, but not 1 mg linagliptin, considerably elevated the increase of GLP-1 levels during the OGTT on day 13 compared with baseline. In line with this, 2.5, 5, and 10 mg linagliptin, but not 1 mg, significantly reduced glucose excursion during the OGTT on days 1 and 13 compared to placebo (104).

1.3.2 Pharmacokinetic properties

1.3.2.1 Preclinical pharmacokinetics and *in vitro* investigations

The pharmacokinetics of linagliptin was mainly investigated in rats and cynomolgus monkeys. The pharmacokinetics of linagliptin was nonlinear in both species (107) accompanied by a dose-dependency of pharmacokinetic parameters like clearance and volume of distribution. After intravenous administration of 5 mg/kg linagliptin to rats and 1.5 mg/kg to cynomolgus monkeys, an apparent clearance (CL) of 37.3 mL/min/kg in rats and 15.8 mL/min/kg in monkeys was determined (100). The volumes of distribution at steady-state (V_{SS}) were 5.4 L/kg in rats and 15.8 L/kg in cynomolgus monkeys (100), both exceeding the total body volume indicating that linagliptin is extensively distributed in the tissues. The gastrointestinal absorption of linagliptin was moderate with an oral bioavailability (F) of ~50% in rats and cynomolgus monkeys. This absolute bioavailability estimate was determined by a comparison of the area under the plasma concentration-time curve of oral 5 mg/kg linagliptin to intravenous 5 mg/kg (rats) and 1.5 mg/kg (monkey) (100). Despite the moderate bioavailability, only a minor first-pass metabolism was observed (107). The mean residence times after oral administration of 5 mg/kg linagliptin were 14.3 h and 17.4 h in rats and cynomolgus monkeys, respectively (100). The terminal half-lives ($t_{1/2}$) of linagliptin after oral administration were long in both species (35.9 h in rats and 41.4 h in cynomolgus monkeys) (100).

Plasma protein binding of linagliptin was investigated for various species including rats, cynomolgus monkeys and humans, by equilibrium dialysis. At plasma concentrations

>30 nM, the fraction bound ranged from 75–89% (107). At lower concentrations, the fraction bound increased to 99%.

In human liver microsomes linagliptin only weakly inhibited cytochrome P450 (CYP) 3A4 and no other CYP isoforms. These findings were confirmed in rats, mice, rabbits, and cynomolgus monkeys. In these animals, metabolism was only a minor elimination pathway (107). Excretion mainly occurred via faeces with a prominent biliary fraction, whereas renal excretion was only of minor importance. After intravenous administration of 1 mg/kg [^{14}C]linagliptin to rats and 1.5 mg/kg to cynomolgus monkeys, the fraction of [^{14}C]linagliptin-related radioactivity excreted in urine was 21.7 and 15.3%, respectively.

1.3.2.2 Clinical pharmacokinetics

The pharmacokinetics of linagliptin after oral administration was investigated in healthy volunteers (103) and type 2 diabetic patients (104). Basic pharmacokinetics was comparable between both groups.

Linagliptin was rapidly absorbed, with a median time of maximum plasma concentration (t_{max}) of ~1.5 h (range: 0.5–6.0 h) after single and multiple dosing (104). Linagliptin exhibited nonlinear pharmacokinetics after single and multiple dosing, in contrast to other DPP-4 inhibitors including sitagliptin, vildagliptin, saxagliptin and alogliptin (108-111). At supratherapeutic doses (25–600 mg), the exposure after a single dose of linagliptin increased more than dose-proportionally (103). In contrast, in the therapeutic dose range (1–10 mg linagliptin once daily), the nonlinearity was characterised by a less than dose-proportional increase in the maximum linagliptin plasma concentration (C_{max}) and the AUC (103). The pharmacokinetic parameters for this dose range, as determined by noncompartmental analysis, are presented in Table 1-1. Both the CL/F and V_{SS}/F were increasing with increasing dose. In general, a low clearance was estimated as well as a high volume of distribution, suggesting an extensive tissue distribution of linagliptin in humans. The terminal half-life of linagliptin was between 113 and 131 h and nearly constant between the therapeutic dose groups. Despite the long terminal half-life, steady-state was reached after few days and only moderate accumulation was observed after once daily treatment. Both the time to reach steady-state and the accumulation ratio decreased with

Table 1-1 Non-compartmental pharmacokinetic parameters of linagliptin (adapted from (104,107))

Parameter	1 mg gMean (gCV [%])	2.5 mg gMean (gCV [%])	5 mg gMean (gCV [%])	10 mg gMean (gCV [%])
$AUC_{0\text{-}24h}$ [nmol·h/L]	40.2 (39.7)	85.3 (22.7)	118 (16.0)	161 (15.7)
$AUC_{\tau,SS}$ [nmol·h/L]	81.7 (28.3)	117 (16.3)	158 (10.1)	190 (17.4)
C_{max} [nM]	3.13 (43.2)	5.25 (24.5)	8.32 (42.4)	9.69 (29.8)
$C_{max,SS}$ [nM]	4.53 (29.0)	6.58 (23.0)	11.1 (21.7)	13.6 (29.6)
t_{max} [1)] [h]	1.50 [1.00–3.00]	2.00 [1.00–3.00]	1.75 [0.92–6.02]	2.00 [1.50–6.00]
$t_{max,SS}$ [1)] [h]	1.48 [1.00–3.00]	1.42 [1.00–3.00]	1.53 [1.00–3.00]	1.34 [0.50–3.00]
$(Vz/F)_{SS}$ [L]	4,510 (32.1)	7,400 (13.1)	12,700 (17.7)	20,800 (22.7)
$(CL/F)_{SS}$ [mL/min]	431 (28.3)	757 (16.3)	1,120 (10.1)	1,850 (17.4)
$CL_{R,SS}$ [mL/min]	14.0 (24.2)	23.1 (39.3)	70.0 (35.0)	59.5 (22.5)
$fe_{0\text{-}24h}$ [%]	Not calculated[2)]	0.139 (51.2)	0.453 (125)	0.919 (115)
$fe_{\tau,SS}$ [%]	3.34 (38.3)	3.06 (45.1)	6.27 (42.2)	3.22 (34.2)
$t_{½,SS}$ [h]	121 (21.3)	113 (10.2)	131 (17.4)	130 (11.7)
Accumulation $t_{½}$ [h]	23.9 (44.0)	12.5 (18.2)	11.4 (37.4)	8.59 (81.2)
$R_{A,AUC}$	2.03 (30.7)	1.37 (8.2)	1.33 (15.0)	1.18 (23.4)

1) Median and range [minimum–maximum]

2) not calculated as most values were below the lower limit of quantification

increasing dose. Steady-state was achieved after 4–6 days for dose groups 1–5 mg and after two days in case of the 10 mg dose. The accumulation ratio was 2.0-fold for the 1 mg dose group and 1.2-fold for the 10 mg dose group. The accumulation half-life[1] decreased accordingly with dose from 24 h for the 1 mg dose group to 8.6 h for the 10 mg dose group. The contribution of renal clearance to overall clearance was small. In the therapeutic dose range of 1–10 mg, the cumulative amount of linagliptin excreted in urine was

[1] calculcated as $\tau \cdot \ln 2 / \ln(R_{A,AUC}/(R_{A,AUC}-1))$

below 1% of the administered dose on day 1 and 3–6% on day 12. With higher single doses, the fraction of dose excreted increased up to 33% in the 600 mg dose group (103).

Further studies revealed that linagliptin is predominantly excreted unchanged via the faeces (107). Metabolism was only of subordinate importance for the elimination of linagliptin. Linagliptin had one main metabolite, CD1790, representing 17% of the drug-related radioactivity in plasma. This metabolite was formed by oxidation of the amino group of the piperidine moiety to a hydroxyl group. CD1790 is pharmacologically inactive and was found in all investigated species (107).

1.3.3 Safety

Binding of linagliptin to DPP-4 is highly selective. The *in vitro* selectivity of binding to DPP-4 is ≥10,000-fold higher compared to dipeptidyl-peptidase 8 (DPP-8) and dipeptidyl-peptidase 9 (DPP-9), and a number of other proteases tested (101). A low inhibition of DPP-8 and DPP-9 is of great importance, as inhibition of these enzymes is assumed to be associated with severe immunotoxic side effects (112). In addition, linagliptin has a low affinity for the hERG channel (100), indicating that the risk for a prolongation of the QT interval is small. In preclinical toxicity studies linagliptin exhibited a very low toxicity with a high safety margin to clinical use (107). No genotoxic or teratogenic effects were observed.

In healthy volunteers, single oral doses of linagliptin up to 600 mg were well tolerated. The incidence of adverse events was not dose-dependent and was not different between subjects treated with linagliptin or placebo (103). This positive safety and tolerability profile after single doses in healthy volunteers was confirmed by a multiple dose study in type 2 diabetic patients. In this study, 1–10 mg oral doses of linagliptin were administered once daily over twelve days (104). Again linagliptin was well tolerated in all dose groups, and no patient discontinued the treatment due to adverse events. In addition, there were no clinically relevant changes in laboratory or electrocardiogram (ECG) parameters and no signs of hypoglycaemia were reported during the study.

1.4 Pharmacometrics in drug development

1.4.1 Pharmacometrics

Pharmacometrics is the development and application of mathematical and statistical methods in order to characterise, understand, and predict the pharmacokinetic and pharmacodynamic properties of a given drug. It allows the differentiation of variability into interindividual, intraindividual, and residual variability (η, κ, and ε, respectively), as well as their quantification, aiding rational drug development and pharmacotherapy (113).

Pharmacometric analyses involve the development of a pharmacokinetic and/or pharmacodynamic model. A pharmacokinetic model describes the relationship between the administered drug and the concentration of the drug in plasma or other body fluids. This relationship is often described using compartmental models. A pharmacodynamic model describes the relationship between the observed exposure of the drug and the observed pharmacodynamic response (e.g. biomarker). A commonly used pharmacodynamic model is for example the E_{max} model. Depending on the availability of data, the knowledge about the drug and the objective of the analysis, pharmacometric models can be empirical, i.e. purely descriptive, or mechanism-based, i.e. reflecting the underlying physiological system as much as possible (114). In pharmacometric analyses, semi-mechanistic models are often used incorporating only the key elements of a physiological system.

Pharmacometric models not only provide estimates for pharmacokinetic and/or pharmacodynamic parameters, but they can also be used for simulations (113). By illustrating the implications of a pharmacometric model, e.g. the amount of drug in the peripheral compartment, simulations can help to understand the pharmacokinetics or pharmacodynamics. Furthermore, clinical trial simulations are a useful tool to answer ‘what if’ scenarios and thereby optimise and evaluate the design of subsequent studies.

1.4.2 Population approach

The models applied in pharmacometrics are often population models using the nonlinear mixed-effect modelling technique. Population analysis is the characterisation of the typical pharmacokinetic and/or pharmacodynamic behaviour of a drug together with the study of sources and correlates of the variability in the drug concentration and/or the pharmacological effect (113,115,116). This includes explorations on the impact of certain patient

characteristics like age or weight (called covariates) on the pharmacokinetic and/or pharmacodynamic behaviour of a drug. A population analysis typically investigates the pharmacokinetics and/or pharmacodynamics of clinically relevant doses of a drug in the patient population (116).

The population approach using the nonlinear mixed-effect modelling technique has several advantages compared to the two-stage approach that has traditionally been used for population analyses (117). In the two-stage approach, the individual parameters are estimated first and then their distribution statistics are calculated. In contrast, in the population approach based on nonlinear mixed-effect modelling the data of all individuals are analysed together, and different kinds of variabilities are directly taken into account. Thereby, the individuality of each subject is maintained and accounted for. In consequence, the population approach based on nonlinear mixed-effect modelling is the more versatile approach (117). It can be applied to different types of data and can be used to analyse extensively as well as sparsely sampled data. The analysis of sparse data is important in situations in which dense sampling is not possible for ethical reasons, e.g. studies in children or severely ill patients. A balanced study design is not required, thus irregular sampling or the combination of data from different studies is possible (115). As the data are analysed together, information can be 'borrowed' between individuals, this is also important for the investigation of nonlinear processes in which every dose group contains different kinds of information (118). Furthermore, the population approach based on nonlinear mixed-effect modelling provides considerably more accurate estimates of the variability compared to the two-stage approach (119,120).

To perform population analyses using nonlinear mixed-effect modelling different software programs are available including NONMEM, NLME in Splus, NLMIX in SAS, and Monolix (121-123). The population analyses presented in this thesis were performed with the NONMEM software (Version V, level 1.1, GloboMax LLC, Hanover MD, USA) (124). NONMEM was the first software for nonlinear mixed-effect modelling, introduced in its first version in the early 1980s by Sheiner, Beal, and Brockman (125) and is still the most widely used software for nonlinear mixed-effect modelling (120,123,126).

1.4.3 Regulatory perspective on pharmacometrics

Pharmacometrics is widely accepted and recommended by authorities to contribute to a better understanding of the pharmacokinetic and pharmacodynamic behaviour of a drug in

order to allow a safe and efficacious therapy. The FDA and the European Medicines Agency (EMEA) have both issued guidances on population analysis. The FDA's *Guidance for industry: Population Pharmacokinetics* (115) elaborates when and how to perform a population analysis while the EMEA guidance (127) focuses on documentation and reporting. In their white paper *Challenge and Opportunity on the Critical Path to New Medical Products* (128), the FDA urges, amongst other approaches, the use of computer-based predictive models to optimise the time-consuming and expensive development of new products. Furthermore, the FDA has published two summaries illustrating the impact of pharmacometrics on new drug approval or labelling (129,130).

1.4.4 Impact of pharmacometrics in different phases of clinical drug development

Pharmacometrics can be applied throughout different phases of drug development (114,117,131,132). Early clinical development includes phase I studies, typically conducted in healthy volunteers as well as phase IIa studies, typically performed in the patient population. The objectives of phase I and IIa studies are to investigate safety and tolerability of a compound, as well as pharmacokinetics and pharmacodynamics. In these studies proof-of-mechanism biomarkers are usually determined to provide evidence of target engagement. Due to the short study period or when the study population is composed of healthy volunteers, disease-related biomarkers are often not meaningful. Usually, in phase I and IIa studies many pharmacokinetic and pharmacodynamic observations are available per subject, but the number of subjects is lower compared to phase IIb and III studies. In pharmacometric analyses, the dense data of phase I and IIa studies can be used to characterise and understand the pharmacokinetics and the relationship between pharmacokinetics and pharmacodynamics of the compound. Due to strict inclusion and exclusion criteria, the variability in the subject-specific characteristics is usually small, and thus the data will only provide limited information about the impact of subject-specific characteristics on the pharmacokinetic or pharmacodynamic model parameters.

In contrast, phase IIb and phase III trials include a larger and more diverse patient population, but the number of pharmacokinetic and pharmacodynamic observations per patient is lower than in early clinical development. The objective of phase IIb trials is to investigate safety and provide the 'proof of concept', i.e. demonstrating positive effects on disease-related biomarkers/surrogate endpoints. The objective of phase III studies is to assess

safety and efficacy in a large patient population. The sparse data of phase IIb and III trials can be analysed by nonlinear mixed-effect modelling techniques to understand and confirm the dose-exposure-response relationship in the target population. Investigations about the relationship between patient characteristics and model parameters may partially explain the variability observed in the drug concentration or effect. By this approach, one may identify subgroups of patients exhibiting a deviant exposure or pharmacological effect. For these patients, safety or efficacy may be compromised, necessitating a dose adjustment.

Throughout all phases of drug development, pharmacometrics is a valuable tool to predict untested scenarios, support dosing recommendations and design future clinical trials. Simulations are of special interest for compounds with nonlinear pharmacokinetics, as for these the pharmacokinetic and pharmacodynamic drug behaviour is difficult to predict.

1.5 Aim of the work

Prior to this thesis, it was known that linagliptin exhibits nonlinear pharmacokinetics with a less than dose-proportional increase in the exposure in various animal species and humans in the therapeutic dose range. The reason for the nonlinearity was unknown. Due to the dependence of the free fraction in plasma on the concentration of linagliptin in the low nanomolar range, it was speculated that the less than dose-proportional increase in the exposure was due to concentration-dependent binding of linagliptin to its target protein DPP-4.

The aim of this work was to characterise the nonlinear pharmacokinetics of linagliptin and the relationship between linagliptin pharmacokinetics and its plasma DPP-4 activity using nonlinear mixed-effect modelling. The developed models were to be applied to support the clinical drug development of linagliptin. This was conducted in a total of five projects.

The aim of Project 1 was to characterise the nonlinear pharmacokinetics and the pharmacokinetic/pharmacodynamic relationship of linagliptin in type 2 diabetic patients. The hypothesis that concentration-dependent binding of linagliptin to DPP-4 is the reason for the nonlinear pharmacokinetics of linagliptin in humans was to be tested.

In Project 2, the population pharmacokinetic/pharmacodynamic model developed in Project 1 was used for clinical trial simulations to support the clinical development of linagliptin.

In Project 2a, simulations were performed to evaluate the adequate dose of linagliptin for a twice-daily dosing strategy. This dosing scheme was required for the fixed dose combination of linagliptin with metformin.

In Project 2b, the impact of a reduced clearance on the exposure of linagliptin was simulated in order to support the definition of the inclusion and exclusion criteria with regard to renal function for Phase IIb studies.

In Project 2c, simulations were performed to investigate the optimal duration of a treatment period in a change-over design, i.e. a cross-over design without a washout between the periods, to adequately test the dose-proportionality of linagliptin at steady-state.

In Project 2d, the model was adapted to describe the single dose plasma concentration-time profiles of a drug-drug interaction trial investigating the influence of ritonavir comedication on linagliptin pharmacokinetics and to simulate the steady-state exposure of linagliptin under ritonavir comedication.

The aim of Project 3 was to characterise the variability in the pharmacokinetics (Project 3a) and the pharmacodynamics (Project 3b) of linagliptin and to identify clinically relevant covariates affecting either drug concentration or DPP-4 inhibition.

In Project 4 a modelling approach was used to determine the absolute bioavailability of linagliptin taking into account its nonlinear pharmacokinetics.

The aim of Project 5 was to test the hypothesis that concentration-dependent binding to DPP-4 is the reason for the nonlinear pharmacokinetics of linagliptin by comparing the plasma concentration-time profiles of wildtype and DPP-4-deficient Fischer rats using a model-based analysis.

2 Methods and studies

2.1 Data acquisition

In this thesis pharmacokinetic and/or pharmacodynamic observations of the DPP-4 inhibitor linagliptin from one nonclinical and six clinical studies were analysed. Table 2-1 provides an overview of these studies. The analytical methods used to quantify the linagliptin plasma concentration and DPP-4 activity are described in the following sections.

Table 2-1 Overview of clinical and nonclinical studies analysed

Study	Pro-ject	Phase	Popu-lation	No. of subjects	Dose	Route	Design	Treatment duration	Obser-vation
I	1+3	IIa	T2D	35	1, 2.5, 5, 10 mg	p.o.	parallel	12 days	PK, PD
II	1+3	IIa	T2D	61	2.5, 5, 10 mg	p.o.	parallel	28 days	PK, PD
III	3	IIb	T2D	170	0.5, 2.5, 5 mg	p.o.	parallel	12 weeks	PK, PD
IV	3	IIb	T2D	196	1, 5, 10 mg	p.o.	parallel	12 weeks	PK, PD
V	2d	I	HV	12	5 mg	p.o.	cross-over (± ritonavir)	SD	PK
VI	4	I	HV	28	0.5, 2.5, 5, 10 mg	i.v.	parallel	SD	PK
					10 mg	p.o.	cross-over vs. 5 mg iv	SD	PK
VII	5	nc	Rats	28	0.01, 0.1, 0.3, 1.0 mg/kg	i.v.	parallel	SD	PK

nc, nonclinical; T2D, type 2 diabetic patients; HV, healthy volunteers; p.o., peroral; i.v., intravenous; SD, single dose; PK, pharmacokinetic; PD, pharmacodynamic (i.e. DPP-4 activity)

2.1.1 Quantification of linagliptin in plasma

For quantification of linagliptin plasma concentrations in the clinical studies, blood was taken from a cubital or forearm vein in potassium ethylendiaminetetraacetic acid (EDTA)-anticoagulant blood drawing tubes. The EDTA-anticoagulated blood samples were centrifuged immediately after collection or within 30 min after collection and stored in an

ice bath prior to centrifugation. The samples were centrifuged for ~10 min at 2,000–4,000 × g at 4–8°C. The plasma samples were stored at about −20°C until analysis. In the nonclinical study of Project 5, blood was taken under isoflurane anaesthesia from the sublingual vein in potassium EDTA-coated tubes. Until centrifugation, the collected blood was stored in an ice bath. Plasma was separated by centrifugation (5 min at 4,000 × g at 4°C) and stored at about −20°C until analysis.

Total (bound plus unbound) linagliptin concentrations in plasma of humans and rats were determined by a set of validated assays based on high performance liquid chromatography coupled to tandem mass spectrometry (HPLC-MS/MS) methods as described (103). Validation of the assays was performed according to the current international guidance on bioanalytical methods (133). The assays comprised sample clean-up by solid-phase extraction in the 96-well plate format. Chromatography was performed on an analytical phenyl-hexyl reversed phase high performance liquid chromatography column with gradient elution. The substance was detected and quantified by HPLC-MS/MS using electrospray ionisation in the positive ion mode with [$^{13}C_3$]-linagliptin as an internal standard.

The validated concentration ranges of linagliptin in undiluted plasma samples varied slightly among the assays applied in the different studies (Appendix, Table 1). The lower limit of quantification of linagliptin was either 0.106 or 0.100 nM, dependent on the study. In the preclinical study (Project 5) [^{14}C]-linagliptin was administered to rats. Since only the unlabelled analyte was directly measured, the resulting concentrations were multiplied with a correction factor of 2.71 for the dose groups 0.01–1 mg/kg to calculate the total concentration. The correction factor was determined from the ratio of total to unlabelled compound in the respective formulation. The analytical range was adjusted accordingly to a lower limit of quantification of 0.271 nM and an upper limit of quantification of 271 nM in the investigated dose groups. Linagliptin plasma concentrations were either measured at the bioanalytical laboratories at the Department of Drug Metabolism and Pharmacokinetics, Boehringer Ingelheim, Biberach, Germany, or at Covance Laboratories Ltd., Harrogate, UK (Appendix, Table 1).

Assay performance during the studies was assessed by back-calculation of calibration standards, tabulation of the standard curve fit function parameters and measurement of quality control samples. Inaccuracy and imprecision data of the plasma quality control samples for linagliptin of the different studies are listed in Appendix, Table 2. An inaccu-

racy value of up to ±15% and an imprecision value of up to 15% was accepted according to the *Guidance for Industry: Bioanalytical method validation* issued by the FDA (133). No relevant interference of endogenous compounds with linagliptin was observed in blank human plasma and blank Fischer rat plasma. The data document the accuracy, precision, and specificity of the HPLC-MS/MS assays employed for the studies. It was therefore concluded that the linagliptin plasma concentration determined in the study samples were reliable within the given inaccuracy and imprecision ranges.

2.1.2 Quantification of DPP-4 activity in plasma

For quantification of plasma DPP-4 activity, blood was collected in potassium EDTA-anticoagulant blood drawing tubes. The EDTA-anticoagulated blood samples were centrifuged immediately or within 30 min after collection. The samples were centrifuged for ~10 min at 1,000 × g or 2,500 × g at 2–8°C or 4–8°C. The plasma samples were stored at about −20°C until analysis.

DPP-4 activity in plasma was analysed by a validated method using a semi-quantitative enzyme activity assay with fluorescence detection as previously described (103). The DPP-4 present in the human plasma samples cleaves the assay substrate alanine-proline-7-amido-4-trifluoro-methylcoumarine yielding the fluorescent product 7-amino-4-trifluoro-methylcoumarine. The higher the DPP-4 activity in the sample, the higher the fluorescence measured as relative fluorescence units (RFU). The fluorescence was detected at 535 nm (emission) using 405 nm excitation wavelength after 10 min of incubation. The assay performance was evaluated during the study by co-analysis of six in-house standards as quality control samples in each run/plate. The plasma DPP-4 activity was measured at the Institut für Klinische Forschung und Entwicklung Mainz (ikfe), Germany.

In Project 1 DPP-4 activity was calculated as percentage of pre-dose DPP-4 activity, thus the individual DPP-4 activities under treatment were normalised to the respective pre-dose measurement of the individual patient. In Project 3 DPP-4 activity as measured in RFU was used in the analysis.

2.2 Datasets

2.2.1 Dataset building

2.2.1.1 General dataset building

The structure of NONMEM datasets is predetermined by the program (124). In general, NONMEM data files contain an identifier for the individual subjects, one or more dependent variables (e.g. linagliptin plasma concentration, plasma DPP-4 activity), independent variables such as dosing information, actual sampling and dosing time and possibly information about subject-specific covariates.

The raw data used to build the NONMEM datasets were provided by Medical Data Services, Boehringer Ingelheim. The NONMEM datasets of Projects 2d, 4, and 5 were prepared manually using Excel (Version 2002, Microsoft, Redmond, WA, USA). The data quality was assured by double data entry, i.e. a dataset was prepared in two independent versions which were then compared. The initial NONMEM datasets of studies I to IV used in Projects 1 and 3 were provided by Medical Data Services, Boehringer Ingelheim. These datasets were created by a well documented SAS (Version 8.02, SAS Institute Inc., Cary, NC, USA) program based on a comprehensive dataset specification document. Problems during the dataset creation were discussed and resolved by both parties to ensure a complete, consistent and accurate reporting database. Subsequently, an intensive data checkout analysis was carried out and documented to assure the quality of the datasets.

Changes of the initial datasets like combination of different datasets, division or modification were performed either manually using Excel or by user-written Splus (Version 7 and 8, Insightful Corporation, Seattle, WA, USA) scripts. All changes of the datasets were checked and documented to allow traceability.

2.2.1.2 Handling of covariates

Information on the following covariates was included in the datasets of studies I–IV:

1. Demographic information: age (years), weight (kg), height (cm), body mass index (kg/m^2), body surface area (m^2), sex, ethnic origin, smoking and alcohol status
2. Laboratory values: serum creatinine (mg/dL), creatinine clearance (ml/min), urea (mM), alanine transaminase (U/L), aspartate transaminase (U/L), alkaline phos-

phatase (U/L), gamma-glutamyl transferase (U/L), total bilirubin (mg/dL), creatine kinase (U/L), cholesterol (mg/dL), C-reactive protein (mg/dL), triglyceride (mg/dL), fasting plasma glucose (mM)

3. Others: study number, randomisation group, formulation, metformin co-treatment, pre-dose DPP-4 activity (RFU)

The derived covariates body mass index, body surface area and creatinine clearance were calculated as follows. The body mass index was calculated according to equation 2-1:

$$\text{Body mass index} = \frac{\text{weight (kg)}}{\text{height (m)}^2} \qquad \text{(Equation 2-1)}$$

Body surface area was derived based on the equation described by DuBois and DuBois (134) as shown in equation 2-2:

$$\text{Body surface area} = 0.007184 \cdot \text{height (cm)}^{0.725} \cdot \text{weight (kg)}^{0.425} \qquad \text{(Equation 2-2)}$$

Creatinine clearance was calculated according to the Cockroft-Gault equation (135) as presented in equations 2-3a and 2-3b:

$$\text{Creatinine clearance}_{\text{male}} = \frac{(140 - \text{age (years)}) \cdot \text{weight (kg)}}{72 \cdot \text{creatinineconcentration (mg/dL)}} \qquad \text{(Equation 2-3a)}$$

$$\text{Creatinine clearance}_{\text{female}} = \frac{(140 - \text{age (years)}) \cdot \text{weight (kg)}}{72 \cdot \text{creatinineconcentration (mg/dL)}} \cdot 0.85 \qquad \text{(Equation 2-3b)}$$

2.2.1.3 Handling of missing observations

If observations of the dependent variables were missing, these values were omitted in the dataset. If date and/or time were missing for an observation, the respective observation was not included into the dataset. Plasma linagliptin concentrations below the limit of quantification were removed *a priori* from the dataset, except when measured during the lag time in which case they were implemented and set to zero. Patients randomised to placebo were excluded from the pharmacokinetic analysis.

2.2.1.4 Handling of missing dosing records

If both date and time of a dosing record were missing, it was assumed that the dose was not taken and the dose was not included in the dataset. If only either date or time of a dosing record was missing, it was assumed that the dose was taken and the dose was implemented

with protocol date or time. If date and/or time of the last dose before an observation was missing, this observation was not included in the dataset.

2.2.1.5 Handling of missing covariates

A covariate completely missing for a particular subject was replaced by the population median of the baseline values for continuous covariates and by the mode for a categorical covariate. If a covariate that was measured more than once within a subject was missing, the last measurement was carried forward until a new measurement was available.

2.2.1.6 Handling of outliers

All data, i.e. dependent variables and covariates, were included in the analysis whenever possible. Data were only exluded if they were not plausible. Whenever possible, outliers which were excluded from the analysis were tested on their impact on the analysis. All outliers are reported in the respective results sections of the projects.

2.2.2 Dataset description

Before start of the actual population pharmacokinetic or pharmacodynamic analysis, the data were extensively explored graphically to further assure the data quality and to allow a comprehensive overview of the investigated data. In general, the distribution of subjects and observations per dose group, visit and time after dose was investigated. Pharmacokinetic and pharmacodynamic observations were plotted versus time and versus each other. Furthermore, frequency distributions of covariates and correlations between covariates were examined. The main results of the dataset description are presented in the respective section of each project.

2.3 Population analysis

The population pharmacokinetic or pharmacodynamic analyses presented within this thesis were performed using the nonlinear mixed-effects modelling software package NONMEM V (124).

2.3.1 Nonlinear mixed-effect modelling

The name of the software NONMEM is derived from *NON*linear *M*ixed-*E*ffects *M*odelling. In a population analysis using nonlinear mixed-effect modelling techniques, data from all individuals are analysed together, but the individuality of the subjects is maintained. This is achieved by simultaneously estimating typical model parameters (so-called fixed effects) together with different levels of variability (so-called random effects). As pharmacokinetic or pharmacodynamic models are nonlinear and comprise both fixed effects and random effects the method was termed nonlinear mixed-effect modelling.

A nonlinear mixed-effect model, referred to as population model in this thesis, consists of the following submodels:

1. Structural model
2. Stochastic model
3. Covariate model (optional)

2.3.1.1 Structural model

The structural model describes the plasma concentration-time profile or the effect-time profile of a typical subject as a function of dose, time and parameters of the underlying model as presented in equation 2-4:

$$y_{ij} = f(x_{ij}, \theta) \qquad \text{(Equation 2-4)}$$

The j^{th} response y (concentration or effect) of the i^{th} individual can be described by a function f that depends on measurable variables x_{ij} like dose or time, as well as estimated typical model parameters θ. Structural models for pharmacokinetic analyses are often compartmental models, while for pharmacokinetic/pharmacodynamic analyses E_{max} models are frequently applied.

2.3.1.2 Stochastic model

Even when subjects receive identical doses and the concentration or response is measured at the same time, they do not exhibit identical concentrations or responses. This is also true for the case when the same dose is given twice to the same subject. To account for this, the stochastic model allows for different levels of variability, called random effects:

1. interindividual variability
2. intraindividual variability
3. residual variability

All variability levels have in common that they are random and thus cannot be predicted in advance. Although it can be expected that all parameters vary between individuals and often also within the single individuum, the data might not allow to account for variability in all parameters.

2.3.1.2.1 Interindividual variability

Interindividual variability accounts for unexplained differences in the model parameters between individuals, as illustrated in equation 2-5:

$$P_i = P_{TV} + \eta_i \qquad \text{(Equation 2-5)}$$

P_i is the model parameter in the i^{th} individual. It is dependent on the typical model parameter of the population P_{TV} and the difference η_i between the individual parameter P_i and the typical parameter P_{TV}. It is assumed that the individual η_i values are independent and normally distributed with a mean of zero and a variance ω^2. The variance ω^2 is estimated by NONMEM and reflects the extent of interindividual variability in the respective model parameter. Most pharmacokinetic parameters follow a log-normal distribution rather than a normal distribution. A log-normal distribution has the advantage that it constrains the individual parameters to be greater than zero and thus avoids the estimation of negative clearance or volume of distribution values. To account for this, interindividual variability was implemented for the model parameters by an exponential model as presented in equation 2-6:

$$P_i = P_{TV} \cdot \exp(\eta_i) \qquad \text{(Equation 2-6)}$$

2.3.1.2.2 Intraindividual variability

Intraindividual variability accounts for the unexplainable differences in the model parameters of a single individual between different study occasions (136). The occasion intervals can be set arbitrarily. Most often, time intervals are chosen based on the available data. For example, in a cross-over study, the occasion intervals may correspond to the different periods. The only constrain in setting the intervals is that more than 1 measurement has to be available per time interval to differentiate between intraindividual variability and residual variability.

Intraindividual variability was implemented like interindividual variability. Exponential models were again chosen to account for intraindividual variability for the same reason as discussed above. Equation 2-7 shows how intraindividual variability was implemented:

$$P_{io} = P_{TV} \cdot \exp(\eta_i + \kappa_{io}) \qquad \text{(Equation 2-7)}$$

P_{io} is the model parameter in the i^{th} individual for the occasion interval o. P_{io} is not only dependent on P_{TV} and η_i, but also on the difference between the individual parameter P_i on different occasions. It is assumed that the individual κ_{io} values are independent and normally distributed with a mean of zero and a variance π^2. The variance π^2 was estimated by NONMEM and reflects the extent of intraindividual variability in the respective model parameter.

2.3.1.2.3 Residual variability

Residual variability accounts for the unexplainable deviation between an observed value and the corresponding model-predicted value, considering inter- and intraindividual variability. Residual variability might be due to errors in the analytical assay, errors in the amount of the administered dose, errors in the recording of the sampling or administration time, model misspecifications, and others. The residual variability can be accounted for by different types of models. Within this work, residual variability was investigated using an additive model, a proportional model, and the combination of both.

An additive residual variability model assumes that errors are additive regardless of the magnitude of the individual prediction. The corresponding mathematical equation is given in equation 2-8:

$$y_{ioj} = \hat{y}_{ioj} + \varepsilon_{ioj} \qquad \text{(Equation 2-8)}$$

In this equation, y_{ioj} is the j^{th} measured response y (concentration or effect) of the i^{th} individual at the o^{th} occasion. $\hat{y}_{ioj}$ is the corresponding response predicted by the model taking into account inter- and intraindividual variability. The random variability ε_{ioj} is the difference of the observed and the predicted response. The individual ε_{ioj} values are assumed to be normally distributed with a mean of zero and a variance σ^2. The variance characterises the extent of residual variability. An additive model is the simplest model, but it often does not reflect the residual variability which increases most often with increasing response. For these cases a proportional residual variability model is more appropriate, as in this model the residual variability is proportional to the magnitude of the individual prediction. The mathematical equation for a proportional variability model is given in equation 2-9:

$$y_{ioj} = \hat{y}_{ioj} \cdot (1 + \varepsilon_{ioj}) \qquad \text{(Equation 2-9)}$$

A third model which was investigated was a combined additive and proportional model, as presented in equation 2-10:

$$y_{ioj} = \hat{y}_{ioj} \cdot (1 + \varepsilon_{1ioj}) + \varepsilon_{2ioj} \qquad \text{(Equation 2-10)}$$

During the analysis, concentrations were log-transformed to increase the stability of the parameter estimation process (137). In consequence, the residual variability models needed to be adapted accordingly. An additive residual variability model used for log-transformed data (equation 2-11) corresponds to an exponential residual variability model for untransformed data (equation 2-12). An exponential model in turn approximately corresponds to a proportional model (equation 2-9), as $\exp(\varepsilon) = 1+\varepsilon$ for small ε.

$$\ln(y_{ioj}) = \ln(\hat{y}_{ioj}) + \varepsilon_{ioj} \qquad \text{(Equation 2-11)}$$

$$y_{ioj} = \hat{y}_{ioj} \cdot \exp(\varepsilon_{ioj}) \qquad \text{(Equation 2-12)}$$

Furthermore, the model presented in equation 2-13 used for log-transformed data approximately corresponds an additive model for untransformed data (138), assuming that $\exp(\theta) = 1+\theta$ for small values of θ.

$$\ln(y_{ioj}) = \ln\left(\hat{y}_{ioj}\right) + \sqrt{\frac{\theta^2}{\hat{y}_{ioj}^{\,2}}} \cdot \varepsilon_{ioj} \qquad \text{(Equation 2-13)}$$

Using this coding, θ was estimated whereas ε_{ioj} was fixed to 1. θ^2 corresponds approximately to the variance σ^2.

2.3.1.3 Covariate model

A covariate model accounts for the impact of a covariate on a model parameter. Parameters of a covariate model are fixed effects. A covariate model should explain the variability of the model parameter, thereby reducing its random, unexplained interindividual (sometimes also intraindividual) variability. Covariates are subject-specific factors. They can be classified in intrinsic factors such as demographics (e.g. age, sex) or laboratory values (e.g. liver enzymes) as well as extrinsic factors (e.g. formulation). Covariates can either be continuous like age or weight, or categorical like sex.

2.3.1.3.1 Continuous covariates

Continuous covariates were implemented into the model based on the graphical relationship between the individual covariate values and the individual model parameters. Most often the correlations were sufficiently described by a linear model, as presented in equation 2-14. The individual covariates cov_i were centered around their median cov_{median} leading to an easier interpretation of the estimates and to a higher numerical stability of the model:

$$P = \theta_1 + \theta_2 \cdot (cov_i - cov_{median}) \qquad \text{(Equation 2-14)}$$

The parameter P is equal to θ_1 if an individual's covariate value equals the median covariate value. If an individual's covariate changes by 1 unit from the median covariate value, P changes by θ_2 from θ_1. If more than one covariate was implemented per parameter, the different covariates were incorporated in a multiplicative way.

2.3.1.3.2 Categorical covariates

Categorical covariates were implemented in two different ways. The first possibility was to estimate separate typical parameters θ_n for each category, as demonstrated in equation 2-15.

$$P = \begin{cases} \theta_1 \text{ for category 1} \\ \vdots \\ \theta_n \text{ for category n} \end{cases} \qquad \text{(Equation 2-15)}$$

If only two categories existed the following coding could be applied (equation 2-16).

$$P = \theta_1 + \theta_2 \cdot cov_i \qquad \text{(Equation 2-16)}$$

θ_1 is the typical parameter of a subject belonging to category 1, whereas the sum of θ_1 and θ_2 is the typical parameter for subjects of category 2. cov_i is the identifier for the categories; it is 0 for subjects of category 1 and 1 for subjects of category 2. Separate categories were only tested if one category contained at least 10% of the subjects in the dataset.

2.3.2 Estimation of population parameters

NONMEM adapts the model function parameters in an iterative process so that they fit the observed data, in order to obtain parameters which describe the observations best (139-141). By using the maximum-likelihood method, NONMEM estimates the fixed (θ) and random effects (ω^2, κ^2, and σ^2) simultaneously. Likelihood is a measure of how likely it is, if the model were true with its current parameters, that the present observations would have been observed. The overall likelihood L is the product of the likelihoods of the individual observations. In order to maximise the likelihood L, NONMEM minimises −2 log likelihood. Maximizing likelihood and minimizing −2 log likelihood are essentially the same thing. However, mathematically, it is easier to take the log of a series of factors, which reduces the problem from one of multiplication to one of sums. The −2 log likelihood function that is minimised by NONMEM is presented in equation 2-17:

$$-2\log(L) = n \cdot \log(2\pi) + \sum_{i=1}^{n}\left(\log(\sigma_i^2) + \frac{(Y_i - \hat{Y}_i)^2}{\sigma_i^2}\right) \qquad \text{(Equation 2-17)}$$

Equation 2-17 consists of a constant term ($n \times \log(2\pi)$) that is dependent on the number n of observations, and of a variable term that is minimised. The squared difference between the individual observed (Y_i) and predicted ($\hat{Y}_i$) observation is weighted by the variance (σ_i^2). A penalty term ($\log \sigma_i^2$) is introduced to prevent minimisation by high variances. The variable term is called extended least square objective function and represents the 'objective function value' in NONMEM.

The −2 log likelihood equation is often difficult to solve as for most population pharmacokinetic/pharmacodynamic models no closed-form solution for $\hat{Y}_i$ and σ_i^2 exists (113,140). Thus, approximation methods are used. The most common ones are the first-

order estimation method (FO), first-order conditional estimation method (FOCE), and FOCE with interaction (FOCE-I). All three use a first-order Taylor series expansion with respect to the random effects η_i, κ_{io}, and ε_{ij}, assuming that they are normally distributed with a mean of zero. The simplest estimation method, FO, expands the nonlinear mixed-effects model as a first-order Taylor series about $\eta = 0$ and then uses a linear approximation to estimate the parameters of the nonlinear model. With FO, estimates for the fixed and random effects, but no individual model parameter estimates are obtained. These are then calculated using the maximum Bayesian estimation method as implemented in the NONMEM 'post-hoc' option (124). FOCE provides estimates of the population parameters as well as the individual random effects during each iteration step. Here, the model is expanded about the conditional estimates of the η's by a first-order Taylor series. When this algorithm is used, estimates of the population parameters as well as the random-effects parameters are obtained during each iteration step. Finally, FOCE-I calculates the objective function allowing for an interaction of ε on η. This is especially useful when a proportional residual variability model is estimated.

In general, the precision of the estimation method increases in the order FO < FOCE < FOCE-I, whereas the calculation speed decreases in that order (126,140). FO was the first method available in NONMEM (139). It performs adequately for sparse data, but it is not recommended for dense data. Today, with the increase in processing power, it is less and less used. FOCE-I was the preferred estimation method in this thesis. In Project 3a, FOCE was used instead to reduce the exceptionally long run times.

2.3.3 Model development

Model development followed a bottom up approach, starting with a simple model and expanding this model in order to allow an adequate description of the data. Whenever possible, this expansion was done in a mechanistic way, reflecting the current knowledge on linagliptin in the model. A separate modelling and simulation strategy was developed for each project, based on the objective of the project, the available data, and the *a priori* information. These individual strategies are outlined in detail in the sections of the respective projects (cf. section 2.5). An analysis plan describing the planned analysis was written prior to the analysis in Projects 1 and 3. At first, a base model was developed consisting of a structural and a stochastic model. This base model was expanded by a covariate model in Projects 1 and 3. Throughout the complete model development, log-transformed linagliptin plasma concentrations were used.

2.3.3.1 Model selection

Model selection was guided by different graphical and statistical methods. For nested models, the likelihood ratio test, a common test for statistical significance, was considered for model selection. Two models are nested if a full model can be reduced to a simpler model by setting one or more parameters to a fixed value. The difference between the objective functions (corresponding to −2·log of the ratio of likelihoods) of a full and a reduced model are approximately χ^2-distributed, with n degrees of freedom, where n is the number of parameters set to a fixed value in the reduced model. Unless stated otherwise, the full model was accepted if the drop in the objective function was >3.84 after addition of one single model parameter, corresponding to a significance level of $p < 0.05$. For the backward elimination procedure during a covariate analysis, a stricter significance level of $p < 0.001$ was applied.

Furthermore, graphical goodness-of-fit analysis (127) was performed utilizing user-written Splus scripts or Xpose (Version 3.104, Uppsala University, Uppsala, Sweden) (142). Plots showing population and individual predictions versus measured observations, as well as weighted residuals versus population predictions and versus time, amongst others, were routinely investigated. To accept a model, the data points were required to be randomly distributed around the line of identity for plots showing predictions versus observations or randomly distributed around zero for residual plots.

Another criterion was the precision of parameter estimates as reported by the relative standard error obtained from NONMEM. A relative standard error of a parameter higher than 50% indicates that this parameter might be redundant. Further selection criteria were the absence of a correlation >0.95 between model parameters, numerical stability of the model, and the plausibility of the parameter estimates.

2.3.3.2 Development of the base model

2.3.3.2.1 Structural model

The aim of the structural model development was to find the model that best described the typical pharmacokinetic or pharmacodynamic profile of linagliptin. If possible, the structural model was to be mechanistic, reflecting the known characteristics of linagliptin. The model selection was based on the criteria described in section 2.3.3.1. The structural pharmacokinetic models were parameterised in terms of clearances and volumes, rather

than rate constants, in order to allow a meaningful implementation and interpretation of interindividual variability and potential covariate effects. The strategy of the development of the structural model is presented separately for the individual projects in section 2.5.

2.3.3.2.2 Stochastic model

The aim of the development of the stochastic model was to characterise the variability within the pharmacokinetics or pharmacodynamics of linagliptin. It was tested whether the residual variability was best described by either an additive, a proportional, or a combined (additive and proportional) model. Interindividual variability was tested sequentially in all model parameters and retained when it improved the data description. As described in section 2.3.1.2.1, interindividual variability was implemented using exponential random effect models. At first, no covariance between the different interindividual variabilities was estimated. If correlations between interindividual variabilities were found by graphical analysis, covariance was implemented and the correlation coefficient was estimated. Intraindividual variability was only explored on selected model parameters.

2.3.3.3 Development of the covariate model

The aim of the covariate analysis was to identify covariates affecting the pharmacokinetics or pharmacodynamics to an extent that their impact may be clinically relevant. The covariate analysis was performed in a stepwise manner: As a first step, a graphical exploratory analysis was performed, then a generalised additive modelling (GAM) analysis was conducted, and finally the covariates suggested by these procedures as well as some pre-selected covariates were tested in NONMEM using the forward inclusion backward elimination procedure.

2.3.3.3.1 Explorative graphical investigation

First, the correlation between the individual covariate values and individual parameter estimates were explored graphically. For continuous covariates, the medians of the individual values of the covariate of interest were plotted against the individual η values. The relationship between categorical covariates and individual η values were investigated using box-whisker plots.

2.3.3.3.2 Generalised additive modelling

In a next step, a GAM analysis was conducted within Splus to statistically investigate the correlation between the covariates and the individual parameter estimates. The GAM

analysis was introduced by Mandema *et al.* (143), to identify possible covariates before further testing in NONMEM. It is a multiple regression analysis in which the influence of different covariates is tested separately per model parameter. The GAM analysis follows a stepwise addition/deletion method. Addition of a covariate is possible through either a linear function or a spline function with one degree of freedom (df). At each step, the model is changed by addition or deletion of the single covariate term resulting in the greatest decrease in the Akaike information criterion (AIC) until a minimum AIC is reached. Equation 2-18 shows how the AIC was calculated. The AIC is dependent of the number of observations n, the number of parameters of the fitted model k, and the weighted least squares wss:

$$AIC = n \cdot \ln(wss) + 2k \qquad \text{(Equation 2-18)}$$

The GAM analysis was performed using the difference between the median individual covariate value and the overall median covariate value for continuous covariates or the respective pre-defined categories for categorical covariates.

2.3.3.3.3 Forward inclusion backward elimination in NONMEM

As mentioned above, the covariates tested further within NONMEM were selected based on the correlation between covariates and individual parameter estimates (exploratory analysis) (144), as well as the results of the GAM analyses (143). Furthermore, the correlation between covariates was considered when selecting the covariates to be tested in NONMEM. Some covariates that were of special interest were pre-selected to be tested in NONMEM, independently of the results of the exploratory analysis or GAM analysis. These covariates are specified under the respective sections in the method part.

The covariate analysis was performed using the forward inclusion and backward elimination procedure (145,146). In the first step of the forward inclusion, all covariates pre-selected as described previously were evaluated one by one in NONMEM with a function that seemed most appropriate from the plots of covariate values versus parameters. Then, the covariates showing a decrease of less than 3.84 in the objective function (OBJF) value (probability (p) ≤ 0.05, chi square distribution (χ^2), 1 df) were removed. The remaining covariates were ranked, starting with the covariate that generated the largest drop in the OBJF value during forward inclusion. In the next step of the forward inclusion, the covariates were added to the base model sequentially in their ranking order. If the addition of a covariate resulted in a drop of the OBJF value of at least 3.84 ($p \leq 0.05$,

χ^2, 1 df), it was retained; otherwise it was removed. This was repeated until the full model was obtained. The forward inclusion of parameter-covariate relationships was followed by a backward elimination, which is essentially the reverse of the forward inclusion. The covariates were removed individually from the full covariate model. The covariates were again ranked according to the increase in the OBJF. If the increase in the OBJF was less than 10.8 points ($p \leq 0.001$, χ^2, 1 df) the corresponding covariate was removed and a new rank order was established based on removing the remaining covariates separately. This was continued until no more terms could be dropped.

In addition to reducing the OBJF, a covariate that was to be retained should explain part of the variability in the model parameters, be physiologically plausible, and have a clinically relevant impact on the pharmacokinetics or pharmacodynamics. If this was not the case, a covariate might not be retained in the final model.

2.3.4 Model evaluation

Different techniques are available to test the performance of a model (115). In this thesis, the choice of evaluation methods was limited by processing power. Computer intensive approaches such as re-estimation of simulated or bootstrapped datasets were not considered. Instead, internal methods based on simulations were applied. The method which was chosen for a given project is outlined in the respective sections.

2.3.4.1 Visual predictive check (VPC)

When a visual predictive check (147) was performed, the response-time profiles of 1,000 subjects were simulated per dose group based on the model to be investigated including interindividual, intraindividual and residual variability as well as the dosing and sampling scheme of the study. The simulations were conducted using the Trial Simulator software (Pharsight Corporation, Version 2.1.2, St. Louis, MO, USA). The median and the 5^{th} and 95^{th} percentiles of the simulated concentrations at every time point were calculated per dose group and plotted against the observed concentration-time profile. The model was considered adequate in describing the observations if most of the data points were within the 5^{th} to 95^{th} percentile interval and were equally distributed around the median.

2.3.4.2 Posterior predictive check

For a posterior predictive check (140,148), one or more variables of interest were defined, which were of importance for the response and which could be directly obtained from the

original dataset, without the use of the model. One thousand new datasets with the same number of patients, the same covariates, and the same dosing history and sampling schedule as the original dataset were simulated in NONMEM, based on the final model. In the posterior predictive checks performed in this thesis the interindividual, intraindividual as well as the residual variability of the model were taken into account, but not the uncertainty in the parameter estimates. The median variable of interest was calculated for each simulated dose group. The distributions of the medians over the 1,000 simulations were presented as histograms and were compared to the observed median, per dose group. For the model to be accepted, the observed median of the variable of interest was to lie within the 90% confidence interval of the simulations.

2.4 Statistical data analysis

Descriptive statistics was applied to quantitatively summarise the contents of the NONMEM datasets as well as the results of the pharmacometric analyses. For categorical values, the mode (most frequently occurring number in a list) and frequency distributions were used. For continuous values, the following measures were used to describe the central tendency, or the average of a list of values.

- Arithmetic mean: sum of all numbers of a list divided by the number of items in the list
- Median: middle number of a group when the numbers were ranked in order
- Geometric mean (gMean): exponential function of the arithmetic mean of the natural logarithms of all numbers of a list

The statistical dispersion, or variability of a list of continuous values were illustrated by the following parameters.

- Range: difference between the highest and lowest value
- Variance: sum of squares of the deviations of the numbers of a list from their mean divided by the number of items minus 1 of the list
- Standard deviation (SD): square root of the variance
- Coefficient of variation (CV%): ratio of the standard deviation to the arithmetic mean
- Geometric coefficient of variation (gCV): square root of the antilog of the variance of log-transformed data minus one times 100%
- 5^{th}, 95^{th} percentile: values below which 5% or 95% of the observations fall, respectively

2.5 Project characteristics

2.5.1 Project 1: Population pharmacokinetic/pharmacodynamic analysis of linagliptin in type 2 diabetic patients

2.5.1.1 Objectives

The pharmacokinetics of linagliptin is nonlinear in the therapeutic dose range (1–10 mg) with a less than dose-proportional increase in exposure. Nonlinear pharmacokinetics can be caused by several mechanisms as discussed in section 4.1.1. Linagliptin exhibited concentration-dependent plasma protein binding in the low nanomolar range (<100 nM). Common plasma proteins like albumin or α-glycoprotein would not yet be saturated at these low concentrations (149). This led to the hypothesis that concentration-dependent binding of linagliptin to its target enzyme, DPP-4 might be responsible for the nonlinear pharmacokinetics of linagliptin.

Thus, the objectives of Project 1 were (a) to characterise the nonlinear pharmacokinetics of linagliptin and the relationship between linagliptin plasma concentration and the DPP-4 inhibition in type 2 diabetic patients and (b) to test the hypothesis that concentration-dependent binding of linagliptin to its target, DPP-4 is responsible for its nonlinear pharmacokinetics in humans. A population pharmacokinetic/pharmacodynamic model incorporating concentration-dependent protein binding was to be developed, describing the nonlinear pharmacokinetics and the DPP-4 inhibition in a semi-mechanistic way. In addition, an initial covariate analysis was carried out to find patient characteristics explaining part of the individual variability in the model parameters.

The final population pharmacokinetic/pharmacodynamic model formed the basis for several simulations contributing to a better understanding of the nonlinear pharmacokinetics of linagliptin and its effects on DPP-4 activity in humans.

2.5.1.2 Study design

Two phase IIa studies with 47 and 77 type 2 diabetic patients (study I (104) and study II) were included in the analysis. Both trials were randomised, placebo-controlled, double-blind multiple dose studies with a parallel group design. Subjects received either placebo, 1, 2.5, 5, or 10 mg linagliptin as a powder in the bottle formulation once daily over twelve days of treatment (study I) or placebo, 2.5, 5, or 10 mg linagliptin as a tablet once daily over 28 days (study II). The studies were conducted at several centres throughout Europe.

Ethics committees reviewed and approved the study protocols and the study was conducted within the ethical standards established by the Declaration of Helsinki (150) and in accordance with applicable regulatory requirements.

Plasma samples for full linagliptin plasma concentration-time and DPP-4 activity-time profiles were collected after the first and the last linagliptin administration in each study. Trough samples were taken at the schedule specified for each study. Due to the long terminal half-life of linagliptin, plasma concentration and DPP-4 activity were measured until 8 or 15 days after the last administration, respectively. The exact sampling schedules are given in the Appendix, Table 3. Linagliptin plasma concentrations and plasma DPP-4 activity were determined as described in section 2.1.

In study I, linagliptin was administered under supervision and date and time of each administration were recorded in the case report form (CRF) by clinic personnel. In study II, linagliptin was administered under supervision during the in-house stay (days 1–6 and days 26–28) and date and time of each administration were recorded in the CRF by clinic personnel. Date and time of tablet intake at home was entered by the patient in a patient's diary and transferred into the CRF by the clinic personnel.

The covariates listed in section 2.2.1.2 were investigated. In study I, demographic characteristics were determined at screening. Laboratory values were measured at screening, optionally at a training visit if screening of safety measurements was done more than 14 days ago and at the following days: −1, 1, 2, 3, 6, 10, 12, 13, 16 and during the end-of-study evaluation (days 20–28). Fasting plasma glucose was determined daily on days −1–13. Pre-dose DPP-4 activity was measured on day 1 before the first administration of linagliptin. In study II, demographic characteristics were determined at screening; weight was also measured on day 30. Laboratory values were measured at screening, at the training visit and at the following days: −1, 2, 6, 12, 19, 26, 28, 30, 36, as well as during the end-of-study evaluation (between days 43−50). Fasting plasma glucose was determined at days –1, 1, 2, 6, 12, 19, 26, 27, 28, 29, 30, 33, 36, 39, 41, and 43. Pre-dose DPP-4 activity was measured at day 1 before the first administration of linagliptin.

2.5.1.3 Modelling strategy

The analysis was performed in a stepwise manner. First, the plasma concentration-time profiles were analysed. Due to the complexity of the structural model it was investigated whether the proposed pharmacokinetic model was identifiable. Finally, DPP-4 activity was

added to the dataset and plasma concentration- and DPP-4 activity-time profiles were analysed simultaneously.

Pharmacokinetic base model. Initially, linear one-, two-, and three-compartment models were tested. To describe the less than dose-proportional increase in exposure, different models were investigated including saturable absorption, which may be caused by saturation of influx transporters, or saturable protein binding. For the protein binding model, the influence of concentration-dependent binding in the central compartment as well as a second binding partner located either in the central or in the peripheral compartment were tested. The second binding partner may reflect tissue DPP-4 (either with or without a distribution process) in contrast to plasma DPP-4.

The way the binding was implemented into the model was derived from literature (151-155). All binding processes were considered to be reversible and competitive. When concentration-dependent binding was assumed at different sites, different amounts of binding partners were estimated but their binding affinities to linagliptin were assumed to be identical. Quasi-equilibrium conditions were assumed for the binding to simplify the estimation, i.e. the binding equilibrium was assumed to be reached faster than all other processes.

Linagliptin was assumed to bind with a high affinity to a binding partner that is present in low amounts and thus has a low capacity for linagliptin. It was further assumed that only linagliptin that was not bound to the high affinity, low capacity binding partner could distribute between the compartments and be eliminated. The concentration of linagliptin bound to the high affinity, low capacity binding partner is referred to as ‘concentration bound’ throughout the thesis. The concentrations of unbound linagliptin and linagliptin linearly bound to other proteins were not distinguishable by the model and thus were regarded as a single concentration, referred to as ‘concentration unbound’. The observed total linagliptin plasma concentration was the sum of unbound linagliptin and linagliptin linearly bound to plasma proteins, as well as the concentration of linagliptin specifically bound to a soluble binding partner in the central compartment.

As only linagliptin plasma concentration-time profiles after oral administration were available in the studies, only relative bioavailabilities could be estimated. Intraindividual variability was tested on all parameters with interindividual variability (bioavailability, rate of absorption, concentration of the binding partner in the central compartment) and on clearance. For intraindividual variability two occasions were defined. The first occasion

included the single-dose profile and the trough plasma concentrations (i.e. concentration at the end of the dosing interval, taken directly before the next administration C_{trough}) until halfway through treatment, followed by the second occasion including the C_{trough} levels of the second half of treatment and the steady-state profile for each study.

Identifiability of the pharmacokinetic model. The pharmacokinetic base model development revealed that a two-compartment model with concentration-dependent protein binding in the central and the peripheral compartment described the plasma concentration-time profiles best. As only total linagliptin plasma concentrations were available, it was unclear whether the data contained sufficient information to identify all model parameters of the complex model structure. Thus, four different approaches were used to investigate whether the model structure with concentration-dependent binding in the central and the peripheral compartment, could be identified given the study designs of Project 1. These investigations were performed based on a preliminary pharmacokinetic model (Table 3-1).

Initially, the influence of the amounts of both binding partners, possibly reflecting plasma and tissue DPP-4, on the plasma concentration-time profiles was evaluated by two approaches. In the first approach, the concentration-time profiles of multiple daily doses of 1, 5, and 10 mg linagliptin were simulated assuming varying amounts of central or peripheral binding partners (originally estimated amount ±50%). In the second approach, log-likelihood profiling was performed for the parameters reflecting the amounts of central and peripheral binding partner.

Similarly to the method used by Waterhouse *et al.* (156), it was explored in the third approach whether NONMEM correctly identified the presence or absence of the peripheral binding. For this method, concentrations were simulated based on the design of study I and two different scenarios. In scenario S1 it was assumed that concentration-dependent binding only occurred in the central compartment. In scenario S2 concentration-dependent binding was assumed in both compartments, central and peripheral. The underlying model parameters used for the simulations were obtained from initial estimations of a model with binding only in the central compartment (M1) and a model with binding in the central and the peripheral compartment (M2) using the original dataset. In the next step, each simulated dataset was re-estimated assuming binding either only in the central compartment (M1) or in both compartments (M2). For each dataset, the performance of the two nested models was compared using the objective function value. Only NONMEM runs reported to have converged successfully were evaluated.

The last method investigated the identifiability of the model using the Fisher information matrix given the study designs of Project 1 as well as a study design where the treatment group with the lowest dose (1 mg linagliptin once daily) was missing. The Fisher information matrix was determined with the WinPOPT software (Version 1.1 (beta), University of Otago, New Zealand) (157). The Fisher information matrix is a measure of the amount of information that is available in a certain model (structural, stochastic) and study design (number of patients, sampling time points, dose groups) (156) to estimate a model parameter. The relative standard errors of the model parameter estimates were determined as the square roots of the diagonal elements of the inverse of the Fisher information matrix (157). In addition, the determinant was investigated as the summary measure of the Fisher information matrix.

Pharmacokinetic/pharmacodynamic base model. To describe DPP-4 activity, standard drug response models (E_{max} and sigmoid E_{max} model) relating the estimated total linagliptin plasma concentration (C_{tot}) to the DPP-4 activity were tested first. These models are described in equations 2-19 and 2-20. The maximum effect parameter E_{max} represents the maximum DPP-4 inhibition in percent. The EC_{50} value is the total linagliptin concentration that leads to half-maximum DPP-4 activity. In the sigmoid E_{max} model the sigmoid character of the curve is determined by the Hill coefficient n.

$$\text{DPP-4 activity} = 100 - \frac{E_{max} \cdot C_{tot}}{C_{tot} + EC_{50}} \qquad \text{(Equation 2-19)}$$

$$\text{DPP-4 activity} = 100 - \frac{E_{max} \cdot C_{tot}^{\,n}}{C_{tot}^{\,n} + EC_{50}^{\,n}} \qquad \text{(Equation 2-20)}$$

Additionally, more mechanistic models were investigated based on the assumption that DPP-4, the target of linagliptin, was its binding partner in the population pharmacokinetic model. These models, described in equations 2-21, 2-22 and 2-23, relate the plasma DPP-4 activity to either the unbound plasma linagliptin concentration (CU_{plasma}) or the plasma DPP-4 occupancy, i.e. the fraction of DPP-4 molecules bound to linagliptin, both estimated by the population pharmacokinetic model:

1. E_{max} model using CU_{plasma}. In this model, the parameter E_{max} specifies the maximum DPP-4 inhibition in percent. The EC_{50} value reflects the unbound linagliptin concentration that leads to half-maximum DPP-4 activity.

$$\text{DPP - 4 activity} = 100 - \frac{E_{max} \cdot CU_{plasma}}{CU_{plasma} + EC_{50}} \qquad \text{(Equation 2-21)}$$

2. Occupancy model. This model assumes a proportional relationship between the plasma DPP-4 activity and the plasma DPP-4 occupancy with linagliptin as ligand. The plasma DPP-4 occupancy can be calculated from the parameters of the pharmacokinetic model in two ways: (a) by dividing the plasma concentration of linagliptin bound to DPP-4 (CB_{plasma}) by the concentration of binding partner in the central compartment ($B_{max,C}$) (b) by dividing CU_{plasma} by the sum of CU_{plasma} and the dissociation constant K_d (see equation 2-22). The parameter E_{max} represents the maximum DPP-4 inhibition. The dissociation constant K_d is a measure of the affinity of the binding between DPP-4 and linagliptin and is derived from the population pharmacokinetic model.

$$\text{DPP - 4 activity} = 100 - E_{max} \cdot \frac{CB_{plasma}}{B_{max}} = 100 - E_{max} \cdot \frac{CU_{plasma}}{CU_{plasma} + K_d} \qquad \text{(Equation 2-22)}$$

The occupancy model is mathematically very similar to the E_{max} model using CU_{plasma} (see equations 2-21 and 2-22). The only difference is that instead of estimating an EC_{50} value, the dissociation constant K_d of the population pharmacokinetic model is used. Pharmacokinetic and pharmacodynamic parameters were estimated simultaneously in all investigated models.

Covariate model. Based on the population pharmacokinetic/pharmacodynamic model, a covariate analysis was performed. All covariates listed in section 2.2.1.2, except metformin co-treatment, were investigated on all parameters that showed interindividual variability. Metformin co-treatment could not be tested as concomitant antidiabetic treatments were excluded by the designs of studies I and II. Although no inter-individual variability was introduced for clearance and the volumes of distribution, the following covariates were pre-defined to be tested in NONMEM: Creatinine clearance and the liver enzymes alanine transaminase and gamma-glutamyl transferase were investigated for their impact on clearance, as well as weight was pre-defined to be tested on the volumes of distribution. To avoid individual outliers in the covariates, the median covariate value per subject was used for covariates measured more than once.

2.5.1.4 Model evaluation

For the evaluation of the final population pharmacokinetic/pharmacodynamic model, a visual predictive check was performed as described under section 2.3.4.1 for linagliptin plasma concentration and DPP-4 activity.

2.5.1.5 Simulation strategy

The final population pharmacokinetic/pharmacodynamic model of Project 1 was used to illustrate the impact of the target-mediated drug disposition on the pharmacokinetics of linagliptin. These simulations were performed using the Berkeley Madonna software (Version 8.0.4, University of California, Berkeley, CA, USA). First, the total linagliptin plasma concentration-time profile was to be compared to the fraction of linagliptin specifically bound to plasma DPP-4. This simulation was conducted for a once daily dosing scheme of 5 mg linagliptin. In a second simulation, the typical profile of plasma occupancy of DPP-4 with linagliptin versus time was investigated for different dose groups (1, 2.5, 5, and 10 mg) assuming once daily dosing.

2.5.2 Project 2: Clinical trial simulations to support the development of linagliptin

The overall aim of the following four simulation projects was to apply the model built in Project 1 to support the clinical development of linagliptin.

2.5.2.1 Project 2a: Simulation to evaluate an equivalent dose for a twice-daily administration

2.5.2.1.1 Objectives

A fixed dose combination was planned in which linagliptin was to be given together with the anti-diabetic drug metformin. As metformin is generally taken twice daily, the fixed dose combination should also adhere to this schedule. Thus, the question was which dose of linagliptin, when given twice daily, would result in a bioequivalent extent of steady-state exposure and similar steady-state DPP-4 inhibition compared to a 5 mg once daily dosing scheme. Due to the nonlinearity, this could not easily be answered without resorting to model-based simulations. Thus, the objective for Project 2a was to evaluate by simulations an equivalent dose for a twice-daily linagliptin administration to be tested in a relative bioequivalence study.

2.5.2.1.2 Simulation strategy

The base population pharmacokinetic/pharmacodynamic model of Project 1 was used for the simulation. This was done under the following assumptions: (a) The pharmacokinetics and the relationship between pharmacokinetics and pharmacodynamics are not different between healthy volunteers and type 2 diabetic patients. (b) The tablet formulation used in the relative bioequivalence study was not different with respect to exposure to the formulations used in Project 1.

Firstly, population mean profiles were simulated using the Berkeley Madonna software assuming that 1, 1.5, 2, and 2.5 mg linagliptin were given twice daily. The area under the plasma concentration-time curve of one day at steady-state ($AUC_{24h,SS}$) was calculated by directly integrating the concentration-time curves over 24 h. These values were then compared to the area under the plasma concentration-time curve at steady-state of one

dosing interval ($AUC_{\tau,SS}$) simulated for 5 mg linagliptin given once daily. The respective DPP-4 activity-time profiles were investigated graphically.

Secondly, a clinical trial simulation was performed based on the following study design. The study was assumed to have a randomised, two-way change-over design with 5 mg linagliptin once daily (treatment A) and the dose determined in simulation 1 twice daily (treatment B). Both treatments were to be administered over seven days until steady-state with no wash-out period in between them. Thus, subjects receiving sequence AB first get treatment A and then treatment B, and vice versa for sequence BA. The number of healthy volunteers included in the study was assumed to be 16. Blood sampling was to take place at the last day of each treatment period, i.e. days 7 and 14, respectively. On both days, the following sampling schedule for linagliptin plasma concentration and DPP-4 activity was used: 0, 0.25, 0.5, 0.75, 1, 1.5, 2, 3, 4, 6, 8, 12, 12.25, 12.5, 12.75, 13, 13.5, 14, 15, 16, 18, 20, and 24 h after the first administration of linagliptin at the respective day. This study design was simulated 1,000 times using the software Trial Simulator.

For each simulated individual and treatment, the $AUC_{24h,SS}$ was calculated using the lin-log computation implemented in Trial Simulator. Then, the geometric means of $AUC_{24h,SS}$ and the gCV were calculated per sequence, and per treatment for each of the 1,000 simulated studies. In the next step, the mean of the gMean $AUC_{24h,SS}$ values and their gCVs of the 1,000 simulated studies were calculated by sequence and treatment. Based on this, the distribution of the $AUC_{24h,SS}$ were compared per sequence, to evaluate whether the treatment period of seven days was long enough, and per treatment to investigate whether the treatments were equal. Finally, the gMean ratio between $AUC_{24h,SS}$ of treatment A and treatment B and its 90% confidence interval were determined for the 1,000 simulated trials and compared to the acceptance interval of 0.80–1.25.

2.5.2.2 Project 2b: Simulation to evaluate the impact of impaired clearance

2.5.2.2.1 Objectives

During the clinical development of linagliptin the question appeared whether patients with renal impairment should be excluded in phase IIb studies. In order to support this decision, alongside other criteria, the impact of an impaired clearance on the exposure of linagliptin was to be investigated. Again, the nonlinear pharmacokinetics made predictions without a model difficult.

2.5.2.2.2 Simulation strategy

The typical linagliptin plasma concentration-time profiles were simulated using the Berkeley Madonna software. The simulations were based on the pharmacokinetic/pharmacodynamic base model developed within Project 1.

The fraction of linagliptin excreted in urine at steady-state was only 3–6% after oral administration of 1–10 mg linagliptin. With higher single oral doses, the fraction excreted increased up to 33% in the 600 mg dose group. In animals the fraction of linagliptin-related radioactivity excreted in urine, which consisted mainly of parent compound, was less than 25% after intravenous administration (cf. section 1.3.2). Based on these results, it was assumed that in the therapeutic dose range renal clearance accounts for a maximum of ~25% of the overall clearance. In addition, a 50% reduction of the overall clearance was simulated to cover a worst case scenario.

For the simulation, it was assumed that 5 mg linagliptin were administered once daily to patients having either 100%, 75%, or 50% of the original clearance of unbound linagliptin estimated within Project 1. The $AUC_{\tau,SS}$ values were calculated by directly integrating the simulated plasma concentration-time profiles using the Berkeley Madonna software. The simulated increase in steady-state exposure ($AUC_{\tau,SS}$) corresponding to a 50% and a 25% decrease in clearance was calculated.

2.5.2.3 Project 2c: Simulation of a design for a dose-proportionality study

2.5.2.3.1 Objectives

A study was planned to assess the dose-proportionality of different dosage strengths of linagliptin tablets (1, 2.5, and 5 mg) at steady-state using the final formulation. Linagliptin was to be given once daily to healthy volunteers in a randomised, three-period cross-over study. Due to the long terminal half-life of linagliptin a change-over design, without any washout between the periods was preferred. The objective of Project 2c was to determine by simulation the optimal treatment duration until a steady-state profile could be obtained within such a change-over design.

2.5.2.3.2 Simulation strategy

The simulations were based on the final population pharmacokinetic/pharmacodynamic model developed in Project 1. In the planned dose-proportionality study the final tablet

formulation was to be used. It was assumed that the final formulation used in this study was not different with respect to exposure to the earlier tablet formulations used in study II. Furthermore, it was assumed that there is no difference in the pharmacokinetics between healthy volunteers and type 2 diabetic patients.

Under these assumptions, a randomised three-way change-over design with treatment groups of 1, 2.5, and 5 mg linagliptin given once daily was simulated using the Berkeley Madonna software. Initially, a treatment period of seven days was tested. It was graphically investigated whether steady-state was achieved for all treatments in all scenarios.

2.5.2.4 Project 2d: Description and steady-state simulation of the drug-drug interaction between linagliptin and ritonavir

2.5.2.4.1 Objectives

A phase I drug-drug interaction study was performed to investigate whether the treatment with the P-glycoprotein and CYP3A4 inhibitor ritonavir had an effect on the pharmacokinetics of linagliptin. In this drug-drug interaction study, linagliptin was administered as a single dose. The objective of Project 2d was to predict the steady-state profile of linagliptin with ritonavir comedication.

2.5.2.4.2 Study design

The study was performed as an open-label, randomised, two-way crossover trial. Two treatments (test and reference) were tested. During the test treatment, volunteers received 200 mg ritonavir twice daily for three days, plus a single oral dose of 5 mg linagliptin on the second day of the ritonavir treatment. During the reference treatment, volunteers received 5 mg linagliptin only. The sequence of treatments was assigned in a random order. The two different treatments were separated by a washout period of at least 35 days. Twelve healthy volunteers were included in the study. The study was conducted at the Boehringer Ingelheim Human Pharmacology Centre in Biberach an der Riß, Germany. Ethics committee reviewed and approved the study protocols and the study was conducted within the ethical standards established by the Declaration of Helsinki (150) and in accordance with applicable regulatory requirements.

Linagliptin plasma concentrations were determined as described in section 2.1.1 and collected at the following time points of each treatment arm: pre-dose, 15, 30, 45 min, and 1.0, 1.5, 2.0, 3.0, 5.0, 7.0, 9.0, 10.5, 12.0, 24.0, 48.0, 72.0, and 96.0 h after the linagliptin

administration. Compliance was ensured by administration of all study medication under supervision of the investigating physician or a designee. The only covariate tested within Project 2d was comedication with ritonavir.

2.5.2.4.3 Modelling strategy

For a reliable prediction of the steady-state profile the semi-mechanistic model developed in Project 1 was to be used. In Project 2d, only plasma linagliptin concentrations after a single dose of 5 mg linagliptin were available. This was not sufficient to support the complex target-mediated drug disposition model. Therefore, the previously developed base model was used as a framework for the current analysis. The model of Project 1 was developed for type 2 diabetic patients, but so far no major differences in the pharmacokinetics of linagliptin between healthy volunteers and patients are known.

The model development was performed in three steps. Firstly, it was investigated which typical model parameters of the Project 1 model (called M3 from here on) had to be adapted to describe the linagliptin concentrations of the reference treatment. In the second step, the impact of the ritonavir interaction on all typical model parameters of linagliptin was explored. Finally, the interindividual variability of the model parameters was investigated.

Firstly, all typical model parameters were fixed to M3 to investigate whether M3 can describe the reference treatment. Then, only one parameter at a time was estimated while all other parameters were fixed to M3. Based on the drop of the OBJF, it was decided which parameter adaptation resulted in the best description of the observations. This was repeated until no further estimated parameter led to a decrease in the OBJF of more than 3.84 points. During the entire procedure the interindividual variability was fixed to 0. The adapted model is referred to as M4.

The next step was to determine the parameter(s) that needed to be adapted to describe the linagliptin concentrations when linagliptin was coadministered with ritonavir. Test and reference treatment were analysed together. First, the typical model parameters were fixed to M4 to investigate whether the adapted model could describe the test treatment. Then, only one parameter was estimated separately for the test treatment, while all other parameters were fixed to M4. Based on the drop of the OBJF it was decided which of the separately estimated parameters resulted in the best description of the test treatment. This

procedure was again repeated until no additional estimated parameter led to a decrease in the OBJF of more than 3.84 points. This adapted model is called M5.

Insufficient information was available to estimate all typical model parameters together. Thus, interindividual variability was estimated by fixing all typical model parameters to M5. Interindividual variability was tested sequentially on all model parameters keeping the variability resulting in the best description of the individual profiles. This procedure was repeated until no further improvement was achieved by adding interindividual variability.

2.5.2.4.4 Model evaluation

The model was evaluated using visual predictive checks and posterior predictive checks as described in section 2.3.4. For the posterior predictive checks C_{max} and the area under the plasma concentration-time curve from time point 0 to infinity ($AUC_{0\text{-}inf}$) were used as variables of interest.

2.5.2.4.5 Simulation strategy

The steady-state concentration-time profiles for both treatments, linagliptin alone and linagliptin in combination with ritonavir, were to be simulated based on the final population pharmacokinetic model of Project 2d. Firstly, the typical model parameters were used to simulate the mean population profiles for a multiple dosing of linagliptin with and without ritonavir comedication. It was assumed that 5 mg of linagliptin was given once daily over seven days for both treatments. The simulations were performed with the Trial Simulator software. It was assumed that a full profile was taken at day 1 and day 7 with samples pre-dose, 15, 30, 45 min, and 1.0, 1.5, 2.0, 3.0, 5.0, 7.0, 9.0, 10.5, 12.0, and 24.0 h after linagliptin administration. In between, daily C_{trough} levels were simulated. Secondly, 1,000 profiles were simulated based on the specified study design and the population pharmacokinetic model including the interindividual and residual variability. These simulated 1,000 profiles were used to calculate the gMean of the area under the plasma concentration-time curve from time point 0 to 24 hours ($AUC_{0\text{-}24h}$) and $AUC_{\tau,SS}$, and the gMean of $C_{max,SD}$ and $C_{max,SS}$ for a once daily treatment with 5 mg linagliptin, with and without ritonavir comedication.

2.5.3 Project 3: Covariate analysis

2.5.3.1 Project 3a: Pharmacokinetic covariate analysis

2.5.3.1.1 Objectives

The objective of Project 3a, extending Project 1, was to characterise the nonlinear pharmacokinetics of linagliptin in a larger patient population with the main focus on investigating the impact of weight, sex and age on the pharmacokinetics of linagliptin. For these covariates, no dedicated phase I studies were planned. In addition, other covariates of clinical relevance for the pharmacokinetics of linagliptin were to be identified.

2.5.3.1.2 Study design

Project 3a was based on four clinical studies: two phase IIa studies with intensive pharmacokinetic sampling schemes and two phase IIb studies with sparse pharmacokinetic sampling. The phase IIa studies were also used in Project 1 and are described in section 2.5.1.2 in detail. A description of the phase IIb studies is given in the following.

The phase IIb studies (study III and study IV) were both randomised, double blind, placebo-controlled studies, each with four parallel treatment arms. In study III, 0.5, 2.5, or 5 mg linagliptin or placebo were administered once daily over twelve weeks. In study IV, 1, 5, or 10 mg linagliptin given once daily were tested versus placebo as add-on treatment to metformin. The treatment duration was again twelve weeks. The tablet formulation used in both studies was identical but differed from that investigated in study II. Table 2-2 summarises the main characteristics of the four studies used within Project 3a.

Table 2-2 Summary of studies used in Project 3

Study	Phase	Formulations	Doses [mg]	Duration	Number of patients treated with linagliptin (planned)	Add-on to metformin
I	IIa	Powder in Bottle	1, 2.5, 5, 10	12 days	36	No
II	IIa	Tablet 1	2.5, 5, 10	4 weeks	60	No
III	IIb	Tablet 2	0.5, 2.5, 5	12 weeks	225	No
IV	IIb	Tablet 2	1, 5, 10	12 weeks	225	Yes

The studies were conducted at several centres throughout Europe, North America, and Australia. Ethics committees reviewed and approved the study protocols and the studies were conducted within the ethical standards established by the Declaration of Helsinki (150) and in accordance with applicable regulatory requirements.

The sampling schemes of the phase IIa studies I and II are presented in section 2.5.1.2. In studies III and IV, the blood samples of linagliptin plasma concentration measurements were taken at four visits (definitions see below) – always before, 1 h (±0.5 h), and 2 h (±1 h) after the linagliptin administration. In addition, one sample was taken at a follow-up visit. In both phase IIb studies, some flexibility was allowed in scheduling the visits according to the following time windows. The time interval between the first (first linagliptin administration) and second visit was 28–35 days (i.e. 4–5 weeks), between the second and the third visit 28–35 days (i.e. 4–5 weeks), between the third and the fourth visit 28–35 days (i.e. 4–5 weeks), and between the fourth and the follow-up visit 14–21 days (i.e. 2–3 weeks). The linagliptin plasma concentrations were determined as described in section 2.1.1.

In both phase IIb studies, the patients had to record the actual administration date and time of the last three doses before a clinic visit on the patient visit card; this information was transferred to the CRF by clinic personnel. The actual date and time of administration at the clinic visit was recorded in the CRF by the clinic personnel.

The demographic characteristics were determined at screening, and weight was also measured at visits 1 and 4. The laboratory values were measured at screening, at the beginning of the placebo run-in, and at the visits 1, 2, 4, and the follow-up visit. Fasting plasma glucose was determined at all clinic visits. Pre-dose DPP-4 activity was measured at visit 1 before the first administration of linagliptin.

2.5.3.1.3 Modelling strategy

The plasma concentrations of the phase IIb studies were to be analysed using the target-mediated drug disposition model developed in Project 1 to allow a meaningful interpretation of the covariates. The sparse sampling scheme performed in phase IIb did not allow estimating all parameters of the model. Thus, the datasets from the phase IIa and IIb studies were combined to perform a well-founded covariate analysis based on a physiologically plausible model. The base population pharmacokinetic model previously developed in Project 1 served as a starting point for the modelling analysis.

Base model. At first, it was tested whether the population pharmacokinetic model of Project 1 could describe the plasma concentrations of studies III (phase IIb mono-therapy study) and IV (phase IIb add-on to metformin study). All model parameters were fixed to the population pharmacokinetic model of Project 1 and individual Bayesian estimates for both studies were obtained. The distribution of the Bayesian estimates around the typical parameters and the description of the concentration-time profiles were investigated separately per study.

Then, the model parameters were estimated based on all four studies. A possible effect of metformin treatment on the linagliptin pharmacokinetics was investigated. Necessary adjustments were implemented into the model. In addition to the variability already implemented in the population pharmacokinetic model of Project 1 (i.e. interindividual variability on relative bioavailability, absorption rate constant, and concentration of binding partner in the central compartment, intraindividual variability on relative bioavailability), interindividual variability on clearance, and the volumes of distribution were investigated. Because of the sparse data, no further intraindividual variability was tested. For the phase IIa studies, the occasions for intraindividual variability were defined in section 2.5.1.3. For the phase IIb studies, every visit in which linagliptin concentrations were measured was handled as a separate occasion, visit 4 and the follow-up visit were treated as one visit as both belonged to one administration. The residual variability was described by an additive residual variability model for log-transformed data corresponding approximately to a proportional residual variability model using untransformed data.

Covariate model. Once the base model was established, the impact of the covariates was investigated. Which covariate was tested on which parameter is listed in Table 2-3. The covariate analysis was mainly performed as described in 2.3.1.3. Due to extensive run times and η-shrinkage (158), the standard approach was adapted as follows. To decrease the run time, the major part of the forward inclusion and backward elimination procedure was conducted separately per model parameter and all model parameters were fixed to the estimates of the base model except the investigated typical pharmacokinetic parameter, its variability and the typical parameter of the covariate effect. In addition, during the forward inclusion, the addition of a covariate was required to result in a drop of the OBJF value of at least 6.635 points ($p \leq 0.01$, χ^2, 1 df) – instead of 3.84 ($p \leq 0.05$, χ^2, 1 df) points in the standard approach – in order to be retained, otherwise the covariate was removed. A forward inclusion criterion closer to the backward elimination criterion was applied to

restrict the inclusion of covariates during the forward inclusion step to the more relevant ones. Due to the η shrinkage, the Bayesian estimates might be biased leading to misleading results of the explorative and GAM analysis. For this reason, the covariates age, sex, and weight, that were of special interest, as well as the covariates found in the initial covariate analysis of Project 1, were pre-defined to be tested in NONMEM.

Table 2-3 Covariates investigated in Project 3a

Model parameter	Covariate
All model parameters with interindividual variability	Demographic information: age, weight, height, body mass index, body surface area, sex, ethnic origin, smoking and alcohol status
	study number, randomisation group
Absorption parameters with interindividual variability	Formulation
Distribution and elimination parameters with interindividual variability (including binding parameters)	Laboratory values: serum creatinine, creatinine clearance, urea, alanine transaminase, aspartate transaminase, alkaline phosphatase, gamma-glutamyl transferase, total bilirubin, creatine kinase, cholesterol, C-reactive protein, triglyceride, fasting plasma glucose
	metformin treatment, pre-dose DPP-4 activity in RFU

Finally, the impact of the statistically significant covariates on the $AUC_{\tau,SS}$ values was to be investigated to evaluate the clinical relevance of the covariates. These investigations were performed using the Berkeley Madonna software. For continuous covariates, the typical concentration-time profiles of a subject with the median or either of the extreme covariate values (5^{th} and 95^{th} percentiles of the covariate distribution) were simulated. For categorical covariates, these simulations were performed for each category. The $AUC_{\tau,SS}$ values were calculated by integrating the typical concentration-time profiles directly using the Berkeley Madonna software.

2.5.3.1.4 Model evaluation

The description of the base model was investigated per study and dose group using a visual predictive check as described in 2.3.4.1. The final model was evaluated by a posterior predictive check performed per dose group as described in 2.3.4.2 using C_{max} and C_{trough} levels as variables of interest.

2.5.3.2 Project 3b: Pharmacodynamic covariate analysis

2.5.3.2.1 Objectives

The objectives of this analysis were to characterise the relationship between linagliptin plasma concentration and plasma DPP-4 activity in type 2 diabetic patients and to identify clinically relevant covariates affecting this correlation.

2.5.3.2.2 Study design

Project 3b used the linagliptin plasma concentrations and DPP-4 activities of the same four clinical studies as Project 3a. The study designs are reported in sections 2.5.1.2 and 2.5.3.1.2 in detail. DPP-4 activity was always measured at the same time points as the respective linagliptin plasma concentrations. Linagliptin plasma concentrations and plasma DPP-4 activity were measured as described in 2.1.

2.5.3.2.3 Modelling strategy

Initially, this analysis was planned to extend the population pharmacokinetic model developed in Project 3a. However, this was not possible due to the very long run time of more than five days of the population pharmacokinetic model. As the linagliptin plasma concentrations and the plasma DPP-4 activity were measured at the same time points and a direct relationship with no hysteresis observed graphically between both measurements, it was possible to correlate the linagliptin plasma concentrations directly to the DPP-4 activity.

For this covariate analysis, the dataset had to be changed as follows: The four single datasets were harmonised, merged, and re-organised to create a dataset containing plasma DPP-4 activity as dependent variable and the corresponding plasma linagliptin concentration measured at the same time points in a separate column. No dosing information was included into the dataset. For reasons unknown, linagliptin concentrations were measured for nine patients before any dose of linagliptin was administered. For these patients, all pre-dose information (linagliptin plasma concentration and plasma DPP-4 activity) was removed. For all other patients, a zero was implemented in the concentration column, when the dependent value column contained a pre-dose DPP-4 activity or when the patients were randomised to placebo. If the patients under linagliptin treatment contained either only a concentration measurement or only a DPP-4 activity at a certain time point the respective

data were not included in the dataset. All modifications were conducted with a user-written Splus script.

Base model. A simple E_{max} model and a sigmoid E_{max} model were tested to describe the correlation between linagliptin plasma concentration and plasma DPP-4 activity. Interindividual variability in all the typical parameters was to be investigated. No intraindividual variability was investigated.

Covariate model. Once the base model was established, the impact of the covariates was investigated. All covariates listed in 2.2.1.2, except formulation and pre-dose DPP-4 activity were tested on all parameters exhibiting interindividual variability. The covariate analysis was performed as described in detail in section 2.3.3.3.

Finally, the impact of the covariates on the model parameter EC_{50} as well as on the concentration leading to 80% inhibition of plasma DPP-4 was to be investigated in order to evaluate the clinical relevance of the covariate. These investigations were performed in Excel. For continuous covariates, the impact of the median and of the extreme covariate values (5^{th} and 95^{th} percentiles of the covariate distribution) on these parameters were determined. For categorical covariates, the impact of each category on the parameters was calculated.

2.5.4 Project 4: Estimation of the absolute bioavailability of linagliptin

2.5.4.1 Objectives

The standard approach (159) to determine the absolute bioavailability is dividing the dose-normalised $AUC_{p.o.}$ by the dose-normalised $AUC_{i.v.}$. However, this standard approach is only valid if the clearance calculated by $CL = F \cdot D/AUC$ of a drug is constant. This is not the case for linagliptin. One possibility to determine the absolute bioavailability despite nonlinear pharmacokinetics is to develop a population pharmacokinetic model that accounts for the nonlinear process (160). This approach was used for linagliptin.

2.5.4.2 Study design

Project 4 analysed a single dose, randomised, placebo-controlled, parallel trial, conducted in healthy men. The study was single-blind in terms of treatment within dose groups. Three treatment groups (1, 2, and 4) received single intravenous doses of linagliptin at dose levels 0.5, 2.5, and 10 mg. In treatment group 3, subjects underwent a two-way randomised cross-

over design, separated by at least 25 days of wash-out, receiving 5 mg linagliptin intravenously, and 10 mg linagliptin as a tablet. The study design is presented in Figure 2-1.

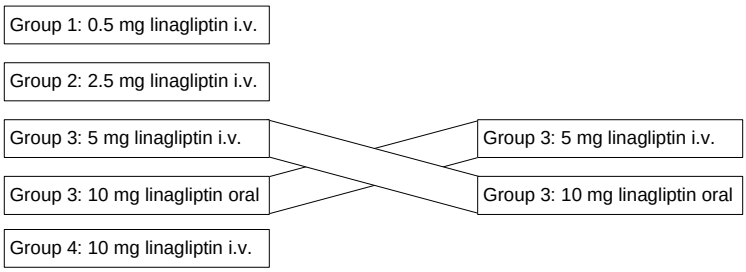

Figure 2-1 Study design of Project 4.

Within groups 1, 2, and 4, six subjects received linagliptin and two subjects received placebo, respectively. In Group 3, ten subjects received linagliptin and two subjects received placebo. The intravenous solutions were administered as an infusion over a time period of 90 min. The study was conducted at PHAROS GmbH, Pharmaceutical Research Outsourcing, Ulm. Ethics committees reviewed and approved the study protocols and the study was conducted within the ethical standards established by the Declaration of Helsinki (150) and in accordance with applicable regulatory requirements.

Plasma samples for pharmacokinetic assessments were taken pre-dose and at 30, 60, 90 (end of infusion), 92, 95, 100, 105 min, 2.0, 2.25, 2.5, 3.0, 3.5, 4.0, 5.0, 6.0, 8.0, 12.0 and 24.0 h after start of the infusion, as well as pre-dose and at 15, 30, 45 min, 1.0, 1.5, 2.0, 3.0, 4.0, 6.0, 8.0, 12.0, and 24.0 h after oral administration. In addition, plasma samples were taken on days 3, 4, 5, 6, 8, and 9, when subjects attended the study unit for walk-in visits. Linagliptin plasma concentrations were determined as described in section 2.1.1. Compliance was guaranteed by administration of the study medication under the supervision of the investigating physician or a designee on all study days.

2.5.4.3 Modelling strategy

The model development was performed in a stepwise manner. Firstly, it was investigated whether the model structure of Project 1 was also adequate to describe the linagliptin plasma concentrations after intravenous administration or whether adaptations were necessary. Then, the plasma concentrations after oral administration were added and both

datasets were analysed simultaneously to estimate the absolute bioavailability of linagliptin.

In order to test whether the model structure of Project 1 was also valid to describe plasma concentrations after intravenous administration, a bottom-up approach was used. First, it was tested whether a one-, two-, or three-compartment model could describe the linagliptin plasma concentrations after intravenous administration and whether incorporating concentration-dependent binding in the central or the central plus a peripheral compartment improved the description of the data. The way the binding was implemented in the model is described in detail for Project 1. When the plasma concentrations after oral administration were added, the disposition of linagliptin was assumed to be identical between intravenous and oral data. To model the absorption of linagliptin a first-order process with lag-time was used. The stochastic model was investigated as described in 2.3.3.2.2.

2.5.4.4 Model evaluation

The evaluation of the population pharmacokinetic model was performed using a visual predictive check as described in section 2.3.4.1.

2.5.5 Project 5: Model-based pharmacokinetic analysis of linagliptin in wildtype and DPP-4-deficient rats

2.5.5.1 Objective

The objective of Project 5 was to test the hypothesis that concentration-dependent binding of linagliptin to its target DPP-4 in plasma and tissue has a major impact on the pharmacokinetics of linagliptin. This was to be tested by comparing the pharmacokinetics of linagliptin in wildtype and DPP-4-deficient rats using a model-based analysis. The model was to describe the pharmacokinetics in both rat strains simultaneously by possibly accounting for concentration-dependent binding of linagliptin to DPP-4 only in wildtype rats. This pharmacokinetic model was used for further simulations illustrating the impact of target-mediated drug disposition on the pharmacokinetics of linagliptin.

2.5.5.2 Study design

Single intravenous doses of 0.01, 0.1, 0.3, 1, 3, 10, and 50 mg/kg of [^{14}C]linagliptin were administered to male DPP-4-deficient or wild-type Fischer rats in a parallel group design. In each dose group, four DPP-4-deficient and four wildtype animals were included, except

for the 0.01 mg/kg dose level which was not investigated in DPP-4-deficient rats due to the limit of quantification of the linagliptin assay and the expected very low plasma levels. The study was conducted by the group Nonclinical Pharmacokinetics, Boehringer Ingelheim. Radiolabelled linagliptin was used because post mortem tissue radioactivity was measured to quantify tissue concentrations from the same animals (161). These concentrations were not used for the pharmacokinetic model.

Male wildtype Fischer rats of the strain F344/DuCrl were supplied by Charles River, Germany and DPP-4-deficient male Fischer rats of the strain F344/DuCrlCrlJ were supplied by Charles River, Japan. In the latter, only a mutant and enzymatically inactive form of the DPP-4 protein is initially synthesised, that is not further processed to the mature DPP-4 and rapidly degraded (81,82).

The compound was dissolved in a small volume of 0.1 M hydrochloric acid and further diluted with sterile 0.9% NaCl solution to the final concentration. The formulation was administered as a single bolus injection into a lateral tail vein.

Blood samples were taken from the sublingual vein under isoflurane anaesthesia 2 and 5 min, as well as 1, 4, 8, 24, 48, and 72 h after administration. Total linagliptin plasma concentrations (labelled and unlabelled compound) were determined as described in section 2.1.1.

2.5.5.3 Modelling strategy

Only the dose groups 0.01–1 mg/kg were included in the model-based analysis, as a DPP-4-related difference was mainly obvious for these doses. At higher dose groups a second nonlinearity with a more than dose-proportional increase in exposure was found in both rat strains. This second nonlinearity is most likely not relevant for the therapeutic concentration range and was therefore not further investigated.

The analysis was carried out in a stepwise manner. Firstly, it was investigated which model adequately described the linagliptin plasma concentration in DPP-4-deficient rats. Due to the linear pharmacokinetics of linagliptin in DPP-4-deficient rats in the investigated dose range (0.1–1 mg/kg), only linear one-, two-, and three-compartment models were tested. In the second step, the plasma concentrations from DPP-4-deficient rats and wildtype rats were analysed together. This analysis was performed under the assumption that the distribution and elimination of linagliptin were identical in both rat strains, with the exception of concentration-dependent binding to DPP-4 which was only existent in wild-

type rats. Thus, the pharmacokinetic model derived from DPP-4-deficient rat data was expanded to include saturable binding in either the central and/or the peripheral compartment(s) in order to test which model adequately described the plasma concentrations of wild-type animals. During model development, the DPP-4 independent parameters were fixed to those from the DPP-4-deficient rat model. In the final model, all parameters were estimated simultaneously.

The concentration-dependent binding was implemented into the model as described in Project 1. For the final model structure, the assumption of quasi-equilibrium conditions for the binding of linagliptin to DPP-4 was tested. In the quasi-equilibrium model, it was assumed that the binding equilibrium was reached faster than all other processes, requiring only an estimation of the state of equilibrium by means of the dissociation constant (K_d). When the assumption of quasi-equilibrium conditions was abandoned, a description of the binding equilibrium by means of the association rate constant (K_{ON}) and the dissociation rate constant (K_{OFF}) was required, with $K_d = K_{OFF}/K_{ON}$. Because of the difficulty in precisely estimating K_{ON} and K_{OFF} together (152), the K_{OFF} value was fixed to the value of 0.108 h^{-1} determined *in vitro* (101).

2.5.5.4 Model evaluation

The models were evaluated using goodness-of-fit plots. In addition, the model parameters for CL, central volume of distribution (V_C), and V_{SS} of unbound linagliptin were compared to those calculated by the noncompartmental analysis for DPP-4-deficient rats. The model-estimated binding parameters were compared to those derived by an equilibrium plasma protein binding study (162).

2.5.5.5 Simulation strategy

The final pharmacokinetic model, which describes the pharmacokinetic profiles of DPP-4-deficient rats and wildtype rats simultaneously, was used for simulations to further characterise the impact of the target-mediated drug disposition on the pharmacokinetics of linagliptin in wildtype rats. The simulations were performed using the Berkeley Madonna software. The time courses of total linagliptin concentration and the DPP-4 bound concentration in the central compartment, as well as the time course of linagliptin in the peripheral compartment(s) in wildtype and DPP-4-deficient rats were simulated. In addition, the influence of altered amounts of binding partner in the central and peripheral compartments (±50% each) on the total linagliptin plasma concentration, the unbound plasma concentra-

tion, and the fraction of DPP-4 bound to linagliptin (i.e. occupancy) were investigated for wildtype animals.

3 Results

3.1 Project 1: Population pharmacokinetic/pharmacodynamic analysis of linagliptin in type 2 diabetic patients

The objective of this project was to characterise the nonlinear pharmacokinetics of linagliptin and the relationship between its pharmacokinetics and the DPP-4 activity in type 2 diabetic patients.

The analysis was based on studies I and II, two multiple dose phase IIa studies with 47 and 77 type 2 diabetic patients, respectively. The vast majority of patients was male, only five female patients participated in study II. The mean ages of patients were 56.0 (range: 36–65) and 60.1 (range: 40–69) years, and the mean body mass indices were 28.6 (range: 22.4–34.6) and 28.8 (range: 20.4–34.9) kg/m^2, respectively. Only Caucasian patients were included in the trials. The distribution of all covariates and the correlation between the covariates are summarised in the Appendix, Tables 4 and 5, as well as Figures 1 and 2, respectively. As the fraction of females included into the studies was less than 10%, sex was not tested as a covariate. No unexpected correlations between the covariates were observed (Appendix, Figures 1 and 2).

The dataset comprised 3,210 pharmacokinetic observations, i.e. plasma samples with a valid measurement of linagliptin plasma concentrations above the limit of quantification, from 96 patients. One patient in study II, randomised to 5 mg linagliptin treatment, was withdrawn from the study for safety reasons (ventricular extra systoles) after the first linagliptin administration (163). The distribution of the numbers of patients and pharmacokinetic observations per dose group is presented in the Appendix, Table 6. As 1 mg linagliptin was tested only in study I, this dose group contained less patients and pharmacokinetic observations compared to the other dose groups. The individual linagliptin plasma concentration-time profiles per study and dose group are shown in the Appendix, Figure 3. Linagliptin exhibited nonlinear pharmacokinetics with a less than dose-proportional increase in the linagliptin plasma concentration-time profiles (104). The pharmacokinetic profiles indicate the low and dose-dependent accumulation of linagliptin as described in section 1.3.2.2. Surprisingly, the profiles in study II were higher compared

to those of study I when the same doses were compared, especially in the higher dose levels, although the formulations had been tested to be bioequivalent in a separate study.

A total of 4,350 plasma DPP-4 activities from 124 patients were included in the dataset. The distribution of DPP-4 activity per dose group is presented in Appendix, Table 6. Again the 1 mg dose group contained less observations compared to the other dose groups. No DPP-4 activity measurement was removed from the dataset. Linagliptin led to a dose-dependent inhibition of DPP-4 with a more than 80% steady-state DPP-4 inhibition over 24 h in the 5 and 10 mg dose groups (Appendix, Figure 4). The linagliptin plasma concentrations and the plasma DPP-4 activity were well correlated in a sigmoid manner with a steep concentration-effect relationship (Figure 3-1).

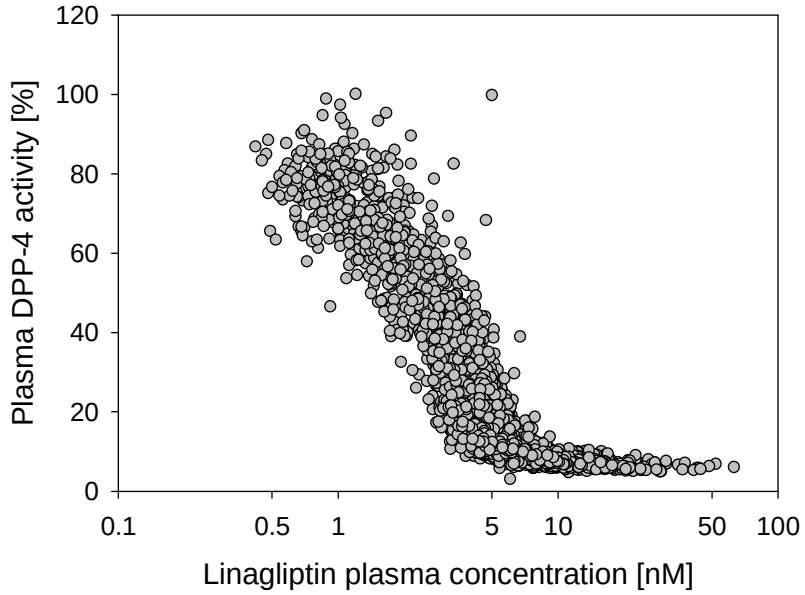

Figure 3-1 Correlation between linagliptin plasma concentration and plasma DPP-4 activity for studies I and II. Placebo and pre-dose observations not shown due to logarithmic scale.

3.1.1 Model development

3.1.1.1 Pharmacokinetic base model

Linear one-, two-, and three-compartment models with first-order absorption and elimination failed to adequately describe the pharmacokinetics of linagliptin. A linear two-compartment model was significantly better than a linear one-compartment model (ΔOBJF −4,423.619) and not inferior compared to a linear three-compartment model (ΔOBJF 0). Including one concentration-dependent binding process in the central compartment of a

two-compartment model improved the model fit significantly (ΔOBJF −2,682.855) and was superior to the implementation of a saturable absorption into a two-compartment model (ΔOBJF −112.003). Adding a second concentration-dependent binding process with equal binding affinity in the peripheral compartment resulted in a significantly better description of the plasma concentration-time profiles (ΔOBJF −142.92), while adding a second peripheral compartment did not improve the model fit (ΔOBJF 0). Adding the second peripheral binding partner to the central compartment, i.e. assuming that linagliptin binds without a distribution process to this second binding partner and linagliptin bound to this second binding partner is not longer measurable in plasma, did likewise not improve the model fit (ΔOBJF 0). Thus, the nonlinear pharmacokinetics of linagliptin was best described by a two-compartment model with concentration-dependent protein binding in the central and the peripheral compartment (Figure 3-2).

Interindividual variability was tested on all pharmacokinetic model parameters in a stepwise manner and implemented on the relative bioavailability, the absorption rate constant and the concentration of the central binding partner. Intraindividual variability was tested on these three parameters as well as on clearance, and was found necessary to be implemented on the relative bioavailability. Addition of further inter- or intraindividual variability on other parameters of the population pharmacokinetic model did either not result in a better description of the plasma concentrations or decreased the stability of the model. The residual variability was adequately described by an additive residual variability model for the log-transformed plasma concentrations (proportional residual variability model for untransformed data). The parameter estimates of the pharmacokinetic base model are presented in Table 3-4.

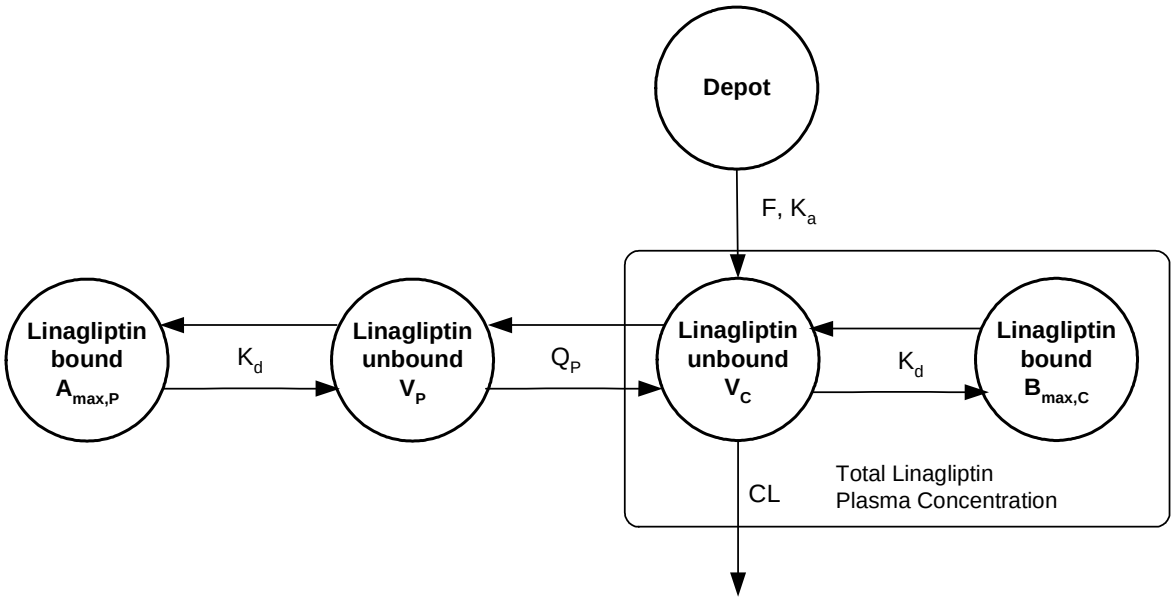

Figure 3-2 Structure of the final population pharmacokinetic model of Project 1. The pharmacokinetic model of linagliptin accounts for concentration-dependent and reversible binding of linagliptin to DPP-4 in plasma and in peripheral tissues. ´Linagliptin bound´ refers to linagliptin bound specifically and concentration-dependently to DPP-4. ´Linagliptin unbound´ refers to free linagliptin as well as to linagliptin bound non-specifically and non-saturably to proteins. The total linagliptin plasma concentration is the sum of unbound and bound linagliptin concentration in the central compartment. F, relative bioavailability; K_a, absorption rate constant; V_C/F, apparent central volume of distribution; V_P/F, apparent volume of distribution of the peripheral compartment; Q_P/F, apparent intercompartmental clearance between central and peripheral compartment; CL/F, apparent clearance; $B_{max,C}$, concentration of binding partner in the central compartment; $A_{max,P}$/F, apparent amount of binding partner in the peripheral compartment; Kd, dissociation constant.

3.1.1.2 Identifiability of the pharmacokinetic model

Due to the complexity of the pharmacokinetic model, it was to be investigated whether the proposed model structure is identifiable given the available data. Structural identifiability is the ability of a model to uniquely estimate all parameters given ideal, error-free data. Deterministic or numeric identifiability is the ability of a model to uniquely estimate all parameters given actual, non-ideal data (140). Different methods were used in the following to investigate whether the structure of a two-compartment model with two concentration-dependent bindings, one in the central and the other in the peripheral compartment, was structurally and numerically identifiable, paying particular attention to the identifiability of the two binding partners.

3.1.1.2.1 Influence of binding on plasma pharmacokinetic profiles

First, the influence of variations in the amount of the binding partner in the central and in the peripheral compartment on the plasma concentration-time profiles was investigated. This was done on the premise that perturbance in a model parameter must have an effect on the resulting plasma concentration-time profiles for the parameter to be estimated by the model. Changes in $B_{max,C}$ affected the concentration-time profiles of all dose groups (Figure 3-3, upper panels).

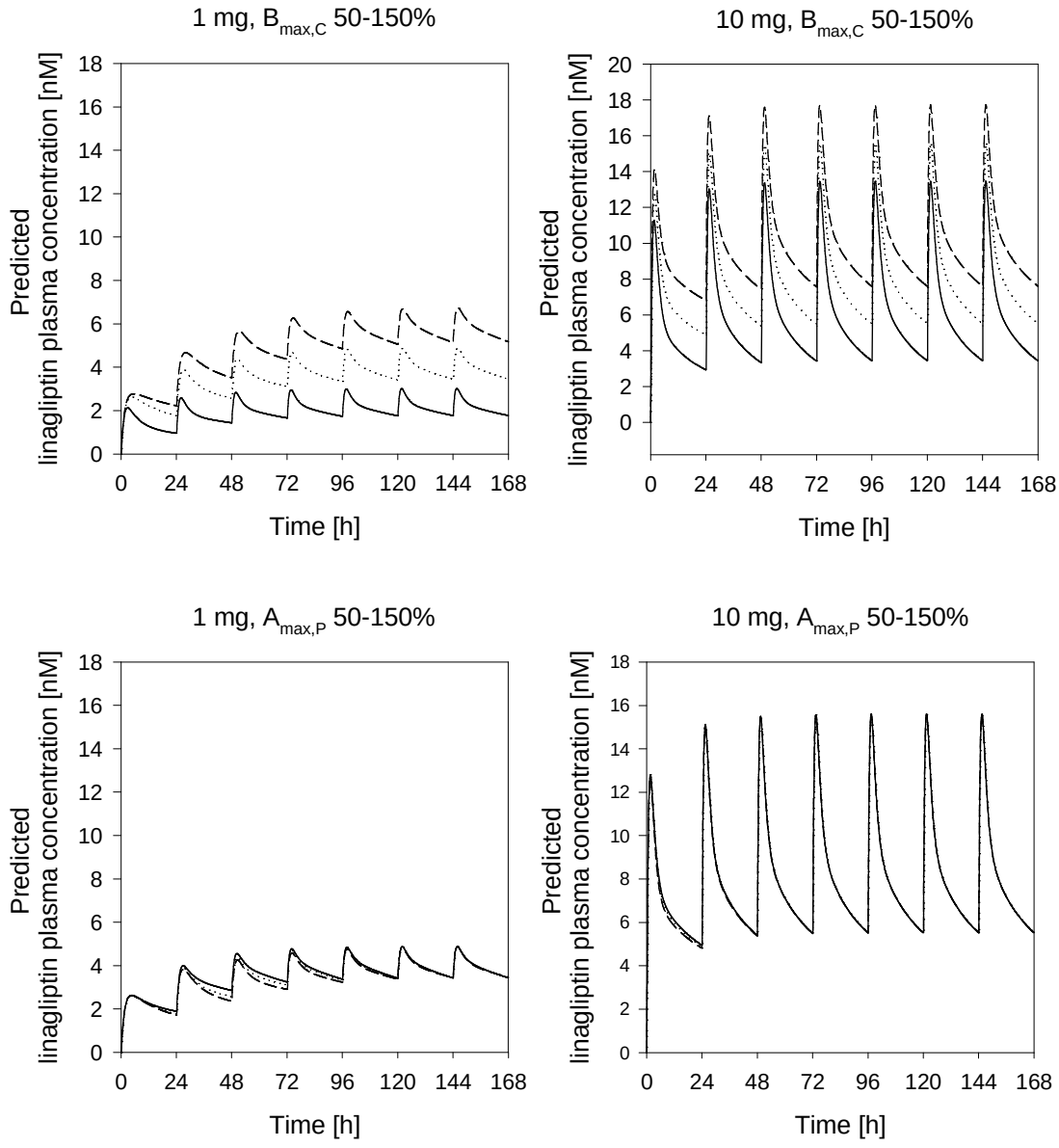

Figure 3-3 Predicted influence of altered (50%, solid line; 100% (original value), dotted line; 150%, dashed line) amounts of central (upper panels) and peripheral (lower panels) binding partner on the plasma concentration-time profiles for the treatment with 1 (left panels) and 10 mg (right panels) linagliptin once daily. Due to the small impact of altered amounts of peripheral binding partner on the plasma concentration-time profiles, the three profiles partly overlap (lower panels).

In contrast, changes in the amount of the binding partner in the peripheral compartment ($A_{max,P}$) affected the 1 mg dose group predominantly, but to a lesser extent (Figure 3-3, lower panels). The same trend was observed with regard to the log-likelihood profiles (Appendix, Figure 5): $B_{max,C}$ was estimated more precisely, with a relative standard error (RSE) of 3.3%, than $A_{max,P}$ (RSE 10.0%). Taken together, both analyses suggest that the binding in both compartments is identifiable.

3.1.1.2.2 Simulation and re-estimation

Whether linagliptin actually binds to a peripheral binding partner has not been experimentally proven thus far. With the following approach it was tested, whether in a simulated scenario for which the existence or non-existence of a peripheral binding is known, the model has the ability to identify the correct scenario. Thus, concentration-time profiles were simulated based on the given study design (study I) and two different simulation scenarios (S1, S2) with the binding partner being available only in the central (S1) or in both (S2) compartments (Figure 3-4). In the next step, each dataset was re-estimated assuming either binding only in the central compartment (M1) or in both compartments (M2). The re-estimations for S1 showed that in 69 out of 70 cases, M2 was not superior to M1 and thus the model was correctly identified (Figure 3-4, left flow chart). In contrast, the re-estimations for S2 showed that in 100% of the simulated datasets M2 was superior to M1 (Figure 3-4, right flow chart). Hence the correct model was chosen for both scenarios.

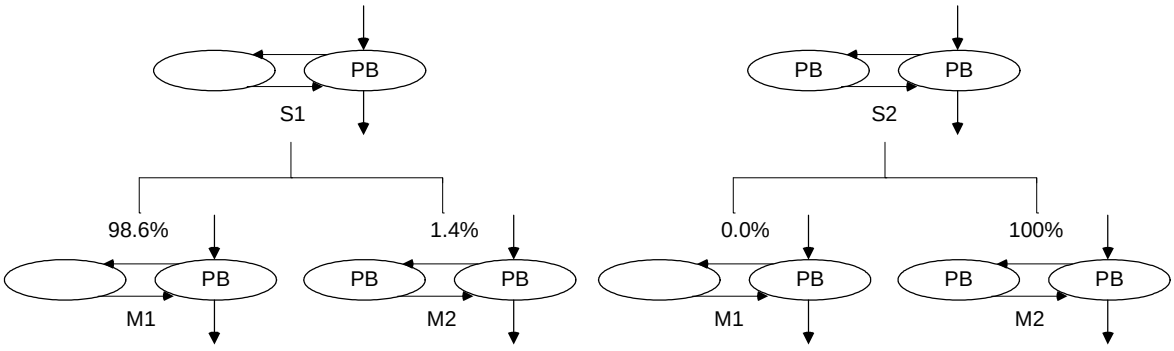

Figure 3-4 Schematic representation of both simulation (S1, S2) and re-estimation (M1, M2) scenarios. PB, concentration-dependent protein binding.

In Table 3-1 the inaccuracy and imprecision of the re-estimated parameters are presented when model M2 was used to re-estimate scenario S2. All population parameters were re-estimated accurately and with an adequate precision, suggesting that the model in general,

and the peripheral binding in particular are identifiable. Again, the standard deviation of the typical population estimates indicated that $B_{max,C}$ was estimated more precisely than $A_{max,P}$ (6.5% versus 22.9%).

Table 3-1 Inaccuracy and imprecision of the re-estimated parameters using model M2 (estimated assuming binding in the central and the peripheral compartment) and simulation scenario S2 (simulated assuming binding in the central and the peripheral compartment)

	K_a	V_C	Q_P	V_P	CL	$B_{max,C}$	K_d	$A_{max,P}$	ωF	ωK_a	$\omega B_{max,C}$	σ_{prop}
Parameters used in the simulation	0.710	701	422	1,980	225	4.34	0.0706	1,630	0.183	0.348	0.0428	0.08
Inaccuracy [%][1)]	-0.01	+4.4	+4.6	+0.8	+3.1	+0.4	+6.0	+2.5	-10.0	-11.5	+0.9	-0.4
Imprecision [%][2)]	11.8	9.0	13.3	16.9	17.7	6.5	9.6	22.9	37.5	26.1	26.2	4.7

1) Inaccuracy was determined as the percent deviation of the re-estimated mean value from the parameter estimate used in the simulation.

2) Imprecision was calculated as the coefficient of variation of the re-estimated parameters.

3.1.1.2.3 Fisher-Information-Matrix

In a third test, the identifiability of the model parameters was investigated using the Fisher-Information-Matrix. The determinant of the Fisher-Information-Matrix was $1.52 \cdot 10^{23}$ and thus far from zero, suggesting that the model is structurally identifiable (Prof. Stephen Duffull, personal communication). The relative standard errors calculated based on the Fisher-Information-Matrix are given in Table 3-2. The binding parameters $B_{max,C}$ and $A_{max,P}$ were supposed to be determined precisely given the investigated study design, with relative standard errors of 4% and 26%, respectively. Interestingly, omitting the 1 mg dose group increased the relative standard errors for $A_{max,P}$ from 26% to 56%. This shows that due to the nonlinear pharmacokinetics, a range of doses is required to reliably estimate all parameters, e.g. low doses were most informative for the estimation of the peripheral binding partner.

Table 3-2 Relative standard errors determined by the Fisher-Information-Matrix

	K_a	V_C	Q_P	V_P	CL	$B_{max,C}$	K_d	$A_{max,P}$	ωF	ωK_a	$\omega B_{max,C}$	$\sigma_{prop.}$
RSE [%]	11.8	8.4	8.9	12.9	7.6	3.9	15.9	25.8	25.1	33.1	24.4	4.0

3.1.1.3 Pharmacokinetic/pharmacodynamic base model

A descriptive sigmoid E_{max} model fitted the DPP-4 activities adequately and was superior to a simple E_{max} model (ΔOBJF −3781.156, E_{max} estimate near the boundary (100%) in the simple E_{max} model). In addition, two semi-mechanistic models were tested, an E_{max} model using CU_{plasma} and a model linking the occupancy, i.e. the fraction of DPP-4 molecules bound to linagliptin, proportionally to the DPP-4 activity. The CU_{plasma} as well as the occupancy were both estimated in the pharmacokinetic part of the model. In the E_{max} model using CU_{plasma} very similar values for K_d and EC_{50} were estimated (K_d: 0.0738 nM, EC_{50}: 0.0723 nM). Both models described the DPP-4 activities equally well (ΔOBJF −0.306). Thus, based on the principle of parsimony, the simpler occupancy model was selected for further development. The performance of the descriptive sigmoid E_{max} model was compared to the occupancy model. As both models were not nested, a comparison based on the OBJF was not possible. The occupancy model was chosen as final model for the following reasons: (a) standard goodness-of-fit plots were similar for both models, (b) the occupancy model required two parameters less, (c) the residual variability for pharmacokinetics and pharmacodynamics was higher in the descriptive sigmoid E_{max} model, (d) relating the DPP-4 activity to the DPP-4 occupancy is in line with the hypothesis that the saturable binding observed in plasma was due to the binding of linagliptin to DPP-4.

The only pharmacodynamic parameter in the occupancy model was E_{max}. Interindividual variability on E_{max} was estimated to be very low (<2%) and was therefore not implemented into the model. The residual variability was adequately described by a proportional residual variability model; adding an additive variability model was not supported by the data. The parameter estimates of the base population pharmacokinetic/pharmacodynamic model are shown in Table 3-4.

3.1.1.4 Covariate selection

The covariate analysis was performed as described in section 2.3.3.3. The covariates preselected by graphical exploration and by GAM analysis are listed in Table 3-3. The preselected covariates and the predefined covariates listed in section 2.5.1.3 were then tested in NONMEM using the forward inclusion backward elimination procedure. The statistically significant covariates depicted by this procedure are presented in Table 3-3.

Table 3-3 Covariates selected during the different phases of the covariate screening process

	Graphical exploration	GAM analysis	Forward inclusion and backward elimination procedure in NONMEM
Bioavailability	Study/formulation	Study/formulation, age	Study/formulation
Rate of absorption	Study/formulation, dose group	Alanine transaminase, triglycerides, alcohol status, dose group	Dose group
Concentration of central binding partner	Baseline DPP-4 activity (raw data) [1)]	Aspartate transaminase, alkaline phosphatase, dose group, triglycerides, C-reactive protein, baseline fasting plasma glucose	Aspartate transaminase
Apparent volumes of distribution	NA	NA	None
Apparent clearance	NA	NA	Alanine transaminase

[1)] Not tested in GAM and NONMEM to allow the detection of otherwise hidden correlations between the concentration of central binding partner and laboratory values, e.g. liver enzymes

NA, not applicable

The effects of the covariates on the linagliptin plasma concentration- and plasma DPP-4 activity-time profile were small. The following covariates were statistically significant but not included into the final covariate model for the stated reasons: The absorption rate constant decreased with increasing dose. This effect was predominantly observed for the powder in the bottle formulation (study I) and not for the tablet (study II) which is the intended formulation for further development. The concentration of the central binding partner increased with increasing aspartate transaminase values. However, this relationship was driven by only four data points. The unbound clearance was slightly increased with increasing aspartate transaminase values. Physiologically, an increase of alanine transaminase, suggesting a deterioration of the hepatic function, is expected to correlate with a decrease of the clearance.

Thus, the only covariate impact remaining in the final covariate model was a 30% decrease of bioavailability in study I compared to study II. Due to the different formulations in both studies, different inter- and intraindividual variabilities were implemented. As the interindividual variability in bioavailability in study I could not be estimated precisely (RSE 353%), it was fixed to zero and only intraindividual variability was implemented. All

covariates mentioned in the previous paragraph were predefined to be tested in NONMEM together with the phase IIb data (Project 3a).

3.1.2 Final model

Supporting the initial hypothesis, that concentration-dependent binding of linagliptin to DPP-4 is responsible for the nonlinear pharmacokinetics of linagliptin, the plasma concentration-time profiles were best described by a two-compartment model with concentration-dependent binding in the central and the peripheral compartments (Figure 3-2). The compound reaches the central compartment by a first-order process. In the central compartment, the unbound compound either binds competitively and reversibly to a high affinity, low capacity binding partner, is eliminated via a first-order process, or is distributed to the peripheral compartment. In the peripheral compartment the compound can again bind competitively and reversibly to a high affinity, low capacity binding partner which has the same binding affinity for the compound as the one in the central compartment. The population pharmacokinetic/pharmacodynamic model was based on the assumption that the high affinity, low capacity binding partner in the population pharmacokinetic model reflects DPP-4. In line with this assumption, the individual estimates for the concentration of binding partner in the central compartment correlated well with the pre-dose DPP-4 activity raw data (Figure 3-5).

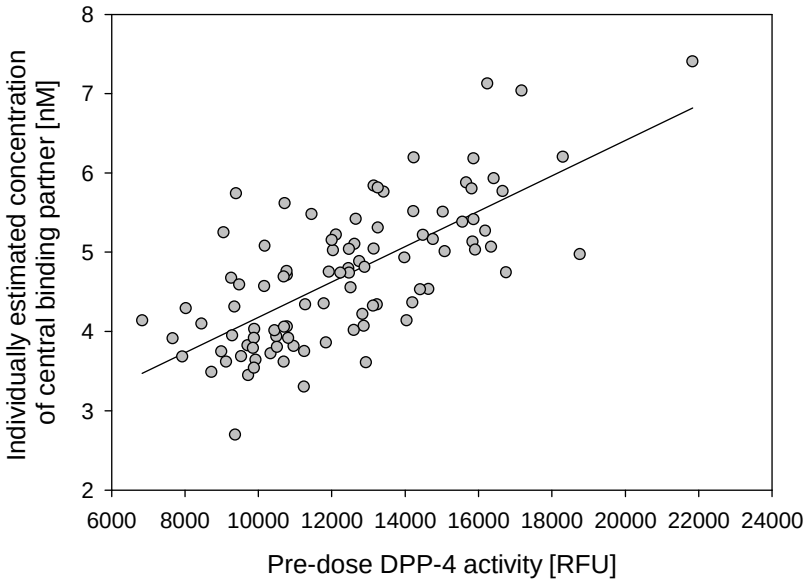

Figure 3-5 Individually estimated concentrations of the central binding partner (most likely DPP-4) versus pre-dose DPP-4 activity in RFU

Plasma DPP-4 activity was incorporated into the model in a semi-mechanistic way using Clark's receptor occupancy theory, which states that drug effect is proportional to occupancy. The more linagliptin is bound to DPP-4, the lower is the DPP-4 activity until all DPP-4 molecules are blocked by linagliptin and the maximal effect is reached.

The parameter estimates of the final population pharmacokinetic/pharmacodynamic model are presented in Table 3-4. The apparent clearance estimated by the model refers to the CL/F of unbound linagliptin. This clearance is independent of dose within the investigated dose range. CL/F was estimated to be high (220 L/h) indicating that linagliptin not bound to DPP-4 is efficiently eliminated. Likewise, the apparent volumes of distribution calculated by the model refer to unbound linagliptin. These values were estimated to be 570 L for the central volume of distribution and 2,090 L for the peripheral volume of distribution, showing that unbound linagliptin is still widely distributed. $B_{max,C}$ was estimated to be 4.62 nM which is within the range expected for the plasma DPP-4 concentration (79,80). The model-estimated dissociation constant for the concentration-dependent binding was 0.0738 nM and is thus in good agreement with the dissociation constant obtained *in vitro* from plasma samples employing equilibrium dialysis (K_d: 0.05 nM, as calculated by $K_d = 1/K_1$) (162). In line with the observed linagliptin concentration-time profiles (Appendix, Figure 3), a lower bioavailability was found for study I during the covariate analysis. This was accounted for by estimating a separate bioavailability in each study.

Interindividual variability could be established for the parameters bioavailability (F), absorption rate constant (K_a), and $B_{max,C}$, and intraindividual variability could be estimated for F. The inter- and intraindividual variability ranged between 18.9% and 60.8% (Table 3-4). The residual variability of the log-transformed linagliptin concentrations was modelled using an additive random effect model corresponding approximately to a proportional model for untransformed data. It was estimated to be low (16.0%, Table 3-4). The residual variability for the DPP-4 activity was adequately described by a proportional random effect model and was also estimated to be low (17.4%, Table 3-4).

Table 3-4 Parameter estimates of the base pharmacokinetic and pharmacokinetic/pharmacodynamic model and the final model

		PK Base Model		PK/PD Base Model		PK/PD Final Model	
	Unit	Estimate	RSE [%]	Estimate	RSE [%]	Estimate	RSE [%]
Typical Parameter							
F study I/II	%	100 fixed	NA	100 fixed	NA	69.8/100 fixed	7.28/NA
K_a	h^{-1}	0.845	13.0	0.631	8.59	0.633	8.29
V_C/F	L	776	12.2	648	7.48	570	10.4
Q_P/F	L/h	412	16.2	508	12.9	446	12.3
V_P/F	L	1,650	10.6	2,390	8.33	2,090	8.09
CL/F	L/h	289	11.9	251	6.53	220	7.36
$B_{max,C}$	nM	4.85	5.15	4.62	2.27	4.62	2.29
K_d	nM	0.0652	9.88	0.0738	7.06	0.0738	7.80
$A_{max,P}/F$	nmol	1,650	12.7	2,170	12.9	1,900	11.2
E_{max}	%	NA	NA	93.5	0.24	93.5	0.24
Inter- and intraindividual variability							
ωF study I/II	CV%	32.7	22.1	37.3	21.2	NA/37.3	NA/23.1
ωK_a	CV%	57.6	16.9	60.7	13.1	60.8	13.0
$\omega B_{max,C}$	CV%	20.2	18.9	18.8	14.7	18.9	14.7
πF study I/II	CV%	34.6	26.5	30.2	19.0	34.1/33.0	16.1/23.7
Residual variability							
$\sigma_{prop,PK}$ [1)]	%	14.1	3.66	16.0	3.89	16.0	3.89
$\sigma_{prop,PD}$	%	NA	NA	17.3	7.91	17.4	7.88

1) Estimated on log-transformed data

NA, not applicable

The parameters of the final model were estimated with good precision (relative standard errors ranging from 0.24–23.7% for the final model, cf. Table 3-4). The goodness-of-fit plots in Appendix, Figure 6 and Figure 7 indicate that the population pharmacokinetic/pharmacodynamic model described the linagliptin plasma concentrations and plasma DPP-4 activity adequately, except for an under-prediction of a few C_{max} values.

3.1.3 Model evaluation

For the evaluation of the final population pharmacokinetic/pharmacodynamic model, a visual predictive check was performed. Generally there was a good agreement between the simulated and the observed linagliptin plasma concentrations and DPP-4 activities (Appendix, Figures 8 and 9). The model slightly over-estimated the variability of DPP-4 activity and the inhibitory effect in the 1 mg dose group.

3.1.4 Simulation

Typical concentration-time profiles for a daily administration of 5 mg linagliptin, which is the therapeutic dose tested in the clinical phase III programme, were simulated. According to these simulations the total $AUC_{\tau,SS}$ is composed to the greater part (~70%) of linagliptin bound to DPP-4, while only the smaller fraction is not bound to DPP-4 (Figure 3-6, left panel). This results in a target-mediated drug disposition that has to be taken into account in the interpretation of the linagliptin pharmacokinetics. Simulations showed that the steady-state occupancy is >90% over 24 h for both the 5 mg and the 10 mg dose group (Figure 3-6, right panel).

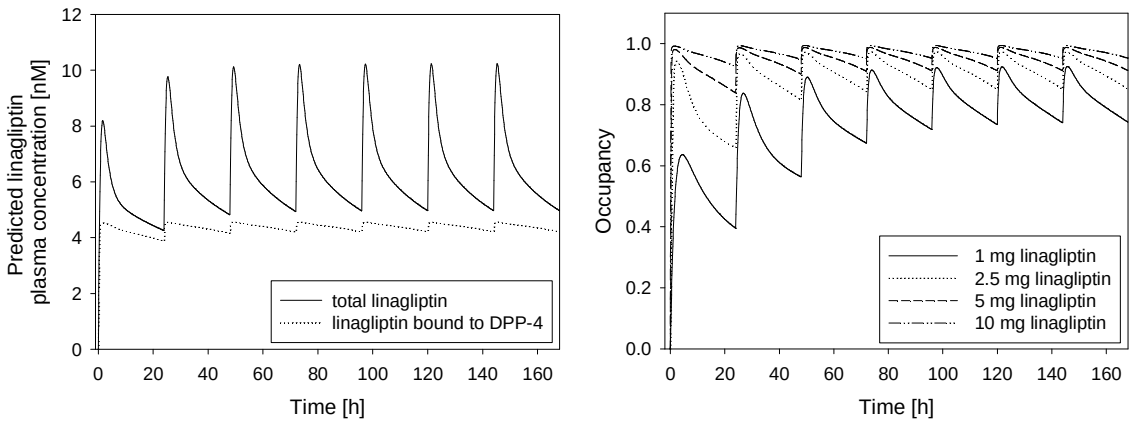

Figure 3-6 Left panel: Predicted linagliptin plasma concentration-time profiles for bound (dotted line) and total (solid line) linagliptin following a once daily 5 mg linagliptin administration. Right panel: Predicted time profile of the occupancy of plasma DPP-4 with linagliptin for the four investigated dose groups, 1, 2.5, 5 and 10 mg linagliptin, following a once daily linagliptin administration.

3.2 Project 2: Clinical trial simulations to support the development of linagliptin

3.2.1 Project 2a: Simulation to evaluate an equivalent dose for a twice-daily administration

The objective of this project was to determine the optimal dose for a twice-daily administration of linagliptin that is bioequivalent with regard to steady-state exposure ($AUC_{24h,SS}$) and shows similar steady-state DPP-4 inhibition as a 5 mg dose given once daily.

The simulation using the base pharmacokinetic/pharmacodynamic model of Project 1 indicated that despite the nonlinear pharmacokinetics, administering 2.5 mg linagliptin twice daily can be expected to result in a very similar exposure and DPP-4 inhibition compared to 5 mg linagliptin once daily (Figure 3-7). The corresponding $AUC_{24h,SS}$ values were 147.1 nM·h for the 5 mg linagliptin once daily (qd) regimen and 116.4, 128.2, 138.4, and 148.0 nM·h for 1, 1.5, 2, and 2.5 mg linagliptin twice daily (bid), respectively.

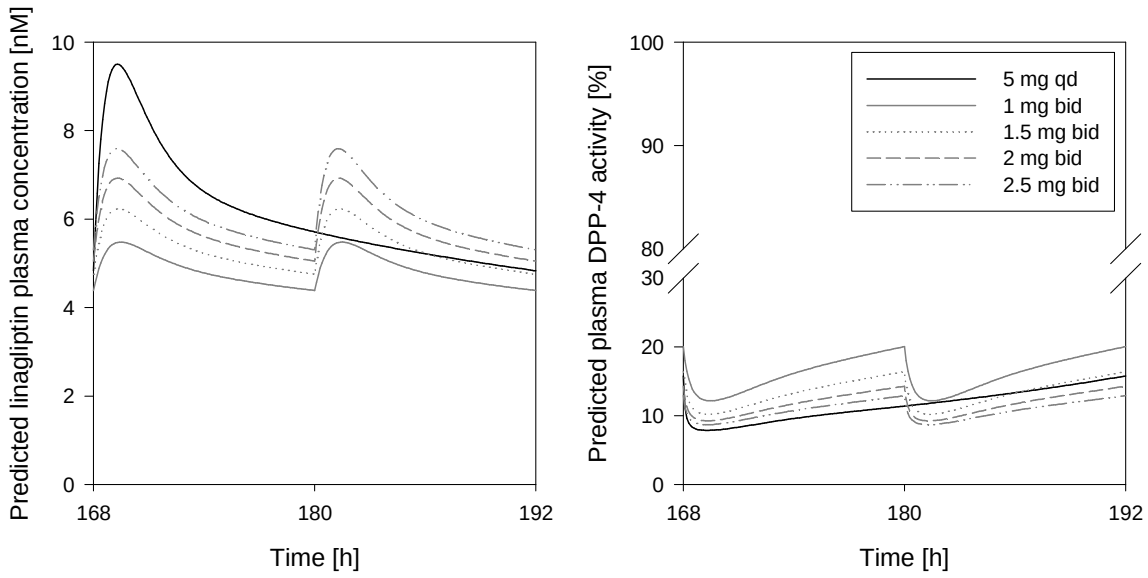

Figure 3-7 Predicted typical plasma concentration- (left panel) and plasma DPP-4 activity- (right panel) time profiles at steady-state of 1, 1.5, 2, and 2.5 mg linagliptin given twice daily (grey lines) in comparison to 5 mg linagliptin given once daily (black line).

In addition, a clinical trial simulation was performed in order to predict the outcome of a relative bioavailability study testing 5 mg linagliptin once daily (treatment A) versus 2.5 mg twice daily (treatment B). Table 3-5 lists the mean of 1,000 simulated geometric

mean (+ gCV) $AUC_{24h,SS}$ values per sequence and treatment. According to the results of the simulation, the exposures at steady-state for treatments A and B are expected to be independent of the tested treatments. In addition, no obvious sequence effect was visible, indicating that a seven day period in the change-over design would be sufficiently long.

Table 3-5 Mean of the geometric mean (+gCV) $AUC_{24h,SS}$ values per sequence and treatment of 1,000 simulated relative bioavailability studies testing 5 mg linagliptin once daily versus 2.5 mg twice daily.

	Treatment A (5 mg linagliptin once daily)		Treatment B (2.5 mg linagliptin twice daily)	
	Mean gMean [nM·h]	Mean gCV [%]	Mean gMean [nM·h]	Mean gCV [%]
Sequence AB	149.97	21.02	151.08	21.03
Sequence BA	149.81	20.71	150.43	20.70

The mean of the gMean ratios between the $AUC_{24h,SS}$ of treatment A and treatment B was 100.90% (90% confidence interval 91.90%–110.80%) for the 1,000 simulated trials. Of the 1,000 simulated trials only one confidence interval was outside the acceptance interval of 0.80–1.25. These simulations clearly supported the use of 2.5 mg linagliptin as adequate dose of a twice-daily treatment.

3.2.2 Project 2b: Simulation to evaluate the impact of impaired clearance

The objective of Project 2b was to investigate the impact of an impaired renal clearance on the nonlinear pharmacokinetics of linagliptin.

The typical linagliptin plasma concentration- and plasma DPP-4 activity-time profiles following 5 mg linagliptin once daily were simulated under the assumption that the clearance of unbound linagliptin is as originally estimated in Project 1 or decreased by 25% and 50% (Figure 3-8). The simulation revealed that for patients with only 75% or 50% of the clearance of a typical patient, the exposure of linagliptin would in average increase by 11% or 31%, respectively. The increased linagliptin exposure is predicted to result in a slightly higher DPP-4 inhibition (Figure 3-8, right panel).

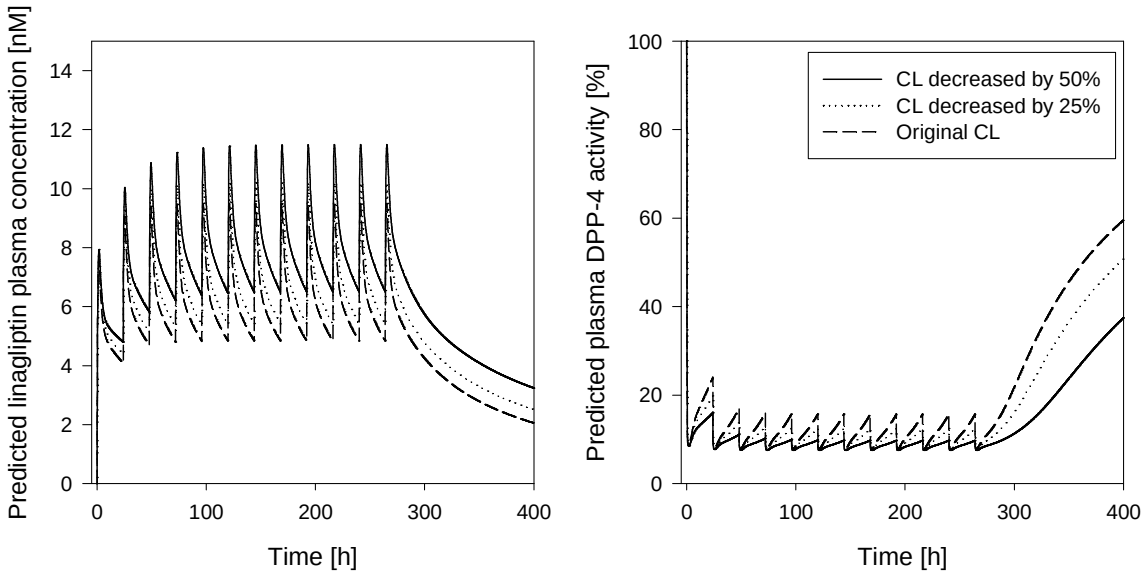

Figure 3-8 Prediction of the typical linagliptin plasma concentration- and plasma DPP-4 activity-time profiles following 5 mg linagliptin once daily under the assumption that the clearance of unbound linagliptin is as originally estimated in Project 1 or decreased by 25 and 50%.

3.2.3 Project 2c: Simulation of a design for a dose-proportionality study

The objective in Project 2c was to determine the treatment duration required for a change-over study to assess dose-proportionality of different dose strengths of linagliptin tablets (1, 2.5, and 5 mg) at steady-state.

The simulations based on the final model of Project 1 suggested that steady-state is achieved by day 5 in all investigated dose groups in every tested scenario (Figure 3-9). Steady-state was reached first in the highest dose group (5 mg) and the time to steady-state increased with decreasing doses. Within the simulated 1 mg dose group, steady-state was reached latest when linagliptin is administered in the first period. For this treatment group, the time to reach steady-state was predicted to be approximately five days. Thus, administering linagliptin over seven days is predicted to assure steady-state in each sequence. In summary, the simulation suggested that the proposed randomised change-over design in which 1, 2.5, and 5 mg linagliptin are administered once daily over seven days is adequate to compare the steady-state profiles of the investigated dose groups.

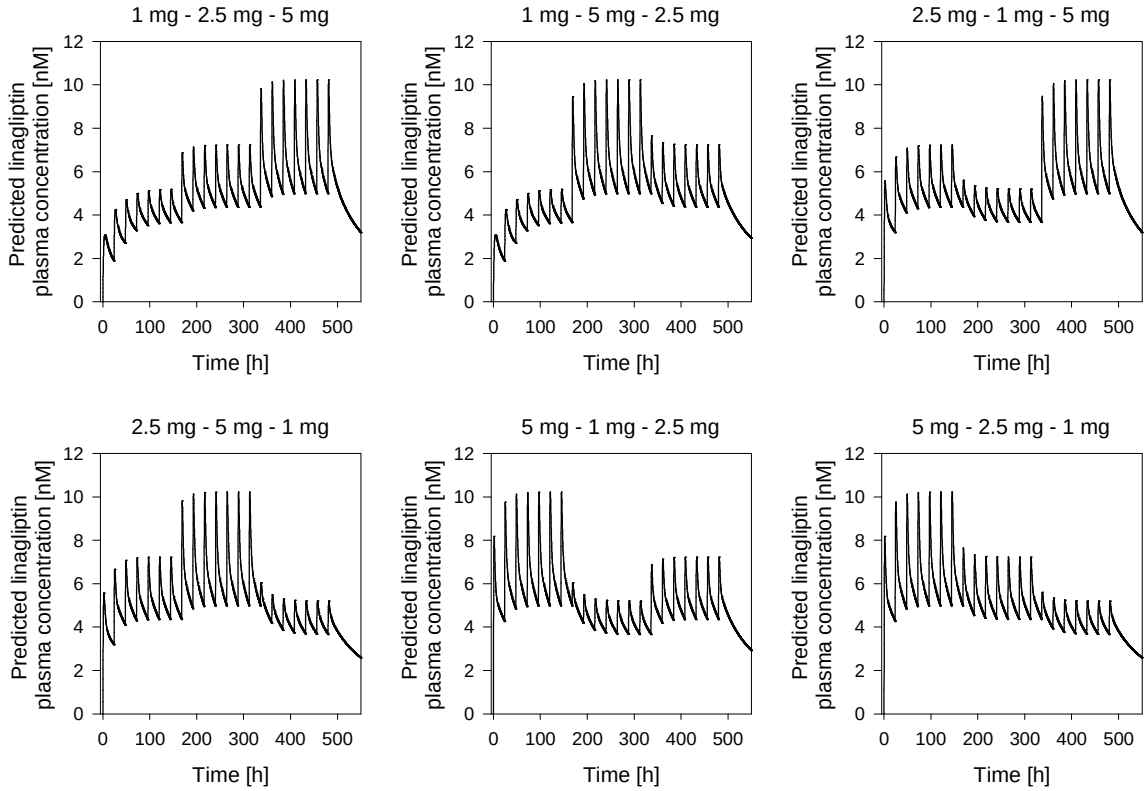

Figure 3-9 Typical profiles of the six possible scenarios for a randomised change-over design where 1, 2.5, and 5 mg linagliptin are given once daily for seven days in each sequence.

3.2.4 Project 2d: Description and steady-state simulation of the drug-drug interaction between linagliptin and ritonavir

The objective of Project 2d was to predict the steady-state profile of linagliptin under ritonavir comedication.

The dataset consisted of linagliptin plasma concentrations from twelve healthy volunteers with a mean age of 37.1 years (range: 25–50 years) and a mean body mass index of 25.4 kg/m^2 (range: 21.8–29.5 kg/m^2). The volunteers received a single dose of 5 mg linagliptin alone and in combination with ritonavir in a cross-over design. Both treatment arms included 192 plasma concentration measurements, respectively. The plasma concentration-time profiles of linagliptin were elevated when linagliptin was given in comedication with ritonavir (Figure 3-10).

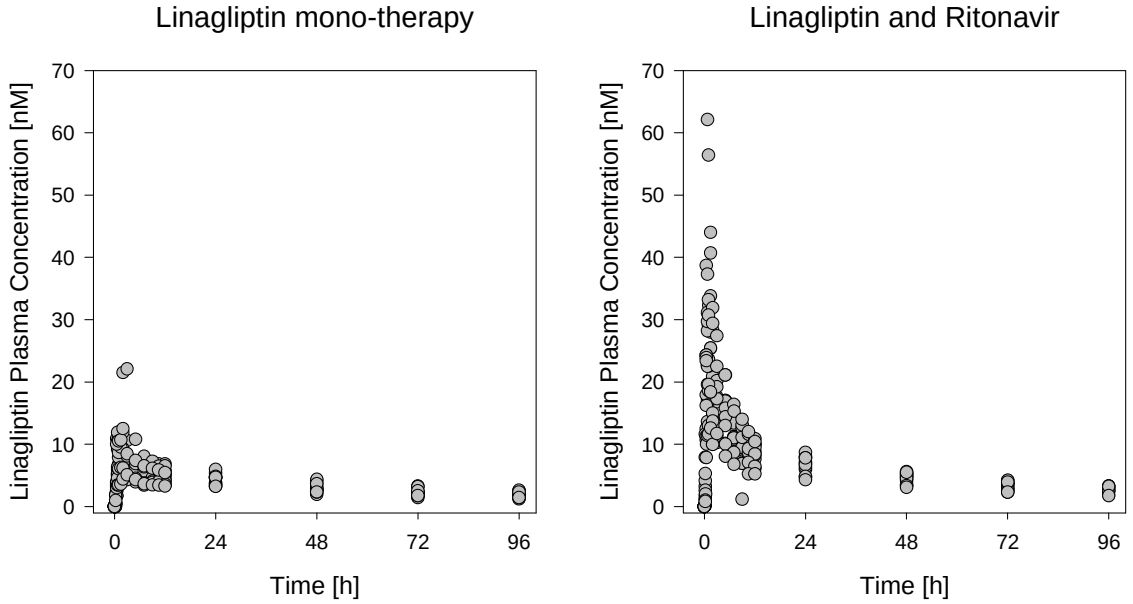

Figure 3-10 Plasma concentration-time profiles of linagliptin after a single dose of 5 mg linagliptin alone (left panel) and in combination with ritonavir (right panel)

3.2.4.1 Model development

The model development was performed in a stepwise manner. Firstly, the model parameters of the base model developed in Project 1 (called M3) were re-estimated to describe the plasma concentrations of linagliptin monotherapy (reference treatment). The thus adapted model (called M4) was then adjusted to describe the plasma concentrations when linagliptin was given in combination with ritonavir (test treatment).

Model adaptation for the linagliptin reference treatment. Based on the approach outlined in section 2.5.2.4.3, re-estimating the parameters dissociation constant (ΔOBJF −18.844), lag time (ΔOBJF −16.231), and apparent central volume of distribution (ΔOBJF −21.785) significantly improved the description of the plasma concentrations following the administration of linagliptin reference treatment compared to model M3. The parameters of the thus adapted model M4 in comparison to M3 are presented in Table 3-6. Figure 3-11 illustrates the influence of the parameter adaptation on the description of the linagliptin plasma concentration-time profiles.

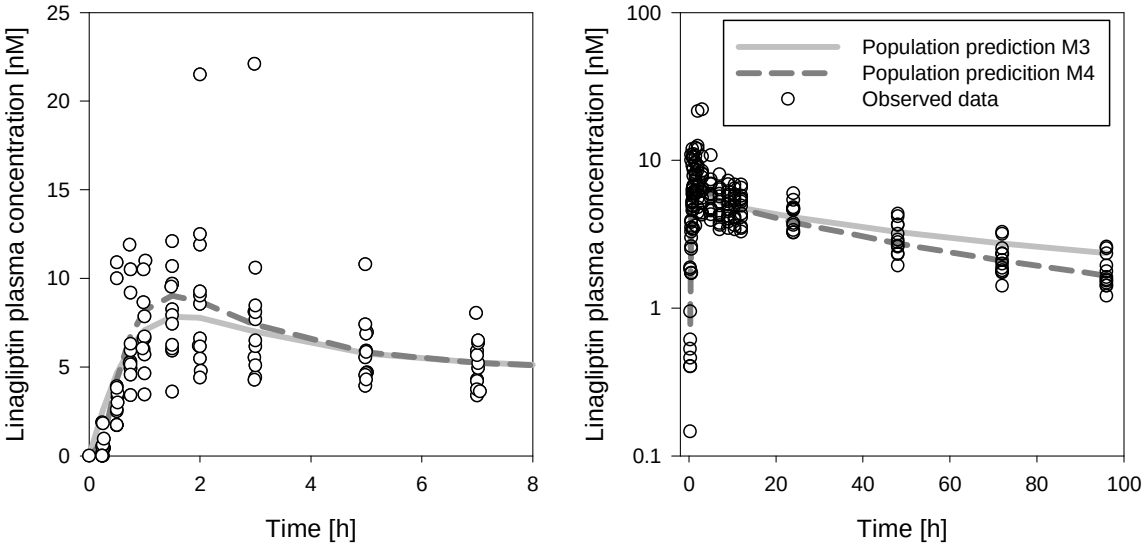

Figure 3-11 Description of the reference treatment of Project 2b using model M3 (previously developed model in Project 1) and the adapted model M4. Straight and dashed lines are the typical profile for model M3 and M4, respectively. The observed plasma concentrations of the reference treatment are presented as open circles.

Model adaptation for the linagliptin test treatment. Re-estimating the parameters relative bioavailability (ΔOBJF −635.374) and lag time (ΔOBJF −55.133) of model M4 resulted in a significantly improved description of the plasma concentrations following the administration of the test treatment. A further decrease in the OBJF of more than 3.84 was estimated for $B_{max,C}$ (ΔOBJF −9.027), K_d (ΔOBJF −7.672), CL (ΔOBJF −7.155) and $A_{max,P}$ (ΔOBJF −4.497). Based only on the OBJF the best model would have been the one with an elevated $B_{max,C}$ when linagliptin was coadministered with ritonavir. However, under ritonavir comedication nearly no metabolite formation was observed. Thus, a decrease in the linagliptin clearance was considered more likely than an increase in $B_{max,C}$. No further decrease in the OBJF of more than 3.84 points was reached when either a separate $B_{max,C}$, K_d, or $A_{max,P}$ was estimated in addition to a separate lag time, bioavailability, and clearance, when linagliptin was coadministered with ritonavir. The parameter estimates of the so adjusted pharmacokinetic model (called M5) are presented in Table 3-6. The influence of the parameter adaptation on the description of the linagliptin plasma concentrations of the test treatment is presented in Figure 3-12.

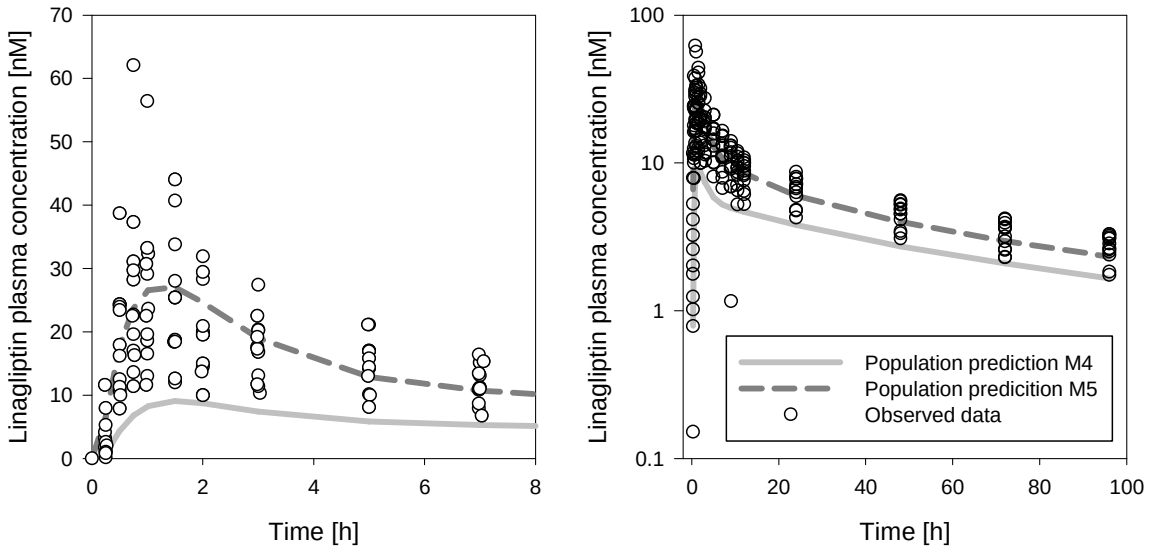

Figure 3-12 Description of the linagliptin plasma concentrations when linagliptin was given together with ritonavir using model M4 (adapted to describe the control group in Project 2b) and model M5 (adapted to describe the treatment group linagliptin plus ritonavir). Straight and dashed lines are the typical profiles for models M4 and M5, respectively. The observed plasma concentrations of the test treatment are presented as open circles.

Testing for interindividual variability in the model parameters. Interindividual variability in F, K_a, $B_{max,C}$ and intercompartmental clearance between central and peripheral compartment (Q_P) improved the description of the individual plasma concentrations of both treatment arms (Table 3-6).

3.2.4.2 Final model

The population pharmacokinetic model of linagliptin developed for Project 2d is based on the previous model M3 (Project 1). To describe the reference treatment adequately, a lag time (0.202 h), a lower apparent central volume of distribution (542 L) and a higher affinity constant (0.106 nM) were estimated. The resulting change in the typical plasma concentration-time profile between M3 and M4 was only small. The elevated plasma concentration-time profiles under ritonavir were best described by estimating a ~4-fold elevated bioavailability, a slightly shorter lag time (0.143 h) and a decrease in the clearance of ~16%. Interindividual variability, implemented on F, K_a, $B_{max,C}$, and Q_P/F, was small to moderate (15.6–44.6%). The residual variability, described by a combined (additive and proportional) residual variability model, was moderate (additive residual variability 0.330 nM, proportional residual variability 21.7%). The parameter estimates of the final

model are presented in Table 3-6. The goodness-of-fit plots in Appendix, Figure 10 suggest an adequate description of the linagliptin plasma concentrations of both treatments.

Table 3-6 Parameter estimates of the structural models M3, M4, and M5 as well as the interindividual variability of the population parameters of the structural model M5

		Original Model M3		Adapted Model M4		Adapted Model M5		Interindividual variability of M5	
	Unit	Estimate	RSE [%]	Estimate	RSE [%]	Estimate	RSE [%]	Estimate	RSE [%]
Typical Parameter									
F	%	100 fix	NA	100 fix	NA	100 fix /394[1)]	NA /11.8[1)]	100/394[1)] fix	NA
K_a	h^{-1}	0.845 fix	NA	0.845 fix	NA	0.845 fix	NA	0.845 fix	NA
ALAG	h	NA	NA	0.202	5.94	0.202 fix /0.143[1)]	NA /24.3[1)]	0.202/ 0.143[1)] fix	NA
V_C/F	L	776 fix	NA	542	17.6	542 fix	NA	542 fix	NA
Q_P/F	L/h	412 fix	NA	412 fix	NA	412 fix	NA	412 fix	NA
V_P/F	L	1650 fix	NA	1650 fix	NA	1650 fix	NA	1650 fix	NA
CL/F	L/h	289 fix	NA	289 fix	NA	289 fix /243[1)]	NA /10.9[1)]	289/243[1)] fix	NA
$B_{max,C}$	nM	4.85 fix	NA	4.85 fix	NA	4.85 fix	NA	4.85 fix	NA
K_d	nM	0.0652 fix	NA	0.106	23.3	0.106 fix	NA	0.106 fix	NA
$A_{max,P}/F$	nmol	1,650 fix	NA	1,650 fix	NA	1,650 fix	NA	1,650 fix	NA
Interindividual Variability									
ωF	CV%	NA	NA	NA	NA	NA	NA	43.2	39.7
ωK_a	CV%	NA	NA	NA	NA	NA	NA	42.8	26.2
ωQ_P	CV%	NA	NA	NA	NA	NA	NA	44.6	47.6
$\omega B_{max,C}$	CV%	NA	NA	NA	NA	NA	NA	15.6	47.3
Residual Variability									
σ_{prop}[2)]	%	39.5	50.3	36.6	32.7	37.1	22.8	21.7	17.9
σ_{add}[2)]	nM	0.590	151.7	0.466	28.7	0.428	44.2	0.330	30.5

1) First value for linagliptin alone, second value for linagliptin in comedication with ritonavir

2) Estimated on log-transformed data

NA, not applicable

3.2.4.3 Model evaluation

The model was evaluated using visual and posterior predictive checks. The visual predictive check displayed an adequate description of the concentration-time profiles by the final model for both treatments (Appendix, Figure 11). The posterior predictive check displayed an adequate description of the $AUC_{0\text{-}inf}$ and C_{max} values for both treatments by the final model with a tendency to slightly overestimate the C_{max} values (Appendix, Figures 12 and 13).

3.2.4.4 Simulation

Using the final population pharmacokinetic model of Project 2d, the impact of ritonavir comedication on the steady-state exposure of linagliptin was simulated. First, the typical concentration-time profiles for 5 mg linagliptin administered once daily either alone or in combination with ritonavir were simulated using M5. Based on the simulated C_{trough} levels, steady-state was reached after ~2 days for both treatments (Figure 3-13). Ritonavir comedication increased the exposure of linagliptin but had no effect on the accumulation ratio of linagliptin. Irrespective of ritonavir comedication, a merely small increase in the predicted exposure for linagliptin treatment after single dose compared to steady-state was predicted (Figure 3-13).

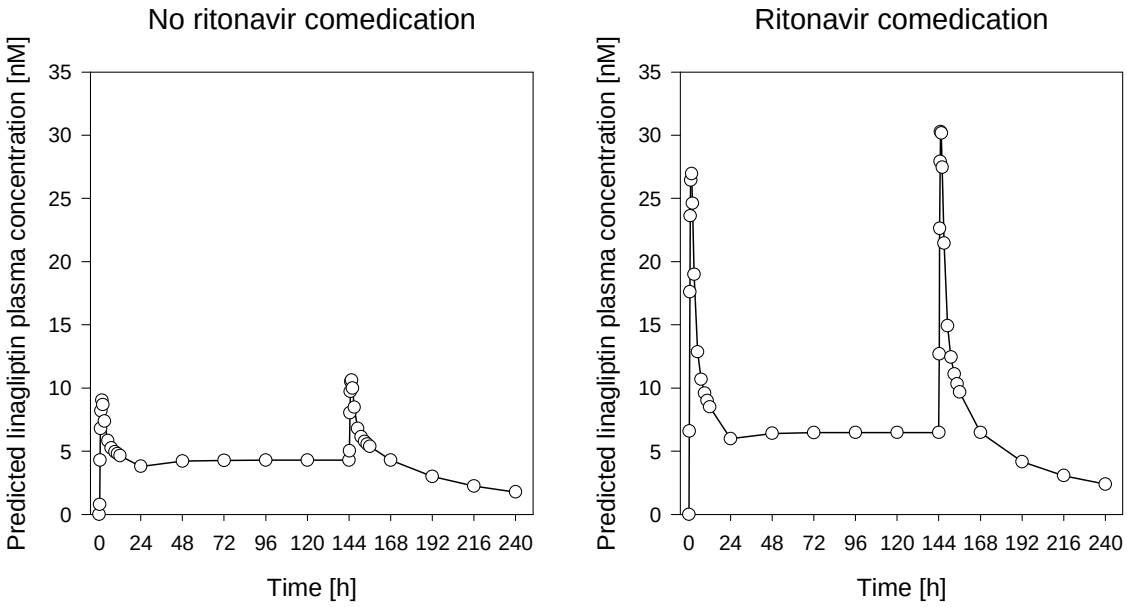

Figure 3-13 Predicted linagliptin plasma concentration-time profiles using the final population pharmacokinetic model of Project 2d for treatment with 5 mg linagliptin administered once daily alone or in combination with ritonavir over seven days. A dense sampling scheme was assumed at day 1 and day 7; at days 2–6, only C_{trough} levels were simulated.

Second, the final population pharmacokinetic model including variability was used to simulate 1,000 $AUC_{\tau,SS}$ and C_{max} values after single dose and at steady-state (day 7) for both treatments. The corresponding gMeans and gCVs are shown in Table 3-7. Based on the AUC, accumulation ratios of 1.20 and 1.13 were predicted by the model for linagliptin administered without and with ritonavir, respectively.

Table 3-7 gMean and gCV of 1,000 predicted AUCτ and C_{max} values for the treatment of linagliptin with and without ritonavir comedication after the first dose and at steady-state

	Linagliptin without ritonavir		Linagliptin with ritonavir	
	First dose (gCV%)	Steady-state (gCV%)	First dose (gCV%)	Steady-state (gCV%)
gMean AUC_{τ} [nM·h]	118 (25)	142 (21)	259 (29)	293 (29)
gMean C_{max} [nM]	10.3 (36)	12.7 (32)	31.7 (45)	35 (41)

3.3 Project 3: Covariate analysis

3.3.1 Project 3a: Pharmacokinetic covariate analysis

The objective of this project was to characterise the nonlinear pharmacokinetics of linagliptin in a larger patient population. The main focus was to investigate the impact of weight, sex, and age on the pharmacokinetics of linagliptin. In addition, other covariates that are of clinical relevance for the pharmacokinetics of linagliptin were to be identified.

The dataset of Project 3a consisted of single dose and steady-state concentration-time profiles of the two phase IIa studies used for Project 1 as well as of two additional phase IIb studies. 462 patients with type 2 diabetes were treated with linagliptin, 302 males and 160 females. The mean age of the population was 59.1 years (56.1, 59.9, 58.1, and 60.2 years per study), ranging from 30–78 years. The mean body mass index was 31.0 kg/m^2 (29.0, 28.8, 31.2, and 31.9 kg/m^2 per study) ranging from 20.4–42.2 kg/m^2. Descriptive statistics of baseline categorical and continuous covariates are shown in Appendix, Tables 7 and 8. Only 0.43% of patients consumed alcohol to an extent that it could interfere with the trial. Also, less than 10% of patients belonged to study I. More than 90% of the patients were Caucasians. Thus, ethnic origin and influence of alcohol consumption were only graphically explored. The ranges of all continuous covariates were relatively wide and thus a robust assessment of their influence was possible. Descriptive statistics of

time-dependent covariates were calculated at baseline and in case of the phase IIb studies also for each visit separately (data not shown). At baseline and at all visits under treatment the descriptive statistics were comparable, indicating that treatment with linagliptin did not significantly influence these covariates. Bivariate scatter plots were prepared to investigate correlations between covariates (Appendix, Figures 14 and 15). No unexpected correlations between covariates were observed.

In total, the dataset of Project 3a consisted of 6,907 linagliptin concentration measurements. For unknown reasons, the phase IIb studies included nine patients with predose linagliptin measurements. These measurements are not plausible and cannot be handled by NONMEM. Therefore, they were removed from this analysis. The distributions of the number of patients and of linaglitin plasma concentrations per dose group are shown in Appendix, Table 9. The distribution of observations and patients per dose group was unbalanced; ~30% of observations and subjects were in the 5 mg treatment group, whereas the 0.5 mg treatment group included merely ~10% of all subjects and observations.

The distribution of linaglitptin plasma concentrations by time after dose per study is shown separately for each dose group in the Appendix, Figure 16. In general, the plasma concentration-time profiles of the phase IIb studies showed higher variability compared to the phase IIa studies. In addition, the linagliptin plasma concentrations were apparently higher for study IV.

3.3.1.1 Model development

3.3.1.1.1 Base model

First, it was tested whether the population pharmacokinetic base model previously developed in Project 1 (called M6 from here onward) could describe the linagliptin plasma concentrations collected during the phase IIb study where linagliptin was given as monotherapy (study III). All parameters were fixed to M6 and individual Bayesian estimates for study III were obtained. The standard goodness-of-fit plots (based on the Bayesian estimates) showed that the linagliptin concentrations of study III could be adequately described by M6 (Appendix, Figure 17). The Bayesian estimates were equally distributed around their typical parameters for F and $B_{max,C}$, whereas the mean of the individual K_a values was lower compared to the previously determined typical parameter for K_a (Appendix, Figure 19, upper panels). In a next step, the model parameters were estimated based on all three studies together. Due to the sparse data from phase IIb, not all model parameters

could be estimated. Therefore, only the typical parameters for which variability was found in M6 (except F which was already fixed to 1 in M6) were estimated. In addition, clearance was estimated as an interesting parameter for the covariate analysis. Hence, the typical parameters for K_a, $B_{max,C}$, CL, and the inter- and intraindividual variabilities as implemented in M6 (η in F, K_a, $B_{max,C}$, and κ in F) were estimated. The parameter estimates for CL and $B_{max,C}$ were very similar to those in M6 (CL: 287 L/h vs. 289 L/h, $B_{max,C}$: 4.77 nM vs. 4.85 nM), whereas K_a was estimated to be slightly lower (0.698 h^{-1} vs. 0.845 h^{-1}).

In a second step, it was tested whether M6 could also describe the linagliptin plasma concentrations of study IV in which linagliptin was given as add-on to metformin. In an exploratory comparison of the pharmacokinetic profiles, a higher exposure was observed for study IV (Appendix, Figure 16). This observation was confirmed when the Bayesian estimates of M6 were investigated for this study: The standard goodness-of-fit plots showed that the linagliptin concentrations were underestimated and could thus not be adequately described by M6 (Appendix, Figure 18). The underprediction by the model was also obvious when investigating the distribution of the Bayesian estimates of study IV around the previously estimated typical parameters. Besides a lower mean of K_a as already observed for study III, higher Bayesian estimates for F and $B_{max,C}$ were obtained compared to the typical parameters of the previous studies I and II (Appendix, Figure 19, lower panels).

When permitting a separate clearance for study IV, this clearance was estimated to be lower than for the other three studies (210 L/h compared to 290 L/h). In addition there was a clear trend towards a higher individual relative bioavailability (high ETABAR-value, indicating that the arithmetic mean of η-estimates (i.e. ETABAR) is not zero). When estimating a separate F for study IV, the relative bioavailability was estimated to be increased by 51% in study IV. The η-distributions of all parameters as well as the goodness-of-fit plots were adequate. The model assuming a separate relative bioavailability for study IV decreased the OBJF by 32.546 points more than the model assuming a separate apparent clearance for study IV. Thus, the higher exposure in study IV was accounted for by estimating a separate bioavailability for this study. During the covariate analysis it was further investigated whether another parameter was needed to be adapted for study IV.

When phase IIa and phase IIb studies were analysed together, higher interindividual (e.g. ωK_a increased from 58% to 87%) and intraindividual variabilities (πF increased from 33% to 55%) as well as higher random residual variability (26.9% compared to 14.1% in M6)

were estimated compared to M6. As the plasma concentrations of the phase IIb studies suggested a higher residual variability than those of the phase IIa studies (Appendix, Figure 16), a separate residual variability dependent on the type of studies was estimated. A drop in the OBJF by 2256.997 points supported this decision. Interindividual variability in CL, V_C, and volume of distribution of the peripheral compartment (V_P) was investigated in addition to the variability already implemented in M6 (i.e. η in F, K_a, $B_{max,C}$, and κ in F). Adding variability on CL and V_C led to a significant decrease in the OBJF and was therefore kept in the model. Diagonal elements of the variance-covariance matrix of interindividual random effects (Ω-matrix) were estimated first. Based on graphical analysis a correlation between the individual F and CL was found. Thus covariance between both parameter was included in the model. The parameter estimates of the base model are presented in the Appendix, Table 10.

3.3.1.1.2 Covariate selection

In the next step a covariate analysis was conducted. Due to η-shrinkage (27% F, 35% CL, 22% K_a, 24% $B_{max,C}$, 58% V_C) the results of the explorative and GAM analyses needed to be regarded with caution as both methods are based on the Bayesian η-estimates (158). Appendix, Table 11 presents the covariates pre-selected by exploratory analysis and GAM analysis, the covariates pre-defined to be tested in NONMEM as well as the covariates that remained in the model after the forward inclusion and backward elimination procedure performed separately per model parameter. The latter, i.e. the remaining covariates (weight on relative bioavailability, formulation and dose group on rate of absorption, gamma-glutamyl transferase on unbound clearance, weight on central volume of distribution, as well as pre-dose DPP-4 activity, dose, age, and sex on the concentration of central binding partner) were tested together in one run. Again, a backward elimination was performed where the covariates were individually eliminated from the model. The OBJF increased less than 10.8 points for weight on volume (ΔOBJF +0.135), gamma-glutamyl transferase on clearance (ΔOBJF +2.284) and sex on $B_{max,C}$ (ΔOBJF +8.695). In addition, for these three covariates the typical parameter describing the covariate-parameter relationship decreased. In the case of weight on volume, there was even a switch from a positive to a negative correlation, indicating that the effect of weight on volume was no longer meaningful. For all other covariates, the typical parameters describing the covariate effect stayed

within the range of the previously estimated value when the covariates were tested individually per parameter.

Based on these results, weight on the apparent central volume of distribution was not included in the final model, because weight was already implemented on the bioavailability and was therefore not required on V_C. During the backward elimination process, gamma-glutamyl transferase on clearance and sex on $B_{max,C}$ did not reach a statistically significant effect. Nevertheless, they were kept in the model as the corresponding runs did not converge properly and could therefore not be considered as final models.

3.3.1.2 Final model

The linagliptin plasma concentrations of both phase IIa and both phase IIb studies were adequately described by a model that takes the binding of linagliptin to its target DPP-4 into account. To describe the pharmacokinetic profiles of study IV (add-on to metformin study) adequately, a separate, significantly elevated relative bioavailability was estimated for this study. During the covariate analysis the following covariates were also found to be statistically significant: F decreased with increasing weight; the formulation and the dose group showed a statistically significant influence on the rate of absorption; the unbound clearance was slightly decreased in case of increased gamma-glutamyl transferase; the model-calculated concentration of the central binding partner was influenced by the pre-dose DPP-4 activity, dose, age, and sex.

Compared to the base model, the variability in the η-parameters only decreased for K_a (76.4% compared to 87.6%) and $B_{max,C}$ (15.0% compared to 29.6%) and was in the same range for F, clearance and V_C, showing that only a small part of the interindividual variability can be explained by these covariates. To finalise the model building process, the necessity to account for intraindividual variability and covariance was re-evaluated. Since the intraindividual variability did not decrease (base model 39.2%, final model 40.0%) and since the correlation between F and CL did not decrease (base model −0.704, final model −0.765) it was concluded that the necessity to account for the intraindividual variability and variance-covariance still existed. The parameter estimates of the final model are given in Table 3-8. The standard goodness-of-fit plots display an adequate description of the plasma concentrations (Appendix, Figure 20).

Table 3-8 Parameter estimates of the final population pharmacokinetic model of Project 3a

	Unit	Estimate	Description
Typical Parameter			
F	%	100 fix	Typical relative bioavailability
$F_{study\ IV}$	%	169	Typical relative bioavailability in study IV (metformin comedication) relative to F
weight_F[1)]	%	-0.00958	% change in F per kg change from the median weight of the population
$K_{a,PIB}$	h^{-1}	0.933	Typical absorption rate constant for the powder in bottle formulation
$K_{a,T1}$	h^{-1}	0.795	Typical absorption rate constant for the tablet 1 formulation
$K_{a,T2}$	h^{-1}	0.441	Typical absorption rate constant for the tablet 2 formulation
Dose_K_a [2)]	%	-0.0651	% change in K_a per dose unit change from the 5 mg dose group
V_C/F	L	715	Typical central volume of distribution
Q_P/F	L/h	412 fix	Typical inter-compartmental clearance between central compartment and peripheral compartment
V_P/F	L	1,650 fix	Typical volume of distribution of the peripheral compartment
CL/F [L/h]	L/h	258	Typical clearance of the unbound concentration
GGT_CL[3)]	%	-0.0339	% change in CL/F per U/L change from the median gamma-glutamyl transferase of the population
$B_{max,C}$	nM	4.97	Typical concentration of binding partner in the central compartment (male)
DPP_ $B_{max,C}$ [4)]	%	0.00332	% change in $B_{max,C}$ per RFU change from the median pre-dose DPP-4 activity of the population
dose_ $B_{max,C}$ [4)]	%	3.41	% change in $B_{max,C}$ per dose unit change from the 5 mg dose group
age_ $B_{max,C}$ [4)]	%	0.561	% change in $B_{max,C}$ per year change from the median age of the population
sex_ $B_{max,C}$ [4)]	nM	0.457	Absolute change in $B_{max,C}$ between males and females
K_d	nM	0.0652 fix	Typical affinity constant of the saturable binding
$A_{max,P}$/F	nmol	1,650 fix	Typical amount of binding partner in the peripheral compartment

Table 3-8 Parameter estimates of the final population pharmacokinetic model of Project 3a (cont.)

	Unit	Estimate	Description
Inter-and intraindividual variability			
ωF	CV%	47.4	Interindividual variability in the relative bioavailability
Corr F_CL		-0.765	Correlation between ωF and ωCL
ωCL	CV%	27.5	Interindividual variability in the clearance of the unbound concentration
ωK_a	CV%	76.4	Interindividual variability in the absorption rate constant
ωV_C	CV%	24.4	Interindividual variability in the central volume of distribution
$\omega B_{max,C}$	CV%	15.0	Interindividual variability in the concentration of central binding partner
πF	CV%	40.0	Intraindividual variability in the absolute bioavailability
Residual variability			
$\sigma_{prop,\ phase\ IIa}$ [5)]	%	13.6	Residual variability phase IIa
$\sigma_{prop,\ phase\ IIb}$ [5)]	%	38.3	Residual variability phase IIb

1) $F_{io} = F \cdot (1+weight\_F \cdot (weight-88)) \cdot \exp(\eta F + \kappa F)$

2) $K_{ai} = K_a \cdot (1+dose\_K_a \cdot (dose-5)) \cdot \exp(\eta K_a)$

3) $CL_i = CL \cdot (1+GGT\_CL \cdot (GGT-33)) \cdot \exp(\eta CL)$

4) $B_{max,C,i} = (B_{max,C}+sex\_B_{max,C} \cdot sex) \cdot (1+DPP\_B_{max,C} \cdot (DPP-12497)) \cdot (1+dose\_B_{max,C} \cdot (dose-5)) \cdot (1+age\_B_{max,C} \cdot (age-60)) \cdot \exp(\eta B_{max,C})$

5) Estimated on log-transformed data

3.3.1.3 Model evaluation

The visual predictive check displayed an adequate description of the linagliptin concentrations by the base model. In the Appendix, Figure 21, the description of the pharmacokinetic profiles at steady-state per dose group and study, respectively, are shown.

The posterior predictive check showed an adequate description of the C_{trough} and C_{max} levels by the final model. In the Appendix, Figures 22 and 23, the simulated distributions of the median C_{trough} and C_{max} levels at steady-state per dose group are shown. The median C_{trough} and C_{max} levels per dose group are well described and lie within the 90% confidence interval. The only exceptions were the C_{max} values of the lowest (0.5 mg) and highest (10 mg) dose groups, which were slightly out of the 90% confidence interval.

3.3.1.4 Simulation

The statistically significant covariates were evaluated for their influence on the pharmacokinetics of linagliptin. The impact of the different covariates on the $AUC_{\tau,SS}$ after a once daily administration of 5 mg linagliptin was <20% for each covariate individually (Table 3-9). In comparison to the overall variability in the plasma concentration-time profiles the impact of weight, age and sex was very small (Figure 3-14). In the two worst-case scenarios, i.e. (a), an old (73 years), low-weight (67 kg), female patient on metformin medication with high gamma-glutamyl transferase (158 U/L) and high pre-dose DPP-4 activity (18,623 RFU), or (b), a young (42 years), high-weight (117 kg), male patient with low gamma-glutamyl transferase (9.4 U/L) and low pre-dose DPP-4 activity (8,025 RFU), the exposure increased or decreased by only 63% or 26%, respectively.

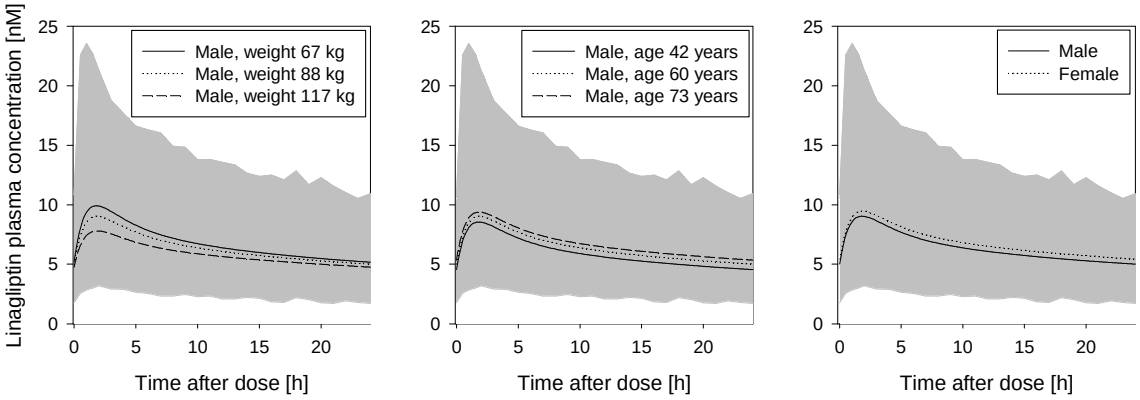

Figure 3-14 Impact of the covariates weight, age and sex on the linagliptin plasma concentration-time profiles after administration of 5 mg linagliptin once daily in comparison to the overall variability (grey shaded area). The overall variability was determined as the 90% confidence interval of 1,000 simulated concentration-time profiles based on the base population pharmacokinetic model of Project 3a.

Table 3-9 Predicted covariate influence on $AUC_{\tau,SS}$ after administration of 5 mg linagliptin once daily

Model Parameter	Covariate	Category	$AUC_{\tau,SS}$ [nM·h]	% difference
F	Study IV (metformin comedication)	No	154.23	NA
		Yes	184.81	+19.8
	Weight	5th percentile (67 kg)	163.38	+5.9
		Mean (88 kg)	154.23	NA
		95th percentile (117 kg)	140.9	-8.7
K_a	Formulation	1	153.66	-0.4
		2	153.75	-0.3
		3	154.23	NA
	Dose	0.5	153.99	-0.2
		5	154.23	NA
		10	154.67	+0.4
$B_{max,C}$	Pre-dose DPP-4 activity	5th percentile (8025 RFU)	137.4	-10.9
		Mean (12497 RFU)	154.23	NA
		95th percentile (18623 RFU)	177.3	+15.0
	Dose	0.5	136.8	-11.3
		5	154.23	NA
		10	173.6	+12.5
	Age	5th percentile (42 years)	142.8	-7.4
		Mean (60 years)	154.23	NA
		95th percentile (73 years)	162.5	+5.4
	Sex	Male	154.23	NA
		Female	164.65	+6.8
CL	Gamma-glutamyl transferase	5th percentile (9.4 U/L)	153.84	-0.25
		Mean (33 U/L)	154.23	NA
		95th percentile (158 U/L)	156.38	+1.4

NA, not applicable

3.3.2 Project 3b: Pharmacodynamic covariate analysis

The objectives of this analysis were to characterise the relationship between linagliptin plasma concentration and the plasma DPP-4 activity in type 2 diabetic patients and to identify clinically relevant covariates impacting this correlation.

The database of Project 3b consisted of the four studies used in Project 3a. 607 patients with type 2 diabetes were included. The mean age of the population was 59.2 years, ranging from 30–78 years, and the mean body mass index was 31.0 kg/m^2 ranging from 20.4–42.2 kg/m^2. Descriptive statistics of categorical and continuous covariates using baseline values are shown in the Appendix, Tables 12 and 13. For the reasons described in Project 3a, the influence of ethnic origin and alcohol consumption were only tested in an explorative manner. The ranges for all continuous covariates were relatively wide and thus a robust assessment of their influence was possible. Bivariate scatter plots were carried out to investigate correlations between covariates (Appendix, Figures 24 and 25). No unexpected correlations between the covariates were observed.

The dataset included 9,674 plasma DPP-4 activities and linagliptin plasma concentrations, respectively, from 607 type 2 diabetic patients. The distribution of the number of patients and the number of observations is given in the Appendix, Table 14. The distribution was unbalanced, as most patients were randomised to either placebo or 5 mg linagliptin. The DPP-4 activity correlated well with the linagliptin plasma concentration (Figure 3-15).

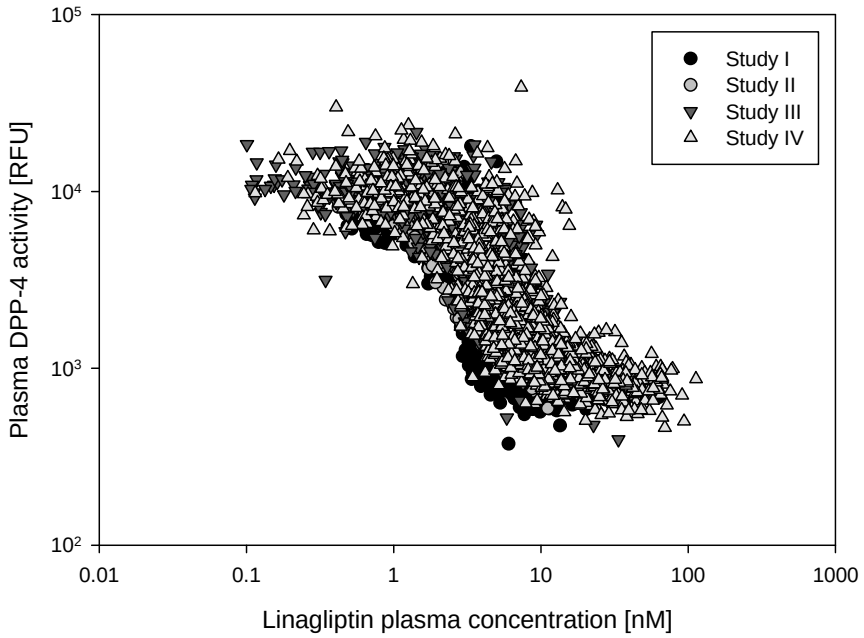

Figure 3-15 Correlation of linagliptin plasma concentration and plasma DPP-4 activity in studies I, II, III, and IV. Placebo and pre-dose observations not shown due to logarithmic scale.

3.3.2.1 Model development

3.3.2.1.1 Base model

A simple E_{max} model and a sigmoid E_{max} model were tested. The sigmoid E_{max} model performed significantly better (ΔOBJF −6,399.422). Interindividual variability was tested sequentially on all model parameters. It was found that interindividual variability in pre-dose DPP-4 activity (BSL) and EC_{50} improved the model fit. Both parameters showed moderate interindividual variability with 21.6% in BSL and 18.4% in EC_{50}. The individual BSL and EC_{50} values were correlated. It was assumed that this correlation is physiologically plausible. The more DPP-4 molecules are available the more linagliptin molecules are needed to reduce 50% of the DPP-4 activity. Previous analyses showed a good correlation between baseline plasma DPP-4 activity and plasma DPP-4 concentration (data not shown). Thus, pre-dose DPP-4 activity can be used as a correlate for DPP-4 concentration. The higher the pre-dose DPP-4 activity, the higher is the DPP-4 concentration which in consequence results in a higher EC_{50} value. Implementing this correlation like a covariate effect of BSL on EC_{50} in the model was significantly better than estimating a correlation between BSL and EC_{50} using the block option (ΔOBJF −75.928). Furthermore, it is advantageous that the covariates that impact the EC_{50} value solely through their effect on pre-dose DPP-4 activity need only be accounted on the pre-dose DPP-4 activity and not on the EC_{50} value. For these reasons, the pre-dose DPP-4 activity was implemented on the EC_{50} value like a covariate effect:

$$EC_{50i} = EC_{50} \cdot (1 + BSL\_EC_{50} \cdot (BSL_i - 11600)) \cdot \exp(\eta_{EC50}) \qquad \text{(Equation 3-1)}$$

In this equation EC_{50i} is the individual EC_{50} parameter which depends on the typical EC_{50} parameter, the typical covariate effect parameter BSL_EC_{50}, the difference between the individual predicted baseline estimate (BSL_i) and the typical baseline value of 11,600 RFU, as well as the interindividual variability of EC_{50} $\eta(EC_{50})$.

The residual variability was adequately described by a proportional residual variability model and was estimated to be 15.7%. The parameter estimates of the base model are presented in the Appendix, Table 15.

3.3.2.1.2 Covariate selection

The covariates selected in the different steps of the covariate analysis are depicted in the Appendix, Table 16. Even though some covariates were found to be significant by the

forward inclusion and backward elimination procedure they were not kept in the model for the following reasons:

There was a study difference in baseline DPP-4 activity as well as in EC_{50}. The baseline DPP-4 activity was 10.3% lower in study II. EC_{50} was estimated to be 2.68 nM in study II, 2.85 nM in study I, and 3.12 nM in studies III and IV. These interstudy differences could not be explained by any of the tested covariates, and were not regarded to be relevant and thus were not included into the final model.

Alanine transaminase and aspartate transaminase both significantly contributed to a better description of the linagliptin plasma concentrations when implemented on the baseline DPP-4 activity. However, as both liver enzymes were highly correlated (Appendix, Figure 25), and the covariate effect of aspartate transaminase was estimated only imprecisely (RSE 69.1%), only alanine transaminase was included into the final model.

Asian ethnicity was not kept in the final model as a covariate on baseline DPP-4 activity because of the small sample size (eleven patients, representing less than 2% of the population). However, for these few patients a significantly higher baseline DPP-4 activity of 13,200 RFU was estimated compared to 10,600 RFU of the residual population. It should be further evaluated whether Asian patients have higher baseline DPP-4 activities.

3.3.2.2 Final model

The correlation between linagliptin plasma concentrations and plasma DPP-4 activity was best described by a sigmoid E_{max} model. The correlation between the individual EC_{50} and BSL values was taken into account by assuming a covariate effect of the individual BSL values on EC_{50}. The final model included a covariate effect of gamma-glutamyl transferase, alanine transaminase, fasting plasma glucose, triglycerides, cholesterol and sex on the baseline DPP-4 activity as well as an additional effect of triglycerides on the EC_{50} parameter. The influence of gamma-glutamyl transferase on baseline was implemented as a hockey-stick function: baseline increased linearly with gamma-glutamyl transferase concentration until a breakpoint of 175 U/L gamma-glutamyl transferase was reached. Beyond the breakpoint, the baseline was constant and elevated by 21.3% compared to the typical baseline DPP-4 activity. The breakpoint was chosen by log-likelihood profiling.

Interindividual variability was reduced compared to the base model (16.9% versus 21.6% for BSL and 15.4% versus 18.4% for EC_{50}). In addition, a smaller residual variability was estimated compared to the base model (14.8% versus 15.7% in the base model). The

parameter estimates of the final model are given in Table 3-10. All parameters were estimated precisely. As demonstrated by the standard goodness-of-fit plots (Appendix, Figure 26), the model described the DPP-4 activities adequately, except for two extreme DPP-4 activity data points of one patient which could not be properly described.

Table 3-10 Parameter estimates of the final population pharmacokinetic/pharmacodynamic model of Project 3b

	Unit	Estimate	RSE [%]	Description
Typical Parameters				
$BSL_{,male}$	RFU	10,700	1.08	Typical baseline DPP-4 activity for males
BSL_{female}[1]	RFU	11,565	20.5	Typical baseline DPP-4 activity for females
E_{max}	%	92.4	0.12	Typical maximum decrease in DPP-4 activity
EC_{50}	nM	3.06	1.56	Typical linagliptin concentration that leads to 50% of maximum decrease in DPP-4 activity
Hill		3.22	1.82	Typical hill coefficient
BSL_EC_{50}[3]	%	0.00792	7.98	% change in EC_{50} per RFU change from the median baseline DPP-4 activity of the population
GGT_BSL[2]	%	0.153	20.39	% change in pre-dose DPP-4 activity per U/L change from the median baseline gamma-glutamyl transferase of the population until 175 U/L
GGT_BSL[2]	%	21.3	18.5	% change in pre-dose DPP-4 activity if gamma-glutamyl transferase > 175 U/L
ALT_BSL[2]	%	0.175	18.5	% change in pre-dose DPP-4 activity per U/L change from the median baseline alanine transaminase of the population
FPG_BSL[2]	%	1.46	12.3	% change in pre-dose DPP-4 activity per mM change from the median baseline fasting plasma glucose of the population
TRIG_BSL[2]	%	0.0294	13.9	% change in pre-dose DPP-4 activity per mg/dL change from the median baseline triglycerides of the population
CHOL_BSL[2]	%	0.0261	43.7	% change in pre-dose DPP-4 activity per mg/dL change from the median baseline cholesterol of the population
TRIG_EC_{50}[3]	%	-0.0153	13.1	% change in EC_{50} per mg/dL change from the median baseline triglycerides of the population

Table 3-10 Parameter estimates of the final population pharmacokinetic/pharmacodynamic model of Project 3b (cont.)

	Unit	Estimate	RSE [%]	Description
Interindividual variability				
ωBSL	CV%	16.9	7.61	Interindividual variability in the baseline DPP-4 activity
ωEC_{50}	CV%	15.4	15.8	Interindividual variability in the EC_{50}
Residual variability				
σ_{prop}	%	14.8	6.64	Residual variability

1) Estimated as BSL_{male}+865 RFU

2) $BSL_i = BSL \cdot (1+GGT\_BSL \cdot (GGT-32.3)) \cdot (1+ALT\_BSL \cdot (ALT-28.8)) \cdot (1+FPG\_BSL \cdot (FPG-8.90)) \cdot (1+TRIG\_BSL \cdot (TRIG-160)) \cdot (1+CHOL \cdot (CHOL-183)) \cdot \exp(\eta BSL)$
if GGT>175: $BSL_i = BSL \cdot (1+GGT\_BSL2)) \cdot (1+ALT\_BSL \cdot (ALT-28.8)) \cdot (1+FPG\_BSL \cdot (FPG-8.90)) \cdot (1+TRIG\_BSL \cdot (TRIG-160)) \cdot (1+CHOL \cdot (CHOL-183)) \cdot \exp(\eta BSL)$

3) $EC_{50i} = EC_{50} \cdot (1+BSL\_EC_{50} \cdot (BSL_i-11600)) \cdot (1+TRIG\_EC_{50} \cdot (TRIG-160)) \cdot \exp(\eta EC_{50})$

3.3.2.3 Simulation

The statistically significant covariates were evaluated for their influence on the EC_{50}, as well as on the concentration leading to 80% DPP-4 inhibition ($EC_{80\%}$)[2]. The individual impact of the different continuous covariates on both parameters was <20% (Table 3-11). Regarding the categorical covariate sex, females had higher EC_{50} and $EC_{80\%}$ values compared to males (3.05 nM versus 2.84 nM, and 5.44 nM versus 5.07 nM, respectively). Even the two worst-case scenarios, i.e. (a), high gamma-glutamyl transferase (139 U/L), high alanine transaminase (64.7 U/L), high fasting plasma glucose (13 mM), high triglycerides (439 mg/dL), high cholesterol (278 mg/dL), and female, or (b), low gamma-glutamyl transferase (10.9 U/L), low alanine transaminase (9.6 U/L), low fasting plasma glucose (5.9 mM), low triglycerides (59.8 mg/dL), low cholesterol (100 mg/dL), and male, led to a minimum EC_{50} value of 2.49 nM and to a maximum EC_{50} value of 4.14 nM ($EC_{80\%}$: minimum 4.44 nM and maximum 7.38 nM), respectively.

[2] 80% DPP-4 inhibition was shown to be maximally effective for glucose lowering. Therefore, the linagliptin concentration resulting in 80% DPP-4 inhibition is of interest. $EC_{80\%}$ is not the same as EC_{80}, the concentration leading to 80% of the maximum effect, as the maximum effect is 92,4% and not 100%.

Table 3-11 Impact of the statistically significant covariates on the EC_{50} and the $EC_{80\%}$ for continuous covariates using the 5th and 95th percentiles of the covariate distribution

	Extreme covariate value		Impact of extreme covariate value on EC_{50} (absolute)		Difference [%]	Impact of extreme covariate value on $EC_{80\%}$ (absolute)		Difference [%]
Percentiles	5th	95th	5th	95th		5th	95th	
Gamma-glutamyl transferase [U/L]	10.9	139	2.76	3.27	16.7	4.92	5.83	16.7
Alanine transaminase [U/L]	9.6	64.7	2.75	3.00	8.2	4.92	5.36	8.1
Fasting plasma glucose [mM]	5.9	13	2.73	3.00	8.8	4.87	5.35	9.0
Triglycerides [mg/dL]	59.8	439	2.81	2.92	3.6	5.01	5.21	3.7
Cholesterol [mg/dL]	100	278	2.79	2.91	3.9	4.97	5.19	4.0

3.4 Project 4: Estimation of the absolute bioavailability of linagliptin

In Project 4, the mean age of the 28 healthy male volunteers was 39.4 years (range: 26–50 years) and the mean body mass index was 25.0 kg/m^2 (range: 18.9–29.4 kg/m^2). One subject was Afro-American, the other 27 subjects were Caucasians.

The dataset comprised 862 linagliptin plasma concentrations from healthy volunteers treated with a single dose of linagliptin administered either orally or intravenously. No subject or concentration was excluded from the analysis. Appendix, Table 17 shows that the distribution of healthy volunteers and concentrations per dose group correspond to the study design. The plasma concentration-time profiles of linagliptin after intravenous administration of 0.5, 2.5, 5, and 10 mg linagliptin increased less than dose-proportionally (Figure 3-16). The variability of linagliptin plasma concentrations after intravenous administration was very small in all dose groups (Figure 3-16), whereas linagliptin exhibited a moderate variability after oral administration (Figure 3-17).

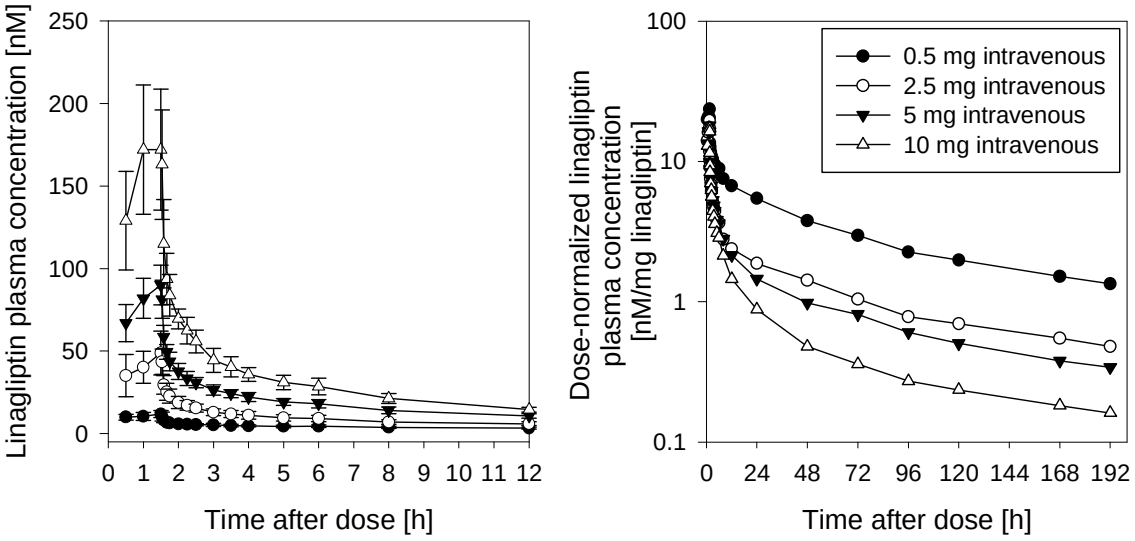

Figure 3-16 Arithmetic mean (±SD) (left panel) and dose-normalised arithmetic mean (right panel) plasma concentration-time profiles of linagliptin after intravenous administration of 0.5, 2.5, 5, and 10 mg linagliptin.

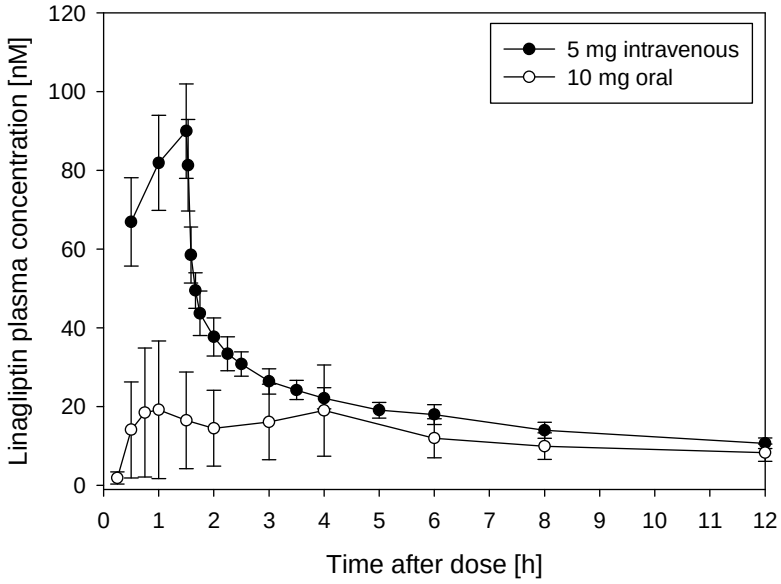

Figure 3-17 Arithmetic mean (±SD) of plasma concentration-time profiles of linagliptin after the administration of 5 mg linagliptin intravenously and 10 mg linagliptin orally.

Due to the nonlinear pharmacokinetics of linagliptin, the standard approach to determine the absolute bioavailability led to dose-dependent estimates. Dividing the dose-normalised $AUC_{p.o.}$ of 10 mg linagliptin by the dose-normalised $AUC_{i.v.}$ of the four different doses resulted in mean values of 12.0% for 0.5 mg, 30.7% for 2.5 mg, 40.3% for 5 mg, and

68.3% for the 10 mg dose. The dose-dependent estimates of the bioavailability illustrate the inappropriateness of this approach for the given data.

3.4.1 Model development

The model development was performed in a stepwise manner. Initially, the plasma concentrations after intravenous administration were analysed separately, then the plasma concentrations after oral administration were included and both datasets were evaluated simultaneously to estimate the absolute bioavailability.

Linear one-, two-, and three-compartment models did not allow a description of the linagliptin plasma concentration-time profiles after intravenous administration of 0.5, 2.5, 5, and 10 mg linagliptin. The fits of all three compartment models were significantly improved by implementing concentration-dependent binding in the central compartment (ΔOBJF −981.577, −802.743, and −795.454 for a one-, two-, and three-compartment model, respectively). Of the models including concentration-dependent binding in the central compartment, a three compartment model performed best (ΔOBJF −249.835 compared to a two compartment model with concentration-dependent binding). Incorporating concentration-dependent binding also in one of the peripheral compartments further led to a significantly better description of the plasma concentrations (ΔOBJF −73.820). This three-compartment model with binding in the central and one peripheral compartment performed significantly better than a two-compartment model with binding in the central and one peripheral compartment (ΔOBJF −216.477). Interindividual variability after intravenous administration was low (Figure 3-16). Addition of interindividual variability on the pharmacokinetic parameters, e.g. CL resulted in a skewed distribution of the individual parameters in the 0.5 mg treatment group and was therefore not implemented. Inclusion of additional nonlinear processes which might be the reason for this observation, e.g. saturable elimination, did not improve the model significantly (ΔOBJF −1.683; parameters for the saturable elimination could only be estimated imprecisely (RSE >145%)). Thus, no interindividual variability was implemented on the disposition parameters.

In the next step, the plasma concentrations after oral administration were included in the analysis. When the disposition parameter were fixed to the typical values of the intravenous model and the absorption was modelled as a first-order process with lag time, the linagliptin plasma concentrations could be described adequately. In addition, when

estimating the model parameters simultaneously using linagliptin plasma concentrations after intravenous and oral administration, the disposition parameter estimates remained nearly identical (Table 3-12). Including interindividual variability for all absorption parameters sequentially was possible and improved the description of the plasma concentrations after oral administration. Therefore, interindividual variability was included for the absorption parameters.

3.4.2 Final model

The plasma concentrations after intravenous and oral administration were best described by a three-compartment model accounting for concentration-dependent binding of linagliptin in the central and one peripheral compartment. The structure of the final model is depicted in Figure 3-18. The model parameters are given in Table 3-12.

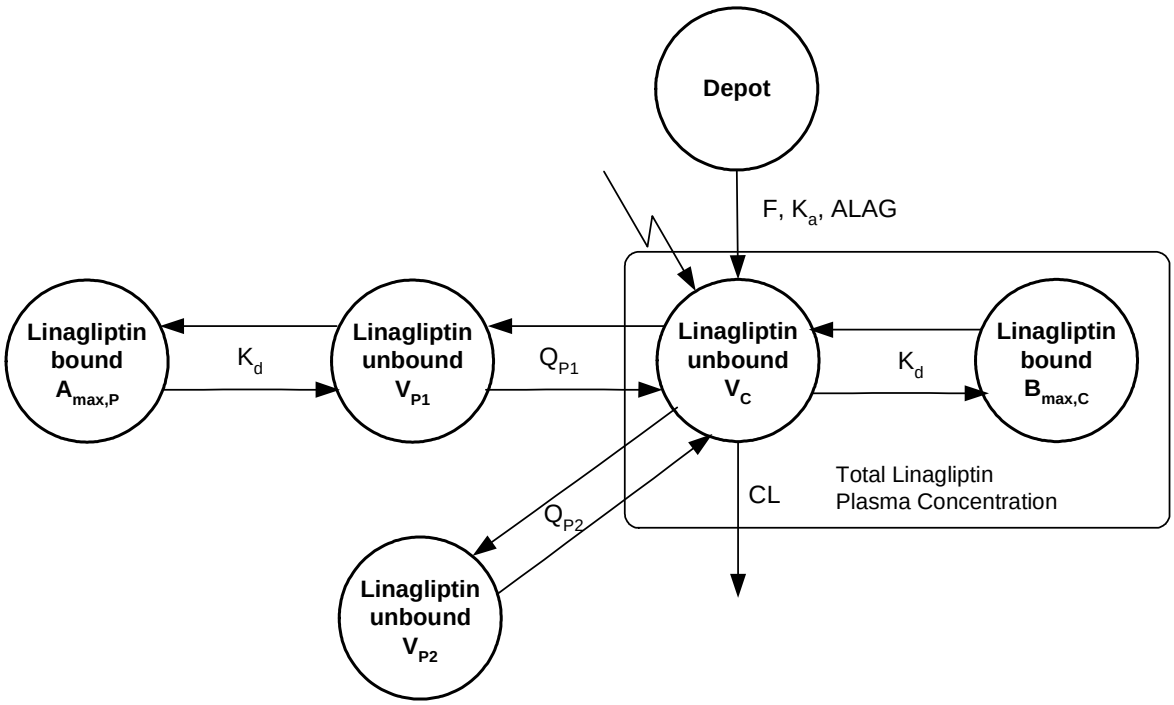

Figure 3-18 Structure of the final pharmacokinetic model of Project 4. F, absolute bioavailability; K_a, absorption rate constant; ALAG, lag time; V_C, central volume of distribution; V_{P1}, volume of distribution of the peripheral compartment 1; Q_{P1}, intercompartmental clearance between central and peripheral compartment 1; V_{P2}, volume of distribution of the peripheral compartment 2; Q_{P2}, intercompartmental clearance between central and peripheral compartment 2; CL, clearance; $B_{max,C}$, concentration of binding partner in the central compartment; $A_{max,P}$, amount of binding partner in the peripheral compartment 1; K_d, dissociation constant. See Figure 3-2 for details.

Table 3-12 Parameter estimates of the population pharmacokinetic models of Project 4

		Population pharmacokinetic model (i.v.)		Population pharmacokinetic model (i.v. and p.o.)	
	Unit	Estimate	RSE [%]	Estimate	RSE [%]
Typical parameter					
F	%	NA	NA	29.5	14.7
ALAG	h	NA	NA	0.234	8.50
K_a	h^{-1}	NA	NA	0.187	27.2
V_C	L	15.0	7.13	15.8	7.66
Q_{P1}	L/h	23.5	9.91	24.3	10.0
V_{P1}	L	291	14.7	293	14.0
Q_{P2}	L/h	70.7	5.46	69.9	5.42
V_{P2}	L	93.8	10.6	93.4	10.2
CL	L/h	26.6	7.86	26.9	7.96
$B_{max,C}$	nM	3.26	11.2	3.44	9.74
K_d	nM	0.0763	10.5	0.0835	11.8
$A_{max,P}$	nmol	437	27.5	548	20.8
Interindividual variability					
ωF	CV%	NA	NA	46.7	34.0
ωALAG	CV%	NA	NA	82.0	29.1
ωK_a	CV%	NA	NA	27.6	66.9
Residual variability					
σ_{prop} [1)]	%	16.6	5.28	17.6	5.14
σ_{add} [1)]	nM	0.277	21.3	0.255	27.3

1) Estimated on log-transformed data

NA, not applicable

All typical parameters could be estimated precisely (RSE ranging from 5.42–20.8%). The concentration of binding partners in the central compartment was 3.44 nM, the dissociation constant for the concentration-dependent binding was 0.0835 nM. The unbound apparent volume of distribution at steady-state was 402.2 L, indicating an extensive DPP-4 independent distribution of linagliptin. The clearance of unbound linagliptin was high (26.9 L/h). Interindividual variability, estimated on the absorption parameters bioavailability, rate constant of absorption, and lag time, was moderate to high (28–82%). The

standard goodness-of-fit plots showed that the model performed adequately (Appendix, Figure 27). For the 10 mg linagliptin dose group the absolute bioavailability estimated by the model was 29.5%, with a high inter-individual variability of 46.7% (range: 12.9–60.8%).

3.4.3 Model evaluation

The visual predictive check presented in the Appendix, Figure 28 demonstrated that the model adequately described the plasma concentrations after oral and intravenous administration of all dose groups.

3.5 Project 5: Model-based pharmacokinetic analysis of linagliptin in wildtype and DPP-4-deficient rats

The objective of Project 5 was to test the impact of concentration-dependent binding of linagliptin to its target DPP-4 on the pharmacokinetics of linagliptin using plasma concentrations from wildtype and DPP-4-deficient rats.

The mean animal weights per dose group and rat strain were comparable (Appendix, Table 18). The dataset included 182 linagliptin plasma concentrations of 28 animals determined after single intravenous administration of 0.01, 0.1, 0.3, or 1.0 mg/kg linagliptin. Each of the four dose groups contained four wildtype and four DPP-4-deficient rats, except for the lowest dose group (0.01 mg/kg) in which only wildtype rats were included. The distribution of observations per dose group and rat strain is summarised in Appendix, Table 19. The number of observations is equally distributed between the dose groups, but it tends to be lower in DPP-4-deficient rats, as for most of these rats linagliptin concentrations after 24 h were below the limit of quantification. No observation was excluded from the analysis. The linagliptin plasma concentration-time profiles of both rat strains are depicted in Figure 3-19.

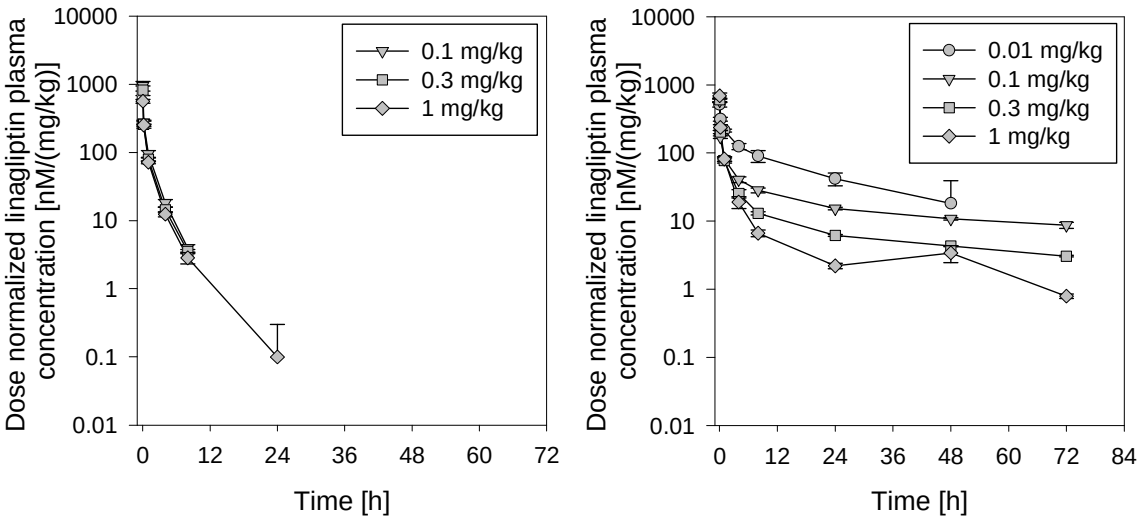

Figure 3-19 Mean (±SD) of dose-normalised linagliptin plasma concentration-time profiles after single intravenous (bolus) administration of linagliptin to DPP-4-deficient (left panel) and wildtype (right panel) rats.

In the dose range up to 1 mg/kg, pronounced differences in the plasma concentration-time profiles of linagliptin were observed between DPP-4-deficient and wildtype rats (Figure 3-19). DPP-4-deficient rats showed a markedly faster decrease in dose-normalised linagliptin plasma concentrations over time, leading to a notably lower exposure in this dose range. The pharmacokinetics was dose-proportional in DPP-4-deficient rats (Figure 3-19, left panel), whereas the pharmacokinetics in wildtype Fischer rats was dose-dependent. This nonlinearity is evident in the dose-normalised pharmacokinetic profiles of wildtype rats not being superimposable due to a less than dose-proportional increase in exposure (Figure 3-19, right panel).

3.5.1 Model development

Linear one-, two-, and three-compartment models were tested to describe the plasma concentration-time profiles of DPP-4-deficient rats. The three-compartment model performed best. It was superior to a one-compartment model (ΔOBJF −223.022) and a two-compartment model (ΔOBJF −133.458). Estimating interindividual variability on the typical population parameters did not improve the description of the plasma concentrations and was thus not implemented. The parameter estimates are listed in Table 3-13.

In the next step, this three-compartment model was extended to describe the pharmacokinetics of DPP-4-deficient and wildtype rats simultaneously by assuming saturable binding

of linagliptin to DPP-4 for wildtype rats. First, concentration-dependent binding to a single binding partner in the central compartment was tested which resulted in a good description of the plasma concentrations. Adding saturable binding also to one peripheral compartment further improved the fit (ΔOBJF −80.085); no further improvement could be reached by additionally implementing saturable binding in the second peripheral compartment (ΔOBJF 0). In addition, implementing the 'tissue' binding partner in the peripheral compartment was superior to incorporating two binding partners in the central compartment, one which is soluble in plasma (i.e. soluble plasma DPP-4) and one which is easily accessible via plasma but not part of the plasma (e.g. membrane bound DPP-4 on lymphocytes or on the endothelium) (ΔOBJF −80.085). In the latter case, the amount of 'tissue' binding partner was estimated to be zero. Accounting for interindividual variability on the binding parameters was not required. During the model development the distribution parameters of unbound linagliptin were fixed to those of the DPP-4-deficient rats' model. When estimating all model parameters simultaneously, the parameter estimates were nearly identical (Table 3-13).

In the last step of model development, the model assumptions were tested if possible (cf. section 2.5.5.3). One model assumption was that the binding affinity of linagliptin to central and peripheral DPP-4 is identical. This assumption was maintained for the model, as the data did not allow to independently estimate two dissociation constants. Another assumption was that the binding equilibrium was reached faster than other pharmacokinetic processes. This assumption of quasi-equilibrium binding had only negligible effects on the model results (e.g. parameter estimates, goodness-of-fit plots), and was therefore abandoned for the final model.

3.5.2 Final model

Confirming the hypothesis, that the nonlinear pharmacokinetics is caused by concentration-dependent binding of linagliptin to DPP-4, the plasma concentrations of both wildtype and DPP-4-deficient rats were best described by a three-compartment model accounting for concentration-dependent binding of linagliptin to plasma and tissue DPP-4 in wildtype rats. The structural model is depicted in Figure 3-20**.**

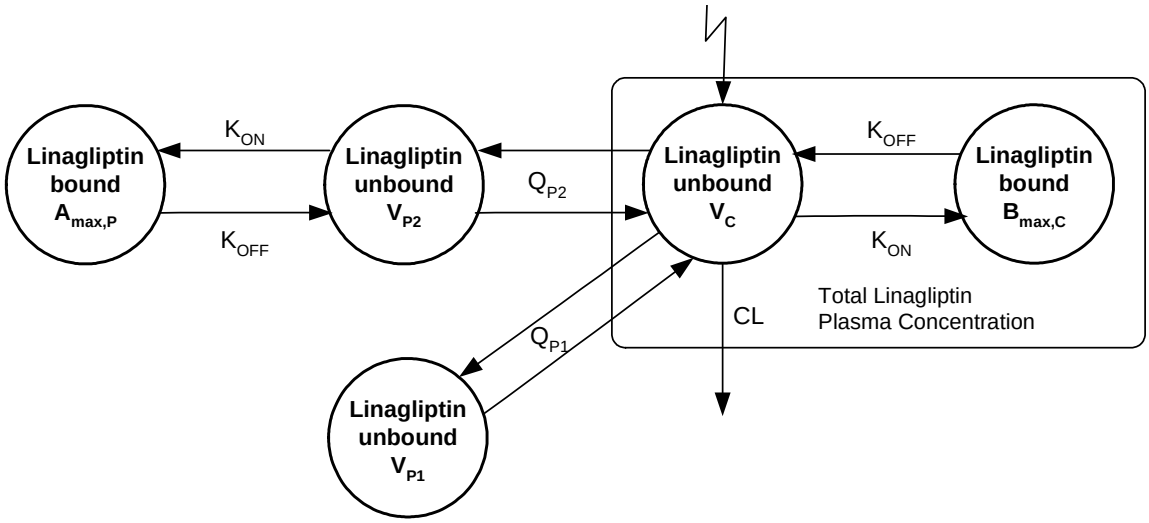

Figure 3-20 Schematic representation of the pharmacokinetic model for linagliptin accounting for concentration-dependent and reversible binding of linagliptin to DPP-4 in wildtype rats. In DPP-4-deficient rats, no binding to DPP-4 is existent simplifying the model to a linear three-compartment model. V_C, central volume of distribution; V_{P1}, volume of distribution of first peripheral compartment; V_{P2}, volume of distribution of second peripheral compartment; Q_{P1}, intercompartmental clearance between central and first peripheral compartment; Q_{P2}, intercompartmental clearance between central and second peripheral compartment; CL, clearance; $B_{max,C}$, concentration of binding partner in the central compartment; $A_{max,P}$, amount of binding partner in the second peripheral compartment; K_{ON}, second-order rate constant of the association of the linagliptin/DPP-4 complex; K_{OFF}, first-order rate constant of the dissociation of the linagliptin/DPP-4 complex.

No interindividual variability was required. The residual variability was 19.9% and was coded as an additive residual variability model for log-transformed data, approximately corresponding to a proportional residual variability model for untransformed data. The parameter estimates are shown in Table 3-13. The standard goodness-of-fit plots (Appendix, Figure 29) highlight that the model performs adequately for DPP-4-deficient and wildtype rats. A slight misspecification can be observed for the linagliptin concentrations at the early time points which may be caused by variations in the actual sampling time of the 2 min values.

Table 3-13 Parameter estimates of the final pharmacokinetic model for DPP-4-deficient and wildtype rats

		DPP-4-deficient model		Combined model	
	Unit	Estimate	RSE [%]	Estimate	RSE [%]
Typical Parameter					
V_C	L	0.487	7.72	0.569	5.18
Q_{P1}	L/h	0.192	8.75	0.173	8.32
V_{P1}	L	1.48	6.30	1.73	12.5
Q_{P2}	L/h	3.31	3.05	4.16	4.62
V_{P2}	L	1.48	2.60	1.81	5.40
CL	L/h	1.44	2.87	1.51	2.56
$B_{max,C}$	nM	NA	NA	2.70	3.68
K_{ON}	L/(h·nmol)	NA	NA	2.50	12.8
K_{OFF}	h^{-1}	NA	NA	0.108 fix	NA
K_d [1)]	nM	NA	NA	0.0432	NA
$A_{max,P}$	nmol	NA	NA	9.86	8.68
Residual variability					
σ_{prop} [2)]	%	14.2	11.6	19.9	8.24

1) Dissociation constant derived from $K_d = K_{OFF}/K_{ON}$

2) Estimated on log-transformed data

NA, not applicable

3.5.3 Model evaluation

The disposition model parameter estimates (V_C, V_{SS}, CL) of unbound linagliptin were comparable to the disposition parameters of DPP-4-deficient rats determined by noncompartmental analysis (Table 3-14). The mean V_{SS} was lower in the noncompartmental analysis, possibly due to the high number of values below the limit of quantification in DPP-4-deficient rats resulting in an underestimation of V_{SS} values.

Table 3-14 Comparison of the parameters for volumes of distribution and clearance between the noncompartmental and the model-based analysis

	V_C (L/kg)	V_{SS} (L/kg)	CL (mL/min/kg)
Model-based	2.28	16.4	100.7
Noncompartmental	2.51	9.2	94.6

The dissociation constant of the saturable binding in wildtype rats was 0.0432 nM, or, reciprocally the association constant was $2.31 \cdot 10^{10}$ M^{-1}. In line with this estimate, the *in vitro* plasma protein binding study determined an association constant of $2.34 \cdot 10^{10}$ M^{-1} for the binding of linagliptin to plasma DPP-4 in rats (162). The concentration of the binding partner in the central compartment was estimated by the model to be 2.70 nM. This parameter essentially reflects the plasma DPP-4 monomer concentration in rat, which was estimated in a previous study to be 3.84 nM (162).

3.5.4 Simulation

Based on the final model, the plasma concentration-time profiles of total linagliptin and linagliptin specifically bound to plasma DPP-4 were simulated for different doses (Figure 3-21). These simulations indicated that in wildtype animals unbound linagliptin was eliminated efficiently and that the long terminal half-life was related to the fraction of linagliptin specifically bound to DPP-4.

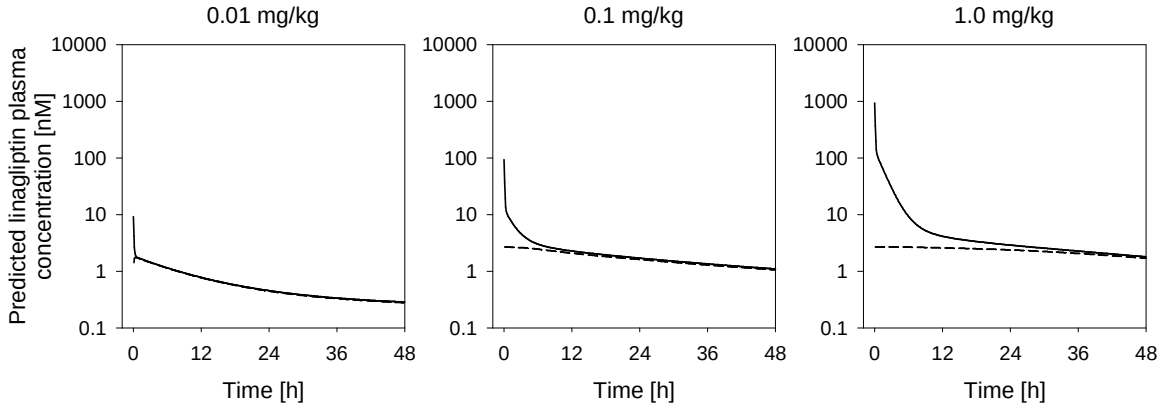

Figure 3-21 Prediction of the plasma concentration-time profiles of total (solid line) and specifically bound (dashed line) linagliptin for the doses 0.01, 0.1, and 1.0 mg/kg. The curves showing the total and the specifically bound plasma concentration-time profiles completely overlap in the left panel, and partly overlap in the middle and right panels.

Furthermore, the time course of linagliptin in both peripheral compartments was simulated and compared between DPP-4-deficient and wildtype rats (Figure 3-22). In DPP-4-deficient rats, the amount of linagliptin in tissue increased linearly with dose and was eliminated rapidly, whereas in wildtype rats the increase of linagliptin in tissue was less than dose-proportional in the dose range from 0.01−1.0 mg/kg. The decline of peripheral linagliptin was predicted to be much slower compared to DPP-4-deficient rats. At the end of the observation period (72 h), the amount of linagliptin in the peripheral compartments was predicted to be much higher in wildtype rats compared to DPP-4-deficient rats (Appendix, Figure 30). In addition, the less than dose-proportional increase of linagliptin in the peripheral compartments of wildtype rats was also evident 72 h after the intravenous bolus administration.

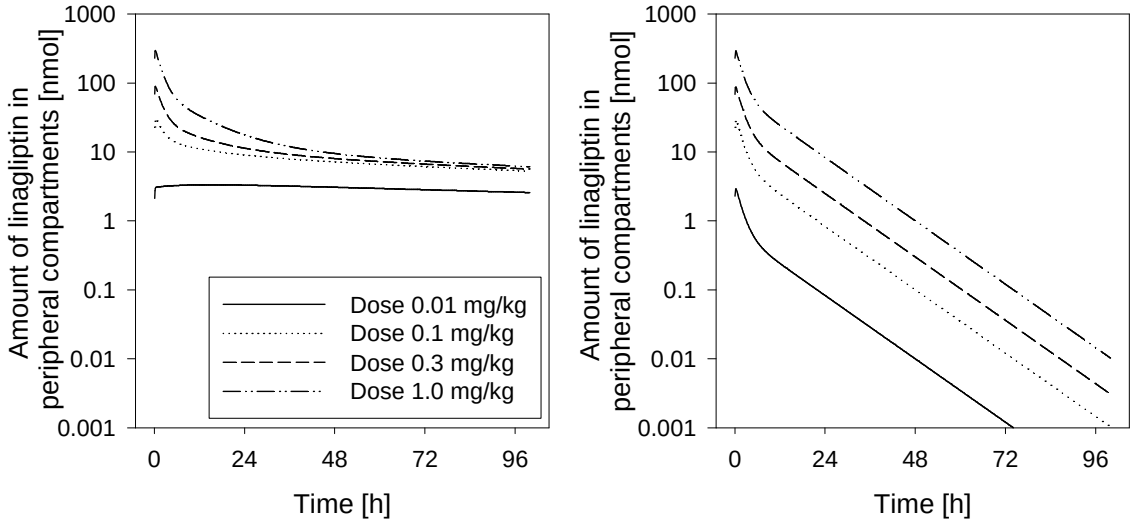

Figure 3-22 Prediction of the amount of linagliptin in both peripheral compartments over time for wildtype (left panel) and DPP-4-deficient rats (right panel) after an intravenous bolus administration of 0.01, 0.1, 0.3, and 1.0 mg/kg linagliptin.

The impact of altered DPP-4 levels on the total linagliptin plasma concentration-time profiles, the plasma concentration-time profiles of unbound linagliptin, and the linagliptin occupancy-time profile of DPP-4 in plasma were to be investigated. Thus, simulations were performed assuming varying amounts of central and peripheral binding partners (original value ±50%). The impact at two dose levels (0.01 and 1 mg/kg) was investigated. Regardless of dose, varying amounts of plasma DPP-4 had an impact on the total linagliptin plasma concentration if linagliptin plasma concentration levels were below the plasma DPP-4 concentration. Interestingly, varying concentrations of plasma DPP-4 only

had a minor effect on the predicted unbound linagliptin concentration and the predicted occupancy (Figure 3-23). In contrast, the impact of varying amounts of peripheral DPP-4 was dose-dependent. In case of the 0.01 mg/kg dose group, a lower amount of peripheral DPP-4 initially led to a higher fraction of unbound linagliptin, as well as higher total plasma concentrations and higher plasma DPP-4 occupancy (Figure 3-24, upper panels). An opposite effect was observed at later time points. At time points >40 h in the 1 mg/kg dose group, a lower amount of peripheral DPP-4 resulted in slightly lower total plasma concentrations, a slightly lower fraction of linagliptin not specifically bound, and a slightly lower occupancy (Figure 3-24, lower panels).

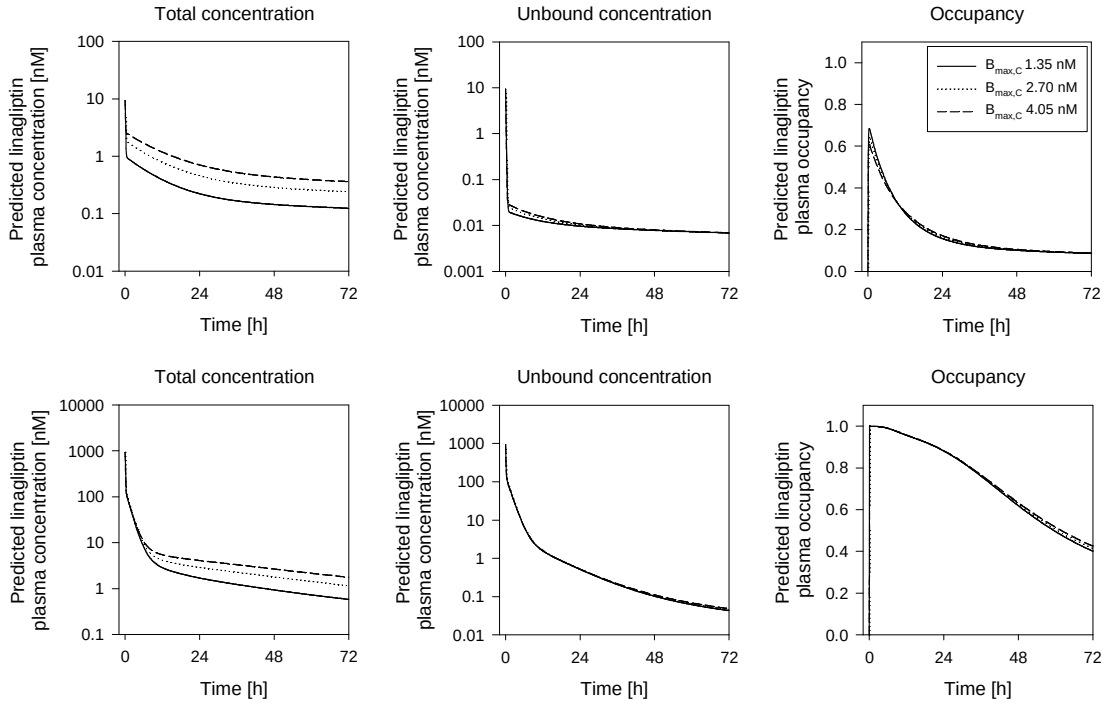

Figure 3-23 Prediction of total plasma linagliptin concentration (left panels), unbound plasma linagliptin concentration (middle panels) and plasma DPP-4 occupancy with linagliptin (right panels) 0-72 h after an intravenous bolus administration of 0.01 mg/kg (upper panels) and 1 mg/kg (lower panels) assuming different concentrations of central binding partner (original value ± 50%).

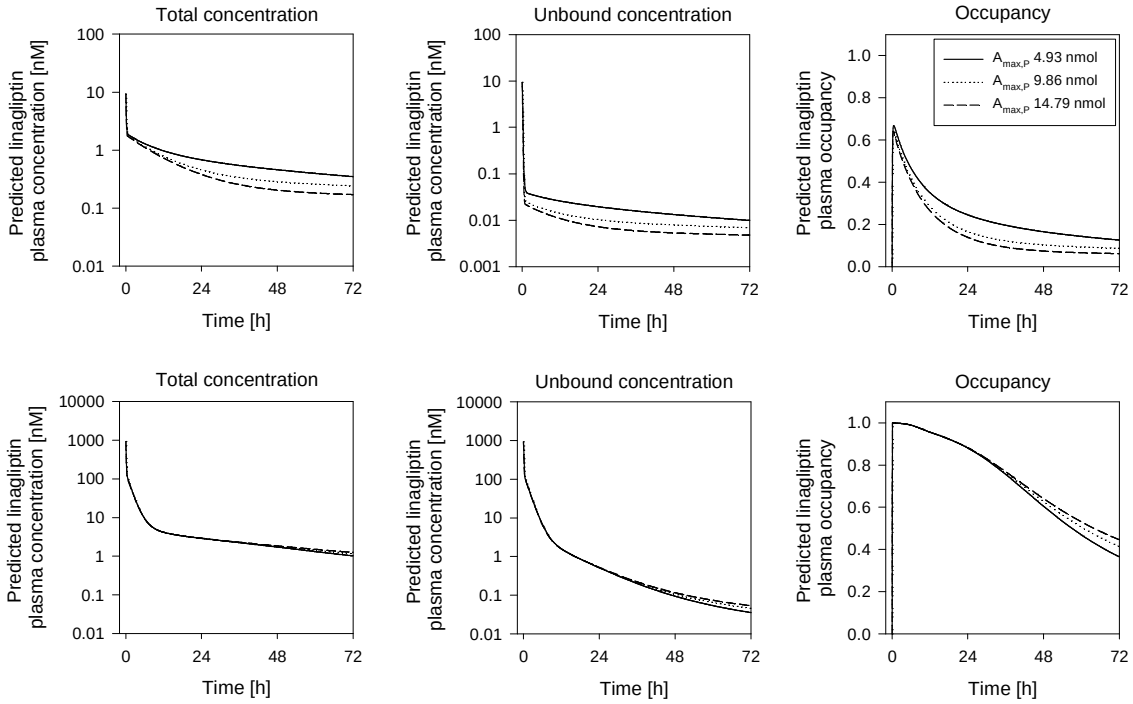

Figure 3-24 Prediction of total plasma linagliptin concentration (left panels), unbound plasma linagliptin concentration (middle panels) and plasma DPP-4 occupancy with linagliptin (right panels) 0-72 h after an intravenous bolus administration of 0.01 mg/kg (upper panels) and 1 mg/kg (lower panels) assuming different amounts of peripheral binding partner (original value ±50%).

4 Discussion

4.1 Nonlinear pharmacokinetics of linagliptin

One major challenge of linagliptin on the way through drug development was its nonlinear pharmacokinetics. For drugs with nonlinear pharmacokinetics it is of great importance to understand the reasons for the nonlinearity to allow a safe and efficacious therapy.

4.1.1 Mechanisms of nonlinear pharmacokinetics

The term ‘linear pharmacokinetics’ implies that concentration-time profiles for a given drug and individual are superimposable when they are normalised for time and dose. In contrast, if these profiles are not superimposable, the pharmacokinetics is termed ‘nonlinear’ (149,164). Nonlinear pharmacokinetics can be caused by nonlinear mechanisms in all kinetic processes, i.e. liberation, absorption, distribution, and elimination. The sources of nonlinearity can be divided into factors dependent on dose or concentration, and factors dependent on time. Table 4-1 summarises possible causes of concentration-dependent and time-dependent pharmacokinetics.

Linagliptin exhibits nonlinear pharmacokinetics already after a single dose (103). This argues for a concentration-dependent effect rather than a time-dependent process. The AUC of linagliptin increases less than dose-proportionally with increasing dose. In consequence, saturation of first-pass metabolism, metabolizing enzymes, and active secretion in liver or kidneys, cannot be responsible for this kind of nonlinearity, as these processes lead to a more than dose-proportional increase in AUC. In addition, saturable liberation was regarded as unlikely because of the high solubility of linagliptin (100) and concentration-dependent renal elimination was considered unlikely due to the small fraction that was renally eliminated (104). Thus, the best explanation for the nonlinearity was either saturable active transport mechanisms in the absorption or saturable protein binding. The latter possibility was supported by human *in vitro* plasma protein-binding data showing concentration-dependent binding for linagliptin in the low nanomolar range (162).

Table 4-1 Common causes of nonlinear pharmacokinetics (adapted from (149))

	Process involved	Parameter primarily affected	Effect on AUC
Dose-dependent processes			
Liberation	Poor solubility, dissolution	Bioavailability ↓	AUC ↓
Absorption	Saturable active transport	Bioavailability ↓	AUC ↓
	Saturable first-pass metabolism	Bioavailability ↑	AUC ↑
Distribution	Saturation of plasma proteins	Volume of distribution ↑, fu_{plasma} ↑ → Clearance ↑	AUC ↓
	Saturation of tissue binding	Volume of distribution ↓, fu_{tissue} ↑	AUC ↔
Metabolism	Saturation of metabolizing enzymes	Hepatic clearance ↓	AUC ↑
Elimination	Saturable renal excretion due to active secretion	Renal clearance ↓	AUC ↑
	Concentration-dependent renal excretion due to active reabsorption	Renal clearance ↑	AUC ↓
	Saturable active biliary excretion	Hepatic clearance ↓	AUC ↑
Time- (and dose-) dependent processes			
Metabolism	Autoinduction	Hepatic clearance ↑ with time	AUC ↓ with time
Elimination	Toxic effects of a drug on its own renal or hepatic elimination	Renal/hepatic clearance ↓ with time	AUC ↑ with time
Others	Diurnal variations in renal function, urine pH, alpha-glycoprotein concentrations, gastrointestinal physiology (food, drink), cardiac output	varies	varies

Concentration-dependent plasma protein binding not only influences the volume of distribution. As the free fraction is increasing with increasing drug concentrations, the clearance is also affected. In literature, there are various examples for drugs exhibiting concentration-dependent plasma binding (149,164). Naproxen, e.g., is a weak acid that binds concentration-dependently to albumin. Nonlinearity is only observed when su-pratherapeutic doses are administered (165). Likewise, valproic acid, a drug with nonlinear pharmacokinetics and a small therapeutic window, exhibits concentration-dependent

binding to albumin, making interpretation of total valproic acid concentrations difficult (166). The basic drug disopyramide binds to α_1-acid glycoprotein. Interestingly, its stereoisomers have different binding affinities (167). The class of angiotensin-converting enzyme (ACE) inhibitors, e.g. trandolaprilat, exhibits nonlinear pharmacokinetics due to concentration-dependent binding to their target enzyme ACE (149). In addition, the distribution and elimination of many therapeutic proteins, peptides, and monoclonal antibodies are likewise determined by target-mediated disposition due to specific high-affinity binding to biological targets (168).

The concentration-dependent plasma protein binding of linagliptin occurred in the low nanomolar range (<100 nM) where common plasma proteins like albumin or α-glycoprotein would not yet be saturated (149). This led to the hypothesis that linagliptin's target enzyme, DPP-4 might be the responsible binding partner.

4.1.2 Nonlinear pharmacokinetics of linagliptin is caused by target-mediated drug disposition

The results of Projects 1 and 5 confirmed the hypothesis that concentration-dependent binding of linagliptin to its target DPP-4 in plasma and tissues is the reason for the nonlinear pharmacokinetics in humans as well as in wildtype rats.

4.1.2.1 Clinical findings in Project 1

The linagliptin plasma concentration-time profiles of type 2 diabetic patients receiving oral doses of 1–10 mg linagliptin once daily over 12 or 28 days were successfully described by a model accounting for concentration-dependent protein binding of linagliptin in the central and the peripheral compartment. This model described the plasma concentrations significantly better than a model assuming saturable absorption, another possible cause for a less than dose-proportional increase in the exposure. Several lines of evidence argue that DPP-4 is the binding partner of linagliptin relevant for its concentration-dependent behaviour. In clinical studies, the concentration of binding partner in the central compartment was estimated to be 4.62 nM, which is in the physiological range expected for the DPP-4 concentration in plasma (79,80). In addition, the individual estimates for the concentration of the binding partner in the central compartment correlated well with the observed pre-dose plasma DPP-4 activity (cf. Figure 3-5). Finally, the observed plasma DPP-4 activity under treatment was linearly related to the estimated plasma occupancy of the binding partner with linagliptin. DPP-4 is available in its soluble form in plasma and to

a great extent in its membrane-bound form in the endothelium and epithelium of various tissues. Thus, concentration-dependent binding of linagliptin in both the central and the peripheral compartment would be in accordance with physiology.

4.1.2.2 Nonclinical findings in Project 5

The findings from the clinical investigations were subsequently confirmed by a comparison of the linagliptin pharmacokinetics between wildtype rats and rats with a DPP-4-deficiency (Project 5). There was a striking difference between the plasma concentration-time profiles of both rat strains after single intravenous administration of up to 1 mg/kg linagliptin. The difference was most pronounced in the lowest dose group (0.1 mg/kg), and decreased with increasing doses. Wildtype rats exhibited a higher exposure and a markedly slower elimination compared to DPP-4-deficient rats. Furthermore, the pharmacokinetics in this dose range was nonlinear in wildtype rats, but linear in DPP-4-deficient rats. The linagliptin plasma concentrations in both rat strains were successfully described by one pharmacokinetic model accounting for concentration-dependent binding of linagliptin in wildtype rats. Like in the model for patients, the binding was implemented in the central and one peripheral compartment, suggesting that concentration-dependent binding of linagliptin to both plasma and peripheral DPP-4 has an impact on the nonlinear pharmacokinetics of linagliptin.

4.1.2.3 Further findings

Beyond the analysis presented here, other nonclinical and *in vitro* experiments also found the concentration-dependent plasma and tissue binding of linagliptin to be caused by DPP-4. Plasma protein binding studies revealed a pronounced concentration-dependent binding of linagliptin in the plasma of wildtype rats and mice, as well as in human plasma (162). This concentration-dependency was characterised by a plasma protein binding of linagliptin >99% for linagliptin concentrations <1 nM, decreasing to 70–80% for linagliptin concentrations >100 nM. In contrast, the plasma protein binding was constant in the concentration range of 0.1–10,000 nM in DPP-4-deficient rats and DPP-4 knockout mice.

Similar findings for the tissue binding of linagliptin were obtained by whole body autoradiography and tissue dissection (161). Tissue levels of drug-related radioactivity increased markedly less than dose-proportional in wildtype rats in all investigated tissues, whereas a nearly dose-proportional increase was observed in DPP-4-deficient rats. In line with the

idea of target-mediated drug disposition, higher levels of linagliptin were observed in the tissues of wildtype rats compared to DPP-4-deficient rats.

4.1.3 Model assumptions

4.1.3.1 Pharmacokinetic models

The pharmacokinetic models developed in this work accounted for the saturable binding of linagliptin to DPP-4 in plasma and peripheral tissues. This is in line with the DPP-4 distribution as well as the current knowledge about linagliptin as presented in section 4.1.2. The tissue binding was implemented in the peripheral compartment as this was superior to implementing a second binding partner in the central compartment which is easily accessible via plasma but not part of the plasma (e.g. membrane bound DPP-4 on lymphocytes or on endothelium). The latter approach has successfully been used previously to describe the target-mediated drug disposition of the angiotensin-converting enzyme inhibitor benazepril (153). A possible explanation for the difference between both models might be that membrane bound angiotensin-converting enzyme is predominantly located in the endothelium of blood vessels (169), whereas DPP-4 is to a high extent also expressed on the epithelia of various tissues (57,72-75). The investigations on the identifiability of the model structure also demonstrated that the proposed model structure not only reflects physiology best, but was also identifiable using the clinical data of Project 1. These investigations further suggested that an analysis of a wide range of doses (1–10 mg) is important to determine all model parameters adequately.

Identical binding affinities of linagliptin for soluble plasma DPP-4 and membrane-bound tissue DPP-4 were assumed in the model. This was necessary as it was not possible to independently estimate two different binding affinities. Assuming identical binding affinities is justified as soluble DPP-4 is most likely a cleavage product of the membrane-bound DPP-4 (57).

The binding of linagliptin to DPP-4 was assumed to be reversible. This is in line with previous *in vitro* experiments (101). However, precisely estimating binding association and dissociation rate constants using a target-mediated drug disposition model is difficult (152). Thus, to simplify the estimation, quasi-equilibrium conditions were assumed for the high-affinity binding of linagliptin to DPP-4, i.e. it was assumed that the binding equilibrium is reached faster than all other processes. This assumption has previously been successfully applied by several authors (151-153,155). In Project 5, the assumption of

quasi-equilibrium conditions for the binding of linagliptin to DPP-4 was tested for the final model structure. Assuming that the binding equilibrium was reached instantly had only negligible effects on the description of the linagliptin plasma concentration-time profiles and the parameter estimates.

4.1.3.2 Pharmacodynamic model

In Project 1 it was assumed that plasma DPP-4 occupancy with linagliptin is directly proportional to the decrease of plasma DPP-4 activity. This implies that the interaction is readily reversible, independent of time, and not cooperative (170). The binding of linagliptin to DPP-4 was found to be reversible in *in vitro* dissociation assays (101). No hysteresis was obvious in the relationship between linagliptin plasma concentration and plasma DPP-4 inhibition (103), suggesting that the interaction is time-independent. DPP-4 monomers have only one active site, i.e. one linagliptin binding site (100). However, as DPP-4 molecules are often associated as dimers (57), cooperativity might be possible (100). Such a cooperative effect would not be covered by the current model.

The basic concept of 'receptor occupancy' was introduced in the 1930s by Alfred J. Clark and has meanwhile been extended to allow the description of more complex scenarios, in which not only receptor occupancy, but also subsequent processes contribute to the response (170). As no processes subsequent to binding are involved in the DPP-4 inhibition by linagliptin, however, the basic model can be applied here.

The pharmacokinetic/pharmacodynamic model of Project 1 assumed the *in vivo* (i.e. in plasma) and *in vitro* (i.e. in the assay) DPP-4 occupancies with linagliptin to be identical. The presumed DPP-4 occupancy with linagliptin *in vitro* may be lower than *in vivo,* however, as the *in vitro* assay requires the plasma samples to be diluted and substrate to be added in excess, affecting the binding equilibrium. Assuming different *in vivo* and *in vitro* DPP-4 occupancies would significantly improve the model fit (ΔOBJF −28.092), but this would also increase the complexity of the model. In addition, visual predictive checks indicated only minor differences between the fits. Therefore, no difference in the *in vitro* and the *in vivo* occupancy was accounted for in the final model.

4.1.4 Implications of the target-mediated drug disposition of linagliptin

Simulations using the pharmacokinetic model of wildtype rats revealed that the binding of linagliptin to DPP-4 in plasma as well as in peripheral tissues has a major impact on the disposition of linagliptin (Project 5). In plasma and tissue, the fraction of linagliptin bound to DPP-4 was not directly available for elimination or re-distribution and acted as a 'reservoir'. In contrast, unbound linagliptin was cleared or re-distributed efficiently. Thus, the high affinity binding in wildtype rats led to a prolonged terminal half-life and a higher exposure of linagliptin in both plasma and tissue compared to DPP-4-deficient rats. With increasing doses, the percentage of linagliptin bound to DPP-4 decreased as DPP-4 became saturated, mitigating the impact of the binding on the pharmacokinetic profiles in both compartments. These simulations are in accordance with the differences observed in the plasma concentration-time profiles between DPP-4-deficient and wildtype rats. In addition, the predicted behaviour of linagliptin in the peripheral tissues very well matched the tissue distribution of [^{14}C]linagliptin-related radioactivity in wildtype and DPP-4-deficient rats (161). Both, the simulated as well as the observed tissue distribution, suggested that saturation of 'tissue' DPP-4 with linagliptin was achieved with single intravenous bolus doses of less than 1 mg/kg linagliptin (0.04 mg/kg based on the model).

Like in the animal model, the target binding of linagliptin plays a considerable role in humans when the compound is administered in the therapeutic dose range. Simulations of the steady-state profiles for the 5 mg linagliptin dose, which is the therapeutic dose tested in the clinical phase III programme, were performed. These simulations predicted that the total $AUC_{\tau,SS}$ is actually composed to the greater part (~70%) of linagliptin bound to DPP-4, while only the smaller fraction is not bound to DPP-4. Thus, the target-mediated drug disposition of linagliptin must be taken into account in the interpretation of the pharmacokinetics of linagliptin.

4.1.4.1 Impact on the pharmacokinetic parameters of linagliptin

In clinical studies I and II, the $AUC_{0\text{-}24h}$ and $AUC_{\tau,SS}$ of linagliptin increased less than dose-proportionally with increasing dose. Both clearance and V_{SS} of linagliptin determined by noncompartmental analysis increased with increasing dose (cf. Table 1-1). Furthermore, despite a long terminal half-life of more than 100 h, the accumulation ratio based on AUC ($R_{A,AUC}$) was small, ranging from 1.2–2.0, and steady-state was reached fast (2–6 days)

(104). Both the accumulation and the time to reach steady-state were dose-dependent for linagliptin.

These particularities of linagliptin pharmacokinetics can be explained by the model accounting for target-mediated drug disposition. The elimination of linagliptin is governed by the high-affinity binding of linagliptin to its target DPP-4, leading to a long terminal half-life. Thus, the clearance of total linagliptin calculated by noncompartmental analysis is not only dependent on the linear clearance of unbound linagliptin but also on the affinity to and the concentration of DPP-4 in plasma and tissue. With increasing doses, the fraction of unbound linagliptin increases as the binding partner becomes saturated. This leads to an increase in the volume of distribution and the clearance of total linagliptin as determined by noncompartmental analysis and thus to a less than dose-proportional increase in the exposure of linagliptin.

The accumulation of unbound linagliptin is low as the fraction of unbound linagliptin is eliminated efficiently (CL/F 220 L/h, in Project 1). The accumulation of linagliptin is dose-dependent as well due to the concentration-dependent binding. When high doses (e.g. 10 mg) are administered, saturation of DPP-4 and thus steady-state is effectively achieved after the first dose already (cf. Figure 3-6, right panel), resulting in a low accumulation ratio of 1.2. Conversely, when low linagliptin doses (e.g. 1 mg) were administered, saturation of DPP-4, and thus steady-state, was not achieved until 4–6 administrations. Accordingly, accumulation is higher (accumulation ratio 2.0) for low doses.

4.1.4.2 Impact on linagliptin DPP-4 inhibition

Due to the direct relationship between pharmacokinetics and pharmacodynamics via the occupancy of DPP-4 with linagliptin, the pharmacokinetic characteristics are also apparent in the DPP-4 inhibition. The plasma DPP-4 inhibition is long-lasting as it is likewise dependent on the slow dissociation of linagliptin from its target. Accordingly, the time until steady-state inhibition is reached is dose-dependent. While low doses of linagliptin are sufficient to elicit a marked DPP-4 plasma inhibition under steady-state conditions, DPP-4 occupancy keeps increasing after the first dose, and thus steady-state DPP-4 inhibition is only reached after several administrations. In contrast, single high doses of linagliptin lead to an instant near-maximum saturation of DPP-4 and thus steady-state DPP-4 inhibition is reached already after the first dose.

4.1.4.3 Comparison to other DPP-4 inhibitors

Interestingly, the impact of target-mediated drug disposition on the pharmacokinetics is higher for linagliptin compared to other DPP-4 inhibitors exhibiting approximately linear pharmacokinetics (108-111). This may be explained by a higher affinity of linagliptin to DPP-4 compared to other DPP-4 inhibitors. A recent study compared the *in vitro* IC_{50} values of several DPP-4 inhibitors (101). Indeed, linagliptin inhibited DPP-4 most effectively with an *in vitro* IC_{50} of ~1 nM, compared to sitagliptin (19 nM), alogliptin (24 nM), saxagliptin (50 nM) and vildagliptin (63 nM). In line with their lower binding affinities, higher therapeutic doses for sitagliptin (100 mg qd), vildagliptin (50 mg qd or bid) and alogliptin (25 mg qd) were required. Also, the AUC values of these compounds are higher compared to linagliptin (Table 4-2).

Table 4-2 Comparison of the therapeutic dose, AUC, fraction unbound, and IC_{50} of saxagliptin, alogliptin, vildagliptin, sitagliptin and linagliptin

	Saxagliptin		Aloglitpin[2)]	Vildagliptin	Sitagliptin	Linagliptin
	Parent	Active Metabolite BMS-510849				
Dose [mg]	5 (qd)	NA	25 (qd)	50 (qd)	100 (qd)	5 (qd)
AUC [nM·h]	180 (111)[3)]	1,355 (111)[4)]	3,194 (110)[5)]	3,395 (173)[6)]	8,500 (108)	158 (104)
fu	1.0 (111)	1.0 (111)	Not specified	0.91 (171)	0.54-0.66 (172)	0.005-22.7(162)
IC_{50} [nM] (101)	50	ND[1)]	24	63	19	1

1) Twofold less potent (111)

2) Active metabolite with similar potency than parent *in vitro*, but only ~1% of AUC parent (110)

3) $AUC_{0\text{-}inf}$ is reported to be 0.06 µg·h/mL and molecular weight of saxagliptin is 333.4 g/mol

4) $AUC_{0\text{-}inf}$ is reported to be 0.43 µg·h/mL and molecular weight of saxagliptin metabolite is 333.4 −16 = 317.4 g/mol

5) $AUC_{\tau,SS}$ is reported to be 1.474 µg·h/mL and molecular weight of alogliptin is 461.5 g/mol

6) $AUC_{0\text{-}inf}$ is reported to be 1.030 µg·h/mL for 50 mg qd and molecular weight of vildagliptin is 303.4 g/mol

NA, not applicable

In contrast, the doses as well as the exposures of saxagliptin and linagliptin are similar. Interestingly, saxagliptin has a pharmacologically active metabolite with a ~7-fold higher exposure than the parent compound which may possibly explain the similar dose and

exposure of linagliptin and saxagliptin despite the 50-fold lower affinity of saxagliptin for DPP-4.

4.1.4.4 Clinical implications

Due to its target-mediated drug disposition, the terminal half-life of linagliptin is not predictive with regard to accumulation. The accumulation for the low dose groups (e.g. 1 mg, 2.5 mg) is dependent on the saturation of DPP-4 as well as the accumulation of unbound linagliptin. For higher doses (e.g. 5 mg, 10 mg), DPP-4 is saturated already after the first dose and thus, the accumulation is predominately dependent on unbound linagliptin. The pharmacokinetics of unbound linagliptin is linear and thus the effective half-life of unbound linagliptin is predictive with regard to the accumulation for higher dose groups. The model-derived effective half-life of unbound linagliptin is 7.7 h. This is in line with the accumulation half-lives of 11.4 h and 8.59 h determined by noncompartmental analysis for the 5 mg and 10 mg dose respectively (104).

One consequence of the short terminal half-life of unbound linagliptin, in conjunction with the nonlinearity in the pharmacokinetics, is a less pronounced increase in the exposure for patients with a reduced CL/F of unbound linagliptin compared to compounds with linear pharmacokinetics (cf. section 4.3.2). The same holds true for increases in the bioavailability or overdosing. If e.g. 10 mg linagliptin was taken instead of 5 mg, the $AUC_{\tau,SS}$ is predicted to increase only by 33% rather than to double.

Conversely, due to the high-affinity binding of linagliptin to its target DPP-4 leading to a long terminal half-life and the long-term effect of linagliptin on the DPP-4 activity, a single missed 5 mg dose would in average still result in a DPP-4 inhibition after 48 h of 71.4%. The long terminal half-life of linagliptin might also be problematic. In case of intolerance for example, linagliptin cannot be eliminated rapidly. This is a theoretical scenario, however, as linagliptin was very well tolerated in all studies performed so far (103,174). Furthermore, only the fraction bound to DPP-4 remains in the body longer, while the major fraction of linagliptin, which is not bound to DPP-4, is eliminated fast.

The fraction of drug which is not bound by DPP-4 will not affect the DPP-4 activity, and will not contribute to the efficacy. Accordingly, and in line with the observed plasma DPP-4 activity, simulations showed that the occupancy for the 5 mg and the 10 mg dose groups is similar and >90% (cf. Figure 3-6, right panel). This favours 5 mg as the therapeutic dose.

4.2 Characterisation of the pharmacokinetics and the pharmacokinetic/pharmacodynamic relationship of linagliptin

4.2.1 Structural model comparison

The structures of the pharmacokinetic models of linagliptin were similar in rats, healthy volunteers, and type 2 diabetic patients. All three models included concentration-dependent protein binding in the central and one peripheral compartment. In Projects 4 and 5, a three-compartment model was required to describe the plasma concentrations adequately, whereas in Project 1 a second peripheral compartment was not supported by the data. This difference between the structural models might be explained by the fact that plasma concentrations after intravenous administration were included in Projects 4 and 5, but not in Project 1. Possibly, the very fast initial distribution phase with α-phase half-lives of linagliptin of 0.085 h in Project 4 and 0.058 h in Project 5 is masked by the relatively slow absorption of linagliptin.

4.2.2 Population parameters

4.2.2.1 Volume of distribution and clearance of unbound linagliptin

The volumes of distribution at steady-state of unbound linagliptin were found to be high in rats (Project 5), healthy volunteers (Project 4) and type 2 diabetic patients (Project 3a) (V_{SS}: 16.6 L/kg, 5.1 L/kg, and V_{SS}/F: 26.2 L/kg, respectively). All estimates by far exceeded the total volume of body water, indicating an extensive tissue distribution of unbound linagliptin. These findings are consistent with the extensive tissue distribution observed for unbound linagliptin in DPP-4-deficient rats as determined by autoradiography (161).

The clearances of unbound linagliptin were estimated to be moderate to high in rats (Project 5), healthy volunteers (Project 4) and type 2 diabetic patients (Project 3a) (CL: 6.09 L/h/kg, 0.34 L/h/kg, and CL/F: 2.86 L/h/kg, respectively). The clearance normalised to body weight was considerably higher in rats compared to humans. This might possibly be caused by differences in the biliary excretion of linagliptin of rats and humans as biliary excretion is generally difficult to predict between different species (175,176). Assuming an absolute bioavailability of 29.5%, a ~2-fold higher clearance was

estimated in diabetic patients compared to the healthy volunteers of Project 4. In line with the lower clearance in Project 4, the linagliptin exposure was 21–41% higher in Project 4 ($AUC_{0\text{-}24h}$: 227 nM·h in Project 4) compared to Project 1 ($AUC_{0\text{-}24h}$: 161 nM·h in study I, 188 nM·h in study II) after oral administration of 10 mg linagliptin. Due to the nonlinearity, the effect of an enhanced clearance on the linagliptin plasma concentration-time profile is lower than would be the case for linear pharmacokinetics. Accordingly, the predicted typical concentration-time profile of Project 4 was only slightly increased compared to those of the other projects (Figure 4-1). The reason for the different exposures in both projects is unknown. A difference between healthy volunteers and patients is unlikely, as similar exposures for healthy volunteers and type 2 diabetic patients were observed in other studies. For example, comparable $AUC_{0\text{-}24h}$ values were found for the healthy volunteers in the control group of Project 2d and the patients of Project 1 (122 nM·h compared to 119 nM·h (study I) and 124 nM·h (study II) after oral administration of 5 mg linagliptin). Also, the plasma concentration-time profiles of the healthy volunteers in Project 4 could be adequately described by the model developed for diabetic patients in Project 1 with only minor model adaptations (cf. section 3.2.4), suggesting that the differences in exposures between Project 4 and Project 3a are random inter-study effects.

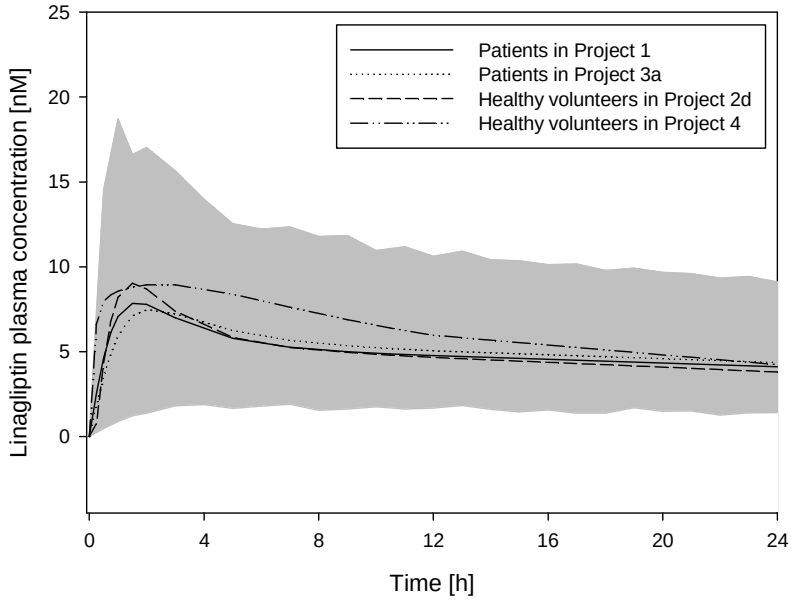

Figure 4-1 Comparison of simulated typical linagliptin concentration-time profiles based on the pharmacokinetic models developed in Projects 1, 2d, 3a, and 4 assuming that a single oral dose of 5 mg linagliptin was administered. The grey shaded area represents the overall variability determined as the 90% confidence interval of 1,000 simulated concentration-time profiles based on the base population pharmacokinetic model of Project 3a.

4.2.2.2 Binding parameters

The concentrations of binding partner in the central compartment were estimated to be 2.70 nM, 3.44 nM, and 4.97 nM for rats, healthy volunteers, and type 2 diabetic patients, respectively, and thus lie within the range expected for the plasma DPP-4 concentration (79,80). Based on the plasma protein binding assay, a similar concentration of plasma DPP-4 monomers of 3.84 nM for rats and 6.36 nM for humans was estimated (162). An elevated plasma DPP-4 concentration for type 2 diabetic patients would be in line with the finding of a higher DPP-4 activity in type 2 diabetic patients compared to healthy volunteers (177,178).

The dissociation constants for the binding of linagliptin to DPP-4 were estimated to be 0.043 nM, 0.0835 nM, and 0.0652 nM for rats, healthy volunteers and type 2 diabetic patients, respectively. Again these estimates are in good agreement with the dissociation constant obtained *in vitro* from plasma samples employing equilibrium dialysis (K_d: 0.043 nM for rats and 0.051 nM for humans, as calculated by $K_d = 1/K_1$) (162).

The total amount of the binding partner (DPP-4) normalised to body weight was estimated to be higher in rats compared to humans (46.0 nmol/kg in rats compared to 7.55 nmol/kg in healthy volunteers and 17.0 nmol/kg in patients, considering a bioavailability of 29.5%). So far no data for comparison have been published. A recent estimate based on differences in the linagliptin distribution of wildtype and DPP-4-deficient rats indicated a total DPP-4 amount of 22 nmol in a 250 g rat corresponding to 88 nmol/kg (personal communication, H. Fuchs).

4.2.2.3 Correlation between pharmacokinetics of linagliptin and DPP-4 activity

The maximum decrease in DPP-4 activity in type 2 diabetic patients was estimated to be 93.5% and 92.4% in Projects 1 and 3b, respectively. This may be an underestimation of the 'true' maximum DPP-4 inhibition *in vivo* due to sample dilution and addition of the competitive substrate alanine-proline-7-amido-4-trifluoro-methylcoumarine during the DPP-4 activity assay (cf. section 2.1.2).

The linagliptin concentration leading to half-maximum DPP-4 inhibition was determined by a sigmoid E_{max} model to be 3.06 nM (Project 3b). This concentration is in line with previous data from healthy volunteers in which a concentration of ~2–4 nM were estimated to lead to 50% inhibition of the DPP-4 enzyme (103).

4.2.2.4 Variability in the pharmacokinetic parameters of linagliptin

Absorption is apparently the major source of variability in the pharmacokinetics of linagliptin. After intravenous administration of linagliptin to rats (Project 5) and healthy volunteers (Project 4) a very low variability in the disposition of linagliptin was observed (cf. Figure 3-16, Figure 3-19), whereas a moderate variability was apparent after oral administration of linagliptin to healthy volunteers and type 2 diabetic patients (cf. Figure 3-17 and Appendix, Figure 16).

A moderate to high variability in the absorption phase was also found during the investigation of inter- and intraindividual variability (Project 3a). This was accounted for by an inter-individual variability on the absorption parameters (ωF: 44.2%; ωK_a: 87.6%) and an intraindividual variability on F (πF: 39.2%). A smaller variability was observed in the distribution and elimination parameters ($\omega B_{max,C}$: 29.6%; ωV_C: 22.6%; ωCL: 23.9%).

4.2.3 Covariate selection

An initial covariate analysis performed in Project 1 using data from two phase IIa studies revealed no major impact of any tested covariate on the pharmacokinetics and the plasma DPP-4 inhibition of linagliptin except an unexplained study difference in the relative bioavailability between studies I and II.

The initial covariate analysis was extended by analyzing the two phase IIa studies and, in addition, two phase IIb studies together. The complexity of the pharmacokinetic model and the amount of analysed data led to extensively long run times. Therefore, two separate analyses, one for the pharmacokinetics and one for the pharmacokinetic/pharmacodynamic relationship, were performed.

Of special interest were the effects of weight, age and sex on the pharmacokinetics and DPP-4 inhibition of linagliptin, because no dedicated studies are planned to investigate these effects.

4.2.3.1 Covariates affecting the pharmacokinetics of linagliptin

The structure of the target-mediated drug disposition model developed in Project 1 was used as the starting point for this analysis. Some model parameters could not be estimated and therefore had to be fixed according to the estimates obtained in Project 1. Neverthe-

less, this model was preferred to a simpler model, as it allowed a physiologic interpretation of the relevant covariates.

A significantly elevated relative bioavailability was estimated for study IV, the add-on to metformin study. In addition, the relative bioavailability decreased significantly with increasing weight. The formulation and the dose group showed a statistically significant influence on the rate of absorption. The unbound clearance tended to be decreased in case of increased gamma-glutamyl transferase but this effect was no longer significant when all parameters were estimated together. The model-calculated concentration of central binding partner was influenced by pre-dose DPP-4 activity, dose, age, and sex. In the following, the effects of the statistically significant covariates on the pharmacokinetics of linagliptin are discussed in detail.

4.2.3.1.1 Age

For linagliptin, the covariate analysis revealed only a minor effect of age on its pharmacokinetics. An average increase of 13.8% in the $AUC_{\tau,SS}$ of a 73-year-old patient compared to a 42-year-old patient (representing the 95^{th} and 5^{th} percentiles of the age distribution, respectively) was found when 5 mg linagliptin were taken once daily. A significant effect of age was only found on the concentration of central binding partner. The older the patients, the higher were their $B_{max,C}$ values. In contrast, in a multiple regression analysis using measured plasma DPP-4 concentrations of phase IIb, no correlation between age and DPP-4 plasma concentration was observed (data not shown). Thus, it cannot be excluded that the underlying physiological reason of the age-dependent $AUC_{\tau,SS}$ is not an increase of plasma DPP-4 levels, but related to a change in another pharmacokinetic parameter of linagliptin. Age-dependent changes in the distribution, metabolism and excretion are reported for many drugs (179). These changes often result in a reduced rate of elimination in elderly patients and in an increased exposure. The volume of distribution of hydrophilic drugs is often reduced in older patients due to reduced total body water, whereas the volume of distribution of lipophilic drugs is often elevated, due to an elevated fat mass (180). With a positive log D value of 0.4, linagliptin can be considered a slightly lipophilic drug and thus no major change in the volume of distribution is expected for linagliptin. In addition, elderly patients often exhibit a lower plasma protein binding due to ~10% lower serum albumin levels (181). The metabolic clearance can be reduced in elderly patients due to a lower phase I metabolism, as well as a reduction in blood flow or liver mass (182). In addition, renal clearance is often reduced in older patients. For linagliptin however, both

metabolism as well as renal elimination are minor pathways as it is mainly excreted unchanged via the faeces.

4.2.3.1.2 Weight

For linagliptin, only a small impact of weight was found on the exposure (5.9% and −8.7% on the $AUC_{\tau,SS}$ after administration of 5 mg once daily for the 5^{th} and 95^{th} percentile of the weight distribution). Weight was found as a covariate for the relative bioavailability; however, since only linagliptin concentrations after oral administration were included in the combined analysis, it could not be differentiated whether weight indeed affected the bioavailability or rather accounted for the variability in the apparent clearance and/or in the apparent volumes of distribution. The second possibility would be physiologically more reasonable considering the typical pharmacokinetic peculiarities in obese subjects (183,184). Overweight subjects have a different tissue composition compared to normal subjects, characterised by a higher proportion of adipose tissue and lower proportions of muscles and body water. Lipophilic drugs typically have a larger volume of distribution in adipose patients, thus these patients often require higher loading doses of lipophilic drugs. In contrast, the pharmacokinetics of hydrophilic drugs is often not or only slightly changed for these subjects. In addition, for obese subjects, plasma protein binding (e.g. due to hyperlipidemia), metabolism (e.g. due to a fatty liver) as well as renal (e.g. due to changes in the glomerular filtration rate) and biliary elimination (e.g. due to gall stones) may also be changed.

4.2.3.1.3 Sex

For linagliptin, a small sex-related difference in the pharmacokinetics was found, leading to a 7% higher $AUC_{\tau,SS}$ in females when 5 mg linagliptin was given once daily. The higher exposure was found to be due to a higher concentration of the binding partner in the central compartment for females. When co-estimating all covariate effects and then performing the backward elimination, the effect of gender on $B_{max,C}$ did no longer reach the required statistical level, but was still kept in the model for reasons of model stability. In accordance with the marginally higher estimated levels of the central binding partner in females, slightly but significantly higher plasma DPP-4 levels were found for females in a multiple regression analysis using observed DPP-4 concentrations from the phase IIb studies (data not shown). In general, pharmacokinetic differences due to sex are rare and if present they are small (185,186). Sex-related differences in the activity of some transporters and

metabolizing enzymes were reported (186). Of these, linagliptin pharmacokinetics might be affected by P-glycoprotein, which shows a higher expression in males. The major linagliptin metabolite CD1790 is produced by CYP3A4, for which no sex-related differences have been reported. In addition, females have a lower body weight and a lower glomerular filtration rate which might possibly also influence linagliptin pharmacokinetics.

4.2.3.1.4 Other covariates

In study IV when linagliptin was given as add-on to metformin, a ~20% higher exposure was observed compared to the mono-therapy linagliptin studies. The effect was best described by an increased bioavailability for this study. A decreased clearance of linagliptin, however, cannot be ruled out. An interaction between metformin and linagliptin affecting the linagliptin clearance might be possible. In a drug-drug interaction study, a ~20% higher linagliptin exposure was observed in combination with metformin whereas the C_{max} concentrations and the terminal half-lives were comparable (187). However, the mechanism of a potential interaction between the two compounds remains unclear. Metformin is not metabolised and mainly excreted renally via the organic cation transporter 2 (OCT2), which is predominately expressed in the distal renal tubules (188). Although linagliptin has been found to be a substrate for OCT2 *in vitro* (personal communication, W. Kishimoto), renal excretion plays a negligible role in the elimination of linagliptin (104). On the other hand, little information is available on the interaction of metformin with other transporters such as P-glycoprotein, which might influence the absorption of linagliptin. Although the higher exposure of linagliptin on metformin background treatment in study IV was in the range observed in the drug-drug interaction study with metformin, a pure study effect cannot be ruled out.

Formulation and dose affected the rate of linagliptin absorption. The powder in bottle solution (study I) showed the fastest absorption (K_a: 0.933 h^{-1}), followed by the tablet given in study II (K_a: 0.795 h^{-1}), while the tablet of the formulation given in the studies III and IV showed the slowest absorption (K_a: 0.441 h^{-1}). Differences due to the formulations are unlikely as their bioequivalence was shown in dedicated bioequivalence studies. The difference between studies I/II and studies III/IV might be due to the different sampling schemes or the fact that in the phase IIb studies, linagliptin was to be taken with a meal whereas it was to be taken fasted in the phase IIa studies. In favour of the latter possibility, a food effect study demonstrated that a high-fat meal reduced the rate of absorption, with the C_{max} values being lowered by 15%. In the same study, no influence of food on the

extent of linagliptin exposure was found (personal communication, U. Graefe-Mody). The reason why dose affected the rate of absorption is unknown. It might be speculated that saturable processes in the absorption are involved.

The model estimated the concentration of central binding partner to be correlated with the pre-dose DPP-4 activities. This physiologically plausible correlation is in line with the assumption that the concentration of central binding partner estimated by the model actually reflected the monomer concentration of plasma DPP-4 (cf. section 4.1.2). The dose correlated slightly with $B_{max,C}$ which might represent a minor model misspecification.

When the impact of the covariates was tested separately per model parameter, the only statistically significant covariate found on the clearance of unbound linagliptin was a minor effect of the liver enzyme gamma-glutamyl transferase. The 95th percentile of the gamma-glutamyl transferase distribution resulted in a clinically not relevant increase in the AUC of 1.4%. When all covariates were tested together, the covariate effect of gamma-glutamyl transferase on clearance was no longer statistically significant, also pointing out the minor importance of this covariate effect. Thus, no major impact on the linagliptin pharmacokinetics resulted from the investigated liver enzymes, suggesting that liver impairment does not alter the pharmacokinetics of linagliptin. However, these results need to be confirmed in a dedicated study including patients with diverse symptoms of liver disease as assessed by the Child-Pugh score.

Creatinine clearance was not found to impact the linagliptin clearance. This is in line with the finding that the renal elimination of linagliptin represents only a minor elimination pathway (in the therapeutic dose range ~4% of the linagliptin dose is eliminated via the kidneys). In addition, in the investigated studies, only patients with no or mild renal impairment were included (90% confidence interval of creatinine clearance: 65–189 mL/min). The impact of moderately and severely impaired renal elimination on the pharmacokinetics of linagliptin needs to be further investigated. This is especially important since renal impairment is common among type 2 diabetics. Furthermore, it was recently shown that renal impairment can also affect the pharmacokinetics of drugs that, like linagliptin, are predominantly eliminated by nonrenal processes (189).

4.2.3.1.5 Clinical relevance

Overall, the individual impact of the statistically significant covariates, including weight, age and sex on the $AUC_{\tau,SS}$ of patients receiving 5 mg linagliptin once daily was less than

±20%. Also the exploratively investigated covariates like creatinine clearance and liver enzymes only showed a minor impact on the linagliptin pharmacokinetics, suggesting that an impairment of renal or hepatic clearance is unlikely to have a substantial impact on linagliptin exposure. However, this needs to be confirmed in dedicated studies including also patients with severely impaired renal and hepatic clearances. The low impact of the individual covariates of less than ±20% on the $AUC_{\tau,SS}$ was regarded to be not clinically relevant, making a dose adjustment based on these covariates unnecessary. Even the combination of all covariates in a worst case scenario is with regard to the largest decrease, −26% for the 5 mg dose, still regarded as effective as the linagliptin exposure is in the range of the 2.5 mg dose group (study I: gMean $AUC_{\tau,SS}$ 2.5 mg: 117 nM·h, 5 mg: 158 nM·h; study II: gMean $AUC_{\tau,SS}$ 2.5 mg: 116 nM·h, 5 mg: 148 nM·h). The worst case with regard to the largest increase (+63%) for the 5 mg dose can still be regarded as safe based on the safety data collected in the phase IIb and in the first-in-man study where a single dose of linagliptin up to 600 mg was administered and well tolerated (103).

One reason for the lack of clinically relevant covariates is the nonlinear pharmacokinetics of linagliptin. The change in the relative bioavailability or clearance must be much more pronounced in case of linagliptin compared to a compound with a linear pharmacokinetics to result in the same decrease or increase in the exposure (Table 4-3, cf. section 4.1.4.4). Thus, even if a covariate affects the bioavailability or the clearance of unbound linagliptin, the clinically relevant influence on the exposure of linagliptin is much smaller.

Table 4-3 Change in bioavailability and clearance required to achieve an increase or decrease of the steady-state exposure in terms of $AUC_{\tau,SS}$. For the pharmacokinetics of linagliptin a once daily administration of 5 mg linagliptin was assumed.

	Linear pharmacokinetics		Pharmacokinetics of linagliptin	
	Change in bioavailability	Change in clearance	Change in bioavailability	Change in clearance
Increase in the exposure ($AUC_{\tau,SS}$) of 25%	+25%	-20 %	+82%	-42 %
Decrease in the exposure ($AUC_{\tau,SS}$) of 25%	-25%	+33%	-68%	+152%

4.2.3.2 Covariates affecting the pharmacodynamics of linagliptin

The correlation between linagliptin plasma concentration and plasma DPP-4 activity was best described by a sigmoid E_{max} model. The correlation between the individual EC_{50} values and the pre-dose DPP-4 activities was taken into account by assuming a covariate

effect of the predicted individual pre-dose DPP-4 activities on EC_{50}. The idea behind this was that a higher pre-dose DPP-4 activity corresponds to a higher DPP-4 plasma concentration. A higher DPP-4 plasma concentration in turn necessitates more linagliptin for half-maximum DPP-4 inhibition to be reached, corresponding to a higher EC_{50}. By this coding the covariates affecting the pre-dose DPP-4 activity also have an indirect impact on EC_{50} and $EC_{80\%}$.

4.2.3.2.1 Age

In the covariate analysis age had no impact on plasma DPP-4 activity. This is in line with the observation by Cordero *et al.* that the DPP-4 levels are not correlated to age. In contrast, different groups reported a significant inverse correlation between age and DPP-4 activity in healthy subjects (190) and type 2 diabetic patients (178). Mannucci *et al.* found an inverse correlation in one group of type 2 diabetic patients and no correlation in another group (177). Thus, the impact of age on DPP-4 activity is only minor, if at all existent.

4.2.3.2.2 Weight

In accordance with published data from healthy volunteers (190) as well as from type 2 diabetic patients (177), neither weight nor body mass index were found to influence the DPP-4 activity.

4.2.3.2.3 Sex

Females had a higher pre-dose DPP-4 activity (11,565 versus 10,700 RFU), and thus higher EC_{50} and $EC_{80\%}$ values compared to males. In contrast to our findings, Durinx *et al.* reported slightly lower DPP-4 activity in females than in males (plasma 23.2 U/L vs. 25.9 U/L), but these differences were no longer significant in their multiple regression analysis (190). No correlation between the DPP-4 levels and sex was reported by Cordero *et al.* (79). Thus, a sex-related difference in the DPP-4 activity is only minor, if at all existent.

4.2.3.2.4 Other covariates

In line with other studies (190-192), pre-dose DPP-4 activity was found to be correlated with the liver enzymes gamma-glutamyl transferase, alanine transaminase, and aspartate transaminase. However, due to the high correlation between alanine transaminase and

aspartate transaminase (cf. Appendix, Figure 25), only alanine transaminase and not aspartate transaminase was implemented in the final model.

The covariate analysis of Project 3b revealed a correlation between fasting plasma glucose and pre-dose DPP-4 activity. This finding was in line with the correlation reported between HbA1c and fasting plasma glucose versus plasma DPP-4 activity in type 2 diabetic patients (177,178). In these reports, also higher DPP-4 activities in type 2 diabetic patients compared to healthy volunteers were found, contradicting the results of Meneilly *et al.* (193). Durinx *et al.* found only a small effect of glucose on the DPP-4 activity in healthy volunteers in a multiple regression analysis (190). This might be explained by the lower plasma glucose concentration in healthy volunteers. Thus, in type 2 diabetic patients the plasma DPP-4 activity is apparently increased with increased plasma glucose levels.

The lipid parameters triglycerides and cholesterol were both correlated to pre-dose DPP-4 activity. When additionally accounting for an effect of triglyceride concentrations on the EC_{50} this covariate effect was negative, counteracting the influence of pre-dose DPP-4 activity. The correlation between cholesterol and pre-dose DPP-4 activity was in line with the findings of Durinx *et al.*, whereas an inverse correlation with triglycerides was reported in the same article (190).

4.2.3.2.5 Clinical relevance

The statistically significant covariates were evaluated for their influence on the EC_{50}, as well as on the concentration leading to 80% DPP-4 inhibition. The individual impact of the different covariates on both parameters was <20%. Even the combined influence of all significant covariates only changed the EC_{50} value from a minimum of 2.49 nM to a maximum EC_{50} value of 4.14 nM ($EC_{80\%}$: minimum 4.44 nM and maximum 7.38 nM), respectively. This may be compared to a median plasma concentration at steady-state for 5 mg linagliptin once daily of 12.5 nM at C_{max} and 5.60 nM at C_{trough} (cf. Appendix, Figures 22, 23). Thus, based on this analysis a dose adjustment does not seem to be justified for the tested covariates.

4.3 Clinical trial simulations to support the development of linagliptin

The nonlinear pharmacokinetics of linagliptin made predictions solely based on noncompartmental parameters difficult. Thus, the target-mediated drug disposition model of Project 1 was not only used to investigate the impact of DPP-4 binding on the pharmacokinetics of linagliptin, but also to support the clinical development of linagliptin.

4.3.1 Simulation to evaluate an equivalent dose for a twice-daily administration

During development of the fixed dose combination of linagliptin with metformin the question for the adequate dose for a twice-daily treatment of linagliptin was addressed by simulations. It was predicted that despite the nonlinear pharmacokinetics, 2.5 mg linagliptin twice daily would result in bioequivalent $AUC_{24h,SS}$ values as well as a similar DPP-4 inhibition compared to 5 mg linagliptin once daily. The likely reason for this is that under steady-state conditions DPP-4 is nearly saturated over 24 h (cf. Figure 3-6, right panel). Thus, linagliptin that is not bound to DPP-4 behaves nearly linearly.

Based on this simulation, a cross-over study was conducted in which 2.5 mg linagliptin administered twice daily (test treatment T) was tested versus 5 mg linagliptin administered once daily (reference treatment R) in 16 healthy volunteers. The 90% confidence interval of the adjusted gMean T/R ratio of the $AUC_{24h,SS}$ was 89.49–98.51% and thus within the acceptance interval of 0.80–1.25 (159,194). Therefore both dosage regimens were considered bioequivalent with regard to the extent of exposure at steady-state. In addition, both regimens resulted in a similar average trough DPP-4 inhibition of 85.3% for the 5 mg once daily regimen and 85.8% for the 2.5 mg twice-daily regimen. This bioequivalence study confirmed the previous simulation and demonstrated that the 2.5 mg linagliptin dose is the adequate dose for a twice-daily regimen. Thus, 2.5 mg linagliptin given twice daily is tested in combination with metformin in the phase III programme.

4.3.2 Simulation to evaluate the impact of impaired clearance

In order to support the decision whether patients with a moderate renal impairment were to be included or excluded in phase IIb, the impact of an impaired clearance on the nonlinear pharmacokinetics of linagliptin was investigated. A 25% and a 50% reduction of the

overall clearance was simulated. The fraction excreted in urine after intravenous administration of linagliptin increased with dose with a maximum of 23% in the 10 mg dose group. Thus, a 25% reduction of the overall clearance would correspond to a complete loss of renal elimination. As renal impairment can also affect other elimination pathways (189), a 50% reduction of the overall clearance can be considered as a worst case scenario.

The simulations revealed that for patients with only 75% or 50% of the clearance of a typical patient, the exposures of linagliptin would in average increase by 11% or 31%, respectively. In contrast, when assuming linear pharmacokinetics the impact of an impaired clearance on the exposure would be higher. Based on the equation $CL = F \cdot D/AUC$ the exposure is expected to increase by a third or to double if the clearance is reduced by 25% or by 50%, respectively (cf. section 4.1.4.4).

4.3.3 Simulation of a design for a dose-proportionality study

Simulations suggested that a change-over study design without any washout between the periods is adequate to assess dose-proportionality of different dose strengths of linagliptin tablets (1, 2.5, and 5 mg) at steady-state when the treatment periods are at least seven days long. Steady-state was predicted to be reached first in the highest dose group (5 mg), and the time to steady-state was predicted to increase with decreasing doses. These predictions are in line with the observed steady-state characteristics reported in study I (104). Within the simulated 1 mg dose group, steady-state was reached latest when linagliptin is administered in the first period. This indicates that the 1 mg dose administered without any previous linagliptin treatment is the treatment determining the duration of the periods. For this treatment group the time to reach steady-state is ~5 days as predicted by this simulation and observed in study I (104). In conclusion, administering linagliptin over seven days is adequate to reach steady-state in each sequence.

4.3.4 Description and steady-state simulation of the drug-drug interaction between linagliptin and ritonavir

Ritonavir is a potent inhibitor of CYP3A4 and P-glycoprotein. In a drug-drug interaction study the $AUC_{0\text{-}inf}$ of linagliptin increased 2-fold under comedication with ritonavir. The model-based analysis of Project 2d revealed a slightly reduced lag time, a 4-fold increase in the bioavailability of linagliptin, and a 16% decrease in the clearance of unbound linagliptin under ritonavir comedication. The high increase in bioavailability is plausible,

considering that the absolute bioavailability was estimated to be ~30% with a high inter-individual variability (values ranged from 12.9–60.8%) (cf. section 4.4). Due to the nonlinear pharmacokinetics, a 4-fold increase in bioavailability does only result in a 2-fold increase in $AUC_{0\text{-}inf}$. Compared to the bioavailability, the clearance of unbound linagliptin is predicted to be less affected by ritonavir. The low impact predicted on the clearance of linagliptin by ritonavir is in line with graphical investigations suggesting that the shapes of the linagliptin plasma concentration-time profiles were only slightly affected by ritonavir. Also the half-lives were comparable between linagliptin alone or in combination with ritonavir. In light of the absence of its major metabolite CD1790, normally representing 17% of all drug-related species in plasma, a decrease in the metabolic clearance of unbound linagliptin under comedication of ritonavir is likely. As the metabolic clearance is only a minor elimination pathway of linagliptin, a low impact on the overall clearance does not contradict the current knowledge about linagliptin (cf. section 1.3.2).

Differentiating between the impact of CYP3A4 or P-glycoprotein inhibition is difficult. However, considering the minor extent of metabolism of linagliptin and the major impact of ritonavir on the bioavailability of linagliptin, it seems likely that the effect of ritonavir is predominately driven by inhibition of P-glycoprotein during the absorption of linagliptin.

Simulations predicted that under ritonavir comedication the increase in linagliptin exposure from the first dose to steady-state was small and comparable to linagliptin treatment alone. The accumulation ratio of the AUC of linagliptin was 1.13 when linagliptin was coadministered with ritonavir compared to 1.20 when linagliptin was given alone. Due to the near-saturation of DPP-4 after the first 5 mg dose, the accumulation of linagliptin is predominantly dependent on the unbound fraction (cf. section 4.1.4.4). Due to the low impact of ritonavir on the clearance of unbound linagliptin, the effective half-life and thus the accumulation of unbound linagliptin were likewise only slightly affected. Thus, as observed after single dose, a ~2-fold increase in $AUC_{\tau,SS}$ was predicted for steady-state.

The predicted typical $AUC_{\tau,SS}$ of 5 mg linagliptin once daily in comedication with ritonavir (293 nM·h) was far smaller than the $AUC_{0\text{-}24h}$ of the single dose administration of 600 mg linagliptin (33,010 nM·h) which was well-tolerated. In addition, 10 mg linagliptin once daily was shown to be well-tolerated over three months (174). Both study results suggest that a ~2-fold increase in the steady-state exposure of 5 mg linagliptin can be expected to be safe. However, this needs to be confirmed by further studies.

4.4 Absolute bioavailability of linagliptin

4.4.1 Estimation of the absolute bioavailability of linagliptin despite its nonlinear pharmacokinetics

The absolute bioavailability is the percentage of the administered dose that reaches the general circulation (160). The standard approach to determine the absolute bioavailability of a compound is to divide the dose-adjusted $AUC_{p.o.}$ by $AUC_{i.v.}$ (159,194). However, this standard approach is only valid if the clearance calculated by CL = F·D/AUC of a drug is linear (160). This is not the case for linagliptin.

One possibility to keep the clearance comparable between the oral and the intravenous treatment despite non-linear pharmacokinetics is to mimic the profile after oral administration by the intravenous administration. Congruent plasma concentration-time profiles after intravenous and oral administration would then allow a noncompartmental assessment of the absolute bioavailability (195). This approach was attempted within this study. Based on preclinical data, the absolute bioavailability was estimated to be ~50% (100). Therefore, a 5 mg intravenous dose was compared to a 10 mg tablet in a cross-over design. As the maximum concentrations after oral administration were generally reached at a median t_{max} of 90 min in humans (104), the 5 mg intravenous dose was infused over 90 min. However, the profiles after intravenous and oral administration differed substantially (cf. Figure 3-17), making a meaningful noncompartmental assessment of the absolute bioavailability impossible. Applying the standard approach of comparing $AUC_{p.o.}$ to $AUC_{i.v.}$ led to dose-dependent estimates of the absolute bioavailability ranging from 12% (10 mg oral compared to 0.5 mg intravenous) to 68% (10 mg oral compared to 10 mg intravenous).

Another possibility to estimate the absolute bioavailability in case of a nonlinear pharmacokinetics is to divide the fraction excreted renally after oral administration by the fraction excreted renally after intravenous administration (160). The prerequisites for this approach are: (a) urine needs to be collected until almost all the drug has been excreted, (b) the ratio of renal clearance and total clearance must not change after intravenous and oral administration, and (c) renal elimination should represent a major elimination pathway. As the renal elimination is only a minor route of elimination for linagliptin and the ratio of renal clearance and total clearance increased with increasing intravenous doses, this approach was considered inadequate to estimate the absolute bioavailability of linagliptin.

An alternative approach to determine the absolute bioavailability despite nonlinear pharmacokinetics is to use a population pharmacokinetic model that accounts for the nonlinear process. Estimating the absolute bioavailability by a population pharmacokinetic model was successfully performed previously (196,197). Thus, the plasma concentrations after oral administration were analysed together with those after intravenous administration using the target-mediated drug disposition model (Project 4). The absorption of linagliptin was described by a first-order process with lag time. The disposition of unbound linagliptin and the binding of linagliptin to DPP-4 were assumed to be identical within a subject after intravenous and oral administration. In this way it was possible to estimate the absolute bioavailability. After accounting for the saturable binding, the absolute bioavailability was estimated to be 29.5% (range of individual values: 12.9–60.8%).

4.4.2 Possible reasons for and consequences of the moderate bioavailability of linagliptin

Linagliptin may be classified within the biopharmaceutics classification system (BCS) (198,199) as a class 3 drug: Linagliptin exhibits a high aqueous solubility in the pH range of 1–7.5 and a low gastrointestinal permeability, based on the extent of absorption (parent plus metabolite) as determined by a mass balance determination in humans (personal communication, U. Graefe-Mody). Wu and Benet postulated that drugs classified in the BCS class 3 are poorly metabolised, but highly dependent on transporters (200). This is in line with the low metabolism observed for linagliptin and the elimination of primarily unchanged linagliptin in the urine and faeces. Thus, according to this theory, the moderate absolute bioavailability of linagliptin may be explained by transporters that prevent the complete absorption of the drug. This explanation is in line with the increase in the exposure of linagliptin in the drug-drug interaction study with P-glycoprotein and CYP3A4 inhibitor ritonavir (cf. section 4.3.4).

Low to moderate bioavailability is often a major source of variability in the pharmacokinetics of a compound (160,201). For example, given an absolute bioavailability of 5%, a subject with a numerically small increase in the absolute bioavailability of another 5% (10% in total) would have a 2-fold higher bioavailability and thus a 2-fold higher exposure assuming linear pharmacokinetics. For linagliptin, the major source of variability is indeed the absorption (cf. section 4.2.2.4).

In addition, compounds with a low to moderate bioavailability exhibit a higher risk for drug-drug interactions as the bioavailability allows room for an increased exposure (160). Due to the absolute bioavailability of linagliptin of ~30%, the absolute bioavailability can rise ~3.4-fold. Indeed, a ~4 fold increase was observed in the bioavailability of linagliptin under comedication with ritonavir (cf. Project 2d) corresponding to the worst case of a drug-drug interaction on the bioavailability of linagliptin, as the bioavailability under ritonavir comedication is most likely in average ~100%. Due to the nonlinear pharmacokinetics of linagliptin, the maximum 4-fold increase in the absolute bioavailability was only related to a 2-fold maximum increase in the AUC.

4.5 Impact of pharmacometrics on the drug development of linagliptin

Different publications describe the potential impact of pharmacometrics on the development of a drug (115,117,131,132). In this section, the impact of the results of this thesis on the clinical development of linagliptin is outlined.

4.5.1 Understanding and characterizing the nonlinear pharmacokinetics of linagliptin in the therapeutic concentration range

One major objective of this work was to contribute to a better understanding and characterisation of the nonlinear pharmacokinetics of linagliptin in the therapeutic dose range. For compounds with nonlinear pharmacokinetics, an in-depth understanding of the reasons for their nonlinearity is important to allow a safe and efficacious therapy.

A population analysis was used to test different hypotheses for mechanisms resulting in nonlinear pharmacokinetics in a clinical setting. A model assuming concentration-dependent protein binding of linagliptin to DPP-4 in plasma and tissues resulted in the best description of the plasma concentrations. This assumption was confirmed by a subsequent nonclinical study comparing the pharmacokinetics of wildtype and DPP-4-deficient rats. Both analyses corroborated the hypothesis that concentration-dependent binding of linagliptin to plasma and tissue DPP-4 is responsible for the nonlinear pharmacokinetics of linagliptin.

The target-mediated drug disposition of linagliptin has several clinically relevant implications (cf. section 4.1.4.4). Alterations of the bioavailability or the clearance of unbound

linagliptin, e.g., only translate to relatively small changes in its $AUC_{\tau,SS}$, a parameter often considered as a correlate for safety and efficacy.

By analytical methods it would not have been possible to determine the fraction of free linagliptin or linagliptin specifically bound to DPP-4, especially in peripheral tissues and for low plasma concentrations where nearly all available linagliptin is bound to DPP-4. The target-mediated drug disposition models developed within Projects 1 and 5 allowed to differentiate between bound and unbound linagliptin in plasma and peripheral tissues and thus allowed further insights into the nonlinear pharmacokinetics of linagliptin.

4.5.2 Covariate analysis

In a written response to a briefing package, the FDA agreed that no further studies were necessary to investigate the impact of age, sex, and weight on the pharmacokinetics of linagliptin. Thus, the population pharmacokinetic analysis presented in Project 3a saved three dedicated phase I studies to investigate these factors. The population analysis, in contrast to phase I studies, also allowed to investigate the impact of covariate combinations on the pharmacokinetics and the pharmacokinetic/pharmacodynamic relationship of linagliptin. None of the investigated covariates warrants a dose adjustment of linagliptin due to their clinically irrelevant impact on the pharmacokinetics or the plasma concentration/plasma DPP-4 activity relationship. Thus, no adjustment of the linagliptin dose is required for e.g. elderly or overweight patients, simplifying the therapy and thereby making it safer.

4.5.3 Clinical trial simulations

In case of the nonlinear pharmacokinetics of linagliptin the availability of a semi-mechanistic model greatly helped to design future studies. The simulation of an adequate linagliptin dose for a twice-daily treatment required for the fixed dose combination with metformin (Project 2a) saved one exploratory dose finding study. Furthermore, it allowed the development of the fixed dose formulation to start earlier, accelerating the fixed dose combination programme by about one year.

The simulation of the impact of impaired linagliptin clearance on the linagliptin exposure (Project 2b), alongside other considerations (e.g. high safety margin, predominantly eliminated by nonrenal processes), allowed including patients with a moderate renal

impairment in the phase IIb programme. Including these patients represented the type 2 diabetic population better, as they often suffer from renal impairment, and thus allowed to investigate the impact of moderate renal impairment on the pharmacokinetics of linagliptin in phase IIb.

The change-over design simulated for the dose-proportionally study in Project 2c helped to reduce the study duration by the length of two wash-out periods of ≥35 days each.

Furthermore, the model-based analysis of the pharmacokinetics of linagliptin under comedication with ritonavir suggested that coadministration with ritonavir resulted in a 4-fold increase in bioavailability and a 16% decrease in the clearance of linagliptin (Project 2d). Based on these assumptions, a simulation of the steady-state exposure of linagliptin was conducted. As observed after single dose, the simulation predicted a 2-fold increase in the AUC at steady-state for linagliptin under comedication with ritonavir. No major accumulation for linagliptin was predicted. These results, alongside other criteria, led to the evaluation that no dose adaptation is required for patients receiving P-glycoprotein or CYP3A4 inhibitors in comedication. However, this needs to be confirmed by future studies.

4.5.4 Further applications of the model

Without a population model that accounted for the nonlinear pharmacokinetics of linagliptin it would have been difficult to determine the absolute bioavailability of linagliptin. With the developed model the absolute bioavailability was estimated to be ~30% (Project 4). Knowledge of the absolute bioavailability is important to identify possible sources of variability and to anticipate possible under- or overexposures of a compound.

4.5.5 Outlook

Plasma DPP-4 inhibition is a valid proof-of-mechanism biomarker. It provides evidence of target engagement and is correlated to glucose lowering as shown for various DPP-4 inhibitors (105,106). In a future model development step, disease-related biomarkers which are more intimately linked to clinical outcome such as glucose or HbA1c may be included into the model. Using such an extended model, the relationship between linagliptin exposure and/or DPP-4 activity and disease-related biomarkers could be characterised, and factors impacting the biomarker response could be identified. Thus, one might differentiate subgroups of patients highly benefiting from linagliptin treatment and potential non-

responders. A disease model quantifying the relationship between glucose and HbA1c, the natural disease progression, and a placebo effect would to a high degree be compound-independent. Such a glucose/HbA1c model would allow long-term predictions based on short-term data, and would thus be of great help in designing phase IIb and phase III trials for the development of subsequent antidiabetic compounds. An example for a disease model applicable for different compounds is the tumour-size survival model for non-small cell lung cancer (202). Also in the field of diabetes, different compound-independent approaches exist, e.g. a glucose-insulin model describing glucose tolerance test data (203,204). Such models, quantitatively summarizing prior knowledge of the compound and the disease, will guide and thereby improve future clinical drug development (202).

Summary

Linaglipin is a novel dipeptidyl-peptidase 4 (DPP-4) inhibitor in clinical development for the treatment of type 2 diabetes. This thesis investigated the nonlinear pharmacokinetics of linagliptin as well as the relationship between linagliptin pharmacokinetics and plasma DPP-4 activity using nonlinear mixed-effect modelling. The developed models supported the clinical drug development of linagliptin by clinical trial simulations.

Based on previous *in vitro* plasma protein binding studies, concentration-dependent protein binding was considered to be the most likely cause of the nonlinear pharmacokinetics of linagliptin. This hypothesis was tested by analysing linagliptin plasma concentrations and plasma DPP-4 activities from two phase IIa studies in type 2 diabetic patients. A model assuming concentration-dependent protein binding of linagliptin in plasma and tissues resulted in the best description of the linagliptin plasma concentrations, supporting the initial hypothesis. Several lines of evidence suggested that the binding partner of linagliptin responsible for the nonlinear pharmacokinetics is its target, DPP-4. Accordingly, plasma DPP-4 activity was included in the model in a semi-mechanistic way by relating it to the model-calculated plasma DPP-4 occupancy with linagliptin. The assumption of target-mediated drug disposition was confirmed in a subsequent nonclinical study. In this nonclinical study, wildtype rats exhibited a higher systemic exposure and a longer terminal half-life of linagliptin compared to DPP-4 deficient rats. These differences could be described by a single pharmacokinetic model assuming concentration-dependent protein binding in the plasma and tissue of wildtype rats and no binding for DPP-4 deficient rats. Taken together, both analyses suggest that concentration-dependent binding of linagliptin to plasma and tissue DPP-4 is responsible for the nonlinear pharmacokinetics of linagliptin.

The nonlinear pharmacokinetics of linagliptin complicate predictions that are based solely on noncompartmental parameters. The availability of the target-mediated drug disposition model allowed simulations that greatly supported the design of future clinical studies. A twice-daily dosing strategy for a fixed dose combination of linagliptin with metformin was simulated. The simulations predicted that despite the nonlinear pharmacokinetics, 2.5 mg linagliptin twice daily would result in a bioequivalent extent of exposure ($AUC_{24h,SS}$) as well as a similar DPP-4 inhibition compared to 5 mg linagliptin once daily. Other simula-

tions demonstrated that due to its nonlinear pharmacokinetics, the impact of impaired linagliptin clearance on the systemic exposure was sufficiently small to allow patients with a moderate renal impairment to participate in the phase IIb programme. Further simulations were performed to investigate the optimal duration of a treatment period in a change-over design to adequately test the dose-proportionality of linagliptin at steady-state. It was shown that a treatment period of seven days was sufficient to attain steady-state for 1, 2.5, and 5 mg linagliptin once daily in each sequence. In addition, steady-state exposure of linagliptin under ritonavir comedication was simulated based on a pharmacokinetic model describing the single dose plasma concentration-time profiles from a drug-drug interaction trial. The simulation predicted a 2-fold increase in the $AUC_{\tau,SS}$ with no major accumulation of linagliptin under ritonavir comedication.

Covariate analyses were performed to identify clinically relevant covariates for the pharmacokinetics and the pharmacodynamics of linagliptin. The analyses were based on linagliptin plasma concentrations and DPP-4 activities of type 2 diabetic patients from two phase IIa and two phase IIb studies. Demographic information, laboratory values including liver enzymes and creatinine clearance, as well as study related factors like metformin co-treatment were investigated. None of the covariates individually affected the $AUC_{\tau,SS}$ of patients receiving 5 mg linagliptin once daily by more than ±20% and thus no covariate was considered to be clinically relevant. Likewise, the impact of the covariates on the EC_{50} or the concentration leading to 80% DPP-4 inhibition was less than ±20%. Based on these analyses, no dose adjustment is expected to be necessary for the tested covariates.

For compounds with nonlinear pharmacokinetics, the standard approach to determine the absolute bioavailability is not valid. Thus, linagliptin plasma concentrations after single oral administration of 10 mg linagliptin and single intravenous administrations of 0.5, 2.5, 5, or 10 mg linagliptin were analysed by the target-mediated drug disposition model. Using this approach, the absolute bioavailability could be estimated despite the nonlinear pharmacokinetics. The absolute bioavailability was estimated to be 29.5%.

In conclusion, the work presented in this thesis contributes to a comprehensive understanding and characterisation of the nonlinear pharmacokinetics of the novel DPP-4 inhibitor linagliptin and significantly supports the clinical development of this promising compound to be used for the treatment of type 2 diabetes.

References

(1) International Diabetes Federation. Diabetes Prevalence [document on the Internet]. International Diabetes Federation 2009 [cited 2009 Jun 21]. Available from: http://www.idf.org/diabetes-prevalence

(2) Wild S, Roglic G, Green A, Sicree R, King H. Global prevalence of diabetes: estimates for the year 2000 and projections for 2030. Diabetes Care 2004;27:1047-53.

(3) World Health Organization. Definition and diagnosis of diabetes mellitus and intermediate hyperglycemia: Report of a WHO/IDF consultation. Geneva: World Health Organization; 2006.

(4) World Health Organization. Definition, diagnosis and classification of diabetes mellitus and its complications: Report of a WHO consultation. Part 1: Diagnosis and classification of diabetes mellitus. Geneva: World Health Organization; 1999.

(5) Genuth S, Alberti KG, Bennett P, Buse J, Defronzo R, Kahn R, et al. Follow-up report on the diagnosis of diabetes mellitus. Diabetes Care 2003;26:3160-7.

(6) Ferrannini E. Insulin resistance versus insulin deficiency in non-insulin-dependent diabetes mellitus: problems and prospects. Endocr Rev 1998;19:477-90.

(7) Lillioja S, Mott DM, Spraul M, Ferraro R, Foley JE, Ravussin E, et al. Insulin resistance and insulin secretory dysfunction as precursors of non-insulin-dependent diabetes mellitus. Prospective studies of Pima Indians. N Engl J Med 1993;329:1988-92.

(8) Andrulionyte L, Zacharova J, Chiasson JL, Laakso M. Common polymorphisms of the PPAR-gamma2 (Pro12Ala) and PGC-1alpha (Gly482Ser) genes are associated with the conversion from impaired glucose tolerance to type 2 diabetes in the STOP-NIDDM trial. Diabetologia 2004;47:2176-84.

(9) Barroso I. Genetics of Type 2 diabetes. Diabet Med 2005;22:517-35.

(10) Harris MI. Epidemiological correlates of NIDDM in Hispanics, whites, and blacks in the U.S. population. Diabetes Care 1991;14:639-48.

(11) Kahn SE, Hull RL, Utzschneider KM. Mechanisms linking obesity to insulin resistance and type 2 diabetes. Nature 2006;444:840-6.

(12) Inzucchi SE. Oral antihyperglycemic therapy for type 2 diabetes: scientific review. JAMA 2002;287:360-72.

(13) Yki-Jarvinen H. Acute and chronic effects of hyperglycaemia on glucose metabolism: implications for the development of new therapies. Diabet Med 1997;14 Suppl 3:S32-S37.

(14) Bergman RN, Ader M. Free fatty acids and pathogenesis of type 2 diabetes mellitus. Trends Endocrinol Metab 2000;11:351-6.

(15) Laakso M. Hyperglycemia and cardiovascular disease in type 2 diabetes. Diabetes 1999;48:937-42.

(16) Intensive blood-glucose control with sulphonylureas or insulin compared with conventional treatment and risk of complications in patients with type 2 diabetes (UKPDS 33). UK Prospective Diabetes Study (UKPDS) Group. Lancet 1998;352:837-53.

(17) Effect of intensive blood-glucose control with metformin on complications in overweight patients with type 2 diabetes (UKPDS 34). UK Prospective Diabetes Study (UKPDS) Group. Lancet 1998;352:854-65.

(18) Ohkubo Y, Kishikawa H, Araki E, Miyata T, Isami S, Motoyoshi S, et al. Intensive insulin therapy prevents the progression of diabetic microvascular complications in Japanese patients with non-insulin-dependent diabetes mellitus: a randomized prospective 6-year study. Diabetes Res Clin Pract 1995;28:103-17.

(19) Nathan DM, Cleary PA, Backlund JY, Genuth SM, Lachin JM, Orchard TJ, et al. Intensive diabetes treatment and cardiovascular disease in patients with type 1 diabetes. N Engl J Med 2005;353:2643-53.

(20) Nathan DM, Lachin J, Cleary P, Orchard T, Brillon DJ, Backlund JY, et al. Intensive diabetes therapy and carotid intima-media thickness in type 1 diabetes mellitus. N Engl J Med 2003;348:2294-303.

(21) Gerstein HC, Miller ME, Byington RP, Goff DC, Jr., Bigger JT, Buse JB, et al. Effects of intensive glucose lowering in type 2 diabetes. N Engl J Med 2008;358:2545-59.

(22) Patel A, MacMahon S, Chalmers J, Neal B, Billot L, Woodward M, et al. Intensive blood glucose control and vascular outcomes in patients with type 2 diabetes. N Engl J Med 2008;358:2560-72.

(23) Holman RR, Paul SK, Bethel MA, Matthews DR, Neil HA. 10-year follow-up of intensive glucose control in type 2 diabetes. N Engl J Med 2008;359:1577-89.

(24) Nathan DM, Buse JB, Davidson MB, Ferrannini E, Holman RR, Sherwin R, et al. Medical Management of Hyperglycemia in Type 2 Diabetes: a Consensus Algorithm for the Initiation and Adjustment of Therapy. Diabetes Care 2008;32:193-203.

(25) Pi-Sunyer X, Blackburn G, Brancati FL, Bray GA, Bright R, Clark JM, et al. Reduction in weight and cardiovascular disease risk factors in individuals with type 2 diabetes: one-year results of the look AHEAD trial. Diabetes Care 2007;30:1374-83.

(26) Van de Laar FA, Lucassen PL, Akkermans RP, Van de Lisdonk EH, Rutten GE, Van WC. Alpha-glucosidase inhibitors for type 2 diabetes mellitus. Cochrane Database Syst Rev 2005;(2):CD003639.

(27) Yki-Jarvinen H. Thiazolidinediones. N Engl J Med 2004;351:1106-18.

(28) United Kingdom Prospective Diabetes Study Group. United Kingdom Prospective Diabetes Study (UKPDS). 13: Relative efficacy of randomly allocated diet, sul-

phonylurea, insulin, or metformin in patients with newly diagnosed non-insulin dependent diabetes followed for three years. BMJ 1995;310:83-8.

(29) Singh S, Loke YK, Furberg CD. Thiazolidinediones and heart failure: a teleo-analysis. Diabetes Care 2007;30:2148-53.

(30) Nissen SE, Wolski K. Effect of rosiglitazone on the risk of myocardial infarction and death from cardiovascular causes. N Engl J Med 2007;356:2457-71.

(31) Singh S, Loke YK, Furberg CD. Long-term risk of cardiovascular events with rosiglitazone: a meta-analysis. JAMA 2007;298:1189-95.

(32) Elrick H, Stimmler L, Hlad CJ, Rai Y. Plasma insulin response to oral and intravenous glucose administration. J Clin Endocrinol Metab 1964;24:1076-82.

(33) Nauck MA, Homberger E, Siegel EG, Allen RC, Eaton RP, Ebert R, et al. Incretin effects of increasing glucose loads in man calculated from venous insulin and C-peptide responses. J Clin Endocrinol Metab 1986;63:492-8.

(34) Efendic S, Portwood N. Overview of incretin hormones. Horm Metab Res 2004;36:742-6.

(35) Kim W, Egan JM. The role of incretins in glucose homeostasis and diabetes treatment. Pharmacol Rev 2008;60:470-512.

(36) Deacon CF. What do we know about the secretion and degradation of incretin hormones? Regul Pept 2005;128:117-24.

(37) Schmidt WE, Siegel EG, Creutzfeldt W. Glucagon-like peptide-1 but not glucagon-like peptide-2 stimulates insulin release from isolated rat pancreatic islets. Diabetologia 1985;28:704-7.

(38) Dupre J, Ross SA, Watson D, Brown JC. Stimulation of insulin secretion by gastric inhibitory polypeptide in man. J Clin Endocrinol Metab 1973;37:826-8.

(39) Ross SA, Dupre J. Effects of ingestion of triglyceride or galactose on secretion of gastric inhibitory polypeptide and on responses to intravenous glucose in normal and diabetic subjects. Diabetes 1978;27:327-33.

(40) Orskov C, Holst JJ, Nielsen OV. Effect of truncated glucagon-like peptide-1 [proglucagon-(78-107) amide] on endocrine secretion from pig pancreas, antrum, and nonantral stomach. Endocrinology 1988;123:2009-13.

(41) Komatsu R, Matsuyama T, Namba M, Watanabe N, Itoh H, Kono N, et al. Glucagonostatic and insulinotropic action of glucagonlike peptide I-(7-36)-amide. Diabetes 1989;38:902-5.

(42) Nauck MA, Kleine N, Orskov C, Holst JJ, Willms B, Creutzfeldt W. Normalization of fasting hyperglycaemia by exogenous glucagon-like peptide 1 (7-36 amide) in type 2 (non-insulin-dependent) diabetic patients. Diabetologia 1993;36:741-4.

(43) Farilla L, Hui H, Bertolotto C, Kang E, Bulotta A, Di MU, et al. Glucagon-like peptide-1 promotes islet cell growth and inhibits apoptosis in Zucker diabetic rats. Endocrinology 2002;143:4397-408.

(44) Perfetti R, Zhou J, Doyle ME, Egan JM. Glucagon-like peptide-1 induces cell proliferation and pancreatic-duodenum homeobox-1 expression and increases endocrine cell mass in the pancreas of old, glucose-intolerant rats. Endocrinology 2000;141:4600-5.

(45) Stoffers DA, Kieffer TJ, Hussain MA, Drucker DJ, Bonner-Weir S, Habener JF, et al. Insulinotropic glucagon-like peptide 1 agonists stimulate expression of homeodomain protein IDX-1 and increase islet size in mouse pancreas. Diabetes 2000;49:741-8.

(46) Trumper A, Trumper K, Trusheim H, Arnold R, Goke B, Horsch D. Glucose-dependent insulinotropic polypeptide is a growth factor for beta (INS-1) cells by pleiotropic signaling. Mol Endocrinol 2001;15:1559-70.

(47) Trumper A, Trumper K, Horsch D. Mechanisms of mitogenic and anti-apoptotic signaling by glucose-dependent insulinotropic polypeptide in beta(INS-1)-cells. J Endocrinol 2002;174:233-46.

(48) Farilla L, Bulotta A, Hirshberg B, Li CS, Khoury N, Noushmehr H, et al. Glucagon-like peptide 1 inhibits cell apoptosis and improves glucose responsiveness of freshly isolated human islets. Endocrinology 2003;144:5149-58.

(49) Wettergren A, Schjoldager B, Mortensen PE, Myhre J, Christiansen J, Holst JJ. Truncated GLP-1 (proglucagon 78-107-amide) inhibits gastric and pancreatic functions in man. Dig Dis Sci 1993;38:665-73.

(50) Willms B, Werner J, Holst JJ, Orskov C, Creutzfeldt W, Nauck MA. Gastric emptying, glucose responses, and insulin secretion after a liquid test meal: effects of exogenous glucagon-like peptide-1 (GLP-1)-(7-36) amide in type 2 (noninsulin-dependent) diabetic patients. J Clin Endocrinol Metab 1996;81:327-32.

(51) Toft-Nielsen MB, Damholt MB, Madsbad S, Hilsted LM, Hughes TE, Michelsen BK, et al. Determinants of the impaired secretion of glucagon-like peptide-1 in type 2 diabetic patients. J Clin Endocrinol Metab 2001;86:3717-23.

(52) Nauck M, Stockmann F, Ebert R, Creutzfeldt W. Reduced incretin effect in type 2 (non-insulin-dependent) diabetes. Diabetologia 1986;29:46-52.

(53) Mitrakou A, Kelley D, Mokan M, Veneman T, Pangburn T, Reilly J, et al. Role of reduced suppression of glucose production and diminished early insulin release in impaired glucose tolerance. N Engl J Med 1992;326:22-9.

(54) Nauck MA, Heimesaat MM, Orskov C, Holst JJ, Ebert R, Creutzfeldt W. Preserved incretin activity of glucagon-like peptide 1 [7-36 amide] but not of synthetic human gastric inhibitory polypeptide in patients with type-2 diabetes mellitus. J Clin Invest 1993;91:301-7.

(55) Zander M, Madsbad S, Madsen JL, Holst JJ. Effect of 6-week course of glucagon-like peptide 1 on glycaemic control, insulin sensitivity, and beta-cell function in type 2 diabetes: a parallel-group study. Lancet 2002;359:824-30.

(56) Hansen L, Deacon CF, Orskov C, Holst JJ. Glucagon-like peptide-1-(7-36)amide is transformed to glucagon-like peptide-1-(9-36)amide by dipeptidyl peptidase IV in

the capillaries supplying the L cells of the porcine intestine. Endocrinology 1999;140:5356-63.

(57) Lambeir AM, Durinx C, Scharpe S, De M, I. Dipeptidyl-peptidase IV from bench to bedside: an update on structural properties, functions, and clinical aspects of the enzyme DPP IV. Crit Rev Clin Lab Sci 2003;40:209-94.

(58) Mentlein R. Dipeptidyl-peptidase IV (CD26)--role in the inactivation of regulatory peptides. Regul Pept 1999;85:9-24.

(59) Mentlein R, Gallwitz B, Schmidt WE. Dipeptidyl-peptidase IV hydrolyses gastric inhibitory polypeptide, glucagon-like peptide-1(7-36)amide, peptide histidine methionine and is responsible for their degradation in human serum. Eur J Biochem 1993;214:829-35.

(60) Mentlein R, Dahms P, Grandt D, Kruger R. Proteolytic processing of neuropeptide Y and peptide YY by dipeptidyl peptidase IV. Regul Pept 1993;49:133-44.

(61) Ahmad S, Wang L, Ward PE. Dipeptidyl(amino)peptidase IV and aminopeptidase M metabolize circulating substance P in vivo. J Pharmacol Exp Ther 1992;260:1257-61.

(62) Bongers J, Lambros T, Ahmad M, Heimer EP. Kinetics of dipeptidyl peptidase IV proteolysis of growth hormone-releasing factor and analogs. Biochim Biophys Acta 1992;1122:147-53.

(63) Wolf M, Albrecht S, Marki C. Proteolytic processing of chemokines: implications in physiological and pathological conditions. Int J Biochem Cell Biol 2008;40:1185-98.

(64) Loster K, Zeilinger K, Schuppan D, Reutter W. The cysteine-rich region of dipeptidyl peptidase IV (CD 26) is the collagen-binding site. Biochem Biophys Res Commun 1995;217:341-8.

(65) Herrera C, Morimoto C, Blanco J, Mallol J, Arenzana F, Lluis C, et al. Comodulation of CXCR4 and CD26 in human lymphocytes. J Biol Chem 2001;276:19532-9.

(66) Kameoka J, Tanaka T, Nojima Y, Schlossman SF, Morimoto C. Direct association of adenosine deaminase with a T cell activation antigen, CD26. Science 1993;261:466-9.

(67) Valenzuela A, Blanco J, Callebaut C, Jacotot E, Lluis C, Hovanessian AG, et al. Adenosine deaminase binding to human CD26 is inhibited by HIV-1 envelope glycoprotein gp120 and viral particles. J Immunol 1997;158:3721-9.

(68) Verstovsek S, Cabanillas F, Dang NH. CD26 in T-cell lymphomas: a potential clinical role? Oncology (Williston Park) 2000;14(6 Suppl 2):17-23.

(69) Carbone A, Gloghini A, Zagonel V, Aldinucci D, Gattei V, Degan M, et al. The expression of CD26 and CD40 ligand is mutually exclusive in human T-cell non-Hodgkin's lymphomas/leukemias. Blood 1995;86:4617-26.

(70) Ruiz P, Mailhot S, Delgado P, Amador A, Viciana AL, Ferrer L, et al. CD26 expression and dipeptidyl peptidase IV activity in an aggressive hepatosplenic T-cell lymphoma. Cytometry 1998 Feb;34:30-5.

(71) Callebaut C, Krust B, Jacotot E, Hovanessian AG. T cell activation antigen, CD26, as a cofactor for entry of HIV in CD4+ cells. Science 1993 Dec;262:2045-50.

(72) Hong WJ, Petell JK, Swank D, Sanford J, Hixson DC, Doyle D. Expression of dipeptidyl peptidase IV in rat tissues is mainly regulated at the mRNA levels. Exp Cell Res 1989;182:256-66.

(73) Fukasawa KM, Fukasawa K, Sahara N, Harada M, Kondo Y, Nagatsu I. Immunohistochemical localization of dipeptidyl aminopeptidase IV in rat kidney, liver, and salivary glands. J Histochem Cytochem 1981;29:337-43.

(74) Hartel S, Gossrau R, Hanski C, Reutter W. Dipeptidyl peptidase (DPP) IV in rat organs. Comparison of immunohistochemistry and activity histochemistry. Histochemistry 1988;89:151-61.

(75) Lojda Z. Studies on dipeptidyl(amino)peptidase IV (glycyl-proline naphthylamidase). II. Blood vessels. Histochemistry 1979;59:153-66.

(76) Mentzel S, Dijkman HB, van Son JP, Koene RA, Assmann KJ. Organ distribution of aminopeptidase A and dipeptidyl peptidase IV in normal mice. J Histochem Cytochem 1996;44:445-61.

(77) Gorrell MD, Wickson J, McCaughan GW. Expression of the rat CD26 antigen (dipeptidyl peptidase IV) on subpopulations of rat lymphocytes. Cell Immunol 1991;134:205-15.

(78) Iwaki-Egawa S, Watanabe Y, Kikuya Y, Fujimoto Y. Dipeptidyl peptidase IV from human serum: purification, characterization, and N-terminal amino acid sequence. J Biochem 1998;124:428-33.

(79) Cordero OJ, Ayude D, Nogueira M, Rodriguez-Berrocal FJ, de la Cadena MP. Preoperative serum CD26 levels: diagnostic efficiency and predictive value for colorectal cancer. Br J Cancer 2000;83:1139-46.

(80) Cuchacovich M, Gatica H, Pizzo SV, Gonzalez-Gronow M. Characterization of human serum dipeptidyl peptidase IV (CD26) and analysis of its autoantibodies in patients with rheumatoid arthritis and other autoimmune diseases. Clin Exp Rheumatol 2001;19:673-80.

(81) Watanabe Y, Kojima T, Fujimoto Y. Deficiency of membrane-bound dipeptidyl aminopeptidase IV in a certain rat strain. Experientia 1987;43:400-1.

(82) Tsuji E, Misumi Y, Fujiwara T, Takami N, Ogata S, Ikehara Y. An active-site mutation (Gly633-->Arg) of dipeptidyl peptidase IV causes its retention and rapid degradation in the endoplasmic reticulum. Biochemistry 1992;31:11921-7.

(83) Marguet D, Baggio L, Kobayashi T, Bernard AM, Pierres M, Nielsen PF, et al. Enhanced insulin secretion and improved glucose tolerance in mice lacking CD26. Proc Natl Acad Sci U S A 2000;97:6874-9.

(84) Nagakura T, Yasuda N, Yamazaki K, Ikuta H, Yoshikawa S, Asano O, et al. Improved glucose tolerance via enhanced glucose-dependent insulin secretion in dipeptidyl peptidase IV-deficient Fischer rats. Biochem Biophys Res Commun 2001;284:501-6.

(85) Mitani H, Takimoto M, Hughes TE, Kimura M. Dipeptidyl peptidase IV inhibition improves impaired glucose tolerance in high-fat diet-fed rats: study using a Fischer 344 rat substrain deficient in its enzyme activity. Jpn J Pharmacol 2002;88:442-50.

(86) Yasuda N, Nagakura T, Yamazaki K, Inoue T, Tanaka I. Improvement of high fat-diet-induced insulin resistance in dipeptidyl peptidase IV-deficient Fischer rats. Life Sci 2002;71:227-38.

(87) Drucker DJ, Nauck MA. The incretin system: glucagon-like peptide-1 receptor agonists and dipeptidyl peptidase-4 inhibitors in type 2 diabetes. Lancet 2006;368:1696-705.

(88) DeFronzo RA, Ratner RE, Han J, Kim DD, Fineman MS, Baron AD. Effects of exenatide (exendin-4) on glycemic control and weight over 30 weeks in metformin-treated patients with type 2 diabetes. Diabetes Care 2005;28:1092-100.

(89) Kendall DM, Riddle MC, Rosenstock J, Zhuang D, Kim DD, Fineman MS, et al. Effects of exenatide (exendin-4) on glycemic control over 30 weeks in patients with type 2 diabetes treated with metformin and a sulfonylurea. Diabetes Care 2005;28:1083-91.

(90) Buse JB, Henry RR, Han J, Kim DD, Fineman MS, Baron AD. Effects of exenatide (exendin-4) on glycemic control over 30 weeks in sulfonylurea-treated patients with type 2 diabetes. Diabetes Care 2004;27:2628-35.

(91) Nauck MA, Hompesch M, Filipczak R, Le TD, Zdravkovic M, Gumprecht J. Five weeks of treatment with the GLP-1 analogue liraglutide improves glycaemic control and lowers body weight in subjects with type 2 diabetes. Exp Clin Endocrinol Diabetes 2006;114:417-23.

(92) Riddle MC, Henry RR, Poon TH, Zhang B, Mac SM, Holcombe JH, et al. Exenatide elicits sustained glycaemic control and progressive reduction of body weight in patients with type 2 diabetes inadequately controlled by sulphonylureas with or without metformin. Diabetes Metab Res Rev 2006;22:483-91.

(93) Amori RE, Lau J, Pittas AG. Efficacy and safety of incretin therapy in type 2 diabetes: systematic review and meta-analysis. JAMA 2007;298:194-206.

(94) Richter B, Bandeira-Echtler E, Bergerhoff K, Lerch CL. Dipeptidyl peptidase-4 (DPP-4) inhibitors for type 2 diabetes mellitus. Cochrane Database Syst Rev 2008;(2):CD006739.

(95) Mu J, Woods J, Zhou YP, Roy RS, Li Z, Zycband E, et al. Chronic inhibition of dipeptidyl peptidase-4 with a sitagliptin analog preserves pancreatic beta-cell mass and function in a rodent model of type 2 diabetes. Diabetes 2006;55:1695-704.

(96) Xu G, Stoffers DA, Habener JF, Bonner-Weir S. Exendin-4 stimulates both beta-cell replication and neogenesis, resulting in increased beta-cell mass and improved glucose tolerance in diabetic rats. Diabetes 1999;48:2270-6.

(97) Rolin B, Larsen MO, Gotfredsen CF, Deacon CF, Carr RD, Wilken M, et al. The long-acting GLP-1 derivative NN2211 ameliorates glycemia and increases beta-cell mass in diabetic mice. Am J Physiol Endocrinol Metab 2002;283:E745-E752.

(98) Pospisilik JA, Martin J, Doty T, Ehses JA, Pamir N, Lynn FC, et al. Dipeptidyl peptidase IV inhibitor treatment stimulates beta-cell survival and islet neogenesis in streptozotocin-induced diabetic rats. Diabetes 2003;52:741-50.

(99) Eckhardt M, Hauel N, Himmelsbach F, Langkopf E, Nar H, Mark M, et al. 3,5-Dihydro-imidazo[4,5-d]pyridazin-4-ones: a class of potent DPP-4 inhibitors. Bioorg Med Chem Lett 2008;18:3158-62.

(100) Eckhardt M, Langkopf E, Mark M, Tadayyon M, Thomas L, Nar H, et al. 8-(3-(R)-aminopiperidin-1-yl)-7-but-2-ynyl-3-methyl-1-(4-methyl-quinazolin -2-ylmethyl)-3,7-dihydropurine-2,6-dione (BI 1356), a highly potent, selective, long-acting, and orally bioavailable DPP-4 inhibitor for the treatment of type 2 diabetes. J Med Chem 2007;50:6450-3.

(101) Thomas L, Eckhardt M, Langkopf E, Tadayyon M, Himmelsbach F, Mark M. (R)-8-(3-amino-piperidin-1-yl)-7-but-2-ynyl-3-methyl-1-(4-methyl-quinazoli n-2-ylmethyl)-3,7-dihydro-purine-2,6-dione (BI 1356), a novel xanthine-based dipeptidyl peptidase 4 inhibitor, has a superior potency and longer duration of action compared with other dipeptidyl peptidase-4 inhibitors. J Pharmacol Exp Ther 2008;325:175-82.

(102) Thomas L, Tadayyon M, Mark M. Chronic Treatment with the Dipeptidyl Peptidase-4 Inhibitor (R)-8-(3-Amino-piperidin-1-yl)-7-but-2-ynyl-3-methyl-1-(4-methyl-quinazoli n-2-ylmethyl)-3,7-dihydro-purine-2,6-dione (BI 1356) Increases Basal Glucagon-Like Peptide-1 and Improves Glycemic Control in Diabetic Rodent Models. J Pharmacol Exp Ther 2008;328:556-63.

(103) Huttner S, Graefe-Mody EU, Withopf B, Ring A, Dugi KA. Safety, tolerability, pharmacokinetics, and pharmacodynamics of single oral doses of BI 1356, an inhibitor of dipeptidyl peptidase 4, in healthy male volunteers. J Clin Pharmacol 2008;48:1171-8.

(104) Heise T, Graefe-Mody EU, Huttner S, Ring A, Trommeshauser D, Dugi KA. Pharmacokinetics, pharmacodynamics and tolerability of multiple oral doses of linagliptin, a dipeptidyl peptidase-4 inhibitor in male type 2 diabetes patients. Diabetes Obes Metab 2009;11:786-94.

(105) Krishna R, Herman G, Wagner JA. Accelerating drug development using biomarkers: a case study with sitagliptin, a novel DPP4 inhibitor for type 2 diabetes. AAPS J 2008;10:401-9.

(106) Roy RS, Wu J, Eiermann GJ, Lyons KA, He H, Weber AE, et al. Plasma DPP-4 inhibition by sitagliptin and other DPP-4 inhibitors correlates with and predicts glucose lowering efficacy. Presented at: ADA 2009. The American Diabetes Association's 69th Scientific Sessions; 2009 Jun 5; New Orleans, LA.

(107) Boehringer Ingelheim. Investigator's Brochure Linagliptin. Biberach: Boehringer Ingelheim; 2008.

(108) Bergman AJ, Stevens C, Zhou Y, Yi B, Laethem M, De SM, et al. Pharmacokinetic and pharmacodynamic properties of multiple oral doses of sitagliptin, a dipeptidyl peptidase-IV inhibitor: a double-blind, randomized, placebo-controlled study in healthy male volunteers. Clin Ther 2006;28:55-72.

(109) He YL, Serra D, Wang Y, Campestrini J, Riviere GJ, Deacon CF, et al. Pharmacokinetics and pharmacodynamics of vildagliptin in patients with type 2 diabetes mellitus. Clin Pharmacokinet 2007;46:577-88.

(110) Covington P, Christopher R, Davenport M, Fleck P, Mekki QA, Wann ER, et al. Pharmacokinetic, pharmacodynamic, and tolerability profiles of the dipeptidyl peptidase-4 inhibitor alogliptin: a randomized, double-blind, placebo-controlled, multiple-dose study in adult patients with type 2 diabetes. Clin Ther 2008;30:499-512.

(111) Fura A, Khanna A, Vyas V, Koplowitz B, Chang SY, Caporuscio C, et al. Pharmacokinetics of the dipeptidyl peptidase 4 inhibitor saxagliptin in rats, dogs, and monkeys and clinical projections. Drug Metab Dispos 2009;37:1164-71.

(112) Lankas GR, Leiting B, Roy RS, Eiermann GJ, Beconi MG, Biftu T, et al. Dipeptidyl peptidase IV inhibition for the treatment of type 2 diabetes: potential importance of selectivity over dipeptidyl peptidases 8 and 9. Diabetes 2005;54:2988-94.

(113) Ette EI, Williams P.J., editors. Pharmacometrics The Science of Quantitative Pharmacology. Hoboken, NJ: Wiley & Sons; 2007.

(114) Lehr T, Staab A, Schaefer HG. Biosimulation in Clinical Drug Development. In: Bertau M, Mosekilde E, Westerhoff V, editors. Biosimulation in Drug Development.Weinheim: Wiley - VCH; 2007.

(115) U.S. Food and Drug Administration. Guidance for Industry: Population Pharmacokinetics [document on the Internet]. Rockville, MD: U.S. Food and Drug Administration; 1999 [cited 2009 Aug 12]. Available from: http://www.fda.gov/downloads/Drugs/GuidanceComplianceRegulatoryInformation/Guidances/UCM072137.pdf

(116) Aarons L. Population pharmacokinetics: Theory and practice. Brit J Clin Pharmacol 1991;32:669-70.

(117) Samara E, Granneman R. Role of population pharmacokinetics in drug development. A pharmaceutical industry perspective. Clin Pharmacokinet 1997;32:294-312.

(118) Jonsson EN, Wade JR, Karlsson MO. Nonlinearity detection: advantages of nonlinear mixed-effects modeling. AAPS PharmSci 2000;2(3):E32.

(119) Sheiner LB, Beal SL. Evaluation of methods for estimating population pharmacokinetic parameters II. Biexponential model and experimental pharmacokinetic data. J Pharmacokinet Biopharm 1981;9:635-51.

(120) Ette EI, Williams PJ. Population pharmacokinetics II: estimation methods. Ann Pharmacother 2004;38:1907-15.

(121) Aarons L. Software for population pharmacokinetics and pharmacodynamics. Clin Pharmacokinet 1999;36:255-64.

(122) Lavielle M, Mentre F. Estimation of population pharmacokinetic parameters of saquinavir in HIV patients with the MONOLIX software. J Pharmacokinet Pharmacodyn 2007;34:229-49.

(123) Mentre F. History and new developments in estimation methods in nonlinear mixed-effects models. Presented at: PAGE 2005. The Population Approach Group Europe's 14th Meeting (Abstr 833); 2005 Jun 16; Pamplona, Spain.

(124) Beal SL, Sheiner LB. NONMEM Users Guides. San Francisco: University of California; 1998.

(125) Sheiner LB, Beal SL. Evaluation of methods for estimating population pharmacokinetic parameters. I. Michaelis-Menten model: Routine clinical pharmacokinetic data. J Pharmacokinet Biopharm 1980;8:553-71.

(126) Bauer RJ, Guzy S, Ng C. A survey of population analysis methods and software for complex pharmacokinetic and pharmacodynamic models with examples. AAPS J 2007;9:E60-E83.

(127) European Medicines Agency. Guideline on reporting the results of population pharmacokinetic analyses. London: European Medicines Agency; 2008.

(128) U.S. Food and Drug Administration. Challenge and opportunity on the critical path to new medical products [document on the Internet]. Rockville, MD: U.S. Food and Drug Administration; 2004 [cited 2009 Aug 12]. Available from: http://www.fda.gov/downloads/ScienceResearch/SpecialTopics/CriticalPathInitiative/CriticalPathOpportunitiesReports/ucm113411.pdf

(129) Bhattaram VA, Booth BP, Ramchandani RP, Beasley BN, Wang Y, Tandon V, et al. Impact of pharmacometrics on drug approval and labeling decisions: A survey of 42 new drug applications. AAPS J 2005;7(3):E503-12.

(130) Bhattaram VA, Bonapace C, Chilukuri DM, Duan JZ, Garnett C, Gobburu JV, et al. Impact of pharmacometric reviews on new drug approval and labeling decisions--a survey of 31 new drug applications submitted between 2005 and 2006. Clin Pharmacol Ther 2007;81:213-21.

(131) Williams PJ, Ette EI. The role of population pharmacokinetics in drug development in light of the Food and Drug Administration's 'Guidance for Industry: population pharmacokinetics'. Clin Pharmacokinet 2000;39:385-95.

(132) Sheiner LB, Steimer JL. Pharmacokinetic/pharmacodynamic modeling in drug development. Annu Rev Pharmacol Toxicol 2000;40:67-95.

(133) U.S. Food and Drug Administration. Guidance for Industry: bioanalytical method validation [document on the Internet]. Rockville, MD: U.S. Food and Drug Administration; 2001 [cited 2009 Aug 12]. Available from: http://www.fda.gov/downloads/Drugs/GuidanceComplianceRegulatoryInformation/Guidances/UCM070107.pdf

(134) Du Bois D, Du Bois E.F. A formula to estimate the approximate surface area if height and weight be known. Arch Intern Med 1916;17:863-871.

(135) Cockcroft DW, Gault MH. Prediction of creatinine clearance from serum creatinine. Nephron 1976;16:31-41.

(136) Karlsson MO, Sheiner LB. The importance of modeling interoccasion variability in population pharmacokinetic analyses. J Pharmacokinet Biopharm 1993;21:735-50.

(137) Grevel J. Log transformation of concentration [Internet user forum entry]. NONMEM UsersNet Archive 2009 [cited 2009 Aug 4]; Available from: http://www.cognigencorp.com/nonmem/current/2009-March/1547.html

(138) Gibiansky L, Karlsson MO. Weighting in NONMEM [Internet user forum entry]. NONMEM UsersNet Archive 2003 May 2 [cited 2009 Aug 4];Available from: http://www.cognigencorp.com/nonmem/nm/98jun022003.html

(139) Beal SL. Population pharmacokinetic data and parameter estimation based on their first two statistical moments. Drug Metab Rev 1984;15:173-93.

(140) Bonate PL. Pharmacokinetic-Pharmacodynamic Modeling and Simulation. Berlin: Springer; 2006.

(141) Fisher D, Shafer S. Fisher/Shafer NONMEM workshop pharmacokinetic and pharmacodynamic analysis with NONMEM basic concepts. 2007 Mar 7; Ghent, Belgium.

(142) Jonsson EN, Karlsson MO. Xpose - An S-PLUS based population pharmacokinetic/pharmacodynamic model building aid for NONMEM. Comput Methods Programs Biomed 1999;58:51-64.

(143) Mandema JW, Verotta D, Sheiner LB. Building population pharmacokinetic-pharmacodynamic models. I. Models for covariate effects. J Pharmacokinet Biopharm 1992;20:511-28.

(144) Maitre PO, Buhrer M, Thomson D, Stanski DR. A three-step approach combining Bayesian regression and NONMEM population analysis: application to midazolam. J Pharmacokinet Biopharm 1991;19:377-84.

(145) Jonsson EN, Karlsson MO. Automated covariate model building within NONMEM. Pharmaceut Res 1998;15:1463-8.

(146) Wählby U, Jonsson EN, Karlsson MO. Comparison of stepwise covariate model building strategies in population pharmacokinetic-pharmacodynamic analysis. AAPS PharmSci [electronic resource] 2002;4:E27.

(147) Karlsson MO, Holford NH. A tutorial on visual predictive checks. Presented at: PAGE 2008.The Population Approach Group Europe's 17th Meeting (Abstr 1434); 2008 Jun 18; Marseille, France.

(148) Yano Y, Beal SL, Sheiner LB. Evaluating pharmacokinetic/pharmacodynamic models using the posterior predictive check. J Pharmacokinet Pharmacodyn 2001;28:171-92.

(149) Rowland M, Tozer T. Clinical Pharmacokinetics: Concepts and Applications. 3 ed. Philadelphia, PA: Lippincott Williams & Wilkins; 1995.

(150) World Medical Association. Declaration of Helsinki: Recommendations Guiding Medical Doctors in Biomedical Research Involving Human Subjects [document on the Internet]. Ferney-Voltaire: World Medical Association; 1996 [cited 2009 Aug 12]. Available from: http://www.wma.net/en/30publications/10policies/b3/index.html

(151) Picard-Hagen N, Gayrard V, Alvinerie M, Smeyers H, Ricou R, Bousquet-Melou A, et al. A nonlabeled method to evaluate cortisol production rate by modeling plasma CBG-free cortisol disposition. Am J Physiol Endocrinol Metab 2001;281:E946-E956.

(152) Mager DE, Krzyzanski W. Quasi-equilibrium pharmacokinetic model for drugs exhibiting target-mediated drug disposition. Pharm Res 2005;22:1589-96.

(153) Toutain PL, Lefebvre HP, King JN. Benazeprilat disposition and effect in dogs revisited with a pharmacokinetic/pharmacodynamic modeling approach. J Pharmacol Exp Ther 2000;292:1087-93.

(154) Toutain PL, Lefebvre HP. Pharmacokinetics and pharmacokinetic/pharmacodynamic relationships for angiotensin-converting enzyme inhibitors. J Vet Pharmacol Ther 2004;27:515-25.

(155) King JN, Maurer M, Toutain PL. Pharmacokinetic/pharmacodynamic modelling of the disposition and effect of benazepril and benazeprilat in cats. J Vet Pharmacol Ther 2003;26:213-24.

(156) Waterhouse TH, Redmann S, Duffull SB, Eccleston JA. Optimal design for model discrimination and parameter estimation for itraconazole population pharmacokinetics in cystic fibrosis patients. J Pharmacokinet Pharmacodyn 2005;32:521-45.

(157) Duffull SB, Eccleston JA, Kimko HC, Denman N. WinPOPT User Guide [document on the Internet]. Dunedin: School of Pharmacy, University of Otago, New Zealand; 2006 [cited 2007 Apr 27]. Available from: http://www.winpopt.com/files/WinPOPT_User_Guide_Ver_1.1.pdf

(158) Karlsson MO, Savic RM. Diagnosing model diagnostics. Clin Pharmacol Ther 2007;82:17-20.

(159) U.S. Food and Drug Administration. Guidance for Industry: bioavailability and bioequivalence studies for orally administered drug products - general considerations [document on the Internet]. Rockville, MD: U.S. Food and Drug Administration; 2003 [cited 2009 Aug 12]. Available from: http://www.fda.gov/downloads/Drugs/GuidanceComplianceRegulatoryInformation/Guidances/ucm070124.pdf

(160) Toutain PL, Bousquet-Melou A. Bioavailability and its assessment. J Vet Pharmacol Ther 2004;27:455-66.

(161) Fuchs H, Binder R, Greischel A. Tissue distribution of the novel DPP-4 inhibitor BI 1356 is dominated by saturable binding to its target in rats. Biopharm Drug Dispos 2009;30:229-40.

(162) Fuchs H, Tillement JP, Urien S, Greischel A, Roth W. Concentration-dependent plasma protein binding of the novel dipeptidyl peptidase 4 inhibitor BI 1356 due to saturable binding to its target in plasma of mice, rats and humans. J Pharm Pharmacol 2009;61:55-62.

(163) Forst T, Uhlig-Laske B, Ring A, Ritzhaupt A, Graefe-Mody U, Dugi KA. The Novel, Potent, and Selective DPP-4 Inhibitor BI 1356 Significantly Lowers HbA1c after only 4 Weeks of Treatment in Patients with Type 2 Diabetes. Presented at:

ADA 2007. The American Diabetes Association's 67th Scientific Sessions; 2007 Jun 22; Chicago; IL.

(164) Ludden TM. Nonlinear pharmacokinetics: clinical Implications. Clin Pharmacokinet 1991;20:429-46.

(165) Davies NM, Anderson KE. Clinical pharmacokinetics of naproxen. Clin Pharmacokinet 1997;32:268-93.

(166) DeVane CL. Pharmacokinetics, drug interactions, and tolerability of valproate. Psychopharmacol Bull 2003;37 Suppl 2:25-42.

(167) Kishino S, Itoh S, Nakagawa T, Miyazaki K. Enantioselective binding of disopyramide to alpha1-acid glycoprotein and its variants. Eur J Clin Pharmacol 2001;57:583-7.

(168) Tang L, Persky AM, Hochhaus G, Meibohm B. Pharmacokinetic aspects of biotechnology products. J Pharm Sci 2004;93:2184-204.

(169) Caldwell PR, Seegal BC, Hsu KC, Das M, Soffer RL. Angiotensin-converting enzyme: vascular endothelial localization. Science 1976;191:1050-1.

(170) Lees P, Cunningham FM, Elliott J. Principles of pharmacodynamics and their applications in veterinary pharmacology. J Vet Pharmacol Ther 2004;27:397-414.

(171) He H, Tran P, Yin H, Smith H, Batard Y, Wang L, et al. Absorption, metabolism, and excretion of [14C]vildagliptin, a novel dipeptidyl peptidase 4 inhibitor, in humans. Drug Metab Dispos 2009;37:536-44.

(172) Beconi MG, Reed JR, Teffera Y, Xia YQ, Kochansky CJ, Liu DQ, et al. Disposition of the dipeptidyl peptidase 4 inhibitor sitagliptin in rats and dogs. Drug Metab Dispos 2007;35:525-32.

(173) Sunkara G, Sabo R, Wang Y, He YL, Campestrini J, Rosenberg M, et al. Dose proportionality and the effect of food on vildagliptin, a novel dipeptidyl peptidase IV inhibitor, in healthy volunteers. J Clin Pharmacol 2007;47:1152-8.

(174) Uhlig-Laske B, Ring A, Graefe-Mody EU, Friedrich C, Herborg H, Woerle HJ, et al. Linagliptin, a potent and selective DPP-4 inhibitor, is safe and efficacious in patients with inadequately controlled type 2 diabetes despite metformin therapy. 5-6-2009. Presented at: ADA 2009. The American Diabetes Association's 69th Scientific Sessions; 2009 Jun 5; New Orleans, LA.

(175) Mahmood I. Comparison of different reduced sampling approaches for the estimation of pharmacokinetic parameters for long half-life drugs in patients with renal or hepatic impairment. Int J Clin Pharmacol Ther 2002;40:53-9.

(176) Rollins DE, Klaassen CD. Biliary excretion of drugs in man. Clin Pharmacokinet 1979;4:368-79.

(177) Mannucci E, Pala L, Ciani S, Bardini G, Pezzatini A, Sposato I, et al. Hyperglycaemia increases dipeptidyl peptidase IV activity in diabetes mellitus. Diabetologia 2005;48:1168-72.

(178) Ryskjaer J, Deacon CF, Carr RD, Krarup T, Madsbad S, Holst J, et al. Plasma dipeptidyl peptidase-IV activity in patients with type-2 diabetes mellitus correlates positively with HbAlc levels, but is not acutely affected by food intake. Eur J Endocrinol 2006;155:485-93.

(179) McLean AJ, Le Couteur DG. Aging biology and geriatric clinical pharmacology. Pharmacol Rev 2004;56:163-84.

(180) Beaufrere B, Morio B. Fat and protein redistribution with aging: metabolic considerations. Eur J Clin Nutr 2000;54 Suppl 3:S48-S53.

(181) Campion EW, deLabry LO, Glynn RJ. The effect of age on serum albumin in healthy males: report from the Normative Aging Study. J Gerontol 1988;43:M18-M20.

(182) Le Couteur DG, McLean AJ. The aging liver. Drug clearance and an oxygen diffusion barrier hypothesis. Clin Pharmacokinet 1998;34:359-73.

(183) Cheymol G. Effects of obesity on pharmacokinetics: Implications for drug therapy. Clin Pharmacokinet 2000;39:215-31.

(184) Derendorf H, Grammaté T, Schaefer HG. Pharmakokinetik. Stuttgart: Wissenschaftliche Verlagsgesellschaft mbH; 2002.

(185) Beierle I, Meibohm B, Derendorf H. Gender differences in pharmacokinetics and pharmacodynamics. Int J Clin Pharmacol Ther 1999;37:529-47.

(186) Meibohm B, Beierle I, Derendorf H. How important are gender differences in pharmacokinetics? Clin Pharmacokinet 2002;41:329-42.

(187) Graefe-Mody EU, Padula S, Ring A, Withopf B, Dugi KA. Evaluation of the potential for steady-state pharmacokinetic and pharmacodynamic interactions between the DPP-4 inhibitor linagliptin and metformin in healthy subjects. Curr Med Res Opin 2009;25:1963-72.

(188) Takane H, Shikata E, Otsubo K, Higuchi S, Ieiri I. Polymorphism in human organic cation transporters and metformin action. Pharmacogenomics 2008;9:415-22.

(189) Zhang Y, Zhang L, Abraham S, Apparaju S, Wu TC, Strong JM, et al. Assessment of the impact of renal impairment on systemic exposure of new molecular entities: evaluation of recent new drug applications. Clin Pharmacol Ther 2009;85:305-11.

(190) Durinx C, Neels H, Van der Auwera JC, Naelaerts K, Scharpe S, De M, I. Reference values for plasma dipeptidyl-peptidase IV activity and their association with other laboratory parameters. Clin Chem Lab Med 2001;39:155-9.

(191) Firneisz G, Lakatos PL, Szalay F. Serum dipeptidyl peptidase IV (DPP IV, CD26) activity in chronic hepatitis C. Scand J Gastroenterol 2001;36:877-80.

(192) Lakatos PL, Firneisz G, Borcsiczky D, Zalatnai A, Selmeci L, Szalay F. Elevated serum dipeptidyl peptidase IV (CD26, EC 3.4.14.5) activity in experimental liver cirrhosis. Eur J Clin Invest 2000;30:793-7.

(193) Meneilly GS, Demuth HU, McIntosh CH, Pederson RA. Effect of ageing and diabetes on glucose-dependent insulinotropic polypeptide and dipeptidyl peptidase IV responses to oral glucose. Diabet Med 2000;17:346-50.

(194) Committee for Proprietary Medicinal Products (CPMP), EMEA. Note for guidance on investigations of bioavailability and bioequivalence [document on the Internet]. London: European Medicines Agency; 2002 [cited 2009 Aug 12]. Available from: http://www.emea.europa.eu/pdfs/human/qwp/140198enfin.pdf

(195) Bialer M, Wu WH, Look ZM, Silber BM, Yacobi A. Pharmacokinetics of cefixime after oral and intravenous doses in dogs: bioavailability assessment for a drug showing nonlinear serum protein binding. Res Commun Chem Pathol Pharmacol 1987;56:21-32.

(196) Hossain M, Jhee SS, Shiovitz T, McDonald C, Sedek G, Pommier F, et al. Estimation of the absolute bioavailability of rivastigmine in patients with mild to moderate dementia of the Alzheimer's type. Clin Pharmacokinet 2002;41:225-34.

(197) He YL, Sadler BM, Sabo R, Balez S, Wang Y, Campestrini J, et al. The absolute oral bioavailability and population-based pharmacokinetic modelling of a novel dipeptidylpeptidase-IV inhibitor, vildagliptin, in healthy volunteers. Clin Pharmacokinet 2007;46:787-802.

(198) U.S. Food and Drug Administration. Guidance for Industry: Waiver of in vivo bioavailability and bioequivalence studies for immediate-release solid oral dosage forms based on a biopharmaceutics classification system [document on the Internet]. Rockville, MD: U.S. Food and Drug Administration; 2000 [cited 2009 Aug 12]. Available from: http://www.fda.gov/downloads/Drugs/GuidanceCompliance RegulatoryInformation/Guidances/ucm070246.pdf

(199) Amidon GL, Lennernas H, Shah VP, Crison JR. A theoretical basis for a biopharmaceutic drug classification: the correlation of in vitro drug product dissolution and in vivo bioavailability. Pharm Res 1995;12:413-20.

(200) Wu CY, Benet LZ. Predicting drug disposition via application of BCS: transport/absorption/ elimination interplay and development of a biopharmaceutics drug disposition classification system. Pharm Res 2005;22:11-23.

(201) Hellriegel ET, Bjornsson TD, Hauck WW. Interpatient variability in bioavailability is related to the extent of absorption: implications for bioavailability and bioequivalence studies. Clin Pharmacol Ther 1996;60:601-7.

(202) Gobburu JV, Lesko LJ. Quantitative disease, drug, and trial models. Annu Rev Pharmacol Toxicol 2009;49:291-301.

(203) Silber HE, Jauslin PM, Frey N, Gieschke R, Simonsson US, Karlsson MO. An integrated model for glucose and insulin regulation in healthy volunteers and type 2 diabetic patients following intravenous glucose provocations. J Clin Pharmacol 2007;47:1159-71.

(204) Jauslin PM, Silber HE, Frey N, Gieschke R, Simonsson US, Jorga K, et al. An integrated glucose-insulin model to describe oral glucose tolerance test data in type 2 diabetics. J Clin Pharmacol 2007;47:1244-55.

Appendix

A-1 Tables

Table 1 Validated linagliptin concentration ranges and measurement sites of the studies investigated

Study	Validated range [nM]	Measurement site
I	0.106 - 106	Boehringer Ingelheim
II	0.106 - 106	Boehringer Ingelheim
III	0.100 - 100	Covance Laboratories
IV	0.100 - 100	Covance Laboratories
V	0.100 - 20	Covance Laboratories
VI	0.100 - 100	Boehringer Ingelheim
VII	0.100 - 100	Boehringer Ingelheim

Table 2 Inaccuracy and imprecision of plasma quality control samples of the studies investigated

Study	Nominal concentration of quality control sample [nM]	Number of replicates	Inaccuracy[1)] [%]	Imprecision[2)] [%]
I	0.265	34	1.0	3.9
	5.29	34	3.1	2.6
	84.6	33	-6.2	2.9
II	0.265	74	1.4	3.6
	5.29	74	4.2	3.5
	84.6	74	-7.3	3.6
III	0.250	62	1.2	11.4
	5.00	64	1.8	4.9
	80.0	64	-4.6	3.9
IV	0.250	84	1.6	7.3
	5.00	84	2.0	5.6
	80.0	84	-3.4	5.5
V	0.250	16	-14.0	7.1
	1.00	16	-0.9	5.2
	15.0	16	-6.0	3.9
VI	0.250	24	4.5	6.1
	5.00	24	5.2	4.2
	80.0	24	-1.1	3.5
VII	0.250	23	-3.4	12.4
	5.00	23	-0.7	6.4
	80.0	24	-5.8	6.8

1) Assay inaccuracy was determined as the percent deviation of replicate analyses from the nominal value in quality control samples.

2) Imprecision was calculated as the coefficient of variation of the quality control samples.

Table 3 Sampling scheme for linagliptin plasma concentration and plasma DPP-4 activity in studies I and II

Sample type	Study	Day	Time
Single-dose profile	I	1	Before and 0.5, 1, 1.5, 2, 3, 4, 6, 8, and 12 h after first administration
	II	1	
C_{trough} levels during treatment	I	2-11	Before linagliptin administration
	II	2, 6, 12, 19, 26, 27	
Overnight sample	I	11	18 h after drug administration of day 10 or 27, respectively
	II	28	
Steady-state profile	I	12	Before, 0.5, 1, 1.5, 2, 3, 4, 6, 8, and 12 h after last administration
	II	28	
Samples after last dose	I	13, 14, 16, 18, 20	In the morning
	II	29, 30, 33, 36, 39, 41, 43	

Table 4 Distribution of categorical covariates in Project 1

Covariate	Categories	Number of patients (percentage)
Alcohol status	No alcohol	39 (31.5%)
	Average alcohol consumption, during studies alcohol was not allowed	85 (68.5%)
Study	I	47 (37.9%)
	II	77 (62.1%)
Sex	Male	119 (96.0%)
	Female	5 (4.0%)
Smoking status	Never smoker	56 (45.2%)
	Ex-smoker	50 (40.3%)
	Current smoker, during studies smoking was not allowed	18 (14.5%)

Table 5 Distribution of continuous covariates in Project 1

Covariate	Unit	N	Mean	Median	Range	5th Percentile	95th Percentile
Age	years	124	58.6	61	36-69	44	68
Weight	kg	124	89.4	89	64-121	71.2	111.9
Height	cm	124	176.7	177	159-198	166	186.9
Body mass index	kg/m^2	124	28.8	28.7	20.4 -34.9	23.3	33.9
Body surface area	m^2	124	2.07	2.07	1.71-2.55	1.81	2.36
Serum creatinine	mg/dL	124	0.98	1.01	0.6-1.15	0.71	1.11
Creatinine clearance	mL/min	124	105.2	101.2	61.4-208.9	67.4	145.6
Urea	mM	124	2.91	2.93	1.42-4.25	2.19	3.51
Alanine transaminase	U/L	124	38.3	33.6	8.71-115.7	17.9	69.5
Aspartate transaminase	U/L	124	32.3	30.0	11.0-93.9	16.0	59.5
Alkaline phosphatase	U/L	124	117.6	106.6	14.6-288.3	52.7	191.2
Gamma-glutamyl transferase	U/L	124	39.1	30.7	9.3-276.6	14.9	91.2
Bilirubin	mg/dL	124	0.61	0.55	0.26-2.15	0.28	1.15
Creatine kinase	U/L	124	209.6	188.4	76.8-492.4	99.3	405.2
Cholesterol	mg/dL	124	187.9	188.5	142.6-237.0	153.5	220.5
C-reactive protein	mg/dL	124	0.21	0.17	0-1.15	0.05	0.46
Triglycerides	mg/dL	124	176.1	164.1	71.7-445.7	89.9	324.9
Fasting plasma glucose	mM	124	8.55	8.35	5.11-13.99	5.80	12.0

Table 6 Distribution of the number of subjects and pharmacokinetic and pharmacodynamic observations per dose group in Project 1

Linagliptin dose group [mg]	Number of subjects	Percentage of total subjects [%]	Number of PK observations	Percentage of total PK observations [%]	Number of PD observations	Percentage of total PD observations [%]
Before treatment	0	0	0	0	201	4.6
Placebo	28	22.6	0	0	937	21.5
1	9	7.3	313	9.8	315	7.2
2.5	35	28.2	1,169	36.4	1,169	26.9
5	24	19.4	786	24.5	786	18.1
10	28	22.6	942	29.3	942	21.7
Total	124	100	3,210	100	4,350	100

Table 7 Distribution of categorical covariates in Project 3a

Covariate	Categories	Number of patients (percentage)
Alcohol status	No alcohol	199 (43.07%)
	Average consumption	261 (56.49%)
	Above-average consumption	2 (0.43%)
Study	I	35 (7.58%)
	II	61 (13.20%)
	III	170 (36.80%)
	IV	196 (42.42%)
Ethnic origin	Caucasian	429 (92.86%)
	Black	8 (1.73%)
	Asian	7 (1.52%)
	Hispanic	18 (3.90%)
Sex	Male	302 (65.37%)
	Female	160 (34.63%)
Smoking status	Never smoker	254 (54.98%)
	Ex-smoker	150 (32.47%)
	Current smoker	58 (12.55%)
Treatment group	0.5 mg linagliptin	58 (12.55%)
	1 mg linagliptin	74 (16.02%)
	2.5 mg linagliptin	92 (19.91%)
	5 mg linagliptin	145 (31.39%)
	10 mg linagliptin	93 (20.13%)
Formulation	Powder in bottle	35 (7.58%)
	Tablet of study II	61 (13.20%)
	Tablet of studies III + IV	366 (79.22%)
Add-on to metformin	No	266 (57.58%)
	Yes	196 (42.42%)

Table 8 Distribution of continuous covariates using the baseline values in Project 3a

Covariate	Unit	Number	Mean	Median	Range	5th Percentile	95th Percentile
Age	years	462	59.1	60	30-78	42.0	73.0
Weight	kg	462	90.3	88.6	57-132	67.1	117.0
Height	cm	462	170.5	171	146-198	155	185
Body mass index	kg/m^2	462	31.0	30.6	20.4-42.2	25.1	38.9
Body surface area	m^2	462	2.02	2.02	1.56-2.56	1.70	2.37
Serum creatinine	mg/dL	462	0.86	0.85	0.45-1.69	0.59	1.12
Creatinine clearance	mL/min	462	177.9	112.2	47.9-318.1	65.0	188.9
Urea	mM	462	3.11	3.04	1.42-5.74	2.30	4.18
Alanine transaminase	U/L	462	35.2	28.8	0-232	9.6	81.7
Aspartate transaminase	U/L	462	26.8	20.8	0-236.5	5.7	65.2
Alkaline phosphatase	U/L	462	154.2	147.3	14.6-513.5	69.2	255.2
Gamma-glutamyl transferase	U/L	462	56.8	34.3	-1.9-1,048.2	9.4	157.4
Bilirubin	mg/dL	462	0.42	0.36	0.02-2.15	0.13	0.93
Creatine kinase	U/L	462	207.1	183.0	51.3-924.7	89.4	425.5
Cholesterol	mg/dL	462	181.5	179.9	14.5-507.2	94.3	279.6
C-reactive protein	mg/dL	462	0.32	0.17	0-3.94	0.06	1.03
Triglycerides	mg/dL	462	208.7	163.7	8.9-4,363.1	56.1	482.5
Fasting plasma glucose	mM	462	10.0	9.9	5.1-20	6.5	13.7
Pre-dose DPP-4 activity	RFU	462	12,809	12,497	1,075-47,519	8,033	18,618

Table 9 Distribution of the number of subjects and pharmacokinetic observations per dose group in Project 3a

Linagliptin dose group [mg]	Number of subjects	Percentage of total subjects [%]	Number of PK observations	Percentage of total observations [%]
Pre-dose values set to 0	0	0	9	0.1
0.5	58	12.55	541	7.8
1	74	16.02	988	14.3
2.5	92	19.91	1,736	25.1
5	145	31.39	1,989	28.8
10	93	20.13	1,644	23.8
Total	462	100	6,907	99.9

Table 10 Parameter estimates of the base pharmacokinetic model of Project 3a

	Unit	Estimate
Typical parameter		
F	%	100 fix
$F_{study\ IV}$	%	151
K_a	h^{-1}	0.549
V_C/F	L	713
Q_P/F	L/h	412 fix
V_P/F	L	1,650 fix
CL/F	L/h	243
$B_{max,C}$	nM	4.82
K_d	nM	0.0652 fix
$A_{max,P}/F$	nmol	1,650 fix
Inter- and intraindividual variability		
ωF	CV%	44.2
Correlation ωF/ ωCL		-0.704
ωCL	CV%	23.9
ωK_a	CV%	87.6
ωV_C	CV%	22.6
$\omega B_{max,C}$	CV%	29.6
πF	CV%	39.2
Residual variability		
$\sigma_{prop,phase\ IIa}$ [1)]	%	13.6
$\sigma_{prop,phase\ IIb}$ [1)]	%	38.1

1) Estimated based on log-transformed data

Table 11 Covariates selected during the different steps of the covariate analysis in Project 3a

	Covariate tested within NONMEM	Explora-tory analysis	GAM	Covariate Selection (Project 1)	Special interest	Selected within NONMEM
ηF	Age		X		X	
	Dose group		X			
	Height[1)]		X			
	Weight				X	X
	Sex				X	
	Study IV (metformin comedication)[2)]					X
ηCL/F	Age		X		X	
	Dose group		X			
	Alanine transaminase		X	X	X	
	Triglycerides		X			
	Creatinine clearance		X		X	
	Metformin comedication					
	Gamma-glutamyl transferase		X		X	X
	C-reactive protein		X			
	Alkaline phosphatase		X			
	Weight				X	
	Sex				X	
ηK_a	Formulation	X				X
	Dose group		X	X		X
	Body surface area		X			
	Age				X	
	Weight				X	
	Sex				X	

Table 11 Covariates selected during the different steps of the covariate analysis in Project 3a (cont.)

	Covariate tested within NONMEM	Explora-tory analysis	GAM	Covariate Selection (Project 1)	Special interest	Selected within NONMEM
$\eta B_{max,C}$	Pre-dose DPP-4 activity	X	X			X
	Dose group		X			X
	Age		X		X	X
	Aspartate transaminase		X	X		
	Triglycerides		X			
	Alkaline phosphatase		X			
	C-reactive protein		X			
	Metformin comedication		X			
	Serum creatinine		X			
	Weight				X	
	Sex				X	X
$\eta V_C/F$	Creatinine clearance		X			
	Age				X	
	Weight[3)]				X	X
	Sex				X	

1) Not further tested, highly correlated to weight, weight resulted in a higher drop in OBJF and was physiologically more plausible

2) Selected during base model development

3) When testing the remaining covariates together in one run, the effect of weight on volume was no longer significant. Thus, only the effect of weight on the bioavailability was retained in the final model, not the effect of weight on V_C.

Table 12 Distribution of categorical covariates in Project 3b

Covariate	Categories	Number of patients (percentage)
Alcohol status	No alcohol	251 (41.35%)
	Average consumption	353 (58.15%)
	Above-average consumption	3 (0.49%)
Study	I	47 (7.74%)
	II	77 (12.69%)
	III	216 (35.58%)
	IV	267 (43.99%)
Ethnic origin	Caucasian	559 (92.09%)
	Black	15 (2.47%)
	Asian	11 (1.81%)
	Hispanic	22 (3.62%)
Sex	Male	401 (66.06%)
	Female	206 (33.94%)
Smoking status	Never smoker	336 (55.35%)
	Ex-smoker	195 (32.13%)
	Current smoker	76 (12.52%)
Add-on to metformin	No	340 (56.01%)
	Yes	267 (43.99%)

Table 13 Distribution of continuous covariates using the baseline values in Project 3b

Covariate	Unit	Num-ber	Mean	Median	Range	5th Percentile	95th Percentile
Age	years	607	59.2	60	30-78	43	72
Weight	kg	607	90.4	89	55-138	67	117
Height	cm	607	170.7	172	142-198	155	185
Body mass index	kg/m^2	607	31.0	30.6	20.4-42.2	25.0	38.7
Body surface area	m^2	607	2.02	2.02	1.54-2.63	1.69	2.37
Serum creatinine	mg/dL	607	0.86	0.85	0.45-1.69	0.60	1.11
Creatinine clearance	mL/min	607	117.9	112.9	47.9-318.1	67.9	191.8
Urea	mM	607	3.09	3.06	1.42-5.74	2.27	4.06
Alanine transaminase	U/L	607	35.7	29.4	0-232	10.6	81.7
Aspartate transaminase	U/L	607	26.9	20.8	-1.9-236.5	5.8	63.2
Alkaline phosphatase	U/L	607	150.7	143.1	14.6-513.5	68.9	251.8
Gamma-glutamyl transferase	U/L	607	57.4	35.1	-1.9-1,048.2	9.5	161.8
Bilirubin	mg/dL	607	0.41	0.35	0.01-2.15	0.13	0.88
Creatine kinase	U/L	607	207.6	183.0	51.3-924.7	86.2	430.7
Cholesterol	mg/dL	607	179.3	177.5	14.5-507.2	91.7	273.9
C-reactive protein	mg/dL	607	0.30	0.17	0-3.94	0.10	0.94
Triglycerides	mg/dL	607	207.7	167.7	8.9-4,363.1	56.4	473.6
Fasting plasma glucose	mM	607	9.99	9.88	5.11-20	6.66	13.7

Table 14 Distribution of the number of subjects as well as pharmacokinetic and pharmacodynamic observations per dose group in Project 3b

Linagliptin dose group [mg]	Number of subjects	Percentage of total subjects [%]	Number of PK and PD observations	Percentage of total observations [%]
Placebo	160	26.4	2,410[1)]	24.9
0.5	53	8.7	545	5.6
1	74	12.2	1,055	10.9
2.5	87	14.3	1,803	18.6
5	140	23.1	2,108	21.8
10	93	15.3	1,753	18.1
Total	607	100	9,674	100

1) The linagliptin plasma concentrations were set to zero for all placebo patients.

Table 15 Parameter estimates of the base pharmacokinetic/pharmacodynamic model of Project 3b

	Unit	Estimate	RSE [%]
Typical Parameter			
BSL	RFU	11,600	1.03
E_{max}	%	92.5	0.12
EC_{50}	nM	2.97	1.69
Hill		3.21	1.90
BSL_EC_{50}[1)]	%	$6.96 \cdot 10^{-3}$	7.31
Interindividual variability			
ωBSL	CV%	21.6	8.84
ωEC_{50}	CV%	18.4	13.8
Residual variability			
σ_{prop}	%	15.7	7.22

1) $EC_{50i} = EC_{50} \cdot (1+BSL\_EC_{50}) \cdot (BSL_i - BSL)) \cdot \exp(\eta EC_{50})$

Table 16 Covariates selected during the different steps of the covariate analysis in Project 3b

	Covariate tested within NONMEM	Exploratory analysis	GAM	Selected within NONMEM
ηBSL	Fasting plasma glucose	X	X	X
	Alanine transaminase	X	X	X
	Aspartate transaminase	X	X	X
	Gamma-glutamyl transferase	X	X	X
	Cholesterol	X	X	X
	Creatine kinase		X	
	C-reactive protein		X	
	Triglycerides		X	X
	Sex	X	X	X
	Alcohol status	X		
	Study	X	X	X (study II)
	Dose group		X	
	Ethnic origin	X	X	X (Asian)
ηEC_{50}	Fasting plasma glucose	X	X	
	Alanine transaminase	X	X	
	Aspartate transaminase	X	X	
	Alkaline phosphatase	X		
	Gamma-glutamyl transferase	X	X	
	Dose group	X	X	
	Study	X	X	X
	Age		X	
	Serum creatinine		X	
	Triglycerides		X	X

Table 17 Distribution of the number of subjects and pharmacokinetic observations per dose group in Project 4

Linagliptin dose group [mg]	Number of Subjects	Percentage of total subjects [%]	Number of PK observations	Percentage of total PK observations [%]
0.5 i.v.	6	21.4	144	16.7
2.5 i.v.	6	21.4	144	16.7
5 i.v.	10	35.7	245	28.4
10 p.o.			185	21.5
10 i.v.	6	21.4	144	16.7
Total	28	100	862	100

Table 18 Mean (±SD) animal weights per dose group and rat strain in Project 5

Dose group linagliptin [mg/kg]	Animal weight (±SD) [g]	
	DPP-4-deficient rats	Wildtype rats
0.01	NA	249 (12.2)
0.1	250 (12.0)	258 (3.7)
0.3	255 (8.8)	266 (9.0)
1	224 (3.1)	233 (5.4)

NA, not applicable

Table 19 Distribution of pharmacokinetic observations per dose group and rat strain in Project 5

Dose group linagliptin [mg/kg]	DPP-4-deficient rats		Wildtype rats	
	Number of observations	Percentage of total observations [%]	Number of observations	Percentage of total observations [%]
0.01	NA	NA	26	21.5
0.1	20	32.8	32	26.45
0.3	20	32.8	32	26.45
1	21	34.4	31	25.6
Total	61	100	121	100

NA, not applicable

A-2 Figures

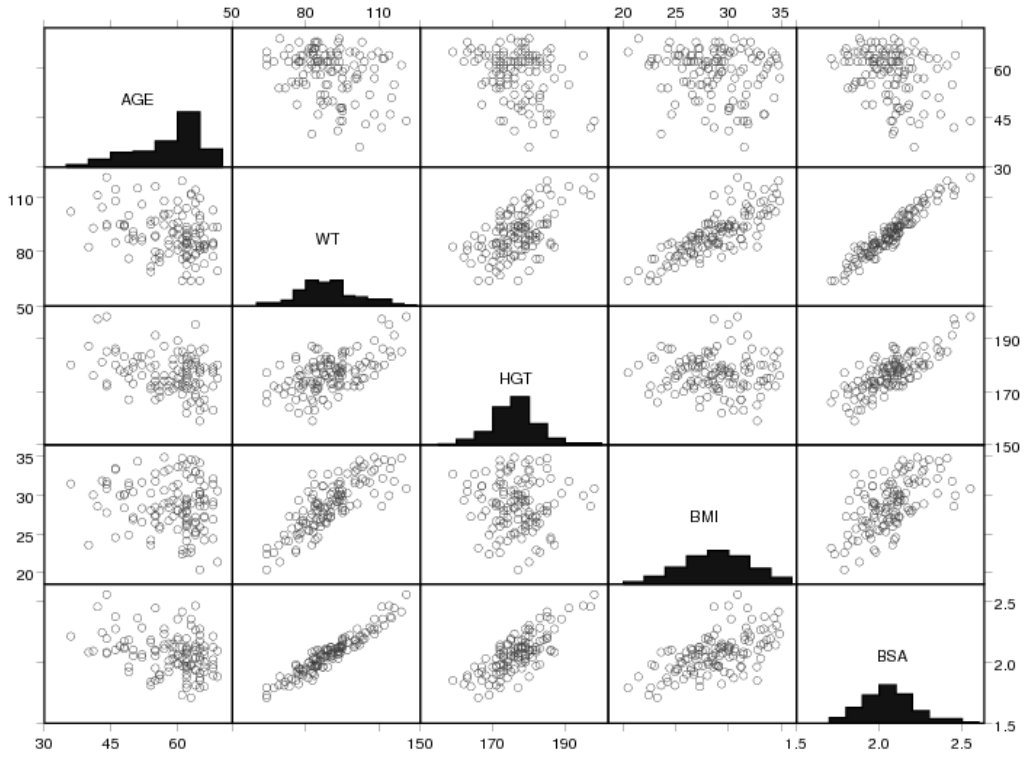

Figure 1 Scatter plots and distributions of the continuous demographic covariates in Project 1. AGE, age (years); WT, weight (kg); HGT, height (cm); BMI, body mass index (kg/m^2); BSA, body surface area (m^2).

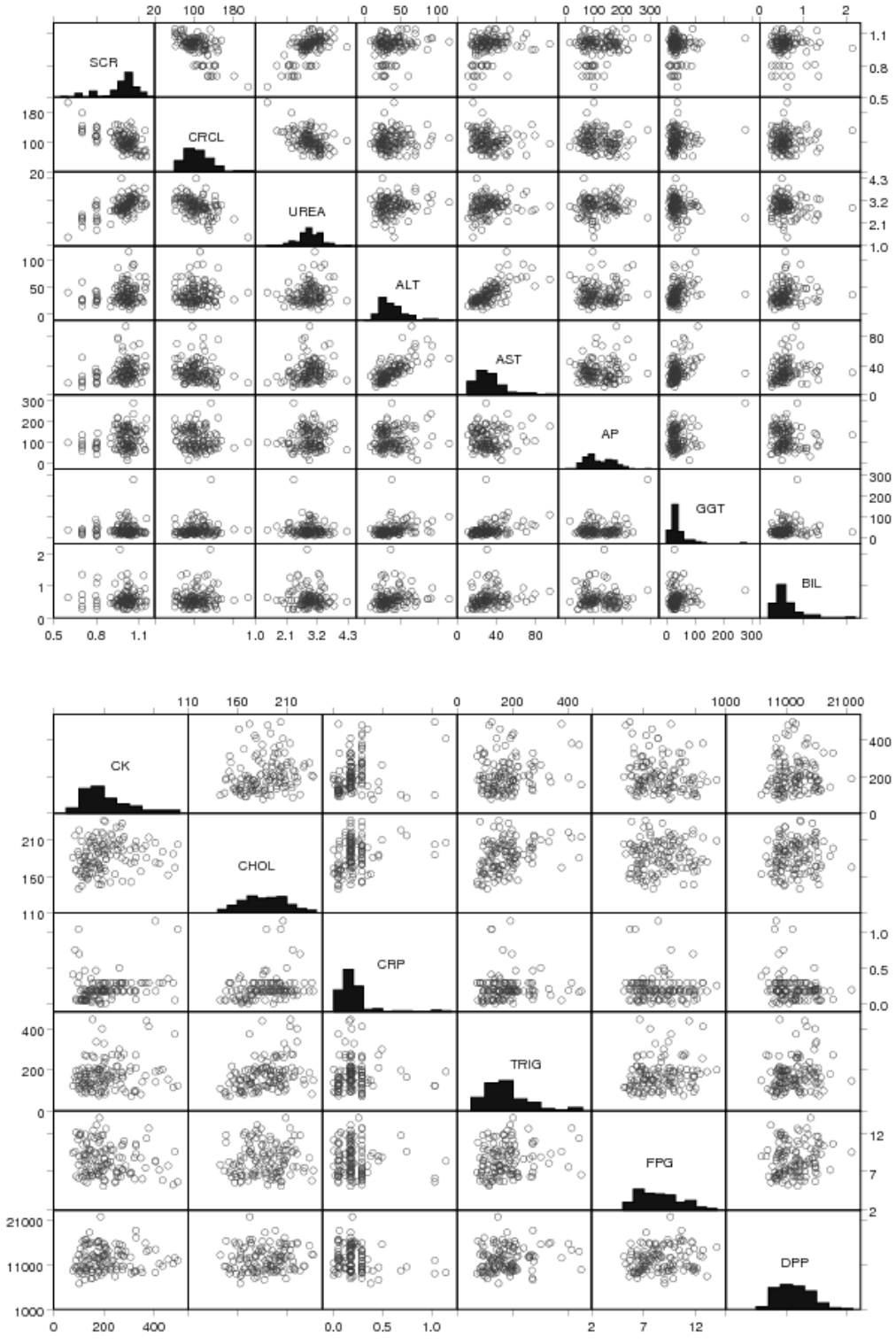

Figure 2 Scatter plots and distributions of the continuous laboratory covariates in Project 1. SCR, serum creatinine (mg/dL); CRCL, creatinine clearance (ml/min); UREA, urea (mM); ALT, alanine transaminase (U/L); AST, aspartate transaminase (U/L); AP, alkaline phosphatase (U/L); GGT, gamma-glutamyl transferase (U/L); BIL, total bilirubin (mg/dL); CK, creatine kinase (U/L); CHOL, cholesterol (mg/dL); CRP, C-reactive protein (mg/dL); TRIG, triglycerides (mg/dL); FPG, fasting plasma glucose (mM); DPP, pre-dose DPP-4 activity (RFU).

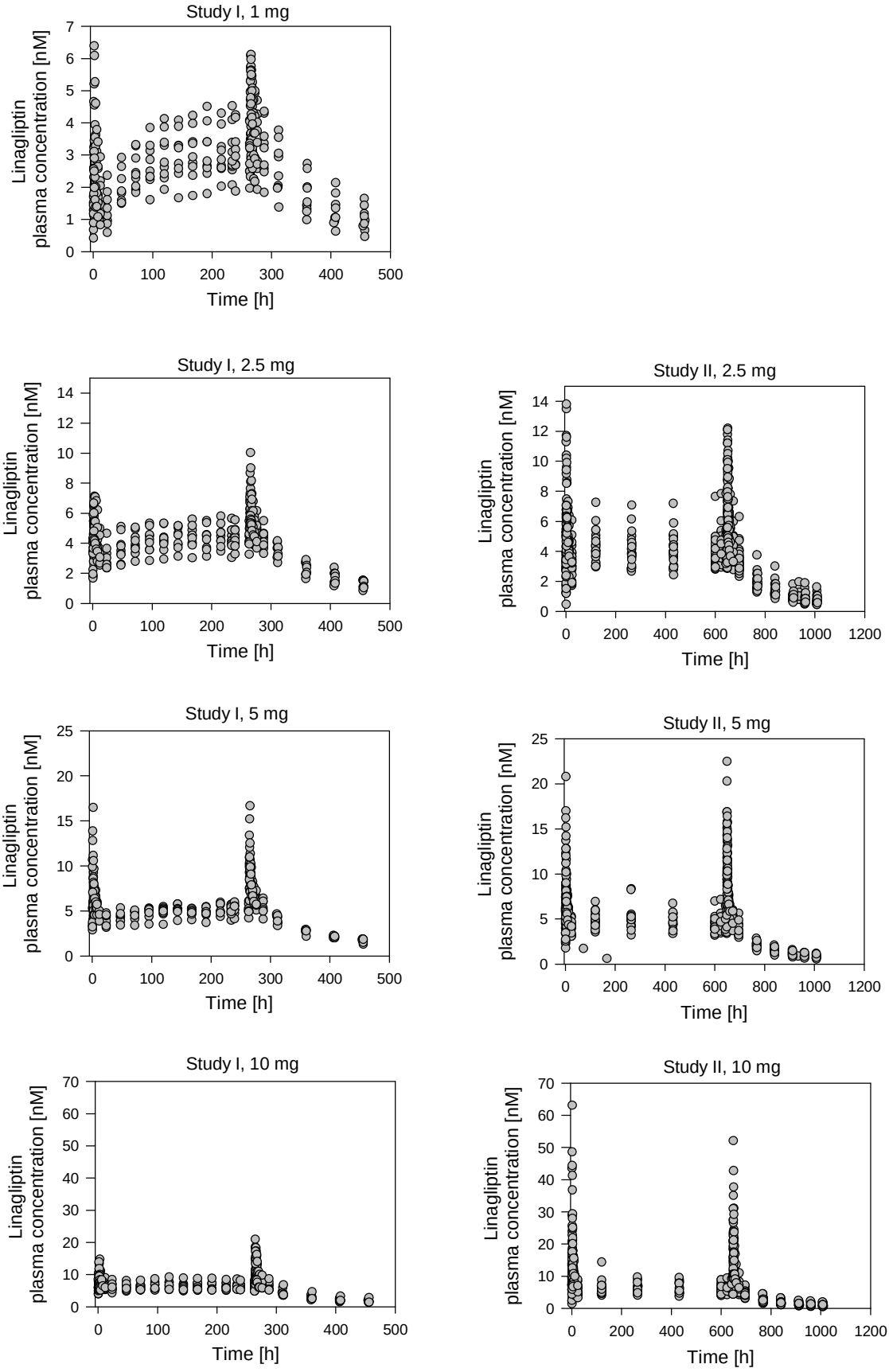

Figure 3 Plasma concentration-time profiles per dose group of studies I (left panels) and II (right panels).

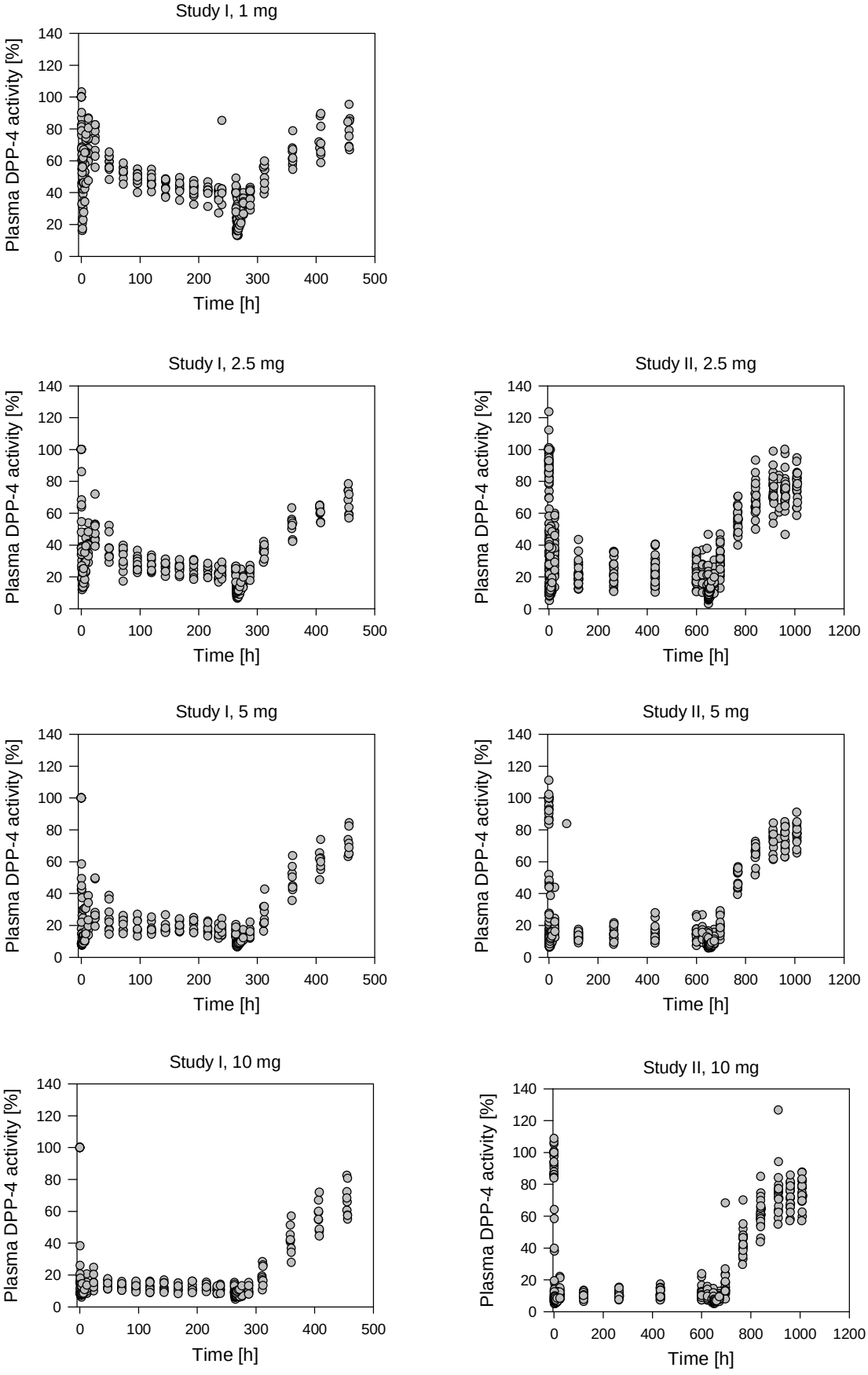

Figure 4 Plasma DPP-4 activity-time profiles per dose group of studies I (left panels) and II (right panels).

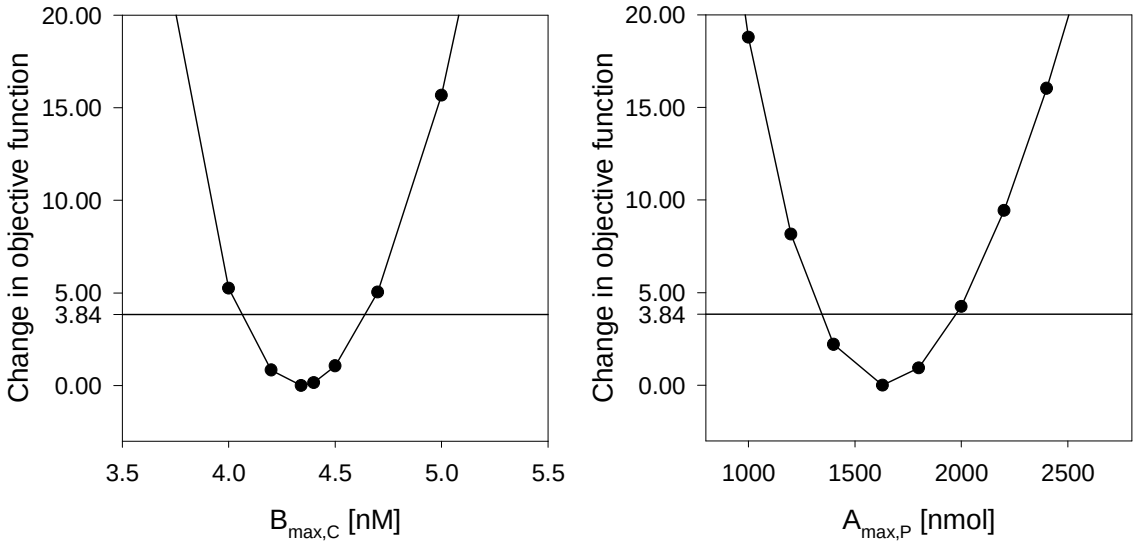

Figure 5 Log-likelihood profiles of the model parameters accounting for the concentration of central binding partner ($B_{max,C}$) and the amount of peripheral binding partner ($A_{max,P}$). The solid horizontal line indicates the cut-off at which the change in the OBJF becomes statistically significant, 3.84 in this case. The 95% confidence intervals for $B_{max,C}$ and $A_{max,P}$ are represented by the points of intersection of the solid horizontal lines and the log-likelihood profiles.

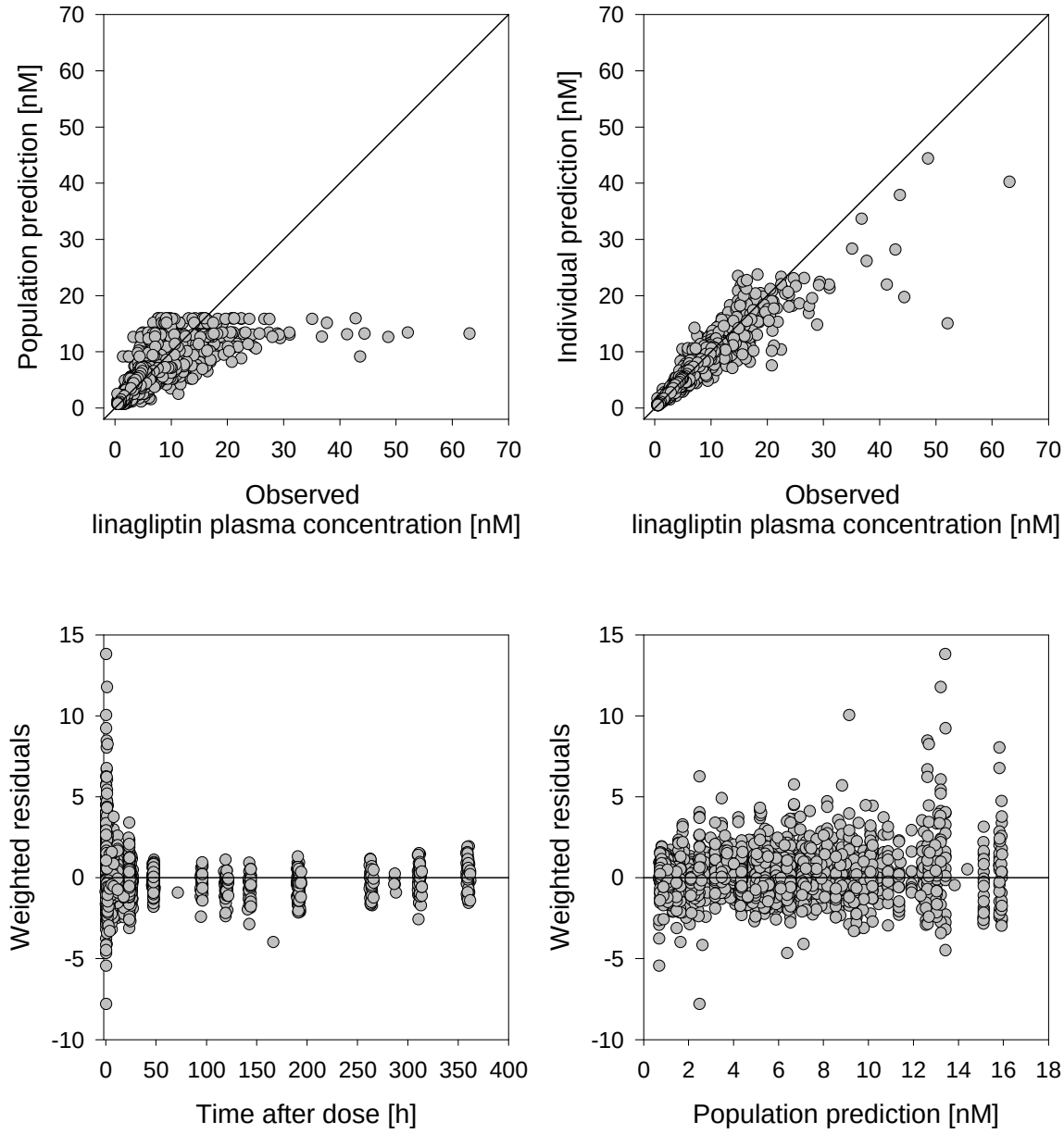

Figure 6 Standard goodness-of-fit plots for the pharmacokinetic part of the final population pharmacokinetic/pharmacodynamic model in Project 1.

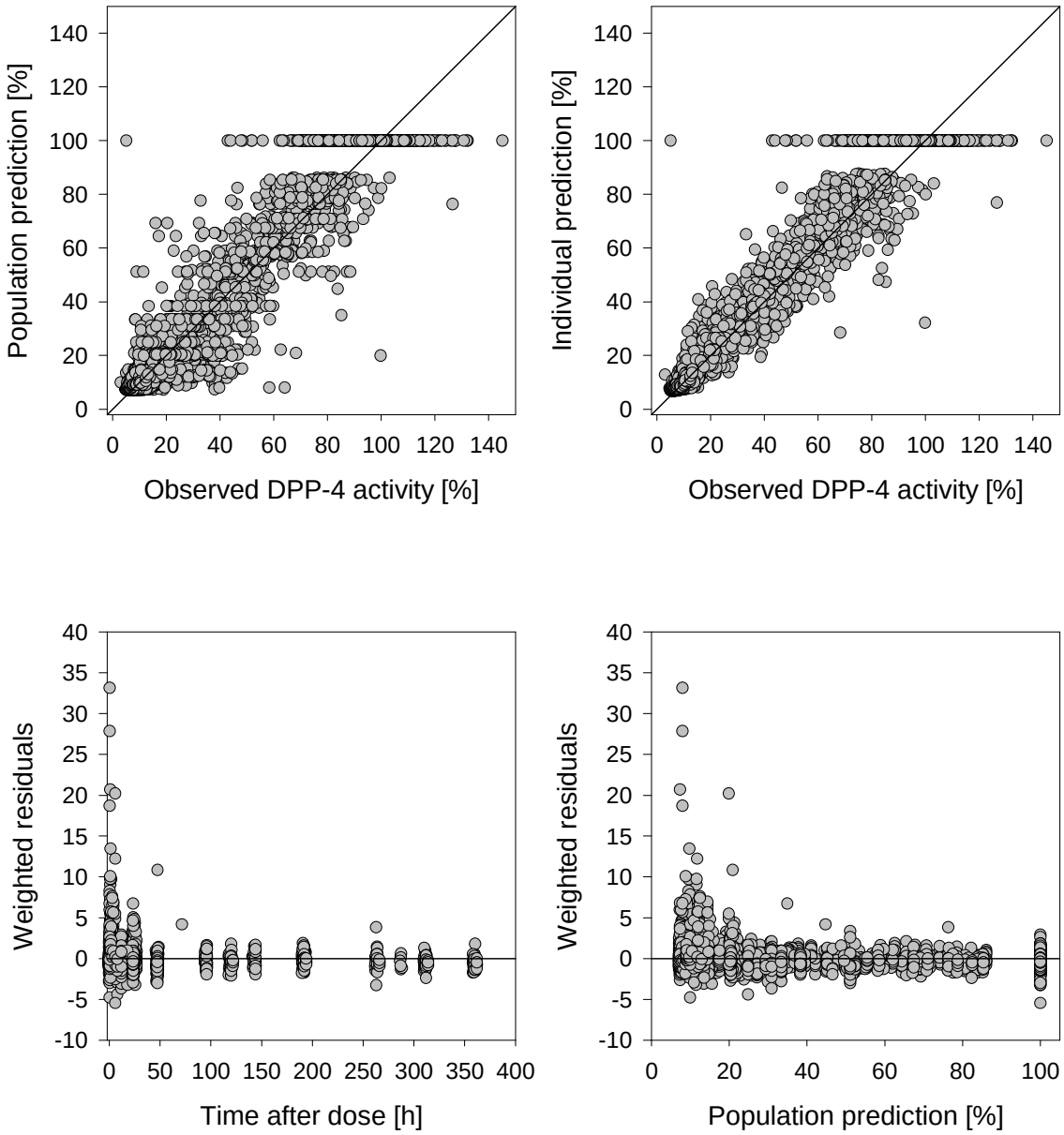

Figure 7 Standard goodness-of-fit plots for the pharmacodynamic part of the final population pharmacokinetic/pharmacodynamic model in Project 1.

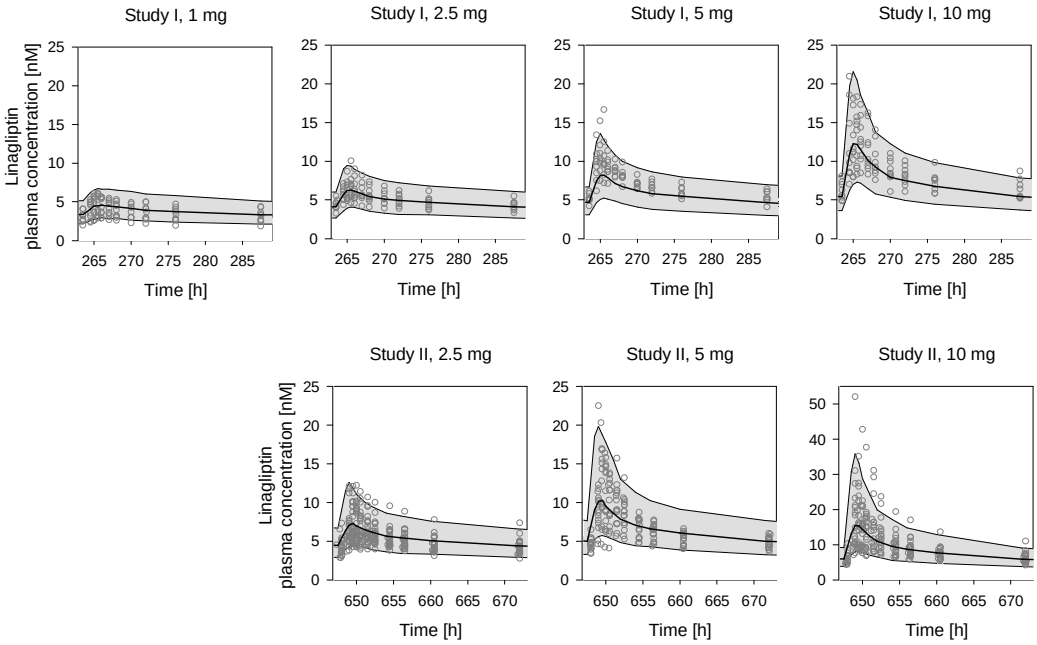

Figure 8 Visual predictive checks. The concentration-time profiles of 1,000 patients per dose group and study were simulated based on the final population pharmacokinetic/pharmacodynamic model of Project 1. The solid lines show the 90% confidence intervals and the median of the simulated concentration-time profiles. The observed linagliptin plasma concentrations are displayed as dots. Only the steady-state profiles are shown.

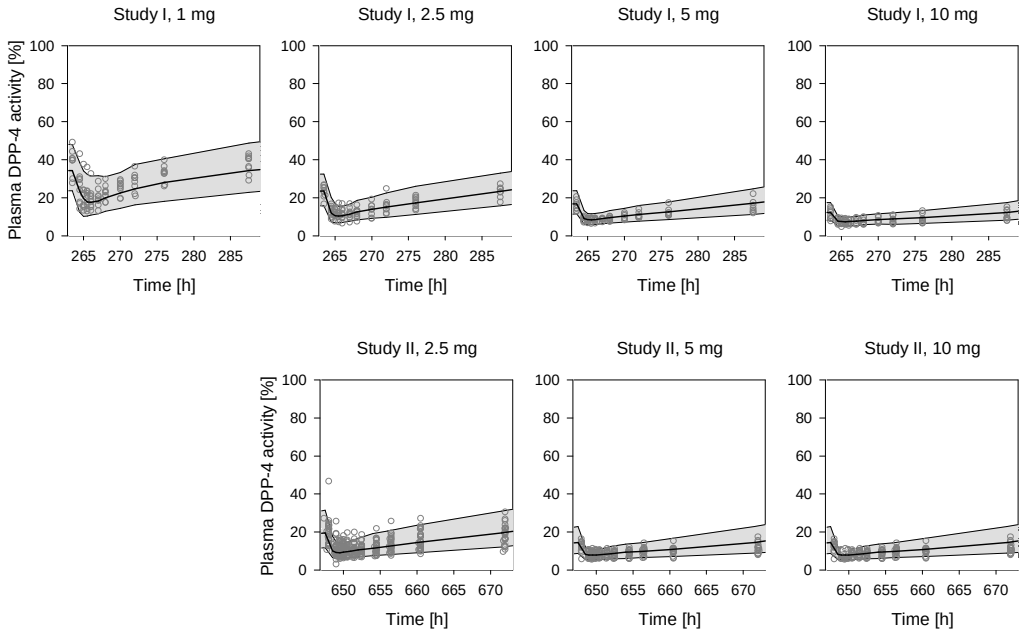

Figure 9 Visual predictive checks. The plasma DPP-4 activity-time profiles of 1,000 patients per dose group and study were simulated based on the final population pharmacokinetic/pharmacodynamic model of Project 1. The solid lines show the 90% confidence intervals and the median of the simulated concentration-time profiles. The observed plasma DPP-4 activities are displayed as dots. Only the steady-state plasma DPP-4 activity-time profiles are shown.

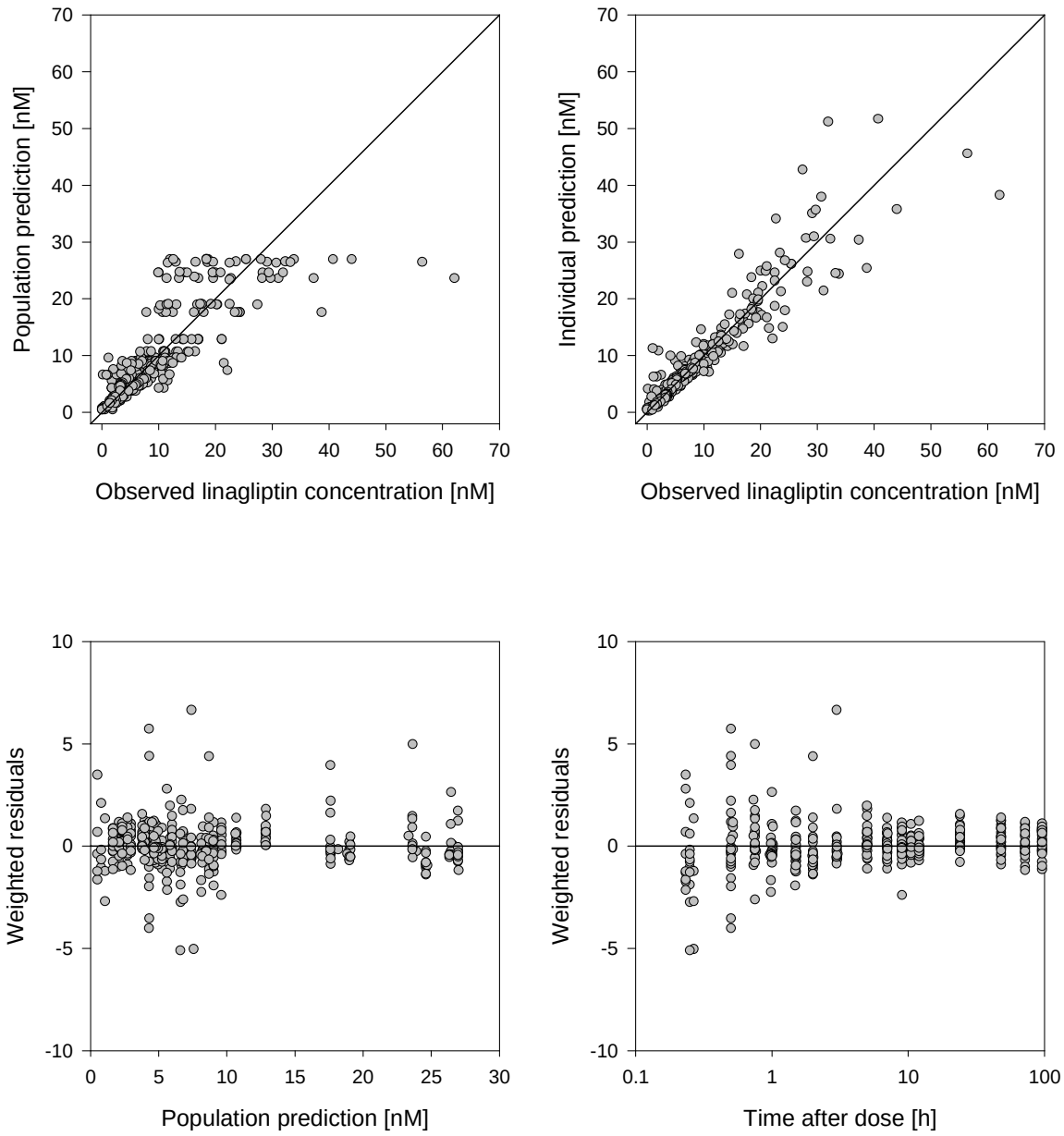

Figure 10 Standard goodness-of-fit plots for the final pharmacokinetic model of Project 2d.

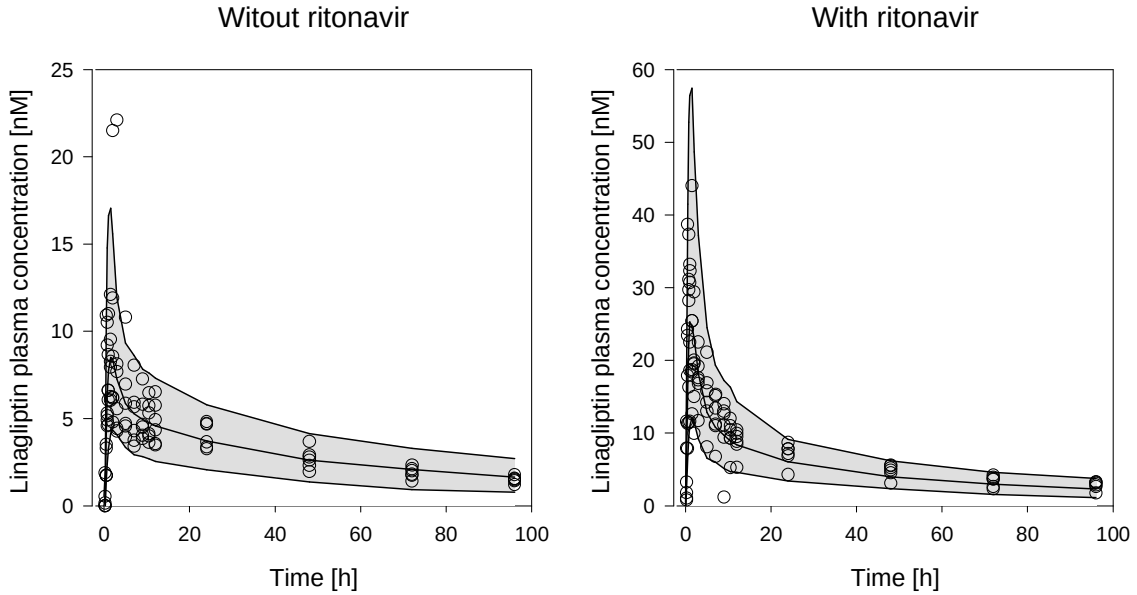

Figure 11 Visual predictive checks. 1,000 patients per treatment group were simulated based on the final population pharmacokinetic model of Project 2d. The solid lines show the 90% confidence interval and the median of the simulated concentration-time profiles. The observed linagliptin plasma concentrations are displayed as dots.

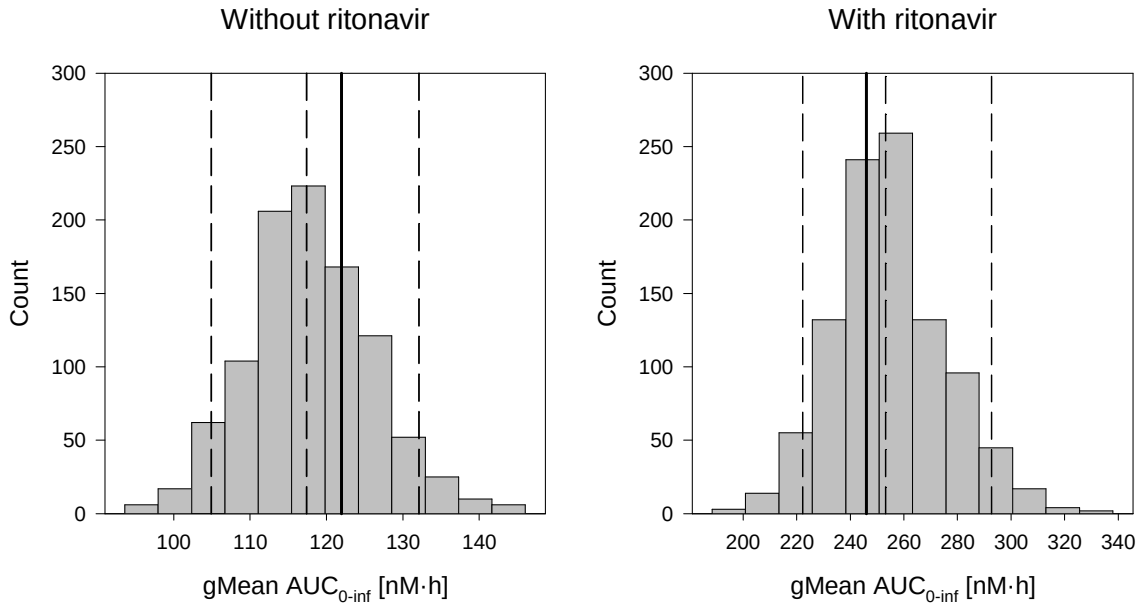

Figure 12 Posterior predictive checks. Distribution of the gMean $AUC_{0\text{-}inf}$ values of 1,000 simulated datasets per treatment group. The dashed lines show the 90% confidence interval and the median of the simulated gMean $AUC_{0\text{-}inf}$ values per treatment group. The observed gMean $AUC_{0\text{-}inf}$ per treatment group is displayed as a straight line.

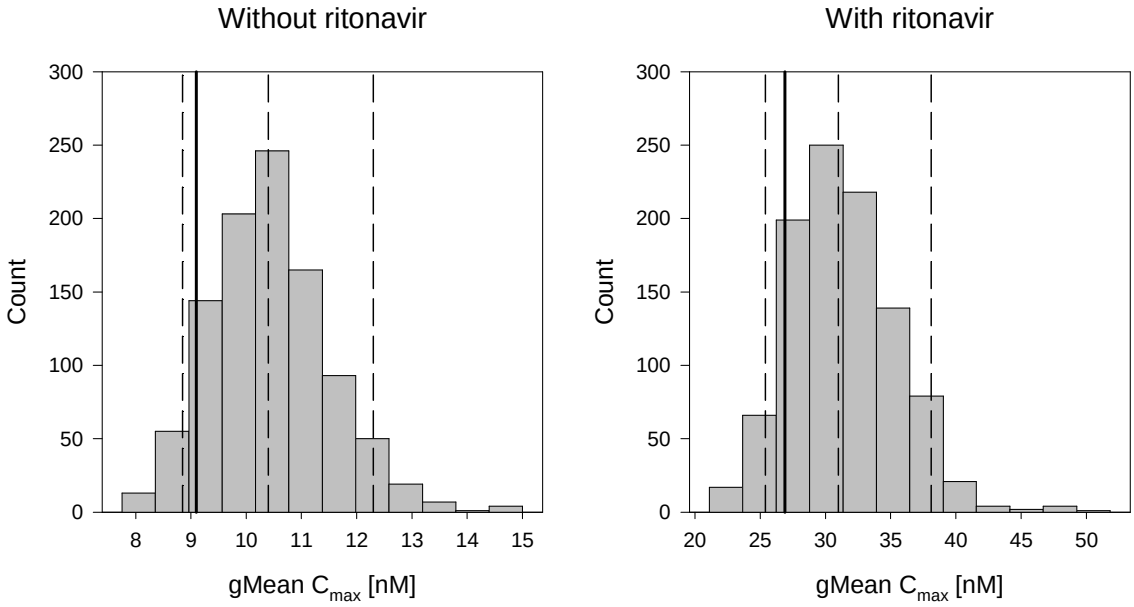

Figure 13 Posterior predictive checks. Distribution of the gMean C_{max} values of 1,000 simulated datasets per treatment group. The dashed lines show the 90% confidence interval and the median of the simulated gMean C_{max} values per treatment group. The observed gMean C_{max} per treatment group is displayed as a straight line.

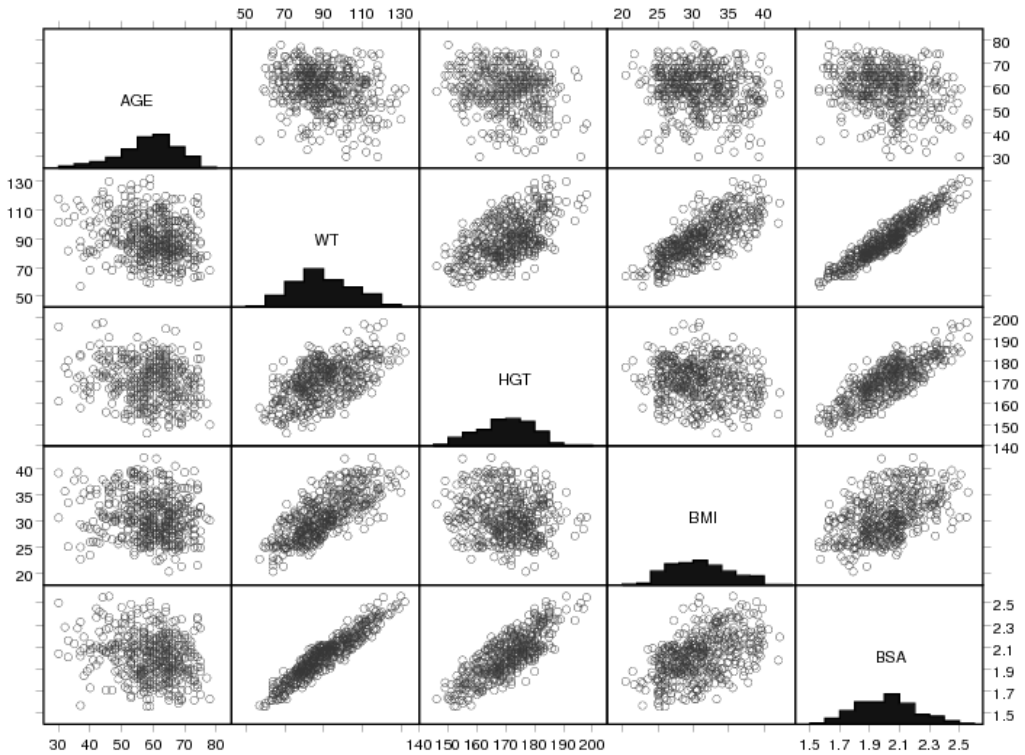

Figure 14 Scatter plots and distributions of the continuous demographic covariates in Project 3a. AGE, age (years); WT, weight (kg); HGT, height (cm); BMI, body mass index (kg/m^2); BSA, body surface area (m^2).

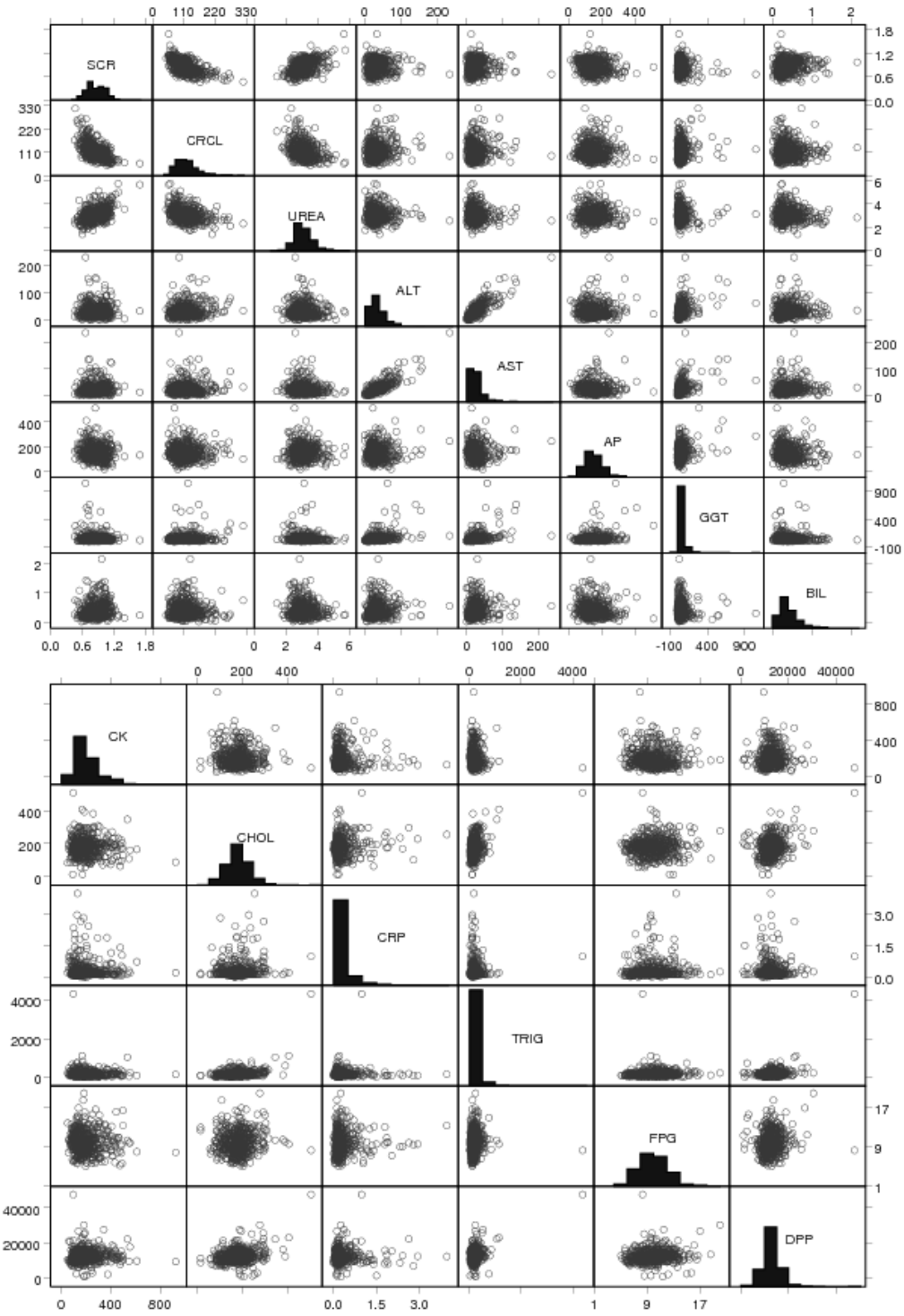

Figure 15 Scatter plots and distributions of the continuous laboratory covariates in Project 3a. SCR, serum creatinine (mg/dL); CRCL, creatinine clearance (ml/min); UREA, urea (mM); ALT, alanine transaminase (U/L); AST, aspartate transaminase (U/L); AP, alkaline phosphatase (U/L); GGT, gamma glutamyl transferase (U/L); BIL, total bilirubin (mg/dL); CK, creatine kinase (U/L); CHOL, cholesterol (mg/dL); CRP, C-reactive protein (mg/dL); TRIG, triglycerides (mg/dL); FPG, fasting plasma glucose (mM); DPP, pre-dose DPP-4 activity (RFU).

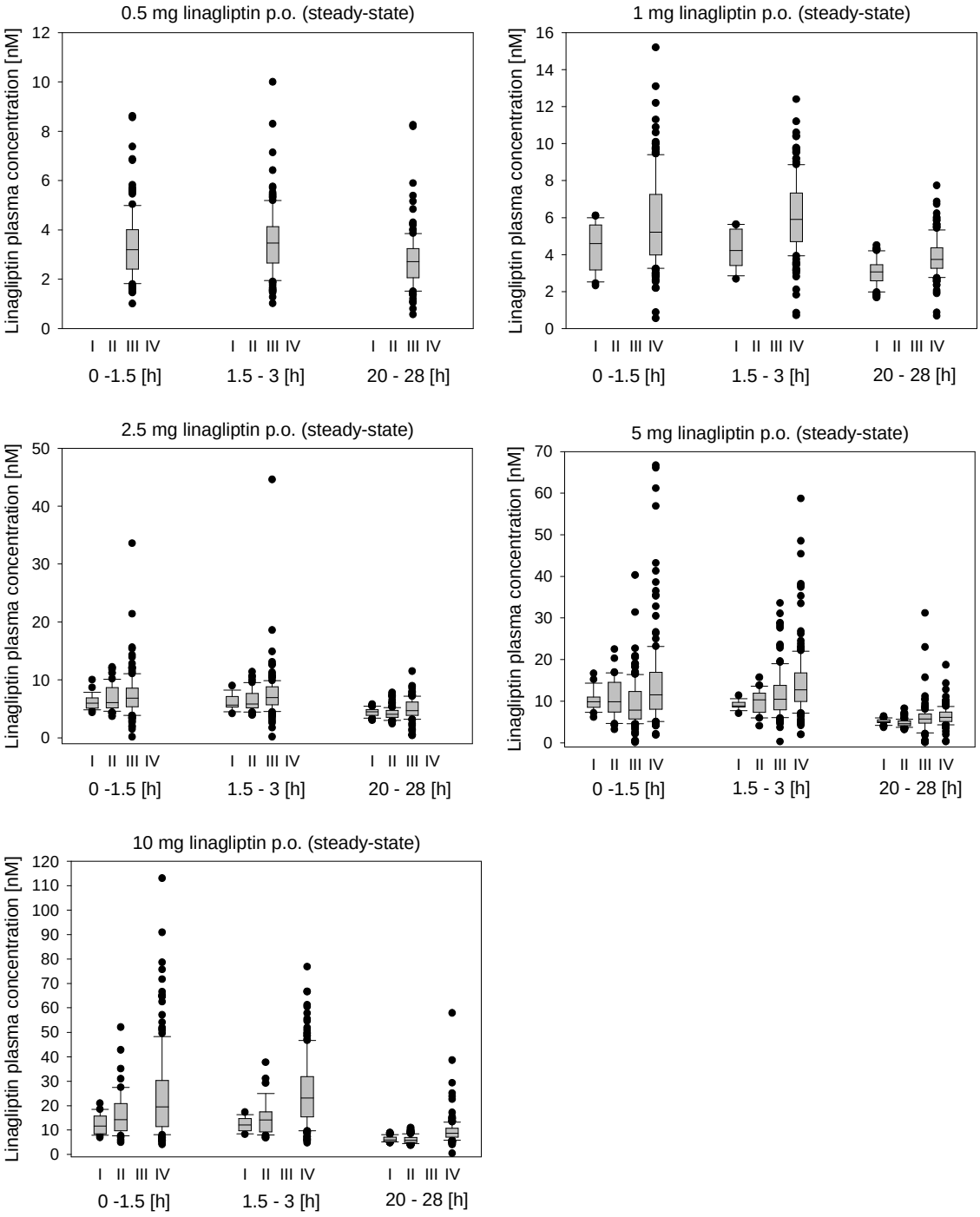

Figure 16 Linagliptin plasma concentrations at steady-state per dose group, time interval, and study (Project 3a).

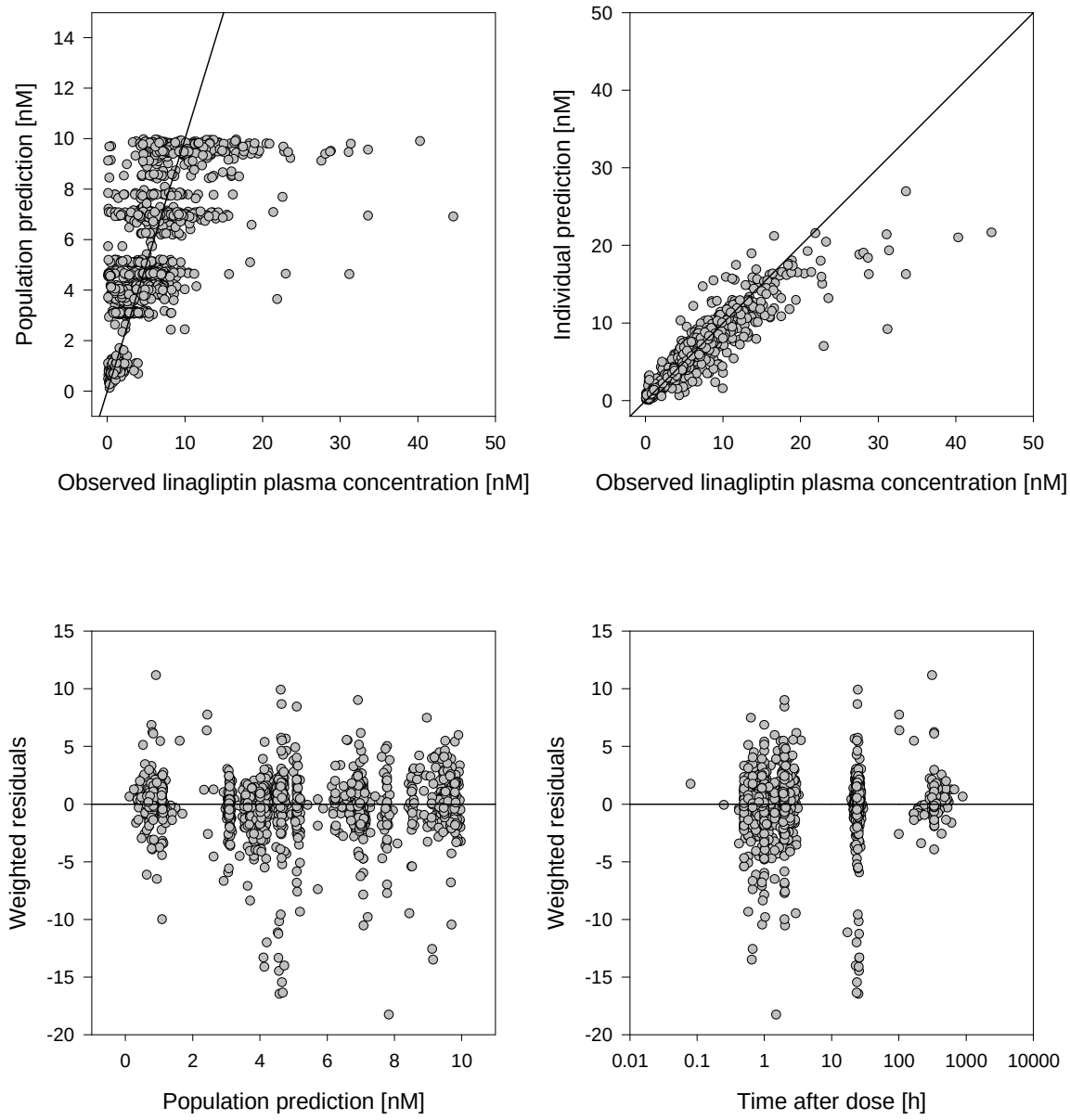

Figure 17 Standard goodness-of-fit plots of the post-hoc estimates of study III derived by applying the base model of Project 1.

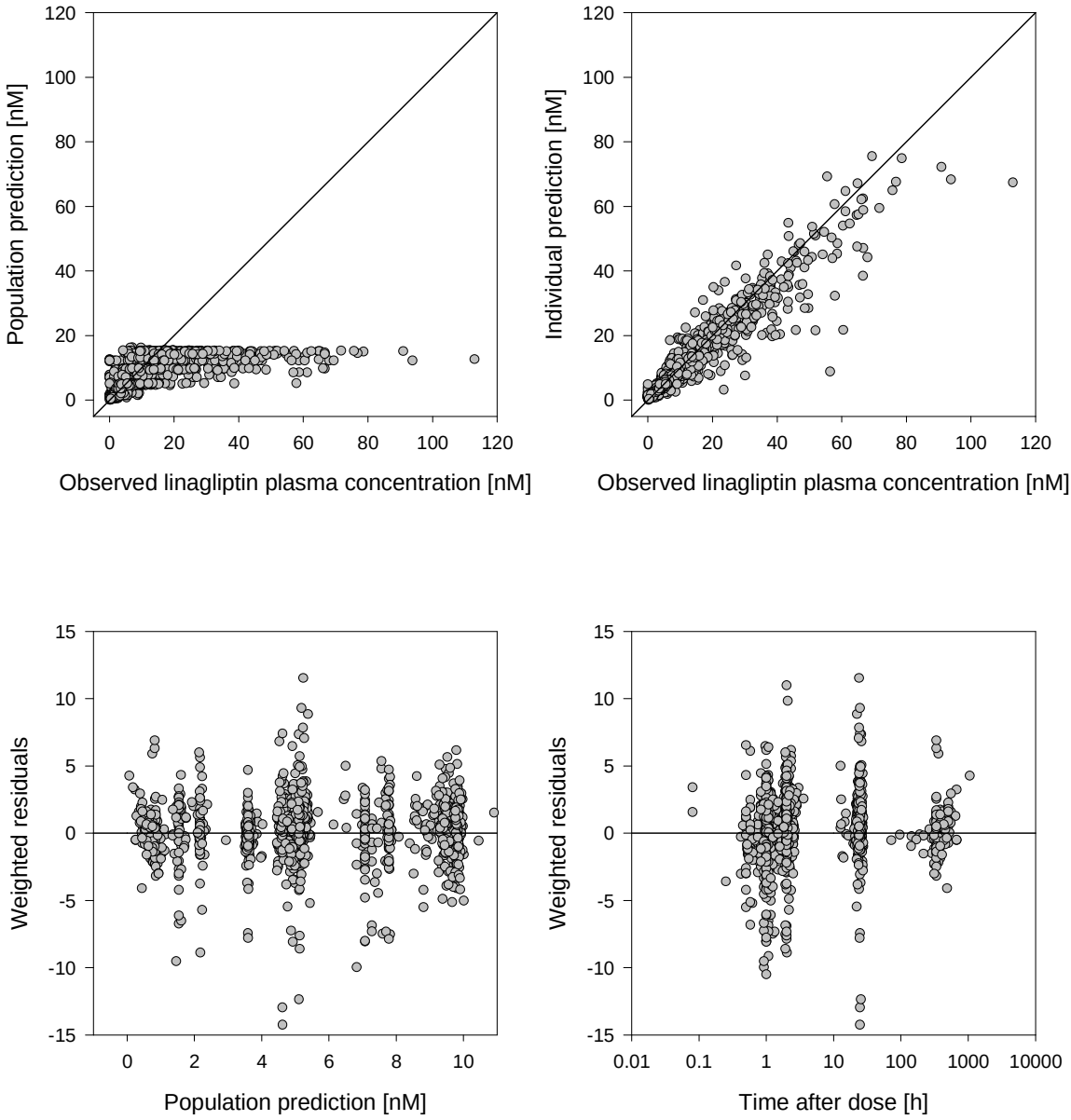

Figure 18 Standard goodness-of-fit plots of the post-hoc estimates of study IV derived by applying the base model of Project 1.

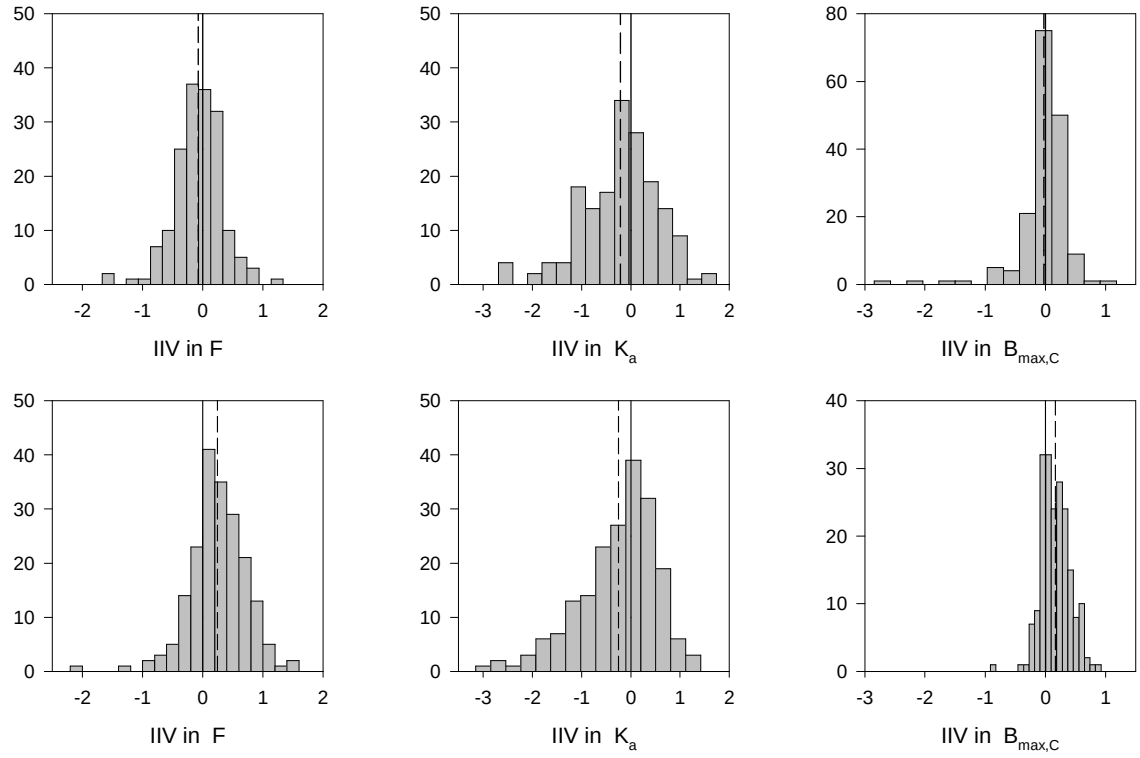

Figure 19 Histograms of the η-distribution of the post-hoc estimates of study III (upper panels) and study IV (lower panels) around the population mean. The solid lines show the assumed means of each distribution (0). The dashed lines show the observed means of each distribution.

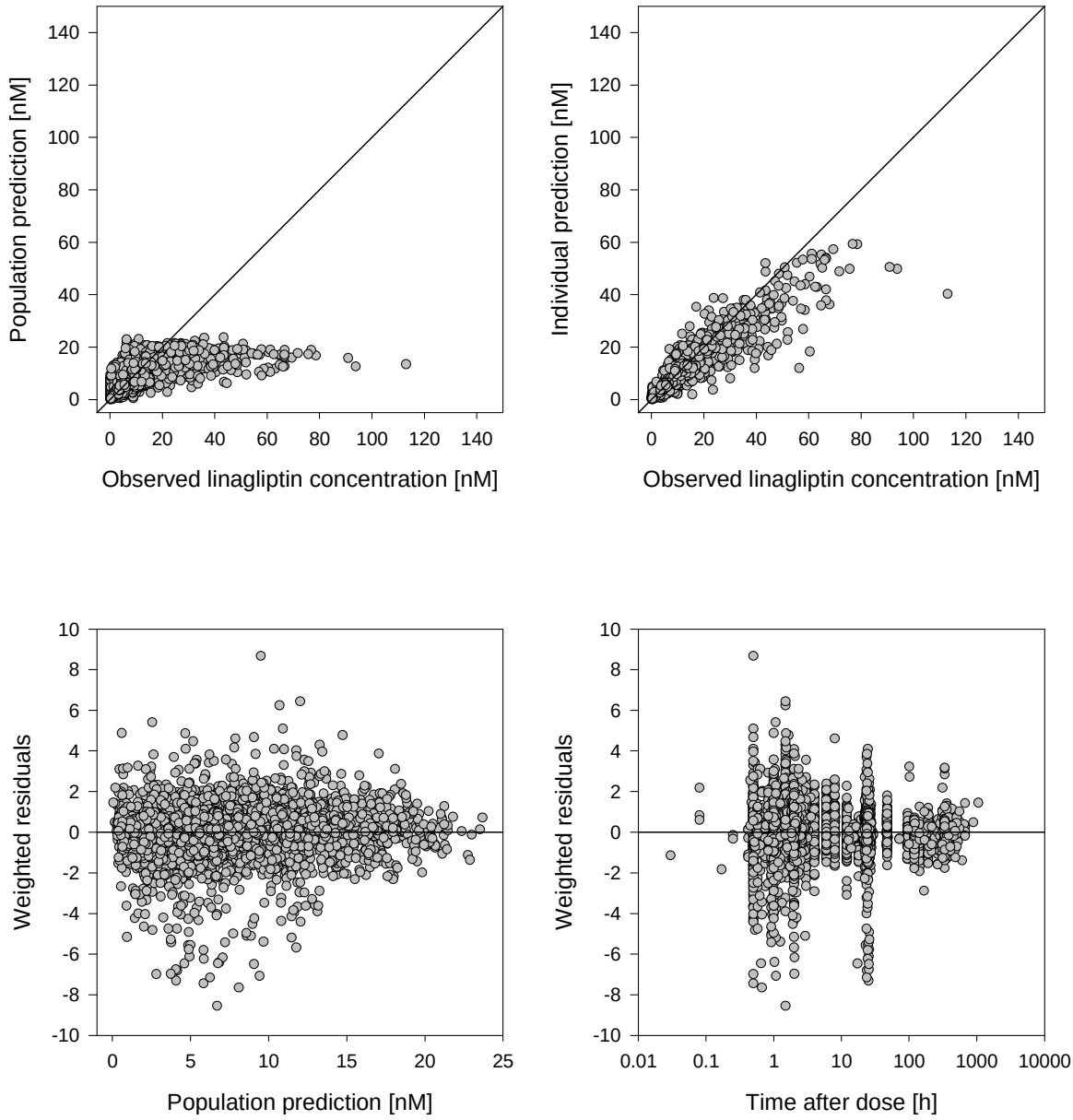

Figure 20 Standard goodness-of-fit plots of the final model of Project 3a.

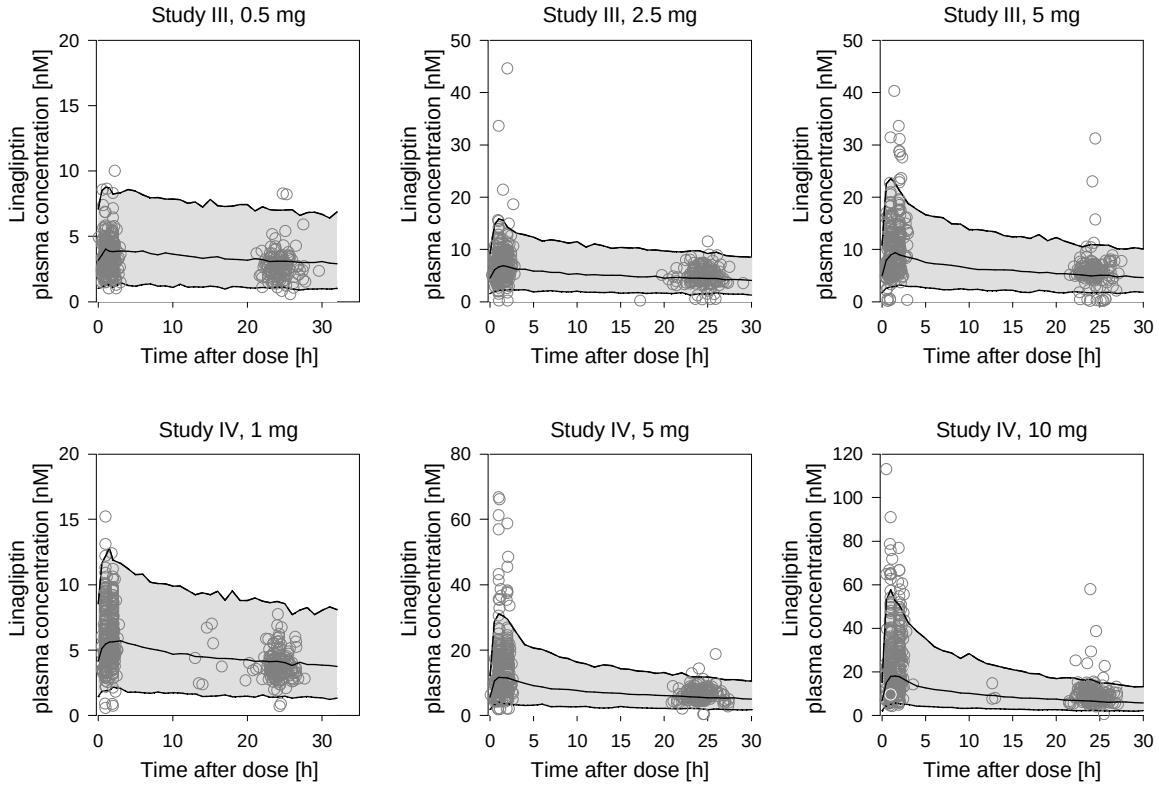

Figure 21 Visual predictive checks. 1,000 linagliptin plasma concentration-time profiles were simulated per dose group and study based on the base population pharmacokinetic model of Project 3a. The solid lines show the 90% confidence intervals and the median of the simulated concentration-time profiles. The observed linagliptin plasma concentrations are displayed as dots. Only steady-state profiles are shown.

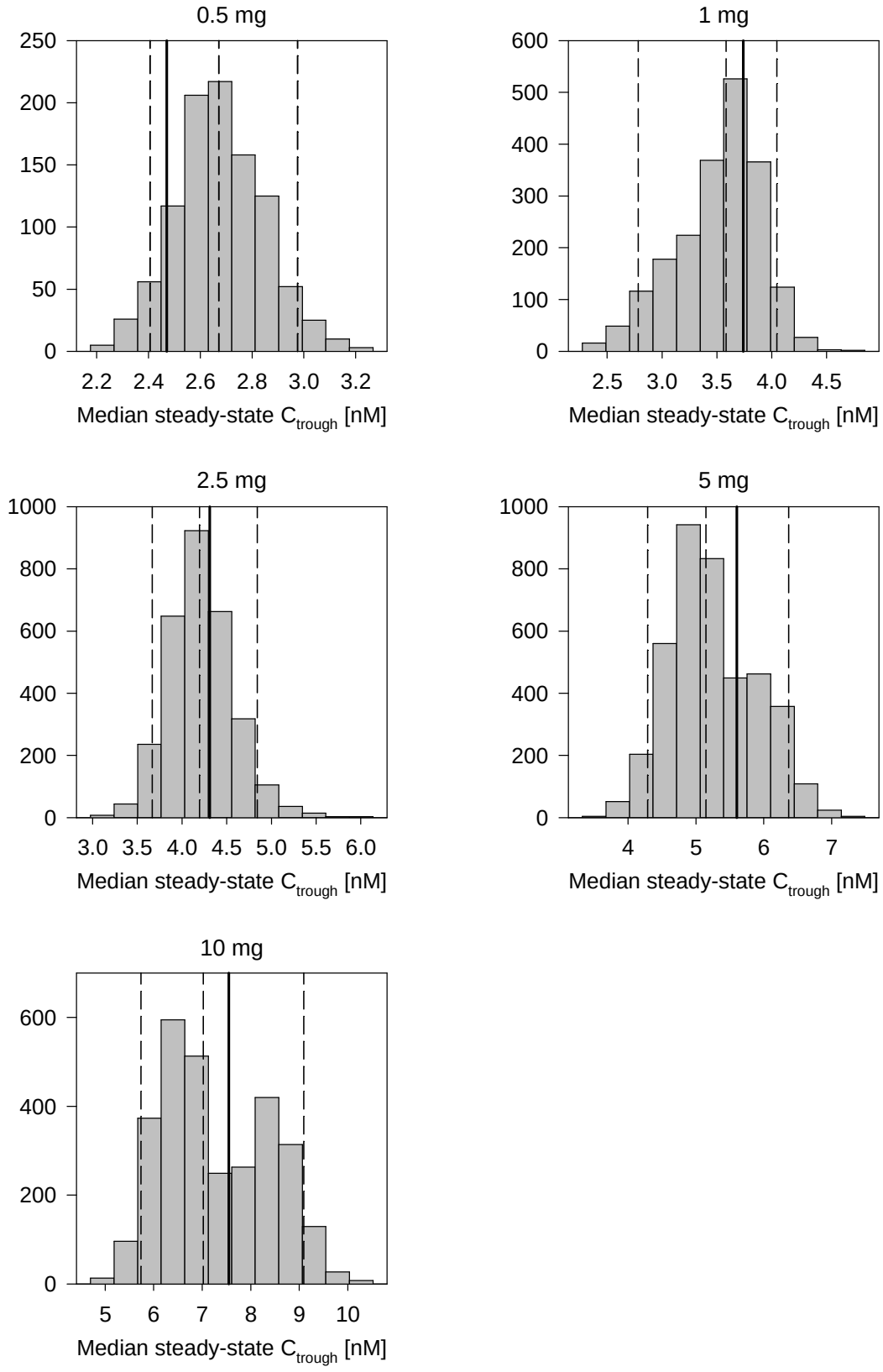

Figure 22 Posterior predictive checks of Project 3a. Distribution of the median C_{trough} levels of 1,000 simulated datasets per dose group. The dashed lines show the 90% confidence intervals and the median of the simulated median C_{trough} levels per dose group. The observed median C_{trough} level per dose group is displayed as a straight line.

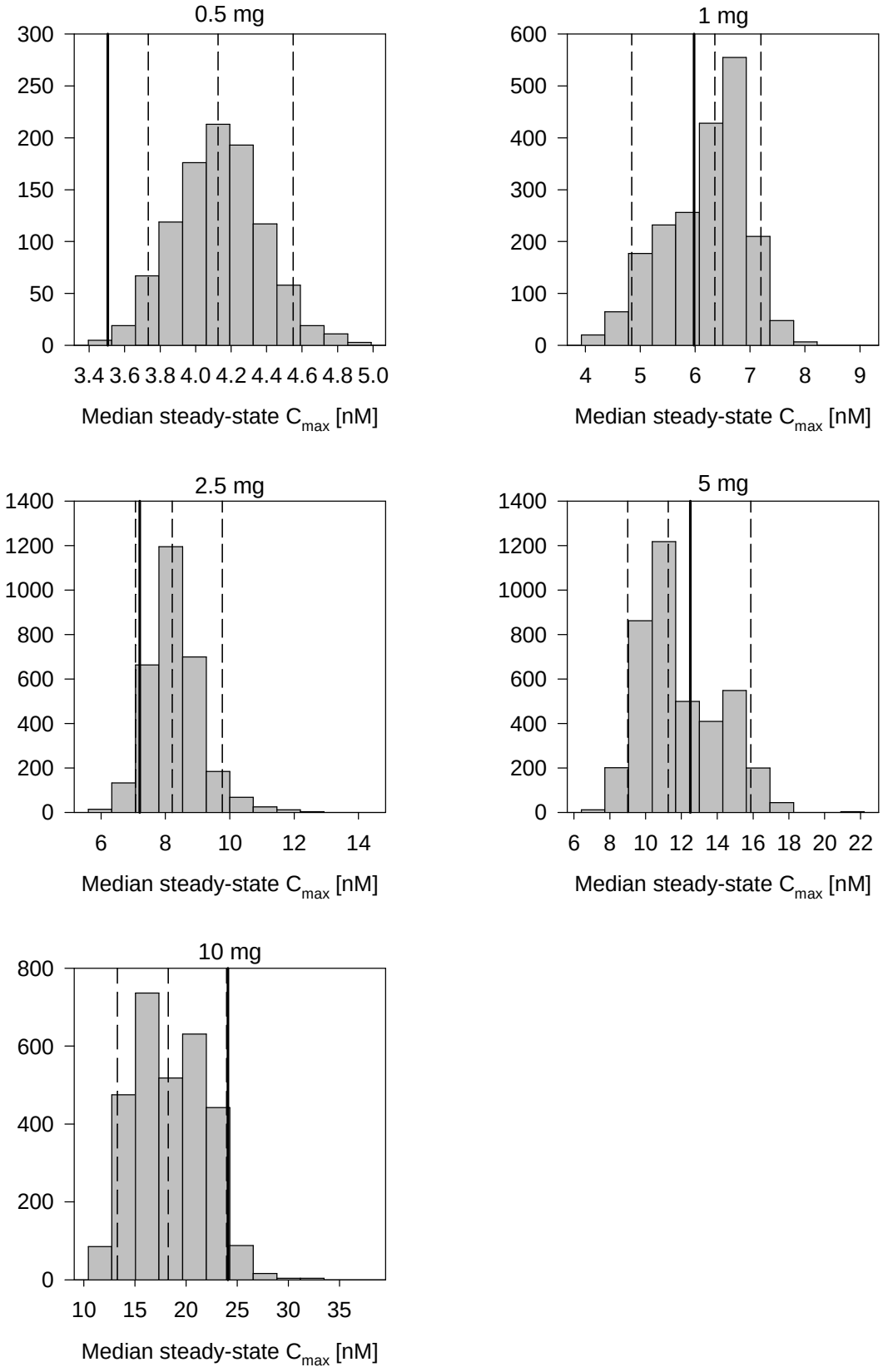

Figure 23 Posterior predictive checks of Project 3a. Distribution of the median C_{max} levels of 1,000 simulated datasets per dose group. The dashed lines show the 90% confidence intervals and the median of the simulated median C_{max} levels per dose group. The observed median C_{max} levels per dose group is displayed as a straight line.

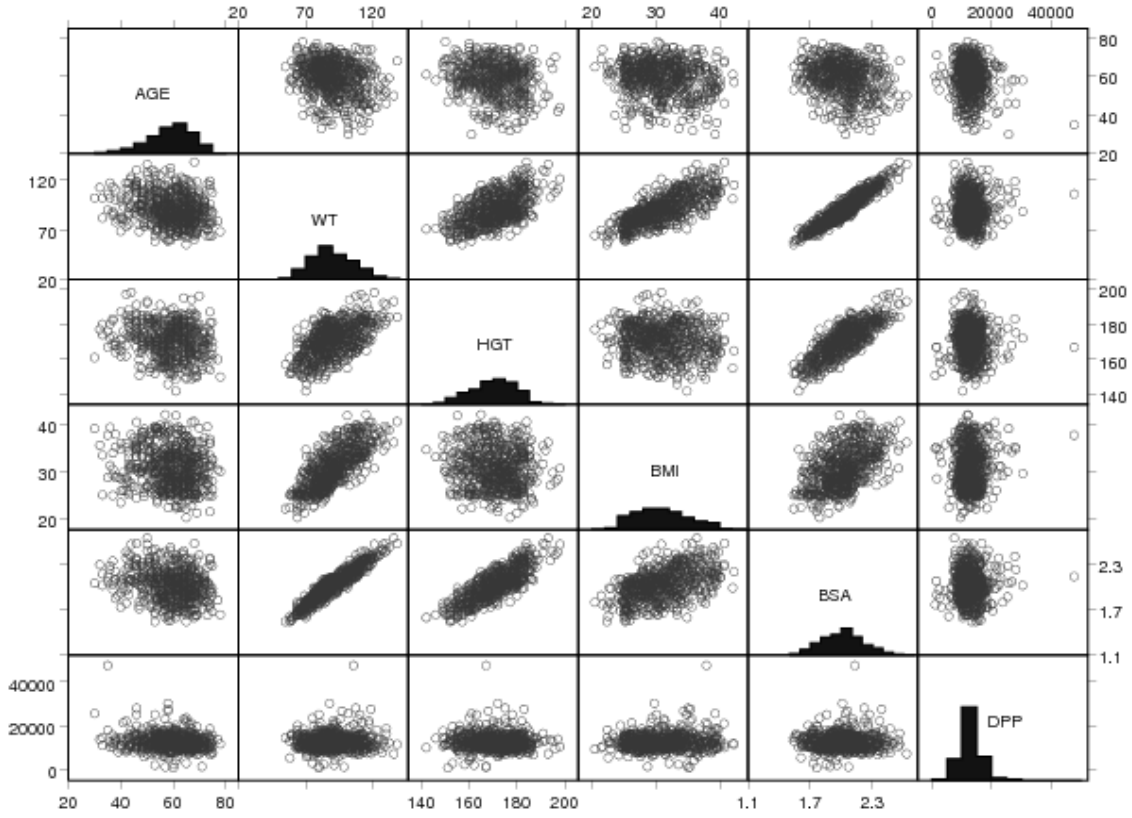

Figure 24 Scatter plots and distributions of the continuous demographic covariates in Project 3b. AGE, age (years); WT, weight (kg); HGT, height (cm); BMI, body mass index (kg/m^2); BSA, body surface area (m^2).

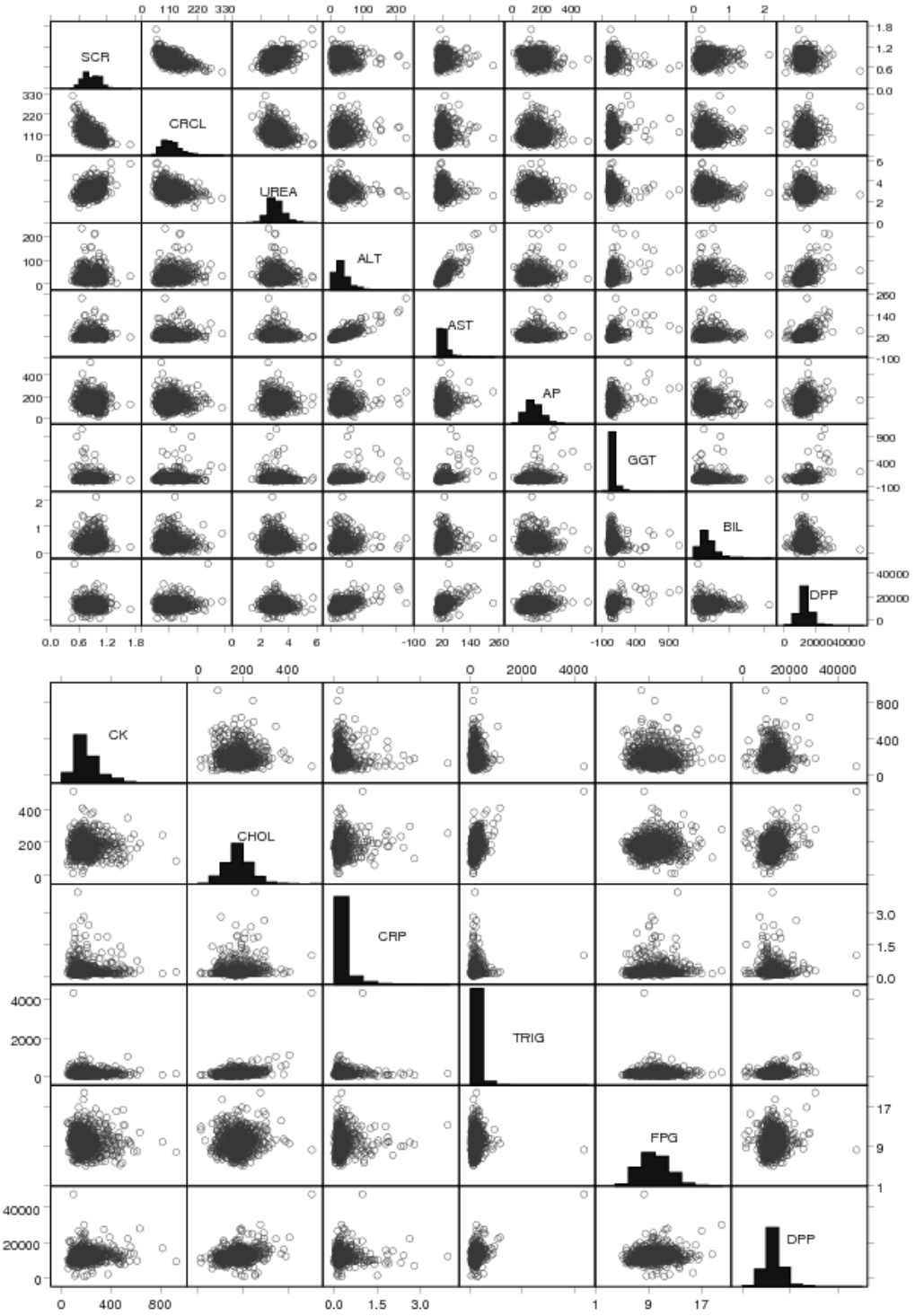

Figure 25 Scatter plots and distributions of the continuous laboratory covariates in Project 3b. SCR, serum creatinine (mg/dL); CRCL, creatinine clearance (ml/min); UREA, urea (mM); ALT, alanine transaminase (U/L); AST, aspartate transaminase (U/L); AP, alkaline phosphatase (U/L); GGT, gamma-glutamyl transferase (U/L); BIL, total bilirubin (mg/dL); CK, creatine kinase (U/L); CHOL, cholesterol (mg/dL); CRP, C-reactive protein (mg/dL); TRIG, triglycerides (mg/dL); FPG, fasting plasma glucose (mM); DPP, pre-dose DPP-4 activity (RFU).

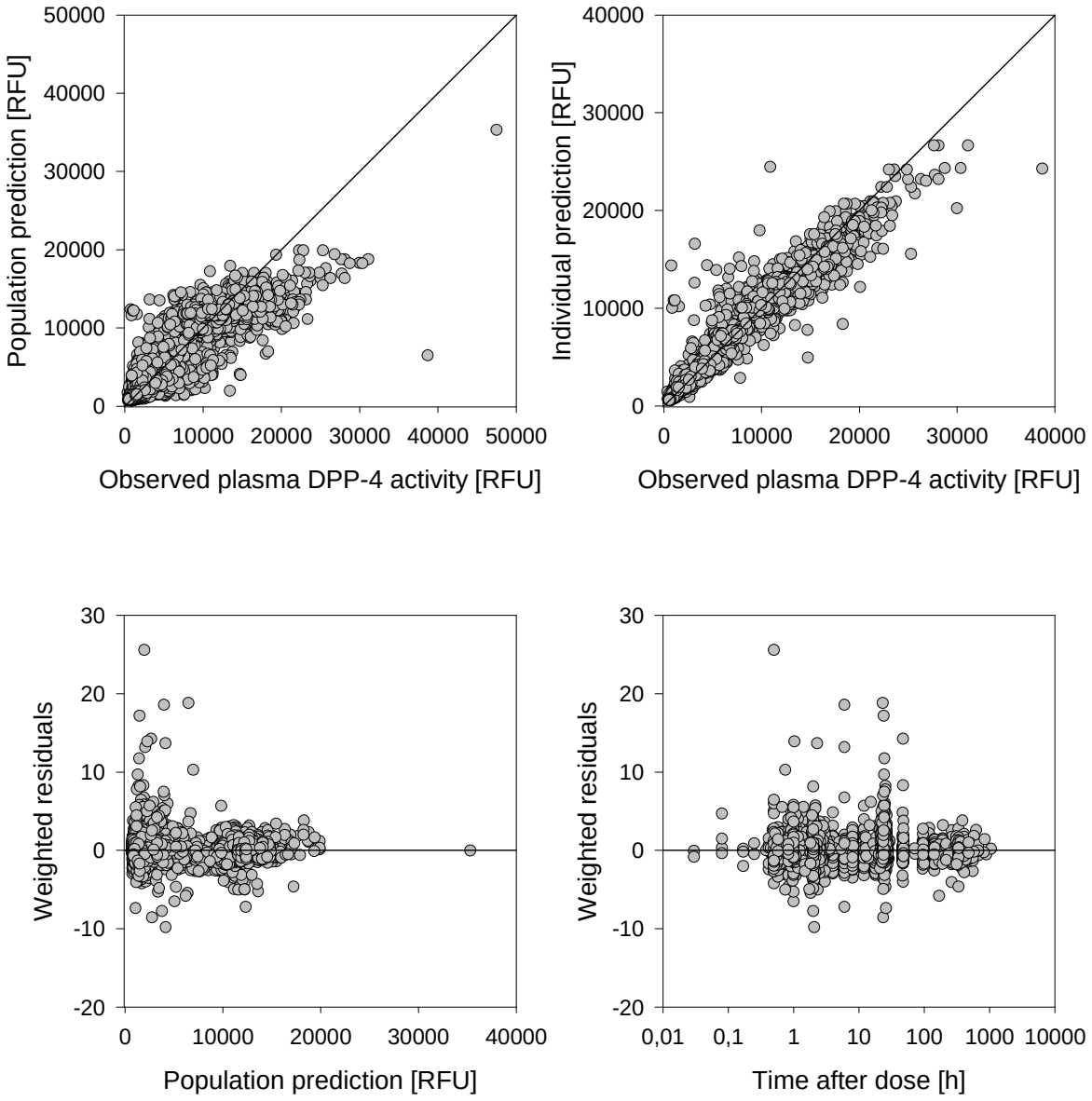

Figure 26 Standard goodness-of-fit plots for the final pharmacokinetic/pharmacodynamic model of Project 3b.

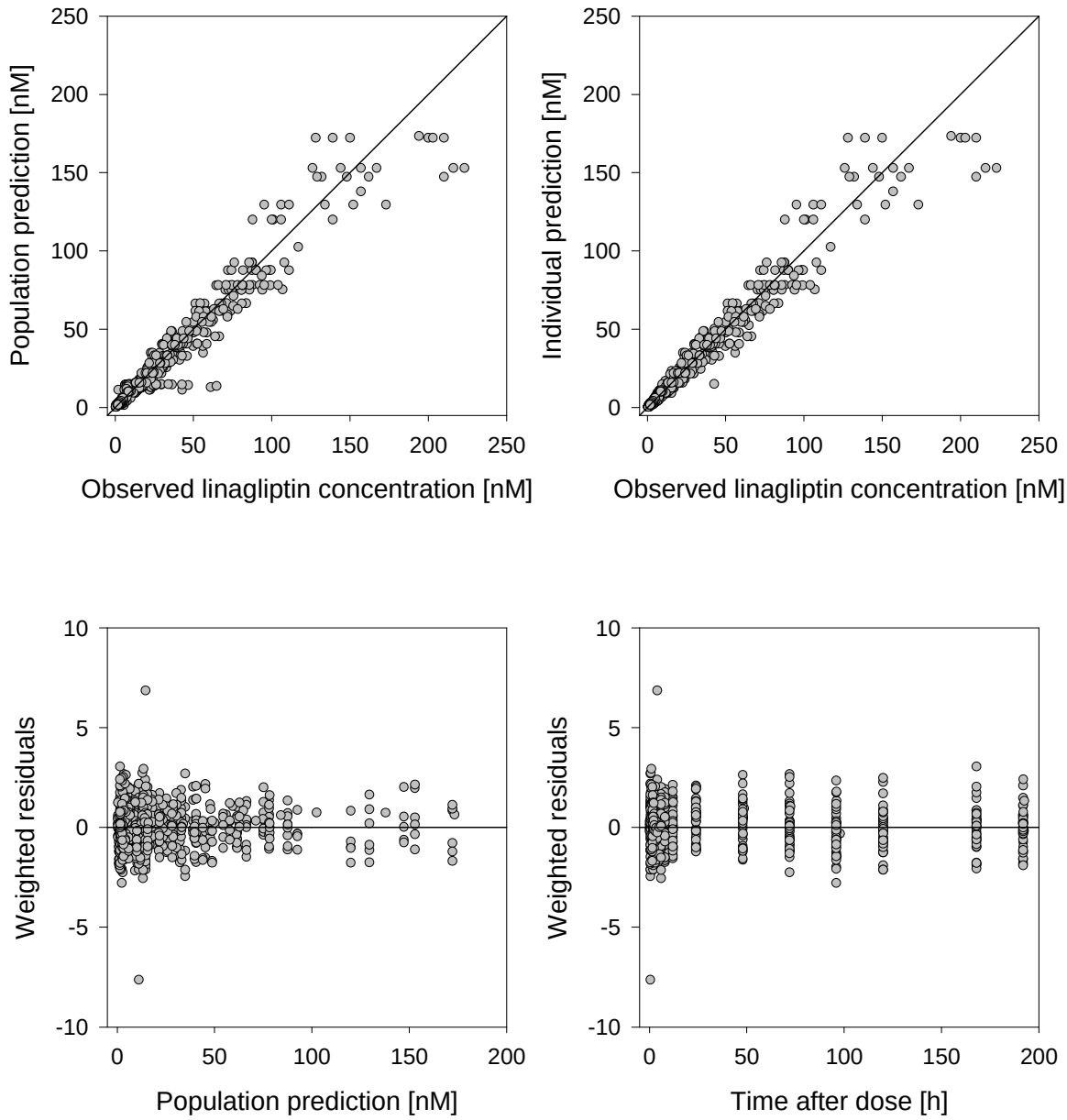

Figure 27 Standard goodness-of-fit plots for the final pharmacokinetic model of Project 4.

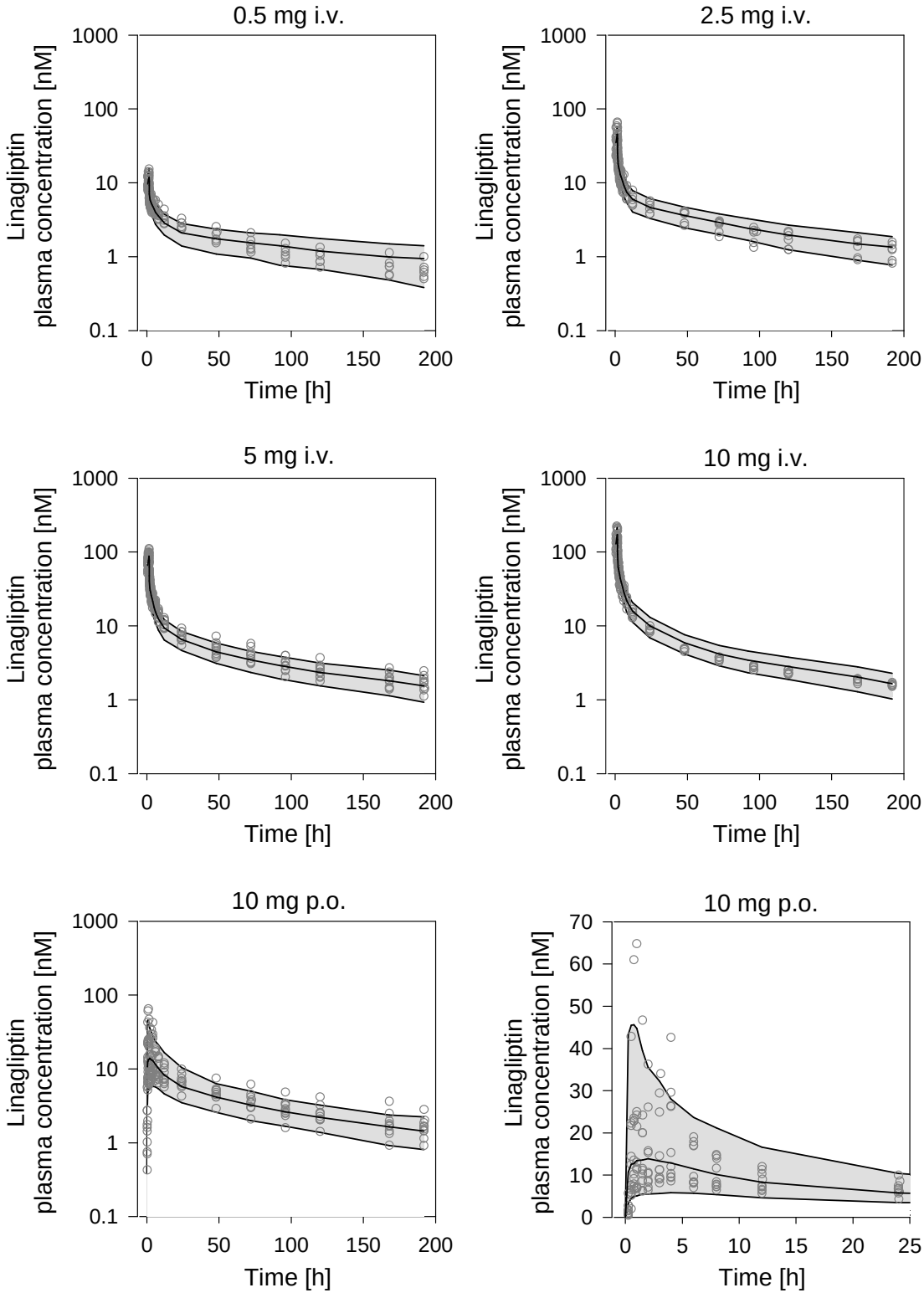

Figure 28 Visual predictive checks. 1,000 patients per dose group were simulated based on the final population pharmacokinetic model of Project 4. The solid lines show the 90% confidence intervals and the median of the simulated concentration-time profiles. The observed linagliptin plasma concentrations are displayed as dots. The visual predictive checks are depicted in semi-logarithmic scale for all dose groups. In addition, the visual predictive check for the oral 10 mg dose is displayed for the first 24 h in linear scale.

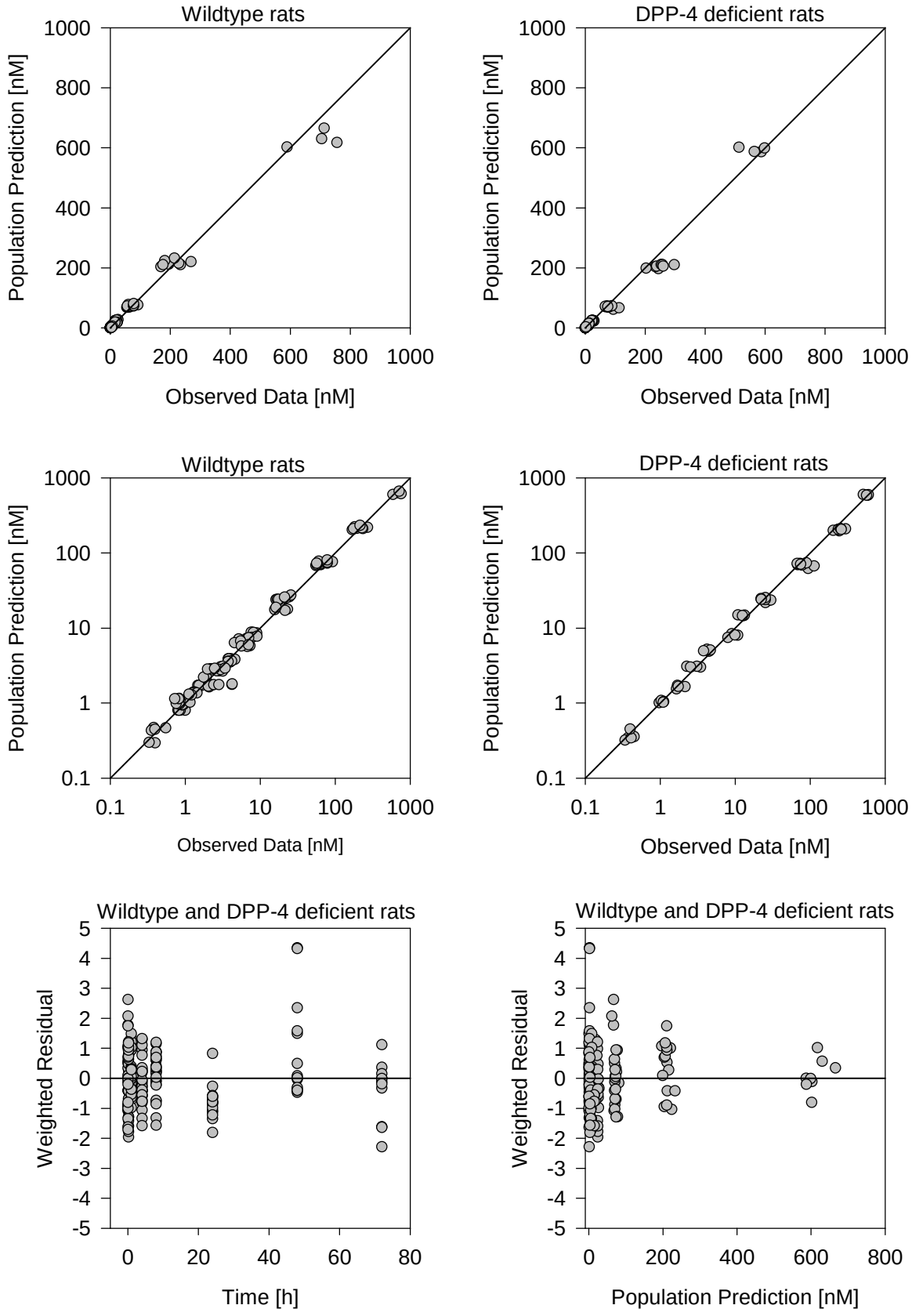

Figure 29 Standard goodness-of-fit plots for the final pharmacokinetic model of Project 5.

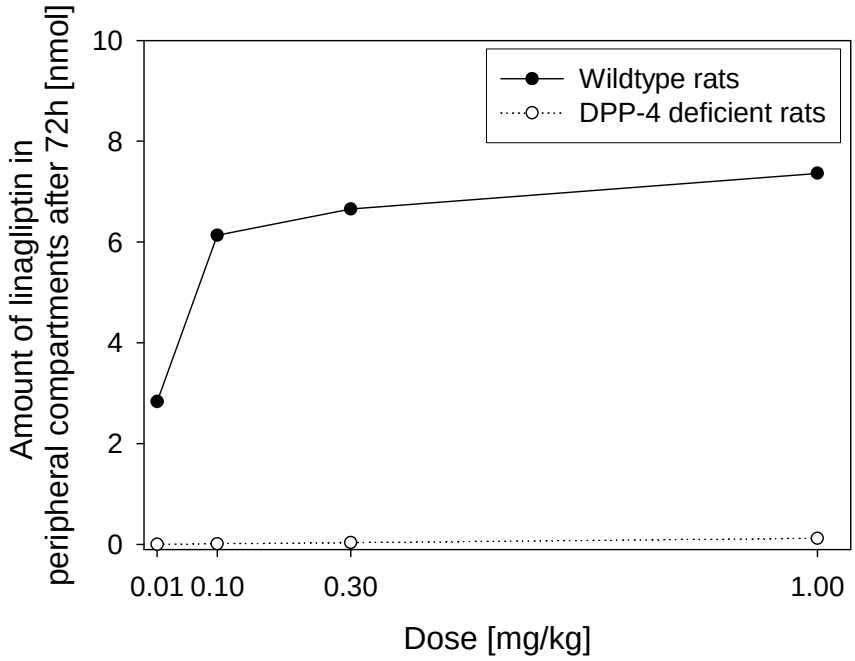

Figure 30 Comparison of the amount of linagliptin in the peripheral compartments 72 h after administration per dose group between wildtype rats (closed circles) and DPP-4 deficient rats (open circles) based on the final model of Project 5.

A-3 Model derivation and code of the target-mediated drug disposition model of linagliptin

A-3.1 Model derivation

The target-mediated drug disposition model of linagliptin assuming quasi-equilibrium conditions for the binding of linagliptin to DPP-4 was derived as exemplified in the following using a one-compartment model with concentration-dependent binding in the central compartment. A one-compartment model with concentration-dependent binding can be described by equations 1 and 2 according to the law of mass.

$$\frac{dA_{unbound}}{dt} = input - K_{ON} \cdot A_{unbound} \cdot \left(B_{\max,C} - A_{bound}\right) + K_{OFF} \cdot A_{bound} - K_{20} \cdot A_{unbound} \quad \text{(Equation 1)}$$

$$\frac{dA_{bound}}{dt} = K_{ON} \cdot A_{unbound} \cdot \left(B_{\max,C} - A_{bound}\right) - K_{OFF} \cdot A_{bound} \quad \text{(Equation 2)}$$

$dA_{unbound}/dt$ can also be expressed as:

$$\frac{dA_{unbound}}{dt} = input - K_{20} \cdot A_{unbound} - \frac{dA_{bound}}{dt} \quad \text{(Equation 3)}$$

$$\frac{dA_{unbound}}{dt} = input - K_{20} \cdot A_{unbound} - \frac{dA_{bound} \cdot dA_{unbound}}{dA_{unbound} \cdot dt} \quad \text{(Equation 4)}$$

Equation 4 can be rearranged to:

$$\frac{dA_{unbound}}{dt} + \frac{dA_{bound} \cdot dA_{unbound}}{dA_{unbound} \cdot dt} = input - K_{20} \cdot A_{unbound} \quad \text{(Equation 5)}$$

$$\frac{dA_{unbound}}{dt} \cdot \left[1 + \frac{dA_{bound}}{dA_{unbound}}\right] = input - K_{20} \cdot A_{unbound} \quad \text{(Equation 6)}$$

By assuming equilibrium conditions ($dA_{bound}/dt = 0$) equation 2 simplifies to equation 7, with $K_d = K_{OFF}/K_{ON}$.

$$A_{bound} = \frac{A_{unbound} \cdot B_{\max,C}}{A_{unbound} + K_d} \qquad \text{(Equation 7)}$$

Equation 7 can be differentiated with respect to $A_{unbound}$ yielding equation 8.

$$\frac{dA_{bound}}{dA_{unbound}} = \frac{B_{\max,C} \cdot \left(A_{unbound} + K_d\right) - A_{unbound} \cdot B_{\max,C}}{\left(A_{unbound} + K_d\right)^2} = \frac{B_{\max,C} \cdot K_d}{\left(A_{unbound} + K_d\right)^2} \qquad \text{(Equation 8)}$$

Substituting $dA_{bound}/dA_{unbound}$ in equation 6 by equation 8 results in equation 9, which was the basis for the target-mediated drug disposition model of linagliptin.

$$\frac{dA_{unbound}}{dt} = \frac{input - K_{20} \cdot A_{unbound}}{1 + \frac{B_{\max,C} \cdot K_d}{\left(A_{unbound} + K_d\right)^2}} \qquad \text{(Equation 9)}$$

A-3.2 Model code

The target-mediated drug disposition model of linagliptin as developed in Project 1 is constituted by the equations 10-13. To be used in the differential equations, the model parameters need to be transformed as follows:

$$A_{max,C} = B_{max.C} \cdot V_C, K_1 = K_d \cdot V_C, K_2 = K_d \cdot V_P, K_{20} = \frac{CL}{V_C}, K_{23} = \frac{Q}{V_C}, \text{and } K_{32} = \frac{Q}{V_P}$$

The linagliptin amount A in the depot compartment (1), the central compartment (2) and the peripheral compartment (3) is described by differential equations 10, 11, and 12, respectively.

$$\frac{dA(1)}{dt} = -K_a \cdot A(1) \qquad \text{(Equation 10)}$$

$$\frac{dA(2)}{dt} = \frac{K_a \cdot A(1) + K_{32} \cdot A(3) - K_{23} \cdot A(2) - K_{20} \cdot A(2)}{1 + \frac{A_{\max,C} \cdot K_1}{\left(A(2) + K_1\right)^2}} \qquad \text{(Equation 11)}$$

$$\frac{dA(3)}{dt} = \frac{K_{23} \cdot A(2) - K_{32} \cdot A(3)}{1 + \frac{A_{\max,P} \cdot K_2}{\left(A(3) + K_2\right)^2}} \qquad \text{(Equation 12)}$$

From this the total linagliptin plasma concentration C_{tot} is calculated as presented in equation 13.

$$C_{tot} = \frac{A(2)}{V_C} + \frac{B_{\max,C} \cdot \frac{A(2)}{V_C}}{K_d + \frac{A(2)}{V_C}} \qquad \text{(Equation 13)}$$

Statutory declaration

I hereby declare that I wrote the present dissertation with the topic

‘Population Pharmacokinetic and Pharmacodynamic Modelling and Simulation of Linagliptin, a Novel Dipeptidyl-Peptidase 4 Inhibitor for the Treatment of Type 2 Diabetes’

independently and used no other aids than those cited. In each individual case, I have clearly identified the source of the passages that are taken word for word or paraphrased from other works.

I also hereby declare that I have carried out my scientific work according to the principles of good scientific practice in accordance with the current „Grundsätze wissenschaftlicher Praxis an der Rheinischen Friedrich-Wilhelms-Universität Bonn“.